



ISF 弘立

# BAUHINIA

## 紫荊花



The Student Research Journal of The ISF Academy  
弘立書院學生研究期刊

Volume VIII  
Issue 2, 2023

Editors: *Ms. C. Brillaux, Mr. B. Coronado-Guerra, Ms. Y. De Soto Gallegos, Ms. E. G. Dixon, Ms. B. Genzlinger, Dr. S. D. J. Griffin, Ms. S. Q. Huang, Ms. D. Ibarra, Ms. H. D. Johnson, Mr. K. Kampen, Mr. C. P. O'Neill, Dr. R. Oser, Dr. M. Pritchard, Ms. S. H. Ratzlaff, Dr. L. Worth, Mr. F. Wynne, Dr. Y. L. Zhang, Dr. J. Zhao*

ISSN 2409-4064

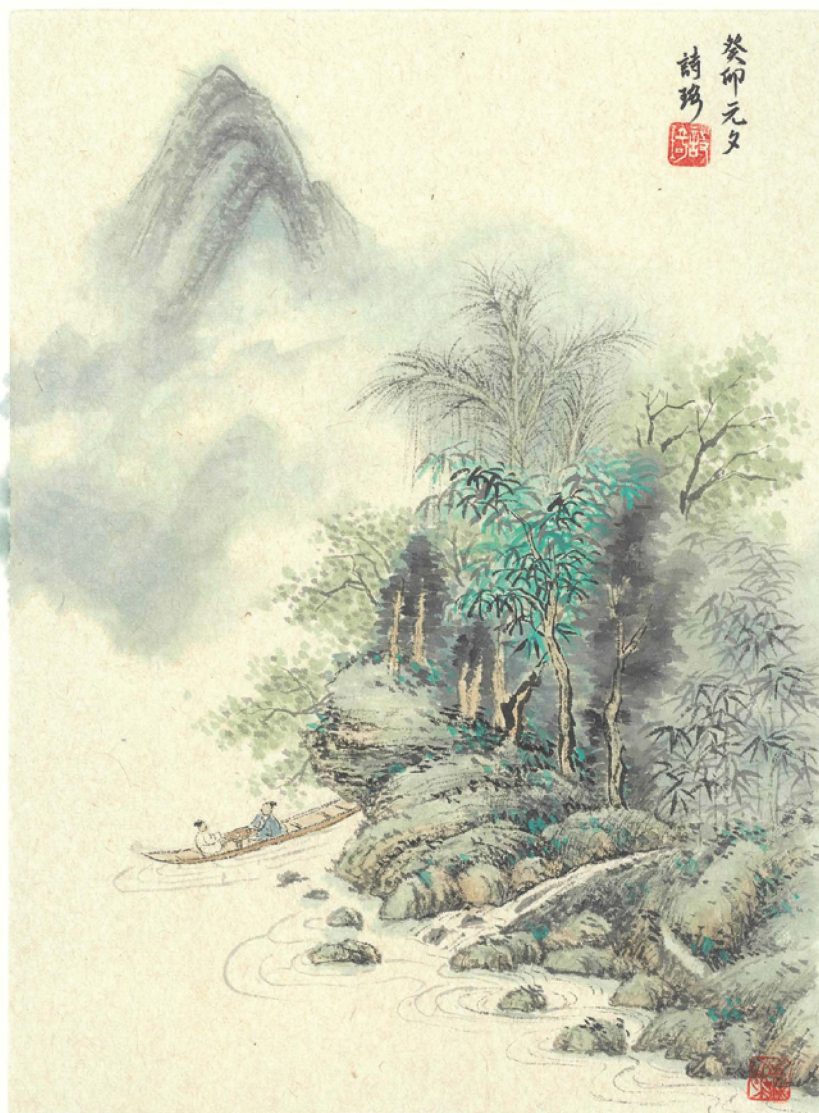


## Table of Contents

<p><b>Bioremediation: isolation and genomic characterisation of bacteria for the degradation of toluene and polystyrene</b>  <i>Angus C.H. Wai</i></p>	1
<p><b>A comparison of the evaluation of <math>\pi</math> by the ancient Chinese, ancient Greek, and modern methods</b>  <i>Henrik H.Y. Ng</i></p>	6
<p><b>Working from home: how can environmental design increase productivity and morale?</b>  <i>Maximillian W.K. Chu</i></p>	15
<p><b>Characterisation of three strains of <i>Escherichia coli</i> isolated from the Equine Gut</b>  <i>Selina W. Y. Hui</i></p>	36
<p><b>To what extent is the diversity of mangrove stands affected by the presence of a breakwater?</b>  <i>Miriam M.C. Cheng</i></p>	43
<p><b>How can drawing a contrast between China and the United States reveal the effectiveness of their solar energy policies in addressing climate change?</b>  <i>a K.H. Pong</i></p>	59
<p><b>Isolation and genomic sequencing of <i>Klebsiella</i> sp. CTHL.F3a, a cellulolytic strain isolated from Korean Kimchi</b>  <i>Chloe T. H. Lee</i></p>	66
<p><b>Lowering the impact of health risk from air pollution and improving commuter comfort in Hong Kong</b>  <i>Harry J. Chee</i></p>	71
<p><b>Generating fire and water through the sun and moon: the mechanism and philosophy behind <i>yangsui</i> 陽燧 and <i>fangzhu</i> 方諸</b>  <i>Ronnie L.C. Cheung</i></p>	89
<p><b>Cognitive behavioural therapy as a treatment for Social Anxiety Disorder (SAD): an analysis of its effectiveness in addressing the etiology of SAD</b>  <i>Marsha C.Y. Lau</i></p>	96
<p><b>What is the relationship between the different types of terrace fields of the same total height and the volume of water needed to fill the terrace fields?</b>  <i>Franklin S. Ke</i></p>	103
<p><b>Tracking COVID-19's genomic and structural evolution</b>  <i>Valerie C.W.D. Huang</i></p>	114
<p><b>Complete genome sequence of <i>Kluyvera</i> sp. CRP, a cellulolytic strain isolated from Red Panda faeces (<i>Ailurus fulgens</i>)</b>  <i>Angus C. H. Wai</i></p>	121
<p><b>The impact of urbanisation on the frequency and length of bat echoes recorded in Hong Kong</b>  <i>Allison C.Y. Cheung</i></p>	127
<p><b>A study into the antibacterial properties of Chinese herbal medicine herb <i>Coptis chinensis</i></b>  <i>Aidan Tam</i></p>	132
<p><b>Genomic analysis of the airborne <i>Micrococcus luteus</i> strain CW.Ay reveals extensive versatility and resilience</b>  <i>Charlotte A.C. M. Wong</i></p>	143
<p>論孫思邈的養生養性觀對中國醫學、養生學的影響  <i>Jamee B.Y. Tsai 蔡寶瑤</i></p>	148



## Editor's note

With awe for the perseverance of our students and the commitment of our editorial board, we humbly present the eighth volume of *Bauhinia*. Legend has it that all *Bauhinia blakeana* trees commonly found in Hong Kong today, originated from the cuttings of one rare tree preserved in the Hong Kong Botanic Gardens (Dunn, 1908). If so, opine Lau *et al.* (2005), clones of this hybrid species should be susceptible to environmental stressors that might cause its extinction, but thus far the tree has thrived. Similarly, despite the environmental stress of the recent pandemic, our students continue to thrive in the pursuit of knowledge, perhaps a merit of our namesake.

The seeds of this journal were first sowed around 10 years ago with the establishment of *Shuyuan* whose programs germinate high-level learning beyond the mainstream curriculum of the school. The seedlings encouraged the pursuit of thoughtful scholarship in all areas of the school, and so this publication highlights the results of research-based tasks completed in any subject. Finally, our students continue to inspire us, and this year we branched out to produce our first faculty journal, *Aquilaria*.

Though *Bauhinia* trees mostly reach a maximum height of eight meters, we know our students will continue these academic pursuits past this eighth year; we've already received our first submission for *Bauhinia* IX, even before the call for submissions!

Expanding to the genus, *Bauhinia* boasts around 300 species, and so too, we invite you to explore the diversity of articles on offer, a culmination of our students' efforts. Whether comparing the cosmological ideas of Pliny the Elder and Laozi, learning about the introduction of chilies to Chinese cuisine and medicine, or examining the impact of urbanization on bat echoes recorded in Hong Kong, there's something for every reader to enjoy. Please feel free to engage with us via [sy\\_team@isf.edu.hk](mailto:sy_team@isf.edu.hk).

Rachel Oser

### References

Dunn, S.T. (1908). New Chinese Plants. *Journal of Botany, British and Foreign*. 46 (550): 324–326.

Lau C.P.Y., Ramsden L., Saunders R.M.K. (2005). Hybrid origin of "*Bauhinia blakeana*" (Leguminosae: Caesalpinioideae), inferred using morphological, reproductive, and molecular data. *American Journal of Botany*; 92(3):525-33. <https://doi.org/10.3732/ajb.92.3.525>

## 編者的話

我們懷著對學生的毅力和編輯委員會的付出的敬畏之心，在此謙卑地推出《洋紫荊》第八卷。傳說中，如今香港常見的洋紫荊樹(*Bauhinia blakeana*)都起源於香港植物園中保存的一棵稀有樹木的剪枝（鄧恩，1908年）。如果是這樣的話，正如劉等人所言，這種雜交物種的克隆體應該對環境壓力十分敏感，這可能會導致其滅絕，但迄今為止，這棵樹一直在茁壯成長。同樣，在近幾年的疫情環境壓力下，我們的學生在追求知識的道路上仍然茁壯成長，這也許是我們名字的優點。

本刊的種子最早在10年前隨著書院的成立而播下，書院的項目孕育了高水平的學術研究，超越了學校的主流課程。這些嫩芽激勵著學校師生們在各個領域，不斷深入地學術追求。因此，本刊重點展示了在學科中完成的基於研究任務的成果。最後，學生們繼續激勵著我們，今年我們擴展出第一本教職員工刊物《菀香》。

儘管洋紫荊樹的高度通常最多達到8米，但我們知道我們的學生會在這第八年之後繼續進行這些學術追求；在征集稿件之前，我們已經收到了第九屆洋紫荊的第一份投稿！

擴展到屬於屬的範疇，洋紫荊約有300個物種，同樣，我們邀請您閱讀本刊，探索文章的豐富性與研究的多樣性，這是我們學生努力的結晶。無論是比較普林尼和老子的宇宙觀念，了解辣椒在中國飲食和醫學中的引入，還是研究城市化對香港蝙蝠回聲的影響，這裡總有一篇文章讓每位讀者喜歡。歡迎通過 [sy\\_team@isf.edu.hk](mailto:sy_team@isf.edu.hk) 與我們互動。

歐睿秋



**Artist:** Ava Osann

**Title:** *Gills*, 2023

**Medium:** Oil on canvas,  
28 x 32 cm

**Description:** This piece explored the connection between mushrooms and neural pathways. I was inspired by the gills of mushrooms and how they resemble neurons. This motif is repeated in other pieces such as *Mytilus Edulis* connecting to how we think subjectively. The bright greens contrast sharply with the black background to create an artificial representation of natural structure connecting to *Sensory Homunculus* in representing the way that reality and the natural world are perceived subjectively.

## A Note about Style

Articles included in this publication are written for many different purposes. Any differences in style are due to the need to adhere to the format required for that purpose. Generally, the Modern Language Association (MLA) citation and format style (8th Ed.) is used for articles written in English as part of the Oxford University Shuyuan Classics Summer Program or the NRI Scholar's Retreat (Needham Research Institute, at Cambridge University). However, articles written in the STEM fields were often adapted from posters students prepared for the American Microbiology Society conference (ASM Microbe) and they adhere to the American Psychological Association (APA) citation and format style (7th Ed.). Articles written in Chinese use footnotes following the style outlined in the Bulletin of the Institute of Chinese Literature and Philosophy. However, articles that were originally submitted as partial fulfillment of the International Baccalaureate (IB) programmes, such as the Diploma Programme's (DP) Extended Essay (EE) or Theory of Knowledge (TOK) course, have followed the specific requirements as outlined by the student's supervisor, and they are published in this journal as they were originally submitted. A footnote under each article indicates the program from which each piece of work was culled.

## 關於文體的說明

本出版物中的文章是為許多不同目的而寫的。任何風格上的差異都是由於需要遵守該目的所需的格式。一般來說，牛津大學書院經典暑期班或劍橋大學NRI研究所(Needham Research Institute)暑期班的英文文章，採用現代語言協會(MLA)的引文和格式(第8版)，而STEM文章則採用美國心理學會(APA)的引文和格式(第7版)。用中文撰寫的文章採用中研院《中國文哲研究集刊》的腳注樣式。但是，如果是作為國際文憑課程(IB)的部分內容而提交的文章，如中學課程(MYP)的個人項目或文憑課程(DP)的擴展論文，則按照學生導師提出的具體要求，按原樣在本刊發表。每篇文章下的腳注都注明了文章入選前所屬的項目。

---

# Bioremediation: isolation and genomic characterisation of bacteria for the degradation of toluene and polystyrene

Angus C.H. Wai

---

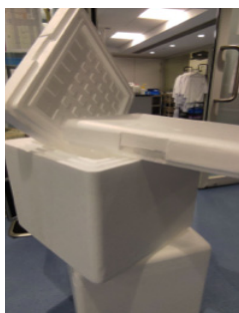
## Introduction

Plastic and microplastic pollution has become a global problem. Microplastics, plastics physically degraded over time, are especially hard to remove with current tools and machinery because of their size and quantity. Of all plastic waste produced, polystyrene ('styrofoam') is perhaps the most alarming. This unrecyclable, low density plastic quickly fills landfills, is blown around by wind and is carried by the ocean (Geyer *et al.*, 2017)

Microbes are known to be able to break down some forms of plastic, such as polyethylene (PE) and polyethylene terephthalate (PET), but to date few microbes that can digest polystyrene have been identified (Atiq, 2010). In this investigation, the ability to use toluene as a carbon source is used to screen bacteria because this common solvent contains almost all of the types of bonds present in polystyrene (Figure 2).

## 1. Toluene and Styrene

Toluene is used to screen bacteria due to its similarity to polystyrene. The structure of the two are highly similar, with only 1 extra C—C bond per phenyl group present in polystyrene (the C=C double bond of styrene is not present in the polymer), as seen in Figure 2. This means that any pathway accomplishing the breakdown of polystyrene must include enzymes capable of toluene



Polystyrene



Toluene

degradation. In Figure 1, degradation pathways from the two molecules to pyruvate have been picked out from the KEGG reference pathway (Kanehisa & Goto, 2010). The pathways differ only slightly from each other.

## 2. Method

The soil sample from which TDs1.5 came from was collected under a pile of polypropylene cups and boxes, under shade and surrounded by plants (Figure 3). TDs3.6a and TDs3.6c came from an old sponge used to apply petroleum-based oil (containing toluene) to horse hooves. TDsB1 was sourced from a pond water sample that happened to survive in the toluene minimal medium.

After suspension in 0.9% saline, 100  $\mu$ L aliquots were used to inoculate LB agar infused with toluene, resulting in 33 colonies. Twelve colonies showing sustained growth after one week were transferred to minimal medium containing 10% toluene as the only carbon source (Figure 4). Three isolates that grew well in this medium were passaged on LB agar before DNA extraction for sequencing via the Illumina MiSeq platform. Draft genomes were assembled using Prinseq-lite (Schmieder & Edwards, 2000) and Newbler (Silva *et al.*, 2013) while hybrid genomes (TDs3.6c) were assembled using Unicycler (Wick *et al.*, 2017). PATRIC (Wattam *et al.*, 2017) was used to annotate and identify enzymes and likely metabolic pathways.

## 3. Results

Experimental results showed that these 4 strains were able to grow in minimal medium with toluene, thus using toluene as the only carbon source. Kirby-Bauer assays, all 3 isolates appeared to tolerate sodium benzoate. TDs3.6c also appeared to be resistant to 8-hydroxyquinoline.

---

The above article was written as a culmination of research presented at the 19th annual meeting of the Asia Oceania Geosciences Society (AOGS), 2021.

**Figure 1.** Degradation pathway of toluene and styrene in enzyme numbers

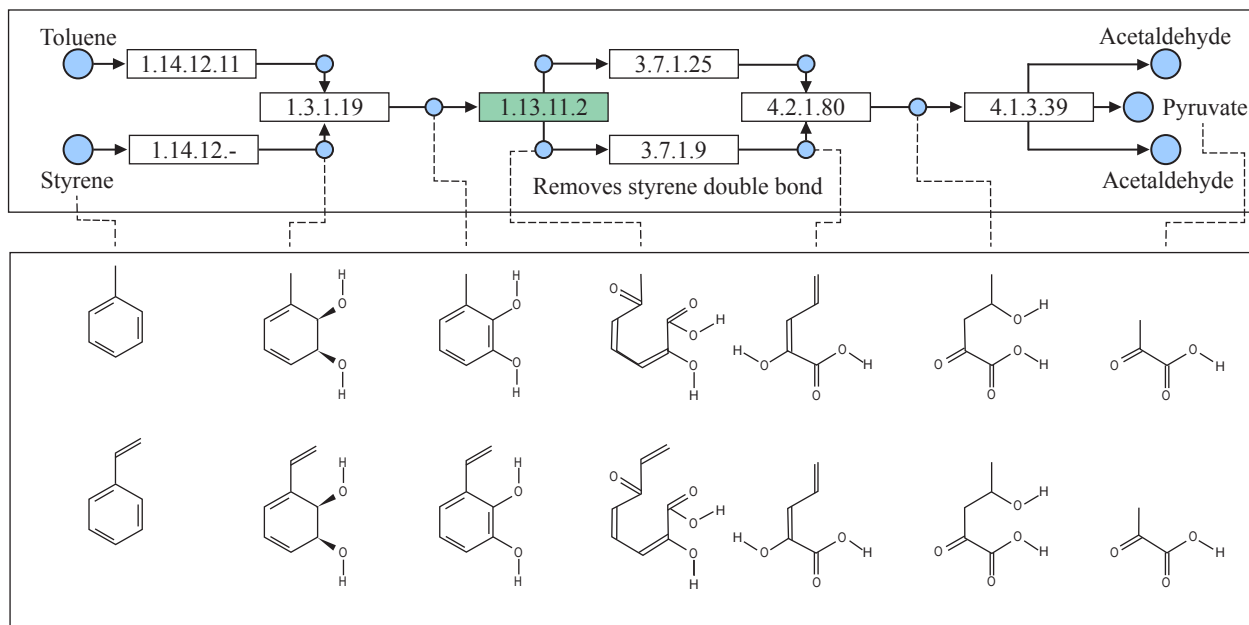


**Figure 2.** Degradation pathway of toluene and styrene in molecules



**Figure 3.** Sample site of TDs1.5



**Figure 4.** Samples in minimal medium with 10% toluene

Draft sequences of 4 strains, TDs1.5, TDs3.6a, TDs3.6c, and TDsB1, were identified through NCBI BLAST (Altschul *et al.*, 1990) to be *Lysinibacillus*, *Sporosarcina*, *Gulosibacter*, and *Acinetobacter oleivorans* respectively. Assembly metrics of TDs1.5, TDs3.6a, and TDs3.6c are shown in Table 1.

## 4. Pathways and Genes

Experimental results have proven that the isolates were able to survive with toluene as the sole carbon source. Enzymes on the reference pathway of toluene and styrene degradation present in the sequences were identified by PATRIC. PATRIC annotation shows that TDs1.5 and TDs3.6c are likely to possess enzymes for styrene and toluene degradation based off of the draft assembly. Table 2 shows the enzymes identified in the sequences.

The hybrid assembly of TDs3.6c did not produce more enzymes on the reference pathway in PATRIC analysis, most likely indicating that it is using a different pathway to degrade toluene.

Fluorescent siderophores were observed around TDs1.5 and TDs3.6a. This combined with the existence of catechol 2,3-dioxygenase in their sequence, it is highly probable that TDs1.5 and TDs3.6a are producing catechol as a part of degradation. This may suggest that they are degrading toluene through a part of the reference pathway.

Sample ID	TDs3.6a	TDs3.6c	TDs3.6c
Input Bases	158,349,060	127,211,866	127,211,866
Aligned Reads	559,446	429,328	429,328
Aligned Bases	154,231,252	115,824,168	115,824,168
Peak depth	43.0	39.0	39.0
Large Contigs	502	56	56
Bases in Large Contigs	3,706,531	2,775,665	2,775,665
Contigs	580	84	84
Bases in Contigs	3,732,354	2,784,141	2,784,141
N50 Contig Size	12,617	115,372	115,372
Estimated genome size	3.7 MB	3.3 MB	3.3 MB
Identity	<i>Sporosarcina</i>	<i>Gulosibacter molinativorax</i>	<i>Gulosibacter molinativorax</i>

**Table 1.** Draft genome assembly metrics of TDs1.5, TDs3.6a, and TDs3.6c

Sample ID	Enzyme	Reference Pathway(s)
(all three)	catechol 2,3-dioxygenase (EC 1.13.11.2)	Xylene degradation, Styrene degradation
TDs3.6c, TDs1.5	2-hydroxy-phenylacetate hydroxylase (EC 1.14.13.-)	Xylene degradation, Styrene degradation
TDs3.6c	Aliphatic nitrilase	Styrene degradation
TDs1.5	Acetaldehyde dehydrogenase	Xylene degradation
TDs1.5	p-cumic alcohol dehydrogenase	Xylene degradation
TDs1.5	Amidase	Styrene degradation

**Table 2.** Enzymes identified in draft assemblies of TDs1.5, TDs3.6a, and TDs3.6c

## 5. Comparison with other Strains

*Gulosibacter Molinativorax* have previously been identified in molinate contaminated runoff (Nunes *et al.*, 2013) and oil contaminated soil (Yang *et al.*, 2013). The petroleum contamination origins of TDs3.6c show resemblance to these identifications.

A strain of *Lysinibacillus* was found dominant in a biodegradation reactor degrading toluene (Wei *et al.*, 2019), while two species of *Lysinibacillus* were found degrading styrene in biotrickling filters (Rezaei *et al.*, 2020). In another study, *Lysinibacillus sp.* was found to

be the most efficient at biofilm formation of polystyrene sheets (Ebciba & Gnanamani, 2000). None of their styrene degrading strains were isolated from soil as TDs1.5 was, instead from environments favorable to perform styrene degradation.

To date, no strains of *Sporosarcina* have been identified with toluene or styrene degradation properties. Interestingly, the genus is commonly found together with *Lysinibacillus* (Markande & Nerurkar, 2016) (Mangwani *et al.*, 2019).



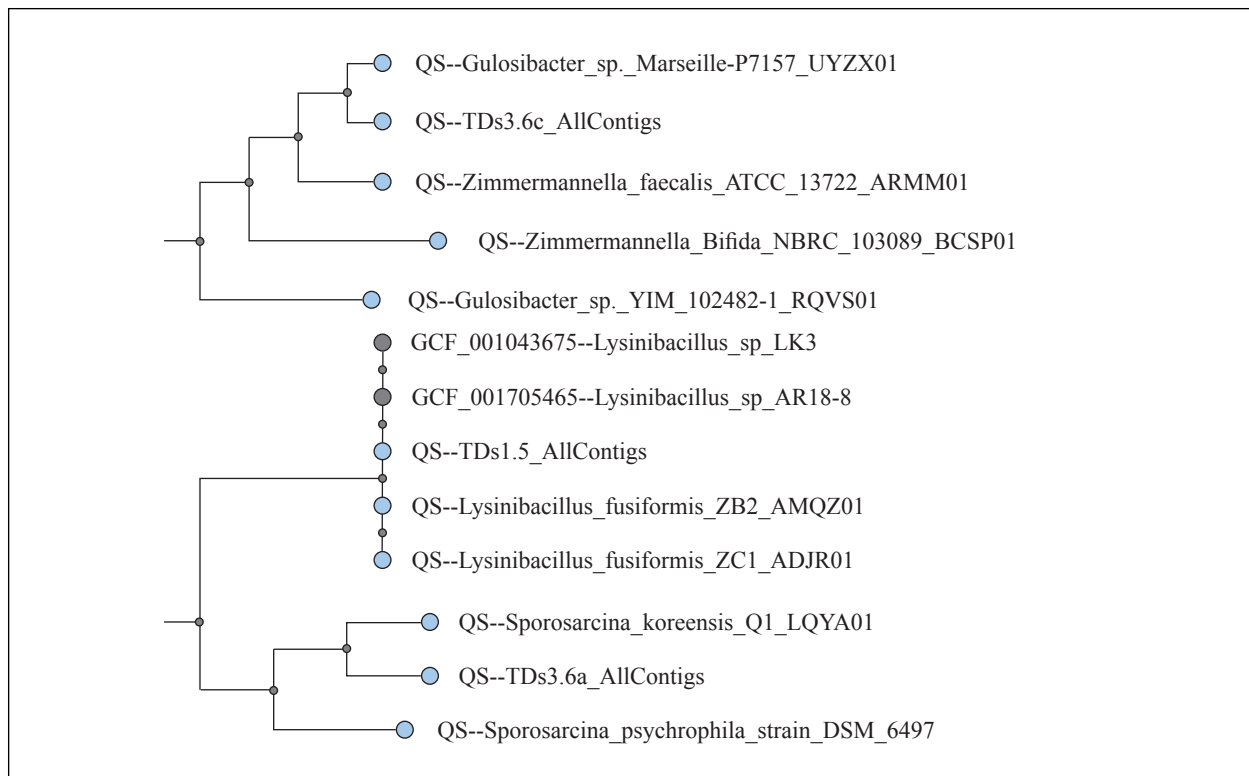


**Figure 5.** Phylogenetic trees of TDs1.5, TDs3.6a, and TDs3.6c [1]

## Conclusion

Polystyrene biodegradation through microbes will have many environmental implications. Most prominently, it provides a method for proper quick disposal of this resilient material in an environmental and sustainable way, as opposed to lengthy UV degradation.

This study has identified strains of bacteria with high chances of being able to degrade polystyrene. The next step is to prove this ability, through either experimental results or analysis of a full genome. If the ability is proven, investigations to the feasibility of industrial application could pave the way to a solution to polystyrene pollution.

However, before bioremediation could become a global solution, there are other factors that are to be considered. For example, by-products of the degradation process; if allowing one species of bacteria to thrive would harm ecosystems; and the economics of implementation.

## References

- Altschul, S. F., Gish, W., Miller, W., Myers, E. W., & Lipman, D. J. (1990). Basic local alignment search tool. *Journal of Molecular Biology*, 215(3), 403–410. [https://doi.org/10.1016/S0022-2836\(05\)80360-2](https://doi.org/10.1016/S0022-2836(05)80360-2)
- Atiq, N., Garba, A., Ali, M., Andleeb, S., Ahmad, & Robson, G. (2010). Isolation and identification of polystyrene biodegrading bacteria from soil. *African Journal of Microbiology Research*, 4, 1537.
- Ebciba, C., & Gnanamani, A. (2020). Detailed studies on microbial adhesion and degradation of polystyrene foam wastes (PSFW) for clean environment. *Environmental Science and Pollution Research*, 27(35), 44257–44266. <https://doi.org/10.1007/s11356-020-10272-7>
- Geyer, R., Jambeck, J. R., & Law, K. L. (2017). Production, use, and fate of all plastics ever made. *Science Advances*, 3(7), e1700782. <https://doi.org/10.1126/sciadv.1700782>
- Kanehisa, M., & Goto, S. (2000). KEGG: Kyoto Encyclopedia of Genes and Genomes. *Nucleic Acids Research*, 28(1), 27–30. <https://doi.org/10.1093/nar/28.1.27>
- Mangwani, N., Kumari, S., & Das, S. (2021). Taxonomy and Characterization of Biofilm Forming Polycyclic Aromatic Hydrocarbon Degrading Bacteria from Marine Environments. *Polycyclic Aromatic Compounds*, 41(6), 1249–1262. <https://doi.org/10.1080/10406638.2019.1666890>
- Markande, A. R., & Nerurkar, A. S. (2016). Microcosm-based interaction studies between members of two ecophysiological groups of bioemulsifier producer and a hydrocarbon degrader from the Indian intertidal zone. *Environmental Science and Pollution Research*, 23(14), 14462–14471. <https://doi.org/10.1007/s11356-016-6625-1>
- Nunes, O. C., Lopes, A. R., & Manaia, C. M. (2013). Microbial degradation of the herbicide molinate by defined cultures and in the environment. *Applied Microbiology and Biotechnology*, 97(24), 10275–10291. <https://doi.org/10.1007/s00253-013-5316-9>
- Rezaei, M., Moussavi, G., Naddafi, K., & Johnson, M. S. (2020). Enhanced biodegradation of styrene vapors in the biotrickling filter inoculated with biosurfactant-generating bacteria under H<sub>2</sub>O<sub>2</sub> stimulation. *Science of The Total Environment*, 704, 135325. <https://doi.org/10.1016/j.scitotenv.2019.135325>
- Schmieder, R., & Edwards, R. (2011). Quality control and preprocessing of metagenomic datasets. *Bioinformatics*, 27(6), 863–864. <https://doi.org/10.1093/bioinformatics/btr026>
- Silva, G. G., Dutilh, B. E., Matthews, T. D., Elkins, K., Schmieder, R., Dinsdale, E. A., & Edwards, R. A. (2013). Combining de novo and reference-guided assembly with scaffold\_builder. *Source Code for Biology and Medicine*, 8(1), 23. <https://doi.org/10.1186/1751-0473-8-23>
- Wattam, A. R., Davis, J. J., Assaf, R., Boisvert, S., Brettin, T., Bun, C., Conrad, N., Dietrich, E. M., Disz, T., Gabbard, J. L., Gerdes, S., Henry, C. S., Kenyon, R. W., Machi, D., Mao, C., Nordberg, E. K., Olsen, G. J., Murphy-Olson, D. E., Olson, R., ... Stevens, R. L. (2017). Improvements to PATRIC, the all-bacterial Bioinformatics Database and Analysis Resource Center. *Nucleic Acids Research*, 45(D1), D535–D542. <https://doi.org/10.1093/nar/gkw1017>
- Wei, Z. S., He, Y. M., Huang, Z. S., Xiao, X. L., Li, B. L., Ming, S., & Cheng, X. L. (2019). Photocatalytic membrane combined with biodegradation for toluene oxidation. *Ecotoxicology and Environmental Safety*, 184, 109618. <https://doi.org/10.1016/j.ecoenv.2019.109618>
- Wick, R. R., Judd, L. M., Gorrie, C. L., & Holt, K. E. (2017). Unicycler: Resolving bacterial genome assemblies from short and long sequencing reads. *PLOS Computational Biology*, 13(6), e1005595. <https://doi.org/10.1371/journal.pcbi.1005595>
- Yang, M.-Q., Li, L.-M., Li, C., & Li, G.-H. (2013). [Microbial community structure and distribution characteristics in oil contaminated soil]. *Huan Jing Ke Xue Huanjing Kexue*, 34(2), 789–794.
- [1] WGS accession numbers of genomes in phylogenetic tree  
Gulosibacter sp. Marseille-P7157, accession UYZX01  
[Zimmermannella] faecalis ATCC 13722, accession ARMM01  
[Zimmermannella] bifida NBRC 103089, accession BCSP01  
Gulosibacter sp. YIM 102482-1, accession RQVS01  
Lysinibacillus sp. LK3, accession LDUJ01  
Lysinibacillus sp. AR18-8, accession MDGU01  
Lysinibacillus fusiformis ZB2, accession AMQZ01  
Lysinibacillus fusiformis ZC1, accession ADJR01  
Sporosarcina koreensis Q1, accession LQYA01  
Sporosarcina psychrophila DSM 6497

# A comparison of the evaluation of $\pi$ by the ancient Chinese, ancient Greek, and modern methods

Henrik H.Y. Ng

## Introduction

Defined as the ratio between the circumference and the diameter of a circle,  $\pi$  is one of the most used constants, being used heavily in academic fields such as engineering, theoretical physics and pure mathematics.

Outside of academia, there are many applications of  $\pi$  in everyday life. For example, you can calculate the volume of your cylindrical bottle by using the formula  $\pi r^2 h$ , simply by finding the height and radius of the bottle. Another example is that every angle can be expressed in terms of  $\pi$  (radians). You can express the angular speed of your fan as  $2\pi \text{ rads}^{-1}$ , which is simply one rotation per second, or 60rpm.

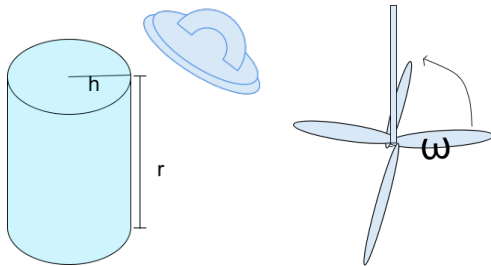


Figure 1. Practical usages of  $\pi$

In fact,  $\pi$  is such an important concept, without which quantities like the formulae for the area of a circle and the volume of a sphere may not be shown or proven using integrals:

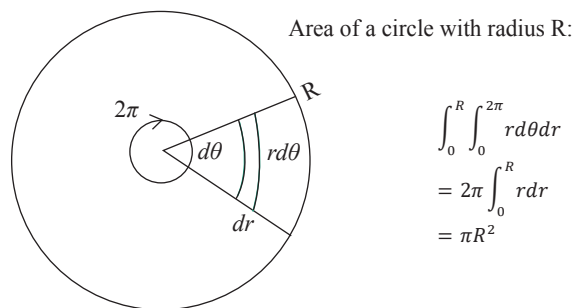


Figure 2. The use of the concept of  $\pi$  to evaluate a very simple double integral.

In the fields of mathematics,  $\pi$  is deeply integrated in a lot of functions, like sine and cosine. With the use of  $\pi$  (or its fraction), we can obtain perfect integer values of those functions. For example,  $\sin(\pi/2)$  is exactly 1, and  $\sin(\pi)$  is exactly 0. Another example is the Euler's equation,  $e^{ix} = \cos x + i \sin x$  - with the use of  $\pi$ , we can get the Euler's identity,  $e^{i\pi} + 1 = 0$  (with  $i$  being the imaginary unit,  $i^2 = -1$ ). Without the use of  $\pi$ , it is also impossible to obtain a neat value through integration of certain functions. In physics,  $\pi$  is an integrated part in many equations, especially in the subfields of waves and circular motion. It is impossible to determine the orbital period of a satellite without using a good approximation of the value of  $\pi$ , and it is also hard to show a mechanical wave neatly without  $\pi$ . Such examples continue indefinitely.

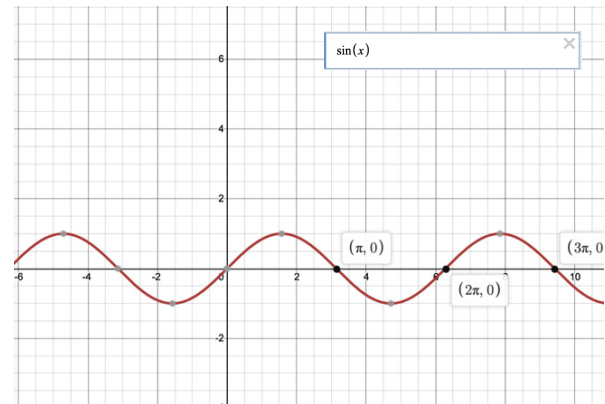


Figure 3. As shown on the graph,  $\pi$  and its fractional forms on the x-axis correspond to the maxima, minima and roots of  $f(x)=\sin(x)$ .

We might take it for granted that the value of  $\pi$  is 3.141592653..... (*ad infinitum*) upon searching Google with a click on the keyboard, but in ancient times across different cultures,  $\pi$  was a mysterious value of which the brightest of mathematicians and scientists tried to approximate the exact value, through a variety of different methods, although some were more successful than others. It was only in the 18th century that Johann Heinrich Lambert proved that  $\pi$  is irrational, which means that it is impossible to reach its exact value. Since then, we humans have abandoned our hopes to exactly find  $\pi$  - although we still approximate  $\pi$  farther than needed to test the arithmetic power of supercomputers - and instead use different levels of approximations for different purposes. For example, a primary textbook might estimate  $\pi$  to 3.14, whilst NASA approximates it to 3.141592653589793, which is to the 15th decimal place (NASA/JPU Edu, 2016).

The derived accuracy of  $\pi$  is a very important indicator of the level of advancement of mathematics and technology of ancient civilizations: when technology advances, humans take mathematics to a higher and more abstract level that goes beyond the scope of everyday life. That leads to more accurate ways (eg. drawing diagrams and applying Pythagoras Theorem instead of actually measuring physically) to evaluate mathematical concepts. My research aims to examine the mathematical advancements of Ancient China and Ancient Greece through comparing and contrasting their methods of obtaining approximations of  $\pi$ , and the level of accuracy of those approximations.

## 1. Ancient China

As late as the Qin Dynasty, the Chinese approximated the ratio between the diameter and circumference to be 1:3, that is, approximating  $\pi$  to be 3. It wasn't until the Han dynasty that the Chinese discovered the irrationality of  $\pi$ , when mathematicians began to derive different values with their own methods (Qu, 2002). Liu Xin, an astronomer and calendar expert of the first century BCE, was said to have been one of the earliest individuals to attempt the improvement (Lam and Ang, 1997).

Liu Hui was a Chinese mathematician who made significant contributions to the field of Mathematics. He lived in the northern Wei kingdom during the 3rd century. His fame rests on publishing the commentary he completed in 263 CE, titled *Jiuzhang suanshu* (*The Nine Chapters on the Mathematical Art*) - a mathematical canon that played a similar role in the East to Euclid's *Elements* in the West. Liu's commentary on *The Nine Chapters* proved the correctness of its algorithms.

These proofs are the earliest-known Chinese proofs in the contemporary sense. However, in contrast to authors of ancient Greek mathematical texts, Liu did not set out to prove theorems so much as to establish the correctness of algorithms. For example, he rigorously proved algorithms for determining the area of circles and the volume of pyramids by dissecting the regions into infinitely many pieces. He also proved algorithms for arithmetic and algebraic operations, such as adding fractions and solving systems of simultaneous linear equations (Chemla, 2006). During the Three Kingdoms period, Liu Hui came up with the cyclotomic method (inscription of polygon inside circle) when annotating "*The Nine Chapters on the Mathematical Art*", which was a milestone of the Chinese evaluation of  $\pi$  (Qu, 2002).



Figure 4. A drawing of Liu Hui (Source: Canzonetti)

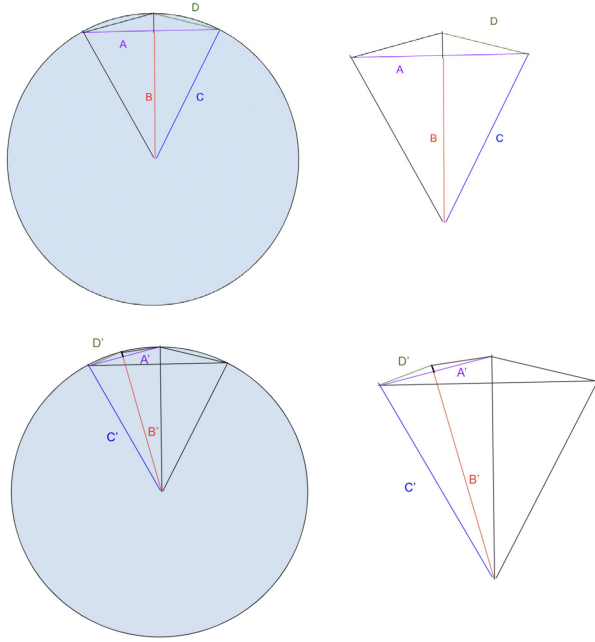


**Figure 5.** Showcase of before and after the second iteration of cyclotomic method

Figure 5 showcases the *cyclotomic method* (割圓術), the method invented by Liu Hui. When the number of sides of the inscribed polygon approaches infinity, the height of one triangle segment (the line from the center point of the polygon to the middle of one side) will approach the length of the radius of the circle. The definition of a circle is that any point of the circumference has the same distance from the center point. As the  $n$ -sided polygon is inscribed in the circle (with  $n$  being a multiple of 6), its new side length (as the number of sides double) can be obtained by Pythagoras Theorem -

$$a^2 + b^2 = c^2$$

$a$  = side of right triangle  
 $b$  = side of right triangle  
 $c$  = hypotenuse

If this process is repeated enough times, the ratio between the circumference and diameter will be close to  $\pi$ . According to Liu's principle of exhaustion, if the process is repeated long enough, eventually a polygon will be reached whose sides are so short that it will coincide with the circle. This explains why the area of the circle is the product of half the circumference and the radius. The value of 3 to 1 for the ratio of the circumference to the diameter is imprecise as this is in fact the ratio of the perimeter of the hexagon to the diameter of the circle. However, this inaccuracy was passed down from generation to generation, Liu explains, without the desire to strive for greater accuracy (Lam and Ang, 1997).

It is appreciable that after each iteration, the number of sides of the polygon increases by two fold. That means, the number of sides increases exponentially. Given that this process starts with an inscribed hexagon, the number of sides ( $n$ ) can be expressed by a formula in which " $i$ " is the number of iterations. It should be noted that Liu's cyclotomic method starts with the following prerequisites:

1. The radius of the circle is 10 units.
2. At iteration 0, a hexagon is inscribed inside the circle, with side lengths of 10 units. The section that is going to undergo the Cyclotomic method is an equilateral triangle that is one sixth of the inscribed hexagon.

What I will show is a slightly simplified version of Liu's method. He calculates the area of the rhombus by calculating the respective areas of two triangles, but as we know, it is simply the height of the rhombus. Before going further to the arithmetics, we should clearly define the variables:

- 
- $A_n$  = Side length of an  $(n/2)$  sided polygon
  - $B_n$  = Distance between circle center and the midpoint of  $A_n$
  - $C$  = 10 units (radius of circle)
  - $D_n$  = Side length of an  $n$ -sided polygon.
  - $D_6$  = 10 units
  - $\alpha_{2^i}$  = Area of the polygon after the  $(i)$ th iteration
- 

Therefore:

$$A_n = D_{0.5n}$$

$$B_n = (10^2 - (0.5A_n)^2)^{0.5}$$

$$D_n = ((0.5A_n)^2 + (10 - B_n)^2)^{0.5}$$

$$\alpha_n = (0.5)(0.5n)CA_n = 2.5nA_n$$

$$n = 6 \times 2^i$$


---

The deficit area is straightforward to calculate (the area of the polygon). The way they calculate the excess area is by  $A = A_{0.5n} + (A_n - A_{0.5n})$ , with  $n$  being the number of sides you reach. Liu Hui continued the process till  $n = 192$  (5th iteration). I am going to demonstrate the first two iterations (rounded up to 11 decimal places) below:

When  $i = 1$ :

$$\begin{aligned} C &= 10 \\ n &= 6 \times 2^1 = 12 \\ A_{12} &= D_6 = 10 \\ B_{12} &= (10^2 - (0.5(10))^2)0.5 = 8.66025403784 \\ D_{12} &= ((0.5(10))^2 + (10 - 8.66025403784)^2)^{0.5} \\ &= 5.17638090205 \\ \alpha_{12} &= (0.5)(0.5n)CA_{12} = 2.5(12)(10) = 300 \end{aligned}$$

When  $i = 2$ :

$$\begin{aligned} C &= 10 \\ n &= 6 \times 2^2 = 24 \\ A_{24} &= D_{12} = 5.17638090205 \\ B_{24} &= (10^2 - (0.5(5.17638090205))^2)^{0.5} \\ &= 9.65925826289 \\ D_{24} &= ((0.5(10))^2 + (10 - 9.65925826289)^2)^{0.5} \\ &= 5.011597044 \\ \alpha_{12} &= (0.5)(0.5n)CA_{12} = 2.5(12)(10) \\ &= 310.582854123 \end{aligned}$$

After three more iterations, Liu Hui estimated the 'deficit value' of  $\pi$  by dividing the area by the radius, which is 98157/31250. The method through which Liu Hui obtained the notation  $A_{circle}/r^2 = \pi$  is unclear, but we can take an educated guess that he did so through evaluating the area of inscribed polygons with the following steps:

1. Divide a polygon into equal slices of isosceles triangles with base length of the polygon's side length,  $L_n$ , and with the other two sides the length of the circle's radius.
2. The area of triangle is half base times height,  $h_n$ , such that  $A_{n-gon} = 0.5nL_n h_n$ . Realise that the parameter of the polygon is  $nL_n$ .
3. Realising if the sides of the polygon increases further and further, the height of the triangle will approach the circle's radius. With modern notations,  $\lim_{n \rightarrow \infty} h_n = r$ ,  $\lim_{n \rightarrow \infty} A_{n-gon} = A_{circle}$ . The parameter of the polygon will also overlap with the circumference of the circle.

4. Provided that the polygon has enough sides, approximate  $A_{n-gon} \approx 0.5nL_n r$ .
5. Hence, get the (approximate) value of half the circumference by dividing the area by the radius. As  $\pi$  is defined as the ratio between circumference and diameter, and that radius is  $0.5d$ , half the circumference divided by radius is equal to circumference divided by diameter. Therefore,  $\pi$  can be approximated by dividing a  $n$ -gon area by radius squared given that  $n$  is big enough.

The excess area is calculated as  $A_{0.5n} + (A_n - A_{0.5n})$  although there is no clear explanation, and in Liu Hui's case,  $A_{96} + (A_{192} - A_{96})$ . Overall, he obtained an inequality:

$$98157/31250 < \pi < 196419/62500$$

In decimal form:

$$3.141024 < \pi < 3.142704$$

Liu Hui's method and the accuracy of  $\pi$  was brought further by Zu Chongzhi around 200 years later. Zu Chongzhi was a Chinese astronomer, mathematician, and engineer who created the *Daming calendar* (大明曆) and found several close approximations for  $\pi$ . Like his grandfather and father, Zu Chongzhi was a state functionary. In around 462 CE he submitted a memorandum to the throne that criticised the current calendar, the *Yuanjia* (created by He Chengtian [370–447]), and proposed a new calendar system that would provide a more precise number of lunations per year and take into consideration the precession of the equinoxes. His calendar, the *Daming calendar*, was finally adopted in 510 CE through the efforts of his son, Zu Geng (Volkov, 2021).



Figure 6. Artistic recreation of Zu Chongzhi (Source: Alchetron)

Zu Chongzhi used Liu's method and inscribed a polygon up to 24576 sides (12th iteration), and obtained the following inequality (converted to decimal form for convenience):

$$3.1415926 < \pi < 3.1415927$$

It was the most advanced achievement worldwide at that time. Such precision was not surpassed until the 15th century when Al-Kashi, a native of Samarkand (now Uzbekistan), calculated  $\pi$  using a similar method. To honor Zu's great contribution to math, some foreign math historians suggested calling  $\pi$  "the rate of Zu". It is astonishing that Zu made the calculation even before the invention of the abacus, so he did all the work using nothing more than wooden counting sticks (ChinaCulture.org, 2021).

## 2. Ancient Greece

Archimedes was a renowned mathematician and scientist in Ancient Greece. While he also attempted to calculate  $\pi$ , his method was slightly different from Liu and Zu despite also using the method of exhaustion. Similar to his Chinese counterparts, Archimedes also calculated two values, between which  $\pi$  lies, using two different methods, in which are of extremely similar principles, except for whether the circle is inscribed in the polygon, or the other way round. Here, I show one of the methods:

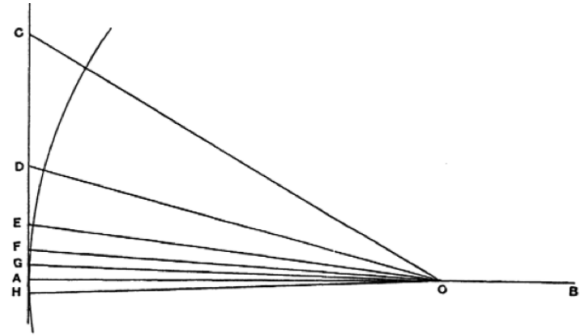


Figure 7. Diagram to excess inflict value (Source: Lennart)

1. Referring to Figure 7, the radius of the circle is  $AO$ , and length  $CH$  is the tangent of the circle at point  $A$ . Angle  $COA$  is 30 degrees, and length  $DO$  bisects angle  $COA$ .
2. According to the angle trigonometric theorem,  $CD:DA = CO:AO$ . Using the trigonometric ratios at  $\theta = 30^\circ$ , we know that  $CO:AO = 2:\sqrt{3}$ ,  $CO:CA = 1:2$ . Archimedes somehow calculated that  $2:\sqrt{3} > 265:153$ .
3. Given the ratio in step 2, we can derive that  $CD+DA:DA = (CO+AO):AO$ , and simply convert it to the form  $CA:DA = AO+CO:AO$ . Swapping terms result in  $CA:AO = AO+CO:DA$ . Using the trigonometric side ratios from step 2,  $OA:DA > 571:153$ .
4. From pythagoras theorem we know that  $DO^2 = AO^2 + DA^2$ , such that  $DO^2:DA^2 = (AO^2 + DA^2):DA^2 > 349450:23409$ .
5. Rooting the values,  $DO:DA > 591.125:153$ .
6.  $EO$  bisects angle  $DOA$ ,  $FO$  bisects angle  $EOA$ , and  $GO$  bisects angle  $FOA$ . Repeat steps 2-5 (using previously derived values) until you reach the values of  $GH$  and  $GO$ .  $GH$  is in fact one side of a 96-sided polygon.
7. Multiply  $GH$  by 96, and divide that by  $GO$ .
8. An excess value of  $22/7$  is derived.

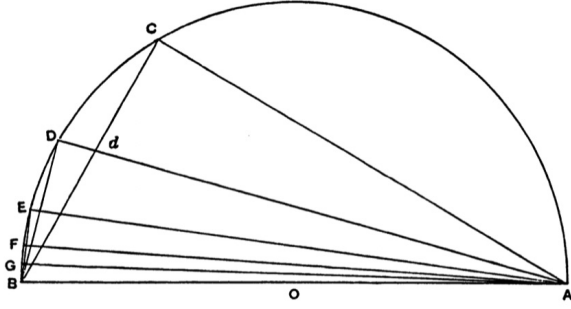


Figure 8. Diagram to evaluate deficit value (Source: Lennart)

The arithmetic principle to finding the default value is the same, except that we are inscribing the polygon in the circle. The length GB has an opposite angle of  $1.875^\circ$ , or  $\pi/96$  radians, such that it is the side length of a 96-sided polygon. Doing the right process yields a deficit value of  $223/71$ .

In summary, Archimedes obtained the following inequality (converted to decimal form for convenience):

$$3.14084507 < \pi < 3.14285714$$

### 3. Comparison and Contrast

Both Archimedes' and Liu's methods utilise the principle of exhaustion - ie. inscribing polygons with many sides in a circle, and the use of Pythagoras theorem was evident in both methods. However, Archimedes utilised special trigonometric ratios ( $\theta = 30^\circ$ ), which is not evident in Liu and Zu's work. Using Liu's method, Zu Chongzhi inscribed a 24,576-sided polygon, the number of sides much more than Archimedes' 96-sided polygon. Zu's accuracy was the best out of all three mathematicians. From Archimedes' inclusion of special trigonometric ratios and the angle bisector theorem, we can see some generalisations of maths theories amongst the Greeks through time, while the Chinese are more focused on the practicality of mathematics instead of abstract theories. That is, possibly, a reason behind the slow advancement of Chinese mathematics beyond the 17th century.

Overall speaking, the Chinese method is simpler to compute compared to the Greek, and that is one of the reasons why Liu and Zu managed to derive a more accurate value of  $\pi$  as compared with Archimedes. However, the Greek's utilisation of mathematical identities shows a fundamentally different approach from the Chinese

### 4. Modern Evaluation of $\Pi$

In modern times, we know that " $\pi$ " is irrational, which can be mathematically proven (see Appendix I for a mathematical proof of irrationality).

Although its exact value can't be reached, there are many ways to approximate  $\pi$  with modern mathematics, and the use of Taylor/Maclaurin series is one of them.

Assume a function,  $f(x)$ , can be expanded into an infinite series, with  $c$  being a constant:

$$f(x) = a_0 + a_1(x - c) + a_2(x - c)^2 + \dots + a_n(x - c)^n$$

$$f(x) = \sum_{n=0}^{\infty} a_n(x - c)^n$$

To obtain the infinite series, we need to find the coefficients  $a_n$ . Realising that differentiating  $f(x-c)$  with accordance to chain rule gives:

$$f(x) = a_0 + a_1(x - c) + a_2(x - c)^2 + \dots + a_n(x - c)^n$$

$$f'(x) = a_1 + 2a_2(x - c) + 3a_3(x - c)^2 + \dots + na_n(x - c)^{n-1}$$

$$f''(x) = 2a_2 + 6a_3(x - c) + 12a_4(x - c)^2 + \dots + n(n-1)a_n(x - c)^{n-2}$$

$$f'''(x) = 6a_3 + 24a_4(x - c) + 60a_5(x - c)^2 + \dots + n(n-1)(n-2)a_n(x - c)^{n-3}$$

...

$$f^n(x) = n! a_n$$

Now, we want to eliminate the non-constant terms. That can be done by setting  $x=c$ :

$$f(c) = a_0$$

$$f'(c) = a_1$$

$$f''(c) = 2a_2, \quad a_2 = \frac{f''(c)}{2!}$$

$$f'''(c) = 6a_3, \quad a_3 = \frac{f'''(c)}{3!}$$

$$f^n(c) = n! a_n, \quad a_n = \frac{f^n(c)}{n!}$$

Such that we can generalise that for  $n \geq 0, n \in \mathbb{Z}$ :

$$a_n = \frac{f^n(c)}{n!}$$



With  $f^n(c)$  being the  $n$ -th derivative of  $f(x)$  evaluated at  $x=c$ . Remember that  $f(x)$  was originally expressed as:

$$f(x) = \sum_{n=0}^{\infty} a_n (x-c)^n$$

Substituting the newly-derived formula into the original equation, we get the Taylor series:

$$f(x) = \sum_{n=0}^{\infty} \frac{f^n(c)}{n!} (x-c)^n$$

Maclaurin series is a special case of Taylor series, with  $c = 0$ . Hence, the expression of Maclaurin series is:

$$f(x) = \sum_{n=0}^{\infty} \frac{f^n(0)}{n!} x^n$$

Trigonometric functions with  $\pi$  typically give perfect integer values, so it is a nice idea to use the Taylor series to approximate  $\pi$ . From instinct, we can directly use trigonometric functions (eg. cosine). We can derive the Maclaurin series of cosine by first listing the derivatives of  $\cos(x)$ , evaluating at  $x=0$ :

$$f(0) = \cos(0) = 1$$

$$\frac{d}{dx} \cos(0) = -\sin(0) = 0 \quad , \quad \frac{d^2 y}{dx^2} \cos(0) = -\cos(0) = -1$$

$$\frac{d^3 y}{dx^3} \cos(0) = \sin(0) = 0 \quad , \quad \frac{d^4 y}{dx^4} \cos(0) = \cos(0) = 1$$

$$\frac{d^5 y}{dx^5} \cos(0) = -\sin(0) = 0 \quad , \quad \frac{d^6 y}{dx^6} \cos(0) = -\cos(0) = -1$$

$$\frac{d^7 y}{dx^7} \cos(0) = \sin(0) = 0 \quad , \quad \frac{d^8 y}{dx^8} \cos(0) = \cos(0) = 1$$

There are 2 patterns:

1. This pattern recurs every four times (is periodic).
2. Only terms ( $x$ ) with a power of even integers have a non-zero coefficient.

Therefore we can construct the Maclaurin series of cosine:

$$\cos(x) = \sum_{n=0}^{\infty} \frac{(-1)^n x^{2n}}{(2n)!}$$

Since we know that  $\cos(\pi)$  is -1, we can put the Maclaurin series of cosine on the right hand side, and put negative one on the left hand side, such that

$$-1 = \sum_{n=0}^{\infty} \frac{(-1)^n x^{2n}}{(2n)!}$$

With the use of technology, it is completely possible to expand the Maclaurin series of cosines to a high power and approximate  $\pi$  by finding the root. However, the solving of such a high-order polynomial requires a lot of memory, such that it is a better idea to use inverse trigonometric functions. We will use arctan as an example, as its Taylor series is easy to compute. Using its Taylor series, we can directly add all terms which approximate  $\pi$  or its fraction, given we substitute a sensible  $x$  value in  $\arctan(x)$  that equals  $\pi$  or its fraction.

Below is the derivation of arctan's series. The first derivative of arctan can simply be evaluated by the following steps:

$$y = \tan^{-1}(x)$$

$$x = \tan(y)$$

$$\frac{d}{dx} x = \frac{d \sin(y)}{dy \cos(y)} \cdot \frac{dy}{dx}$$

Applying quotient rule,  $u'/v' = (u'v - v'u)/2v^2$ :

$$1 = \frac{dy}{dx} \cdot \frac{\cos^2(y) + \sin^2(y)}{\cos^2(y)}$$

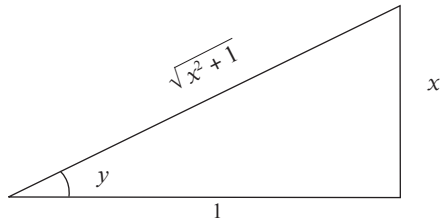
Remembering that  $\sin^2 x + \cos^2 x$  always equals 1:

$$\frac{dy}{dx} = \cos^2(y)$$

However, we want the derivative to be in terms of  $x$ , not  $y$ . Therefore, substituting  $y = \tan^{-1}(x)$ :

$$\frac{dy}{dx} = \cos^2(\tan^{-1}(x))$$

We can further simplify this with the aid of a triangle diagram:



$$\cos(y) = \frac{1}{\sqrt{x^2 + 1}}$$

$$\cos^2(y) = \frac{1}{x^2 + 1}$$

$$\tan^{-1} x = y$$

Combining terms yields:

$$\frac{d}{dx} \tan^{-1}(x) = \frac{1}{1 + x^2}$$

Now, according to the extension of binomial theorem,  $(1+x^2)^{-1}$  can be expanded into the following infinite convergent series given that  $|x| < 1$ ;

$$(1 + x^2)^{-1} = \sum_{n=0}^{\infty} (-1)^n x^{2n}$$

Since  $(1 - x^2)^{-1}$  is the 1st derivative of arctan, we simply integrate the infinite series to obtain the Taylor series for arctan (and therefore skipping the step of evaluating all those other derivatives of arctan), given that  $|x| < 1$ :

$$\begin{aligned} \tan^{-1}(x) &= \int \sum_{n=0}^{\infty} (-1)^n x^{2n} dx \\ &= \sum_{n=0}^{\infty} \frac{(-1)^n x^{2n+1}}{2n + 1} + c \end{aligned}$$

Where  $c$  is the constant of integration. However, substituting  $x=0$ ,  $\tan^{-1}(0)$  is 0. Equating left hand side and right hand side yields  $c=0$ , so therefore, the integration constant can be discarded, such that

$$\tan^{-1}(x) = \sum_{n=0}^{\infty} \frac{(-1)^n x^{2n+1}}{2n + 1} \approx x - \frac{x^3}{3} + \frac{x^5}{5} - \frac{x^7}{7} + \dots$$

Now having the equation, we can now substitute special values on left hand side that would result in a fractional  $\pi$ . Simply sum the terms on the right (the more terms, the better the accuracy), multiply it by the denominator under  $\pi$ , and thus approximate the value of  $\pi$ . Set  $x=1$ , and  $\tan(\pi/4) = 1$ . (Don't set  $x=0$ , as all the terms will become 0).

$$\pi = 4 \cdot \sum_{n=0}^{\infty} \frac{(-1)^n 1^{2n+1}}{2n + 1}$$

## 6. Comparison between Contemporary and Ancient Methods

There are fundamental differences between the ancient and contemporary methods of determining the most accurate approximate of  $\pi$ . Whilst Ancient Chinese and Greeks used methods of exhaustion, modern mathematics utilise algebraic methods and trigonometric functions to precisely evaluate digits of left hand side. Moreover, as mathematics progresses, mathematicians are able to dig deeper into the nature of  $\pi$ , by proving its irrationality with calculus. The utilisation of exhaustion methods showcases ancient understandings of the 'infinitesimal' concept, which to a large extent, amounts to an early form of integral calculus (University of British Columbia, 2021).

It is also interesting how our understanding of trigonometry broadened over centuries: in Archimedes' method, he utilised special trigonometric ratios, like  $1/2$  and  $\sqrt{3}/2$ , whilst with modern mathematics, we are able to approximate trigonometric ratios of any angle with Taylor expansions as precise as we want to, and make applications out of that.

The transition to an algebraic approach reflects the evolution of mathematics to a huge extent. For the past thousand years, Maths heavily relied on geometric computations and proofs, as late as the publication of *Summa de Arithmetica* in the 15th century (Norman, 2013). As Maths developed, however, the reliance on geometry plummeted, for computation efficiency and the inclusion of concepts, like imaginary numbers.

## Appendix I: Contemporary Exploration - Proving Irrationality



### References

- Berggren, L. *et al.* (2000).  $\pi$ : *A Sourcebook (2nd ed.)*. Springer.
- Chemla, K. (2022). Liu Hui | Chinese Mathematician | Britannica. *Encyclopædia Britannica*. [www.britannica.com/biography/Liu-Hui](http://www.britannica.com/biography/Liu-Hui).
- Lam, L.Y. and Ang, T.S. (1997). Circle Measurements in Ancient China.  $\pi$ : *A Sourcebook*, edited by Lennart Berggren, Springer, 20-35.
- Lloyd, G.E.R. (2009). What was Mathematics in the Ancient World? Greek and Chinese Perspectives. *The Oxford Handbook of the History of Mathematics*, edited by Eleanor Robson and Jacqueline A. Stedall, Oxford UP, 7-25.
- Needham, J. (1959). Evaluation of  $\pi$ . *Science and Civilisation in China. Mathematics and the Sciences of the Heavens and the Earth. Vol. III*, Cambridge UP, 99-102.
- NASA/JPL (2016). How Many Decimals of Pi Do We Really Need? *Edu News*. [www.jpl.nasa.gov/edu/news/2016/3/16/how-many-decimals-of-pi-do-we-really-need/](http://www.jpl.nasa.gov/edu/news/2016/3/16/how-many-decimals-of-pi-do-we-really-need/).
- Pacioli Issues ‘Summa de Arithmetica’, the First Great General Work on Mathematics : History of Information. *Historyofinformation.com*, 2013, [www.historyofinformation.com/detail.php?id=1711](http://www.historyofinformation.com/detail.php?id=1711).
- The Method of Exhaustion. [personal.math.ubc.ca/~cass/courses/m446-03/exhaustion.pdf](http://personal.math.ubc.ca/~cass/courses/m446-03/exhaustion.pdf).
- Volkov, A. (2022). Zu Chongzhi | Chinese Astronomer, Mathematician, and Engineer | Britannica. *Encyclopædia Britannica*, 2022, [www.britannica.com/biography/Zu-Chongzhi](http://www.britannica.com/biography/Zu-Chongzhi).

#### Images:

Canzonetti and Gentile. “Liu Hui by Elisa.gentile on Genially.” Genial.ly, Genial.ly, 23 Apr. 2021, [view.genial.ly/6083087a2766ae0d9143f458/presentation-liu-hui](http://view.genial.ly/6083087a2766ae0d9143f458/presentation-liu-hui).

“Zu Chongzhi - Alchetron, the Free Social Encyclopedia.” Alchetron.com, 25 Dec. 2017, [alchetron.com/Zu-Chongzhi](http://alchetron.com/Zu-Chongzhi).

#### Tools:

“Online LaTeX Equation Editor - Create, Integrate and Download.” Codecogs.com, 2022, [latex.codecogs.com/eqneditor/editor.php](http://latex.codecogs.com/eqneditor/editor.php).

# Working from home: how can environmental design increase productivity and morale?

Maximilian W.K. Chu

## 1. Problem

### 1.1 Analysis of a design opportunity

Due to the recent pandemic of COVID-19, 'close to 70% of the workforce in the world have been searching for alternative work environments, most of them being working from home (WFH)' (Apollo Technical, 2021). Consequently, educational sectors in Hong Kong were greatly affected. According to Vyas & Butakhieo, "85% of employees in Hong Kong were required to work at home." During this time, people are starting to face a range of issues at home, where their busy work life is brought into an environment of comfort and rest.

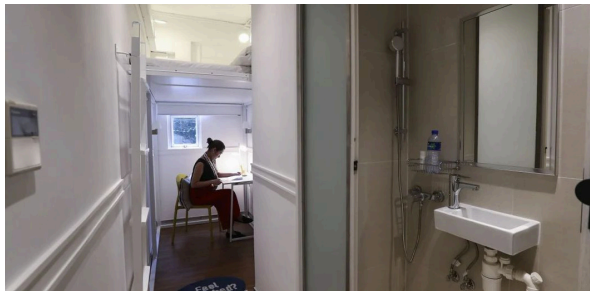


Figure 1. Employee, Nora Tam, working from home in an apartment in Hong Kong.

A percentage of people are finding it flexible and more beneficial to work at home. Stated by the FastLane Team:

*"89% of Hong Kong employees surveyed have benefited from working from home, suggesting it as a long term sustainable plan"*

This could lead to a potential long term continuation of working at home. Alongside this, it was stated that a common solution to fatigue in WFH would be 'the prioritization of self-care and the balance in one's mood and emotion' (Pocklington, 2021).



Figure 2. The increase in Hong Kong employee adoption for working from home practices.

Despite this fact, working at home may not always be the most productive method. Issues such as having a blurred line between work and family, distractions, social isolation, balance, comfort and other costs can all reduce the motivation and attitude of one's performance during work. While this issue gains more exposure due to the pandemic, it has placed a great impact on the productiveness and fatigue of individuals. According to SCMP, "85% of teachers polled this year said they felt "relatively high" or "very high" pressure at work with reasons cited including challenges brought by online classes"

On a scale of 1-5, when working at home, how easily do you get distracted?

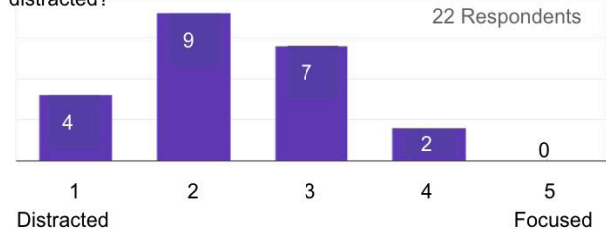
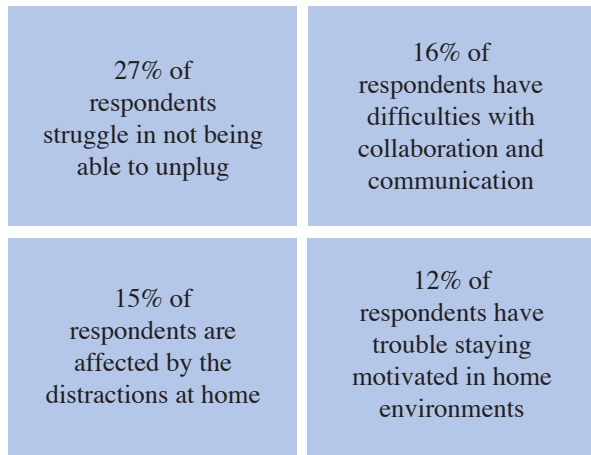


Figure 3. According to a survey by the author, 59.1% of respondents from an educational sectors found that working from home is distracting for them.



**Figure 4.** Statista online survey data: Presentation on the biggest struggles with working remotely, 2020.

## 1.2 Investigate the problem to develop a design brief

### Situation

“Over two-thirds, or 69%, of employees are experiencing burnout symptoms while working from home” (Fox, 2020) People working at home are facing issues such as distractions, demotivation, fatigue and many other effects which have caused them to work ineffectively at home. Reasons such as struggling to balance out work life or having a lack of communication has become quite a commonality in this situation.

### Goal

The goal is to help workers structure their life better, improving their scheduling and balance in life, providing ease when working from home.

- Consider meeting physio and psycho pleasures (IB Textbook)
- Have emotionally and physically interactive elements
- Provide interactive ergonomics

### Limitations/Constraints

- Research conducted will be constrained only to audiences within Hong Kong.
- Only a prototype of product is produced
- Limited access to resources at school
- Time constraint is limited

## Persona mapping

Primary Personae: Self-employed tutors confined to WFH

Secondary Personae: Members of labor force in educational sector(including teachers, mentors, admissions, etc.)

Age	26
Profession	Business Management Tutor
Income	500HKD (hourly)
Work Location	Home (transitioned from tuition firm)
Situation	Faces the issue of blurring the line between his work and family
Result	Fatigue, leading to ineffective performance

## Product

The product would seek to improve the comfort and motivation of self-employed tutors through a emotionally responsive green desk accessory concept consisting of gardening and responsive light.

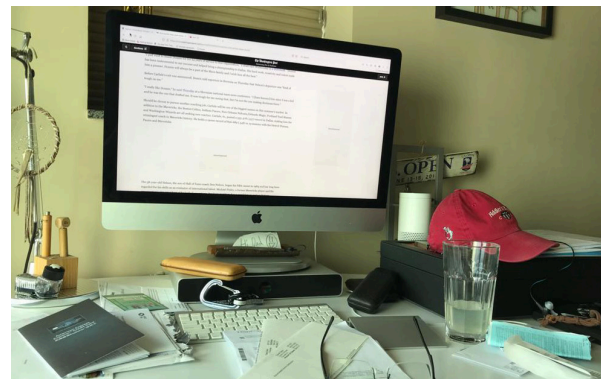




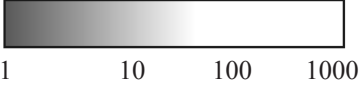

**Figure 5.** Observation of an employee’s desk while working from home, facing fatigue.


# Working from home




## 1.3 Develop a design specification

Product Analysis		
Product	Advantages	Disadvantages
Plant Container 	<ul style="list-style-type: none"> <li>• Solid and can function well by holding the plant and soil</li> <li>• Incorporates easy operation through ergonomic textured design</li> <li>• Compact and convenient for strong user efficiency</li> </ul>	<ul style="list-style-type: none"> <li>• Minimal adjustability and interactive aspects</li> <li>• Lack of aesthetic and design for emotion/pleasure</li> <li>• Material is non-recyclable and cannot meet the cradle-to-cradle philosophy (IB Textbook)</li> </ul>
Desk Organizer 	<ul style="list-style-type: none"> <li>• Strong adjustability and range of designs in holders</li> <li>• Reduced complexity in design for usability</li> <li>• Environmentally considerate through the use of biodegradable material</li> </ul>	<ul style="list-style-type: none"> <li>• Priced at 1370 HKD which can be expensive to purchase as a accessory</li> <li>• Lack of design for emotion/pleasure</li> <li>• Incorporates no elements of green in its design</li> <li>• Minimal emotional response and interaction</li> </ul>

Specification	Priority	Description	Justification
Function	2	<p>2.1: Include watering mechanic for gardening</p> <p>2.2: Mechanism for light should be adjustable</p> <p>2.3: The range of light emitted should be between 500 - 2500 lux units</p>  <p style="text-align: center;">Logarithmic scale of light intensity (units in lux)</p>	<p>2.1: A function for the input of water would hold necessary for the nurturing of the plant during its growing stages. (Bertacchi, 2020)</p> <p>2.2: Uncontrollable output of light can affect user experience and attitude as well as growth of plant.</p> <p>2.3: 500 - 2500 lux is an average output of low light indoor plants (Robinson, 2020)</p>
Aesthetic	4	<p>4.1: Design should be simplistic and cohesive</p> <p>4.2: The product's color have elements of green or white</p>  <p>4.3: Light emitted should contain a close to neutral color temperature</p>	<p>4.1: This can increase the clarity of the design allowing for an ease of use (Drouillat, 2020)</p> <p>4.2: The portrayal of green will provide a sense of nature and refreshment. "Spending time in natural green environments has been linked to stress relief, better impulse control, and improved focus." (Cherry, 2021)</p> <p>4.3: Can enhance a user's psycho-pleasure. "neutral light provides the stimulation needed to regulate human circadian rhythms, or the internal body clock" (Delaney, 2019)</p>
Safety	3	<p>3.1: The product must account for safety features such as materials and environments</p> <p>3.2: Structure should be balanced and stable</p>	<p>3.1: Hazards such as cuts and discomfort can occur during user interaction. Especially in a home environment.</p> <p>3.2: Unbalanced structure when used can cause a poor user engagement and harmful interaction through the collapsing of product.(IB Textbook)</p>
Size	6	<p>6.1: The framework of the product should be 7 x 8 inches</p> <p>6.2: Different components can vary in sizes within the framework</p>	<p>6.1: Product should have reasonable dimensions, that of which can serve as a desk accessory. "Common desk size dimensions are 48, 60, and 72 inches wide" (Randall <i>et al.</i>, 2020)</p> <p>6.2: Multiple components will need to maintain suitable proportions to assure stability.</p>

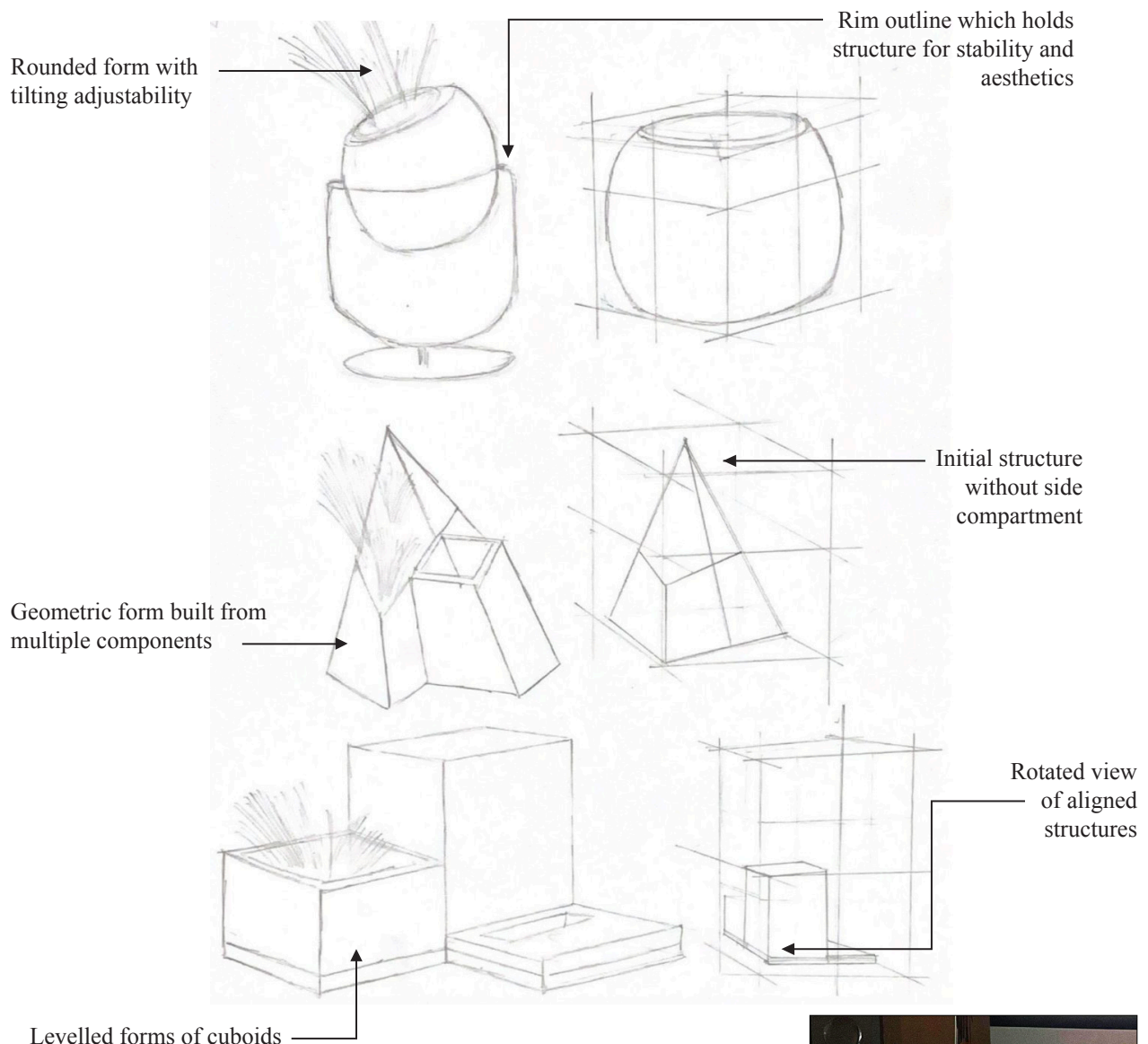
Specification	Priority	Description	Justification
Material	7	<p>7.1: Structure of product will be made out of ABS plastic (Acrylonitrile butadiene styrene)</p> <p>7.2: LED lights will be used as lighting components</p>  <p>LED Temperature gradient</p>	<p>7.1: ABS plastic is very stable and neutral to plants. “It is a thermo-plastic material, meaning it can be easily recycled” (Rogers)</p> <p>7.2: LED lights provide low usage of energy and heat, being more user-friendly for both the plant and user. “They are super-efficient, long lasting and can stimulate stronger roots, ensuring peak growth” (“How to Choose a Grow Light”, n.d.)</p>
Ergonomics	1	<p>1.1 Consist of smooth textures and clear design to meet physio and psycho pleasure and increase usability</p> <p>1.2 Planting and lighting system will be interactive through the sense of touch and visuals</p>	<p>1.1: This can meet cognitive demands, enhancing user learnability and attitude. “Surfaces, temperatures and other attributes of textures can have a significant impact on our emotions” (Oliver, 2020)</p> <p>1.2: The interactive function of the product can meet the “Attract/Converse/Transact (ACT) model (Van Gorp, Adams 2012), a framework for creating designs that improve the relations of users with a product and intentionally trigger emotional responses.” (Trumpold)</p>
Consumer	5	<p>5.1: Employees or workers who are in a home environment hindered by the unbalance in work life (secondary personae can apply to those working in remote environments)</p>	<p>5.1: Employees and workers are at the highest level of being affected by the negative implications during working at home. Their fatigue and loss of motivation leads them to a low output of work efficiency. (Intalex, 2019)</p>
Manufacturing	9	<p>9.1: Product will be made through assembly-line mass production</p> <p>9.2: The use of computer aided design (CAD) will be included in the assistance of manufacturing the design</p>	<p>9.1: Assembly-line mass production will cater to a larger demographic of users, lowering the products costs. (Trumpold)</p> <p>9.2: Will allow for prototyping and efficient visualization, providing easy testing and adjustments to model. (Trumpold)</p>



Specification	Priority	Description	Justification
Constraints	10	<p>10.1: Audiences and testing are limited to only within Hong Kong</p> <p>10.2: Only a prototype modelling of the product can be made</p> <p>10.3: There will be limited access to resources for manufacturing of the product</p>	<p>10.1: Extent of testing leads to a smaller range of data for testing and information collection.</p> <p>10.2: Prototype of modeling might have limiting implications in the products performances and effects on users.</p> <p>10.3: Certain components and materials will not be obtainable at school</p>
Environment	8	<p>8.1: Withuse a cradle to cradle approach, making it sustainable for long term use through its material</p> <div style="border: 1px solid black; padding: 10px; margin: 10px auto; width: fit-content;"> <p>Extraction of material →  Transportation →  Manufacturing →  Distribution → Use →  Reuse Recycle → Repeat</p> </div>	<p>8.1: Using a cradle-to-cradle approach can allow for a product to reach sustainability throughout its life cycle. The philosophy “centres on products which are made to be made again.” (Trumpold)</p> <div style="text-align: center;">  </div>
Cost	12	<p>12.1: The cost for this product should range between 300 - 600 HKD</p>	<p>12.1: Other similar products can amount to 700 - 4000 HKD (Click &amp; Grow Asia). 300 - 600 HKD would be a lot more modest of a price for a wider range of users. Even so, the pricing will need to take into consideration material and manufacturing processes.</p>
Market/ innovative considerations	11	<p>11.1: Indoor gardening system markets hold moderate competition</p> <p>11.2: Market could still be open for innovative opportunities</p>	<p>11.1: Indoor gardening system markets hold moderate competition</p> <p>11.2: Market could still be open for innovative opportunities</p>

## 2. Development of Ideas

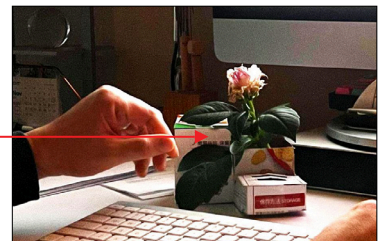
### 2.1 Initial designs



#### Specification Summary

- Enhancement of usability through considering physio and psycho pleasures
- A mechanism for light will be equipped into a component of each iteration
- Each structure consists of a wide base to maintain stability
- All designs conforms to elements of clarity and simplicity

Mock-up model for environment testing



Size and form suitable for user space



## 2.2 Developed sketches

Initial design (1)



Initial design (2)



Initial design (3)



Initial design (4)



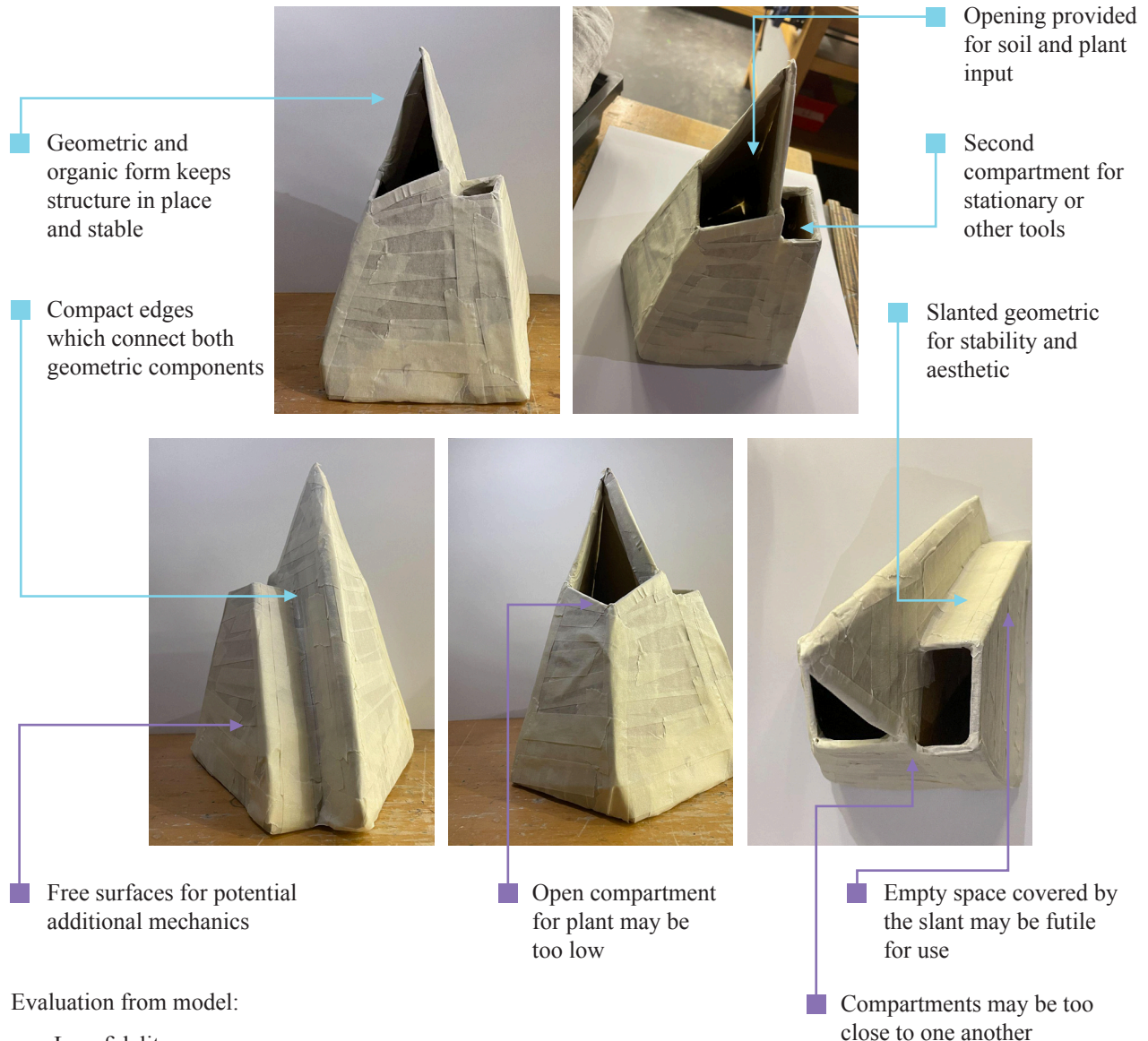
### 2.3 Initial physical modelling

Assessment of designs: (in correlation to specification)

Design 1: (4/5) | Design 2: (5/5) | Design 3: (2/5) | Design 4: (3/5)

Influence of designs (Chosen Design: Developed Design 2) Inspiration will be taken from each design:

- Design 1: Organic and simple aesthetic will be maintained and improved
- Design 3: Durability and thickness of structure will be taken into account
- Design 4: Ease of use and utilization of layers will be focused for ergonomics

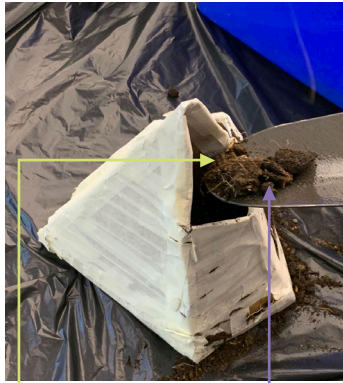


Evaluation from model:

- Low fidelity
- Account for thickness of the structure
- Consider use of material
- Examine weight with/without soil
- Be wary of free surfaces, make room for other function

Reference - ■ Specification ■ Limitations

## User interactive experience: soil application



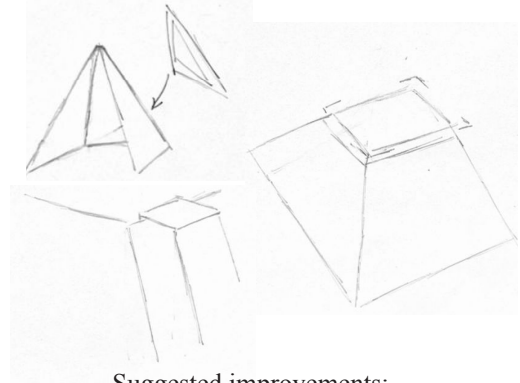
Accessible and stable compartment



Potential spilling of soil into second compartment

Suitable amount of soil fitting within compartment

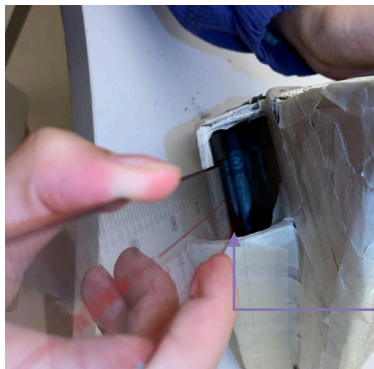
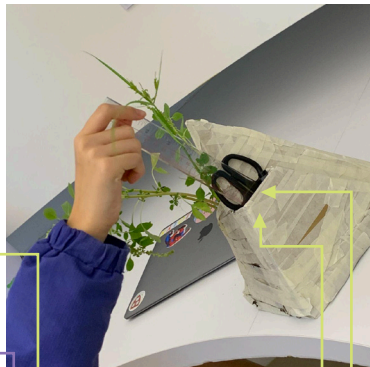
Quick Sketches in reflection of model



Suggested improvements:

- Top component is rounded at tip
- Second compartment is elevated
- Soil compartment opening is widened

## User interactive experience: planting



Product holding plants and soil

Compartment size may hinder open space for plant

Inconvenience with stationary getting stuck due to slant of compartments

Interactive use with plants and stationary within compartments

Usage of compartments are viable and durable

Product in user environment

Organic feel and sense of nature achieved

Size of model may be too high scaled

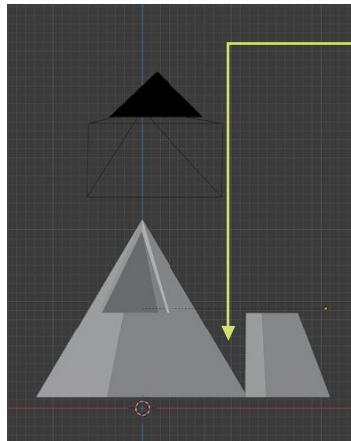
Evaluation from model:

- Provides viable user access and interaction
- Stable and feasible for withholding contents
- Fix slant component
- Be cautious over the space provided for plant
- Reconsider size to user ratio, potentially too big

Reference - ■ Observation ■ Limitations

## 2.4 3D conceptual modelling

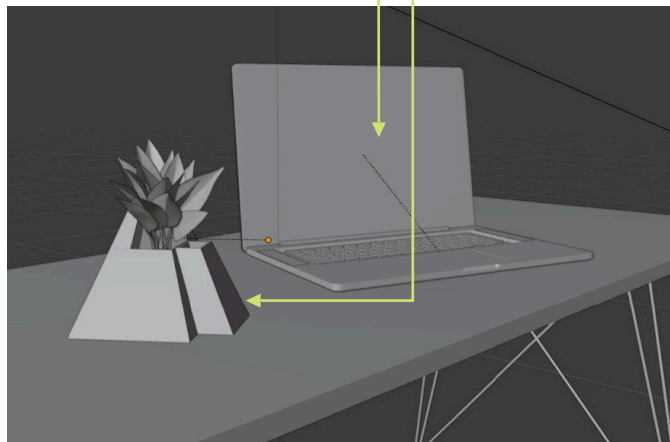
### 3D program renders



Two components are merged to form both compartments

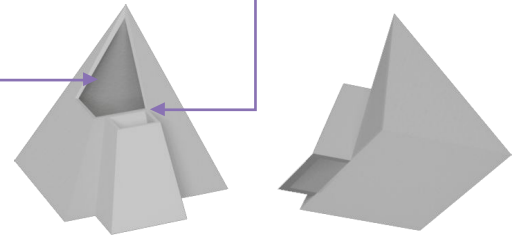
Inclusion of other environmental factors

Structure remains geometric and organic



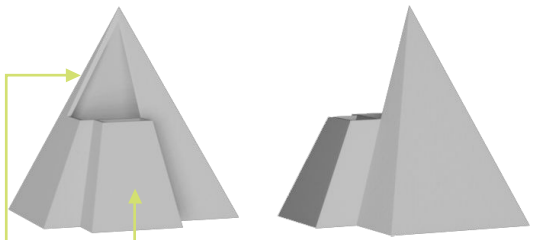
Plant compartment may hinder user experience

Compartments may still be too close to one another



Opening for plant compartment was widened

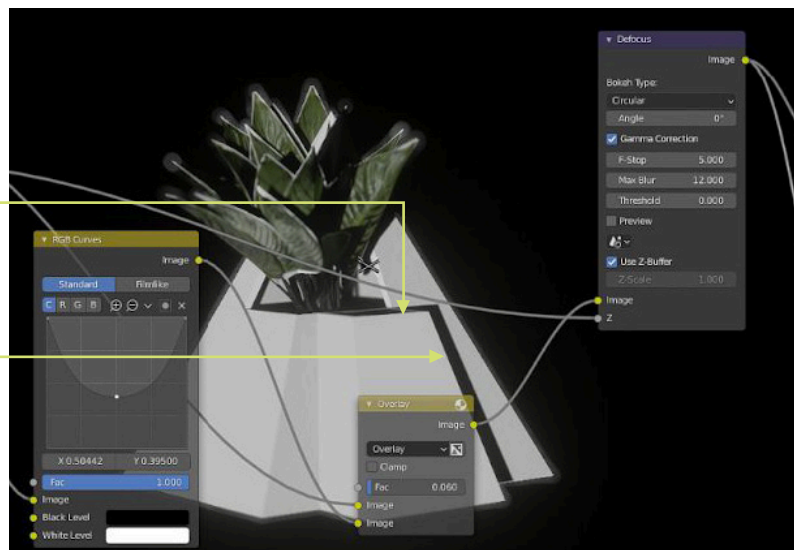
Slant of the second compartment has been moved back



### Adjustment to lighting and textures

Texture was added for ABS plastic material

Lighting was set to apply a more realistic environment

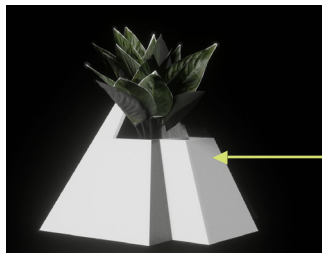


Evaluation from model:

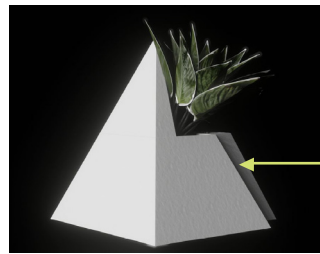
- Material testing
- Product weight
- Protection for electronic components
- Moisture resistance

Reference - ■ Observation ■ Limitations

## Model renders with plant

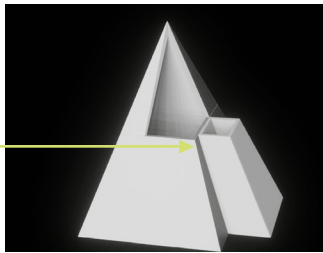


■ Flatter and more compact structure

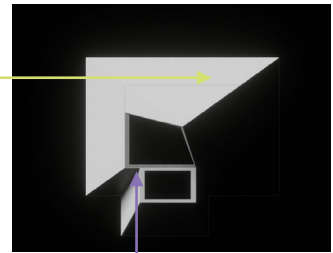


■ Symmetrical balance in sides

■ Compartment lowered for more space



■ Form of the overall structure has been changed (more rectangular)



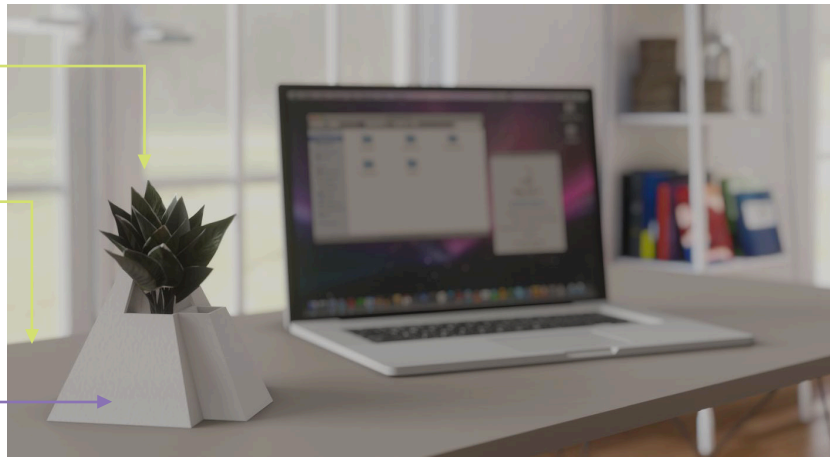
■ Compartments are still too close to one another

## Environmental renders

■ Feasible for holding plant

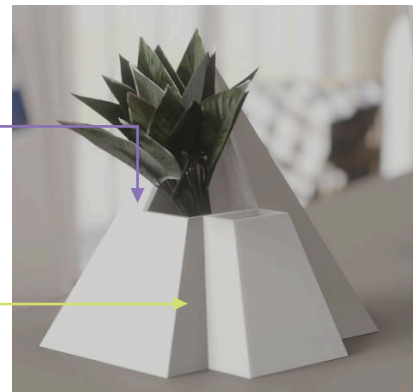
■ Meets optimal sizing for desk to product ratio

■ Instead of white, color selection can be more organic



■ Free surfaces which could be used

■ Pushed further out to create more space between compartments

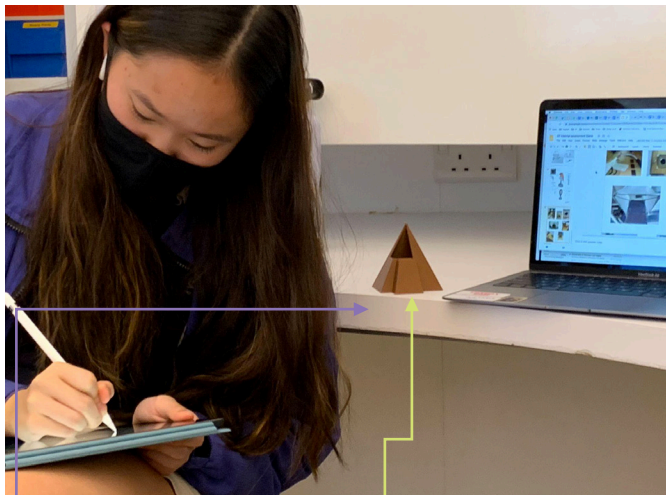


Evaluation from model:

- High fidelity (digital)
- Consider space at the top of the compartment
- Other than plastic there may be other materials to use as options
- Continue to find concepts to include onto the open surfaces

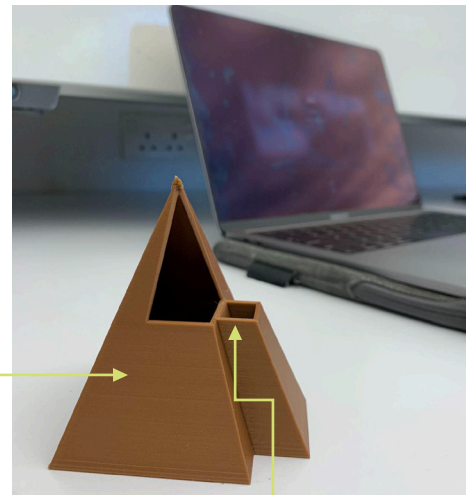
Reference - ■ Observation ■ Limitations

### 3D model prototype



Print size is scaled too small for precise user interaction

Prototype model printed through laser cutter

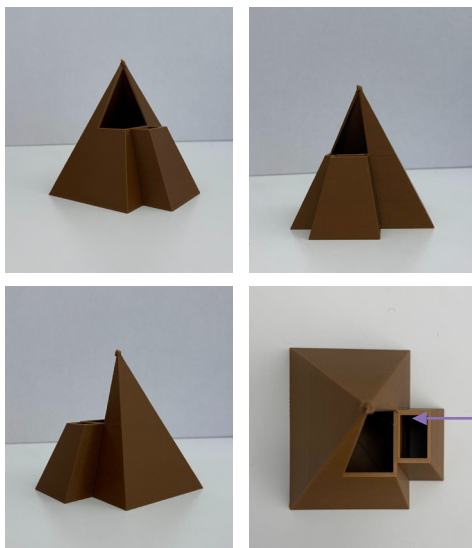


Structure and stability hold well on flat surfaces

Compartments are intact

User feedback: (Total: 2/5)

- Interactive experience provided a sense of clarity and peace in mind (+2)
- Suited the environment well, stress relieving during work (+2)
- The space of holding the plant and soil is too compact (-1)
- Top piece may be a safety hazard (-1)



User interaction with plant

Openings of compartments are too close, risk the spillage of soil



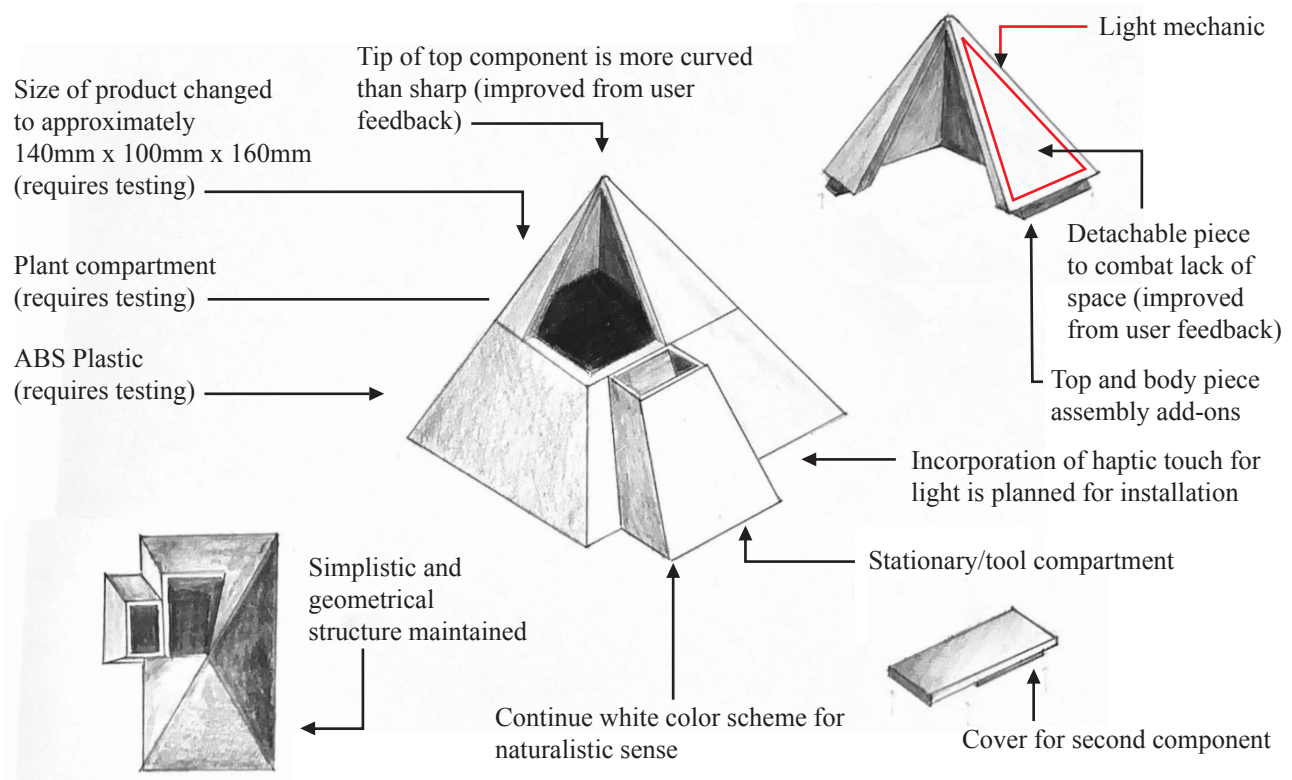
Evaluation from model:

- High fidelity (model)
- Reflect on inconsistency of soil application
- Consider top component and the space it provides for plant
- Adjust size to suitable scale

Reference - ■ Observation ■ Limitations









## 2.5 Final design



Justification	Specification	Condition
Initial Design (2) has been developed for the final design. Through the evaluation of previous models and their environmental and interactive aspects, several changes have been made. The top component of the plant compartment is now detachable. Inspired by the layer concept from initial design (4), a cover has been added to the second compartment to prevent soil spillage in advance from the user feedback provided. To enhance durability and thickness in account of design (3), the size of the product has been set to '140mm x 100mm x 160mm' being a suitable scale in cohesion with the environment. Incorporation of a haptic touch for the control of light will also be established to enhance interactive functions and user experience, making use of free surface areas. Having the user to be more connected with the product will fulfill its purpose of emotional design. With the addition of haptic technology it places the product under a niche market, allowing it to protrude with its unique functions targeted towards the educational sector. Taking into account aspects of design (1), its uses in materials and its embodiment with the feel of nature lets it meet factors such as the physio and psycho factors of the pleasure framework, enabling users to be attached to the product at use.	1.1 Meet physio and psycho pleasure and increase usability	Met
	1.2 Planting/lighting system are interactive through sense of touch and visuals	Met
	2.2: Mechanism for light will be adjustable	(In progress)
	3.1 Product will account for safety features such as materials and environments	Met
	3.2 The product's structure should be balanced and stable	Met
	4.1 Design of the product should be simplistic and cohesive	Met
	4.2 Color have elements of green or white	Met
	6.2 Different components can vary in sizes within the framework	Met
	7.1 Structure will be made out of ABS plastic (Acrylonitrile butadiene styrene)	(In progress)

### 3. Choice of Materials, Components, and Techniques

#### 3.1 Material and processes

Component	Material	Cost	Advantages	Disadvantages	Accepted/ Rejected
Light	1.1 PLWS3000C Circular LED Array	\$194.32	<ul style="list-style-type: none"> <li>Thin and flat</li> <li>Includes cool daylight tone</li> </ul>	<ul style="list-style-type: none"> <li>Exceeds size</li> <li>High cost for resize process</li> </ul>	Rejected
	1.2 LED Light Strip Ribbon 	\$203.66 per 5m	<ul style="list-style-type: none"> <li>Adjustable and meets lx range</li> <li>Eco Friendly</li> <li>Simple installation</li> <li>Cuttable and linkable</li> </ul>	<ul style="list-style-type: none"> <li>High initial cost</li> <li>Sensitive to temperature levels</li> <li>Produce fairly low light (McCloy, 2019)</li> </ul>	Accepted
	1.3 RS PRO Neutral White LED Strip 1m 12V	\$133.47	<ul style="list-style-type: none"> <li>Easy setup with flexibility</li> <li>Wide range of exposure</li> </ul>	<ul style="list-style-type: none"> <li>Non-adjustable light</li> <li>Such strong light is too excessive</li> </ul>	Rejected
Material	2.1 ABS Plastic 	\$0.5 per cubic m	<ul style="list-style-type: none"> <li>High impact resistivity</li> <li>Extensive toughness and stiffness</li> </ul>	<ul style="list-style-type: none"> <li>Low chemical resistant</li> <li>Strenuous to recycle</li> </ul>	Rejected
	2.2 PLA Plastic 	\$0.6 per cubic m	<ul style="list-style-type: none"> <li>Biodegradable</li> <li>High strength</li> <li>Water resistant</li> <li>Easily malleable</li> <li>Lightweight</li> </ul>	<ul style="list-style-type: none"> <li>Weak thermal resistance</li> <li>Fragile from strong force</li> </ul>	Accepted
	2.3 Ceramic 	\$200 per 2.85mm	<ul style="list-style-type: none"> <li>Great hardness</li> <li>Low density</li> <li>Available and inexpensive</li> <li>Surfaces are hard to stain</li> </ul>	<ul style="list-style-type: none"> <li>Tensile strength is weak</li> <li>Weak shock resistance</li> <li>Fragile and easy to crack</li> <li>Potentially heavy</li> </ul>	Rejected
Haptic	3.1 UHDK5-AA1: Ultrahaptics 	\$597.85	<ul style="list-style-type: none"> <li>Engages user experience</li> <li>High precision</li> <li>Easy accessibility</li> </ul>	<ul style="list-style-type: none"> <li>High cost</li> <li>Complex design and technology required for incorporation</li> </ul>	Accepted
	3.2 UL-SIR170-01- C-E V SIR170 Hand Tracking Module Evaluation Kit	\$1950.9	<ul style="list-style-type: none"> <li>Achieves user engagement</li> <li>Tracks movement for great accuracy</li> </ul>	<ul style="list-style-type: none"> <li>High cost</li> <li>May require high maintenance with such advanced technology</li> </ul>	Rejected
Component Protection	4 Silicone Resin Conformal Coating 	\$166.92 per 200ml	<ul style="list-style-type: none"> <li>Protects electronic components</li> <li>Resistant to moisture, humidity, heat, dust, etc.</li> </ul>	<ul style="list-style-type: none"> <li>Low abrasion resistance (Vsi Parylene, 2021)</li> <li>Mildly costly</li> <li>Time consuming from curing</li> </ul>	Accepted

Method	Tools and Materials	Advantages	Disadvantages	Accepted/ Rejected
Resin Molding	Epoxy resin injection moulding machine	<ul style="list-style-type: none"> <li>• Cost effective process</li> <li>• Flexibility with material</li> <li>• Consistent production in accuracy (Plastikcity)</li> </ul>	<ul style="list-style-type: none"> <li>• High tooling cost and time consuming</li> <li>• Limitations from design restrictions</li> </ul>	
3D Printing	3D Printer	<ul style="list-style-type: none"> <li>• Flexible designing</li> <li>• Rapid prototyping with easy accessibility</li> <li>• Cost effective and environmentally friendly (TWI)</li> </ul>	<ul style="list-style-type: none"> <li>• Part structures can delaminate under stresses (TWI)</li> <li>• Post process will be required for refinement</li> </ul>	
Fused Deposition Modeling	Filament, 3D Printer	<ul style="list-style-type: none"> <li>• Allows use for CAD</li> <li>• Suitable for PLA, ABS filaments</li> <li>• Rapid prototyping with scalability</li> </ul>	<ul style="list-style-type: none"> <li>• High qualities are hard to achieve (Games, 2020)</li> <li>• Outcomes can turn out brittle</li> </ul>	
Stereolithography	Filament, Resin printer	<ul style="list-style-type: none"> <li>• Achieves rapid prototyping with high quality and detail</li> <li>• Suitable for multi-part assembly</li> </ul>	<ul style="list-style-type: none"> <li>• With great quality comes a high cost</li> <li>• Components may turn out brittle (3d stereolithography)</li> </ul>	

Cost of materials					
Parts	Volume	Quantity	Material	Justification (linked to specification)	Cost
General Structure	12600 mm <sup>3</sup>	1	2.2 PLA plastic (Color: Organic white)	With two downsides of being fragile to strong force and having weak thermal resistance. The PLA plastic would be suitable for the modelled product, meeting specifications of being biodegradable, water resistant and having high strengths and stiffness. (spec point: 3.1, 4.2, 8.1)	\$75.6
	10800 mm <sup>3</sup>	1			\$64.8
	540 mm <sup>3</sup>	1			\$3.24
	3040 mm <sup>3</sup>	1			\$18.24
Lighting sources	960 mm <sup>3</sup>	1	1.2 LED (Color temperature: Warm)	The LED strips although having high initial cost, can be fitting to the lighting compartments as it is both cuttable and linkable. Alongside this, it has also met specifications in being eco-friendly. (spec point: 2.2, 7.2, 8.1)	\$203.66
Haptic functions	1920 mm <sup>3</sup>	1	3.1 UHDK5-AA1: Ultrahaptics	Placed at a higher price, the haptic still comes with many benefits, being a significant component for engaged user experience, improving accessibility. (spec point: 1.2, 3.1)	\$597.85
Electronic component Protection	200 ml	1	4 Conformal coating	Coating will protect electronic components, allowing resistance for moisture, dust, humidity, heat, etc.	\$166.92

### 3.2 Orthographic drawing

Component 1



Component 2



Component 3



Component 4

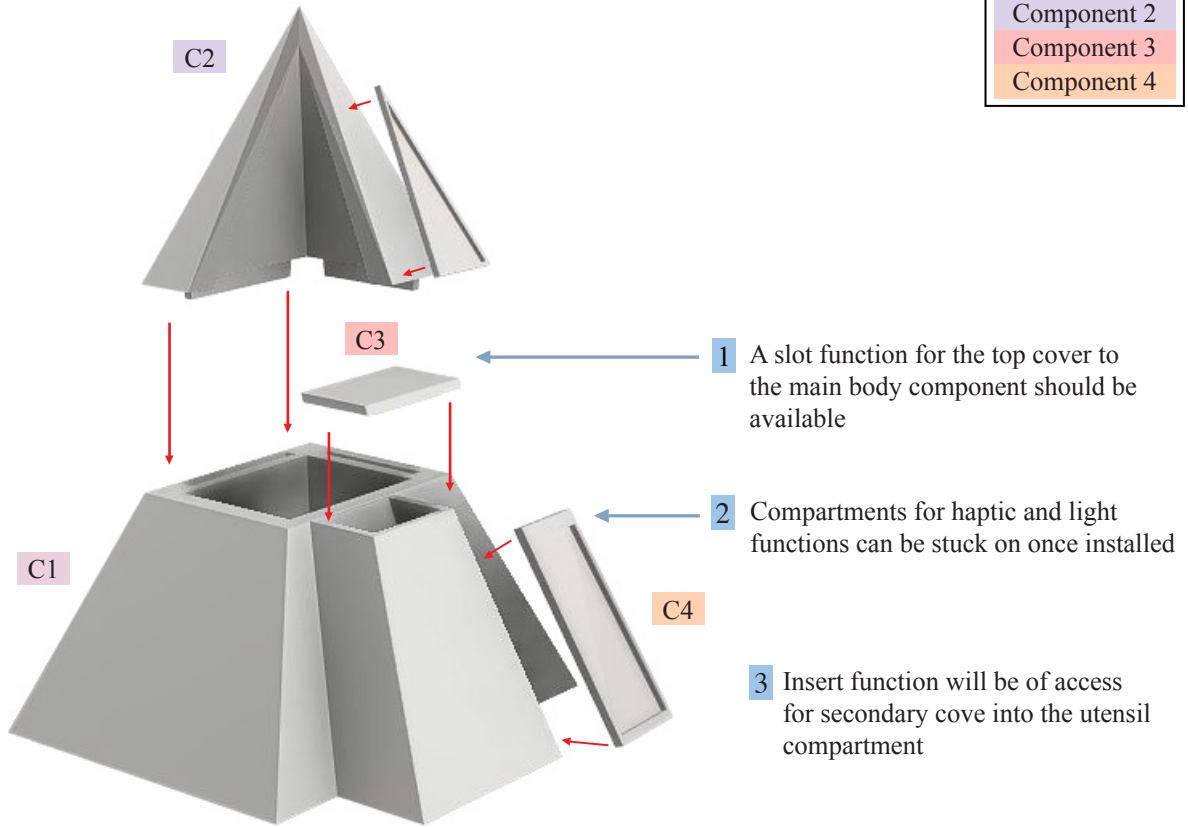


### 3.3 Plan of production

Processes	Equipment	Time	Quality Control	Risk Assessment
Finalizing prototype on CAD (4 components)	Laptop, Computer	10h	Confirm correct and accurate measurements for components	Imprecise measurements can result in delays for product development and compatibility
Adjust CAD files to print orientation and transfer to print file	Laptop, Computer	30 mins	Ensure for any printing precautions and verify printing settings	File transfers and printing precautions that are disregarded may lead to readjustments to CAD
3D Print Prototype model	Laptop, Computer, 3D printer, PLA filament	24h	Confirm placement and dimensions of PLA filament	Invalid dimensions could lead to errors throughout printing process
Post process: Excess removal after completion of printing	Model components, Sand paper, Filers	20 mins	Handle process with caution, maintain composure	The remanence on excess material on the model can hinder functionality
Post process: Refinement and sanding	Model components, Sand paper, Filers	30 mins	Remain controlled in this process, avoid uneven sanding	Inconsistent alignments in the model can affect aesthetic and user appeal
Outsourcing: LED Lighting and Ultrahaptics (Sources: LEDJUMP, Verical)	Laptop, Computer, Manufacturing list	1h	Make sure that the order is completed, processed and tracked on time	The delay in components can hinder the assembly of components
Conformal Coating process	Outsourced electric components, Conforming coat	48h	Make sure that the electronic components of the product are fully coated	Errors with the conformal coating can affect the performance of the product and harmful risks may arise
Assembly of components (refer to diagram for assembly)	Model components	20 mins	Secure each assembly for every component	Unviability in function if components do not fit, avert from forceful appliance
Examination of assembled product (refer to diagram for assembly)	Final model	10 mins	Make sure product is prepared and ready for inspection	Errors identified could cause setbacks for process, affecting time constraints

# Product assembly

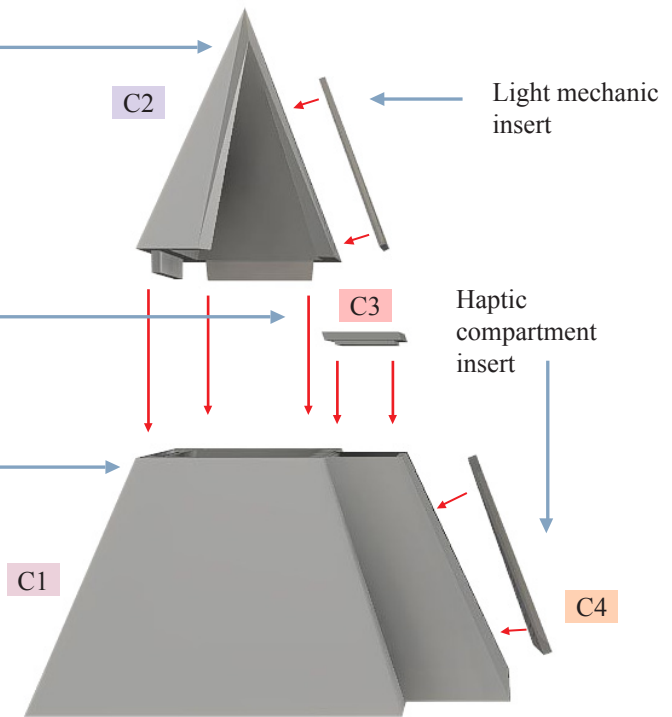
Component 1
Component 2
Component 3
Component 4



Tip will be sanded for prevention of user harm risk

Secondary cover consist of extended lengths for further ergonomics

Slot compartments included in main body for top cover to be inserted



## References

Acrylonitrile Butadiene Styrene. *Acrylonitrile Butadiene Styrene - an Overview* | ScienceDirect Topics, [www.sciencedirect.com/topics/materials-science/acrylonitrile-butadiene-styrene](http://www.sciencedirect.com/topics/materials-science/acrylonitrile-butadiene-styrene).

Advantages and Disadvantages of Stereolithography–Sla.(2017) *3d Stereolithography*. [www.3d-stereolithography.com/advantages-and-disadvantages/](http://www.3d-stereolithography.com/advantages-and-disadvantages/).

*Amazon.com*: Ledjump Bright High Power Output Lumen Flexible. [www.amazon.com/LEDJump-Bright-Flexible-2500-2700k-Dimmable/dp/B0091L0GTU](http://www.amazon.com/LEDJump-Bright-Flexible-2500-2700k-Dimmable/dp/B0091L0GTU).

Bertacchi, D. (2020). Importance of Water to Plants. *Garden Guides*, [www.gardenguides.com/78292-importance-water-plants.html](http://www.gardenguides.com/78292-importance-water-plants.html).

Brower, T. (2020). Why Working From Home Is So Exhausting- And How To Reinvigorate. *Forbes*, Forbes Magazine. [www.forbes.com/sites/tracybrower/2020/03/30/why-working-from-home-is-so-exhausting-and-how-to-reinvigorate/?sh=410a7d7f55ab](http://www.forbes.com/sites/tracybrower/2020/03/30/why-working-from-home-is-so-exhausting-and-how-to-reinvigorate/?sh=410a7d7f55ab).

Cherry, K. (2021). How Does the Color Green Make You Feel? *Verywell Mind*. [www.verywellmind.com/color-psychology-green-2795817](http://www.verywellmind.com/color-psychology-green-2795817).

Colorpalette. (2019). Nature Green Tree Color Palette. *Colorpalette.org*, [www.colorpalette.org/nature-green-tree-color-palette-5/](http://www.colorpalette.org/nature-green-tree-color-palette-5/).

Cradle to Cradle Model Offers next Step in Zero Waste. (2016) *Waste Wise Products Inc*. [www.wastewiseproductsinc.com/blog/zero-waste/cradle-to-cradle-model-offers-next-step-in-zero-waste/](http://www.wastewiseproductsinc.com/blog/zero-waste/cradle-to-cradle-model-offers-next-step-in-zero-waste/).

Cradle to Cradle.(2020) *EPEA Intl. Umweltforschung GmbH Taiwan Branch*. [www.c2cplatform.tw/en/c2c.php?Key=1](http://www.c2cplatform.tw/en/c2c.php?Key=1).

Drouillat, B. (2020). Ease of Use and Attractiveness for Interface Design. *Medium*, Designers Interactifs. [www.medium.com/designers-interactifs/ease-of-use-and-attractiveness-for-interface-design-5ea8c3394ea1](http://www.medium.com/designers-interactifs/ease-of-use-and-attractiveness-for-interface-design-5ea8c3394ea1).

EHSQ Alliance Affiliate. (2019) 7 Signs of Fatigue and How It Affects the Workplace: Posts. *Intelex Community*. [www.community.intelex.com/explore/posts/7-signs-fatigue-and-how-it-affects-workplace](http://www.community.intelex.com/explore/posts/7-signs-fatigue-and-how-it-affects-workplace).

Electronic Components and Parts Distributor. *Verical*, [www.verical.com/pd/ultrahaptics-sensor-development-tools-uhdk5-aa1-5903398](http://www.verical.com/pd/ultrahaptics-sensor-development-tools-uhdk5-aa1-5903398).

Electronics Potting and Encapsulation Services by Appli-Tec. (2020). *Appli*. [www.appli-tec.com/services/potting-and-encapsulation/](http://www.appli-tec.com/services/potting-and-encapsulation/).

FastLane Team. (2020). Infographic: Work From Home Hong Kong Survey COVID-19. *FastLane*. [www.fastlanepro.hk/work-from-home-hong-kong-infographic/](http://www.fastlanepro.hk/work-from-home-hong-kong-infographic/).

Flaherty, C. (2020). *Working from Home during COVID-19 Proves Challenging for Faculty Members*. [www.insidehighered.com/news/2020/03/24/working-home-during-covid-19-proves-challenging-faculty-members](http://www.insidehighered.com/news/2020/03/24/working-home-during-covid-19-proves-challenging-faculty-members).

Fox, M. (2020). Remote Work Burnout Is Growing as Pandemic Stretches on. Here's How to Manage It. *CNBC*. [www.cnbc.com/2020/07/28/remote-work-burnout-is-growing-as-coronavirus-pandemic-stretches-on.html](http://www.cnbc.com/2020/07/28/remote-work-burnout-is-growing-as-coronavirus-pandemic-stretches-on.html).

Goal 11: Sustainable Cities and Communities. *The Global Goals*, [www.globalgoals.org/11-sustainable-cities-and-communities](http://www.globalgoals.org/11-sustainable-cities-and-communities).

Grames, E. (2020). What Is FDM 3D Printing? – Simply Explained. *All3DP*. [www.all3dp.com/2/fused-deposition-modeling-fdm-3d-printing-simply-explained/](http://www.all3dp.com/2/fused-deposition-modeling-fdm-3d-printing-simply-explained/).

How to Choose an LED Grow Light: Gardener's Supply. *Garden Tools, Planters, Raised Garden Beds + More* | Gardener's Supply, [gardeners.com/how-to/how-to-choose-a-grow-light/5020.html](http://gardeners.com/how-to/how-to-choose-a-grow-light/5020.html).

How to Make an Impressive Website That Will Help You Sell Better. Use Emotional Purchases. *Cadabra Studio - Your Reliable Design Partner.*, [cadabra.studio/blog/how-to-make-an-impressive-website-that-will-help-you-sell-better-use-emotional-purchases](http://cadabra.studio/blog/how-to-make-an-impressive-website-that-will-help-you-sell-better-use-emotional-purchases).

India Today Web Desk. (2021). 9 Tips to Manage Stress at Work on World Day for Safety and Health at Work. *India Today*, [www.indiatoday.in/education-today/jobs-and-careers/story/9-tips-to-manage-stress-at-work-on-world-day-for-safety-and-health-at-work-1795945-2021-04-28](http://www.indiatoday.in/education-today/jobs-and-careers/story/9-tips-to-manage-stress-at-work-on-world-day-for-safety-and-health-at-work-1795945-2021-04-28).

Jain, S. (2019). Impact of Light and Color on A Customer's Mood. *innotecgroup.com/impact-of-light-and-color-on-a-customers-mood/?locale=en*.

Layceramic Ceramic Filament - 2.85mm (1kg). *MatterHackers*, [www.matterhackers.com/store/1/layceramic-ceramic-filament-285mm-1kg/sk/M7RE5J6P](http://www.matterhackers.com/store/1/layceramic-ceramic-filament-285mm-1kg/sk/M7RE5J6P).

Li, S. (2020). As Hong Kong Tenants Call the Shots, Can Work-from-Home Dent Office Market? *South China Morning Post*, [www.scmp.com/business/article/3085960/tenants-call-shots-can-work-home-inflct-more-damage-hong-kong-office](http://www.scmp.com/business/article/3085960/tenants-call-shots-can-work-home-inflct-more-damage-hong-kong-office).

Light. *Zeitgeber*, [zeitgeber.net/light/](http://zeitgeber.net/light/).

Luger. (2016) LED Light Spectrum Enhancement with Transparent Pigmented Glazes. *LED Light Spectrum Enhancement with Transparent Pigmented Glazes - LED Professional - LED Lighting Technology, A plication Magazine*. [www.led-professional.com/resources-1/articles/led-light-spectrum-enhancement-with-transparent-pigmented-glazes-by-light-spectrum-glazes](http://www.led-professional.com/resources-1/articles/led-light-spectrum-enhancement-with-transparent-pigmented-glazes-by-light-spectrum-glazes).

McCloy, J. (2019). Pros and Cons of LED Lighting: Should You Use Them? *GreenCoast*. [www.greencoast.org/pros-and-cons-of-led-lighting/](http://www.greencoast.org/pros-and-cons-of-led-lighting/).

Mlitz, K. (2021). Remote Work Prior to COVID-19 Worldwide 2020. *Statista*. [www.statista.com/statistics/1220141/remote-work-prior-covid-worldwide/](http://www.statista.com/statistics/1220141/remote-work-prior-covid-worldwide/).

Mlitz, K. (2021). Struggles with Working Remotely 2021. *Statista*. [www.statista.com/statistics/1111316/biggest-struggles-to-remote-work/](http://www.statista.com/statistics/1111316/biggest-struggles-to-remote-work/).

Mok, D. (2020). Nightmares, More Stress, Nowhere to Hide: the Strain of 'Zoom Fatigue'. *South China Morning Post*. [www.scmp.com/news/hong-kong/health-environment/article/3081314/bad-dreams-more-stress-and-nowhere-hide-zoom](http://www.scmp.com/news/hong-kong/health-environment/article/3081314/bad-dreams-more-stress-and-nowhere-hide-zoom).

Oliver, R. (2020). The Power of Touch: How Do Textures Affect Our Emotions? *Truly Experiences Blog*, [www.trulyexperiences.com/blog/textures-emotions/](http://www.trulyexperiences.com/blog/textures-emotions/).

Philips, M. (2017). Design for Emotion to Increase User Engagement. *Toptal Design Blog*, Toptal. [www.toptal.com/designers/product-design/design-for-emotion-to-increase-user-engagement](http://www.toptal.com/designers/product-design/design-for-emotion-to-increase-user-engagement).

Pla vs ABS vs Nylon. *Markforged*, [www.markforged.com/resources/blog/pla-abs-nylon](http://www.markforged.com/resources/blog/pla-abs-nylon).

- Plessey PLWS3000CA84000, PLWS3000C Circular Led Array, 42 Neutral White Led (4000k). Plessey PLWS3000CA84000, PLWS3000C Circular LED Array, 42 Neutral White LED (4000K) | RS Components, [www.hken.rs-online.com/web/p/led-circular-arrays/1696965](http://www.hken.rs-online.com/web/p/led-circular-arrays/1696965).
- Plessey PLWS3000CB83000, PLWS3000C Circular Led Array, 42 White Led (3000k). Plessey PLWS3000CB83000, PLWS3000C Circular LED Array, 42 White LED (3000K) | RS Components, [hken.rs-online.com/web/p/led-circular-arrays/1696962](http://hken.rs-online.com/web/p/led-circular-arrays/1696962).
- Pocklington, A. (2021). How To Successfully Conquer Working-From-Home Fatigue. *Forbes*. [www.forbes.com/sites/forbescommunicationscouncil/2021/01/21/how-to-successfully-conquer-working-from-home-fatigue/?sh=607e9698731e](http://www.forbes.com/sites/forbescommunicationscouncil/2021/01/21/how-to-successfully-conquer-working-from-home-fatigue/?sh=607e9698731e).
- Randall, S. (2020). Standard Desk Dimensions & Layout Guidelines (with Photos). *Upgraded Home*. [www.upgradedhome.com/desk-dimensions/](http://www.upgradedhome.com/desk-dimensions/).
- Robinson, P. (2020). How Much Light Do My Indoor Plants Need? *PlantMaid*. [www.plantmaid.com/how-much-light-do-my-indoor-plants-need/](http://www.plantmaid.com/how-much-light-do-my-indoor-plants-need/).
- Trumpold, R. Design Tech for IB Students. *Design Technology*, [ruthtrumpold.id.au/destech/](http://ruthtrumpold.id.au/destech/).
- UL-SIR170-01-C-EV by Ultraleap - Arrow.com. *UL-SIR170-01-C-EV - Ultraleap*. [www.arrow.com/en/products/ul-sir170-01-c-ev/ultraleap](http://www.arrow.com/en/products/ul-sir170-01-c-ev/ultraleap).
- Ultimaker Polypropylene Filament - 2.85mm (0.5kg). *MatterHackers*. [www.matterhackers.com/store//ultimaker-polypropylene-filament-300mm/sk/MMFT177W](http://www.matterhackers.com/store//ultimaker-polypropylene-filament-300mm/sk/MMFT177W).
- Vyas, L., & Nantapong B. The Impact of Working from Home during COVID-19 on Work and Life Domains: an Exploratory Study on Hong Kong. *Taylor & Francis*, [tandfonline.com/doi/full/10.1080/25741292.2020.1863560](http://tandfonline.com/doi/full/10.1080/25741292.2020.1863560).
- What Are the Advantages and Disadvantages of 3D Printing? *TWI*. [www.twi-global.com/technical-knowledge/faqs/what-is-3d-printing/pros-and-cons](http://www.twi-global.com/technical-knowledge/faqs/what-is-3d-printing/pros-and-cons).
- What Are the Advantages and Disadvantages of Ceramic? - 09scigthekacassite. (2019). *Google Sites*, [sites.google.com/site/thekacassite/ceramic/what-are-the-advantages-and-disadvantages-of-ceramic](https://sites.google.com/site/thekacassite/ceramic/what-are-the-advantages-and-disadvantages-of-ceramic). "What Are the Advantages and Disadvantages of Injection Moulding?" *PlastikCity Blog*. [www.plastikcity.co.uk/blog/advantages-disadvantages-of-injection-moulding/](http://www.plastikcity.co.uk/blog/advantages-disadvantages-of-injection-moulding/).
- Williamson, C. (2015). Desk Accessories Made of Cork and Aluminum. *Design Milk*. [design-milk.com/niu-desk-accessories-made-cork-aluminum/](http://design-milk.com/niu-desk-accessories-made-cork-aluminum/).
- Wood, C. (2021). Why Gardening Is Good for Your Mind as Well as Your Body. *The Conversation*. [theconversation.com/why-gardening-is-good-for-your-mind-as-well-as-your-body-50094](http://theconversation.com/why-gardening-is-good-for-your-mind-as-well-as-your-body-50094).
- Work-at-Home After COVID-19-Our Forecast. (2020). *Global Workplace Analytics*. [www.globalworkplaceanalytics.com/work-at-home-after-covid-19-our-forecast](http://www.globalworkplaceanalytics.com/work-at-home-after-covid-19-our-forecast).
- Rogers, T. (2014). All You Need to Know about Polypropylene. Part 2. *ALL YOU NEED TO KNOW ABOUT POLYPROPYLENE*. Part 2. [www.creativemechanisms.com/blog/all-you-need-to-know-about-polypropylene.-part-2](http://www.creativemechanisms.com/blog/all-you-need-to-know-about-polypropylene.-part-2).
- Rogers, T. (2015). *Everything You Need to Know About ABS Plastic*. [www.creativemechanisms.com/blog/everything-you-need-to-know-about-abs-plastic](http://www.creativemechanisms.com/blog/everything-you-need-to-know-about-abs-plastic).
- RS pro 1.75mm White ABS 3D Printer Filament, 1kg. *RS PRO 1.75mm White ABS 3D Printer Filament, 1kg* | RS Components, RS PRO, [hken.rs-online.com/web/p/3d-printing-materials/8320315](http://hken.rs-online.com/web/p/3d-printing-materials/8320315).
- RS pro 1.75mm White Pla 3D Printer Filament, 300G. *RS PRO 1.75mm White PLA 3D Printer Filament, 300g* | RS Components, RS PRO. [hken.rs-online.com/web/p/3d-printing-materials/8320400](http://hken.rs-online.com/web/p/3d-printing-materials/8320400).
- RS pro Neutral White Led Strip 1M 12V. *RS PRO Neutral White LED Strip 1m 12V* | RS Components, RS PRO. [hken.rs-online.com/web/p/led-strip-lights/1533639](http://hken.rs-online.com/web/p/led-strip-lights/1533639).
- RS pro Transparent Silicone Resin Conformal Coating, 200 MI Aerosol, -70°C Min, +200°C Max. *RS PRO Transparent Silicone Resin Conformal Coating, 200 MI Aerosol, -70°C Min, +200°C Max* | RS Components, [hken.rs-online.com/web/p/conformal-coatings/0494714](http://hken.rs-online.com/web/p/conformal-coatings/0494714).
- Salman, A. (2019). Haptic Technology - Feedback, Devices, Working Principle, Applications. *Electricalfundablog.com*. [www.electricalfundablog.com/haptic-technology/](http://www.electricalfundablog.com/haptic-technology/)
- Smart Indoor Garden Systems Market Size, Trends and Forecast -2027. *Allied Market Research*, [alliedmarketresearch.com/smart-indoor-garden-systems-market-A09426](http://alliedmarketresearch.com/smart-indoor-garden-systems-market-A09426).
- South China Morning Post. Hong Kong Teachers Are More Stressed Because of Covid-19 than the Protests. *Young Post*, [scmp.com/yp/discover/news/hong-kong/article/3114153/coronavirus-hong-kong-teachers-more-stressed-during](http://scmp.com/yp/discover/news/hong-kong/article/3114153/coronavirus-hong-kong-teachers-more-stressed-during).
- Statistics On Remote Workers That Will Surprise You. (2021). *Apollo Technical LLC*. [apollotechnical.com/statistics-on-remote-workers/](http://apollotechnical.com/statistics-on-remote-workers/).
- Sullivan, E.J. (2021). Covid Lockdowns Turned Buying Plants into the next Big Pandemic Trend — for Good Reason, *THINK*. [www.nbcnews.com/think/opinion/covid-lockdowns-turned-buying-plants-next-big-pandemic-trend-good-ncna1256223](http://www.nbcnews.com/think/opinion/covid-lockdowns-turned-buying-plants-next-big-pandemic-trend-good-ncna1256223).
- The Essential Conformal Coating Comparison Guide. (2021). *VSi Parylene*. [vsiparylene.com/the-essential-conformal-coating-comparison-guide/](http://vsiparylene.com/the-essential-conformal-coating-comparison-guide/).
- The Smart Garden 3. *Click & Grow Asia*, [asia.clickandgrow.com/products/the-smart-garden-3](http://asia.clickandgrow.com/products/the-smart-garden-3).
- Times of India. (2021). Coronavirus Symptoms: Extreme Fatigue and Weakness Could Be Signs of Covid-19, Here's What You Need to Know." *The Times of India*, Times of India. [www.timesofindia.indiatimes.com/life-style/health-fitness/health-news/coronavirus-symptoms-extreme-fatigue-and-weakness-could-be-signs-of-covid-19-heres-what-you-need-to-know/photostory/82290296.cms](http://www.timesofindia.indiatimes.com/life-style/health-fitness/health-news/coronavirus-symptoms-extreme-fatigue-and-weakness-could-be-signs-of-covid-19-heres-what-you-need-to-know/photostory/82290296.cms).
- Trinklein, D.H. Lighting Indoor Houseplants. *University of Missouri Extension*, [extension.missouri.edu/publications/g6515?\\_\\_cf\\_chl\\_jschl\\_tk\\_\\_=pmd\\_63e86f3f1d2b28974c792980cd860ecc7f7a8e5c-1627229412-0-gqNtZGzNAiKjcnBszQii](http://extension.missouri.edu/publications/g6515?__cf_chl_jschl_tk__=pmd_63e86f3f1d2b28974c792980cd860ecc7f7a8e5c-1627229412-0-gqNtZGzNAiKjcnBszQii).



---

# Characterisation of three strains of *Escherichia coli* isolated from the Equine Gut

Selina W. Y. Hui

---

## Abstract

Antimicrobial resistance (AMR) is a growing global problem as it makes infections harder to treat in both humans and animals (Ventola, 2015). The extensive use of antibacterial agents and antibiotics in human and veterinary medicine (and especially in certain types of intensive farming) enriches for resistant bacterial strains. This project examined *Escherichia coli* strains isolated from horses in Hong Kong to determine their susceptibility to antibiotics and to establish the nature and distribution of AMR genes. Three isolates were characterized with complete genomic sequences that enabled both chromosomes and plasmids to be compared. They came from two different horses: the first was isolated from an older horse undergoing long-term treatment for a persistent bacterial infection; and, the second from a recent import from the UK, treated briefly for a respiratory infection that appeared during transport. While the presence of tetracycline-resistance genes seemed consistent with recent or ongoing treatment, a closely associated group of four AMR genes, *sul2*, *aph(3'')-I*, *aph(6)-Id*, and *dfrA17* could not be explained by previous exposure and the group was found to be highly mobile.

---

## Introduction

Antibiotic resistance is increasingly spreading worldwide in communities and is a dire threat to human health because it makes infections more difficult to treat in both humans and animals (Ventola, 2015). The extensive use of antibiotics in human and veterinary medicine (and especially in certain types of intensive farming) enriches for resistant bacterial strains. Tetracycline is a class of broad-spectrum antibiotics used to treat a number of bacterial infections. For example, China has largely reduced the consumption of antibiotics in the agricultural sector (administered to animals) by 57% between 2014 and 2018, to less than 30,000 tonnes (Schoenmakers, 2020).

*Escherichia coli* is a Gram-negative, coagulase-negative, facultative anaerobic enterobacterium commonly found in the guts of most warm-blooded animals (Lim *et al.*, 2010). Even though it was one of the first fully-characterized bacteria, there is far less research into *E. coli* from non-human sources, especially the tracking of the dynamics of resistance-gene transfer within an individual and its effects in a community.

*Escherichia coli* can be readily isolated using selective media (Lupindu, 2017), hence it can serve as an indicator

species not only for levels of antibiotic resistance within the gut microbiome but also as a window on the types and range of antibiotic resistance genes present.

The genomic comparison of the three horse *E. coli* isolates detailed here illustrates that a number of resistance genes are transferred between bacteria and their hosts. The genes were partly due to the oxytetracycline treatment of the host, while others were transferred with a plasmid via bacterial conjugation or via those involving mobile elements.

## 1. Method

### 1.1 Sample collection from subjects and screening

Faecal samples were collected from horses that were housed in the same stable in Hong Kong. 1 g of each sample was suspended in 9 mL of 0.9% w:v sterile saline (to give a 10% w:v suspension), with serial dilution in saline to give 0.01% and 0.001% w:v solutions. 1 mL of each diluted extract was applied to a 3M Petrifilm™ *E. coli*/coliform plate, on which *E. coli* appears as blue colonies with gas bubbles. Colonies were counted in order to compare the relative concentrations of *E. coli*. 16 colonies were also picked and transferred initially to a grid on McConkey agar.

---

The above article is a culmination of research undertaken at ISF's Molecular Biology Laboratory, and is a modification of a Genome announcement, currently in submission.

## 1.2 Isolation and passaging

Selected colonies from the MacConkey agar plates were passaged on Luria agar plates at least 10 times (all with aerobic incubation overnight at 37 °C) to obtain pure isolates. Isolates were also tested for antibiotic susceptibility (assessed by growth on agar containing 0.01% w:v ampicillin, kanamycin, augmentin, and tetracycline).

## 1.3 DNA extraction and tests

Three isolates were selected for sequencing and genomic DNA was extracted using the Invitrogen PureLink® Genomic DNA Mini Kit and then submitted for sequencing via the Illumina MiSeq platform to generate complete sequences. NCBI BLAST and autoMLST were used for identification (Johnson *et al.*, 2008). PATRIC (Wattam *et al.*, 2016) and Proksee (<https://proksee.ca/>) were used to identify presumed plasmid sequences and create circular plasmid maps. Antibiotic resistance genes were identified using Resistance Gene Identifier (RGI) 5.2.1 at the Comprehensive Antibiotic Resistance Database (CARD) (Alcock *et al.*, 2020).

## 2. Results and Discussion

### 2.1 Characterisation of three *E. coli* isolates

Using PATRIC, all three isolates were identified as strains of *E. coli*. Sequencing data for the three isolates are shown in Table 1.

	SWYH.B349aT	SWYHX138.33gt	SWYHX138.261ft
Total sequence length	4,918,847 bp	4,613,682 bp	4,613,682 bp
GC content	51.61%	50.82%	50.86%
Long reads	13,443	9,629	12,620
Short-read contigs	179	140	113
Total aligned bases	345,619,563 bp	348,014,259 bp	349,150,667 bp
Genome coverage	70.0x	70.0x	74.0x
Circular chromosome	4,800,990 bp	4,695,496 bp	4,710,641 bp
Circular plasmid 1	109,860 bp	76,063 bp	90,138 bp
Circular plasmid 2	5,969 bp	6,821 bp	6,821 bp
Circular plasmid 3	2,028 bp		

**Table 1.** Complete genomes of three equine gut *E. coli* isolates were generated by the hybrid assembly.

## Antimicrobial resistance and AMR genes

SWYH.B349aT is an isolate recovered from a 22-year-old Thoroughbred horse (gelding) under long-term treatment for a persistent sinonasal infection. The isolate showed unrestricted growth in the presence of tetracycline, augmentin, ampicillin, and kanamycin. CARD identified numerous AMR genes, including *tetR*, *tetB* and *tetC* (tetracycline resistance); *aph(3'')-I* and *aph(6)-Id* (aminoglycoside resistance); *sul2* (sulfonamide resistance); and, *dfrA17* (diaminopyrimidine/Trimethoprim resistance). It also contains the mercuric resistance operon *merRTPCADE*.

SWYHX138.261ft and SWYHX138.33gt are isolates recovered from a 4-year-old Thoroughbred cross (gelding) recently imported to Hong Kong from the UK. SWYHX138.261ft was from a sample collected immediately after release from quarantine, where the horse had received a 5-day treatment with oxytetracycline for a respiratory infection acquired during transport. SWYHX138.33gt was recovered from the same horse five weeks later.

Both SWYHX138.261ft and SWYHX138.33gt grew well in the presence of tetracycline. While an IncF plasmid in SWYHX138.261ft contains *tetA-tetR*, these genes are not present in SWYHX138.33gt. Instead, the *AcrAB-TolC* efflux pump, which is present in both, is likely to confer resistance to tetracycline here (Chetri *et al.*, 2019).

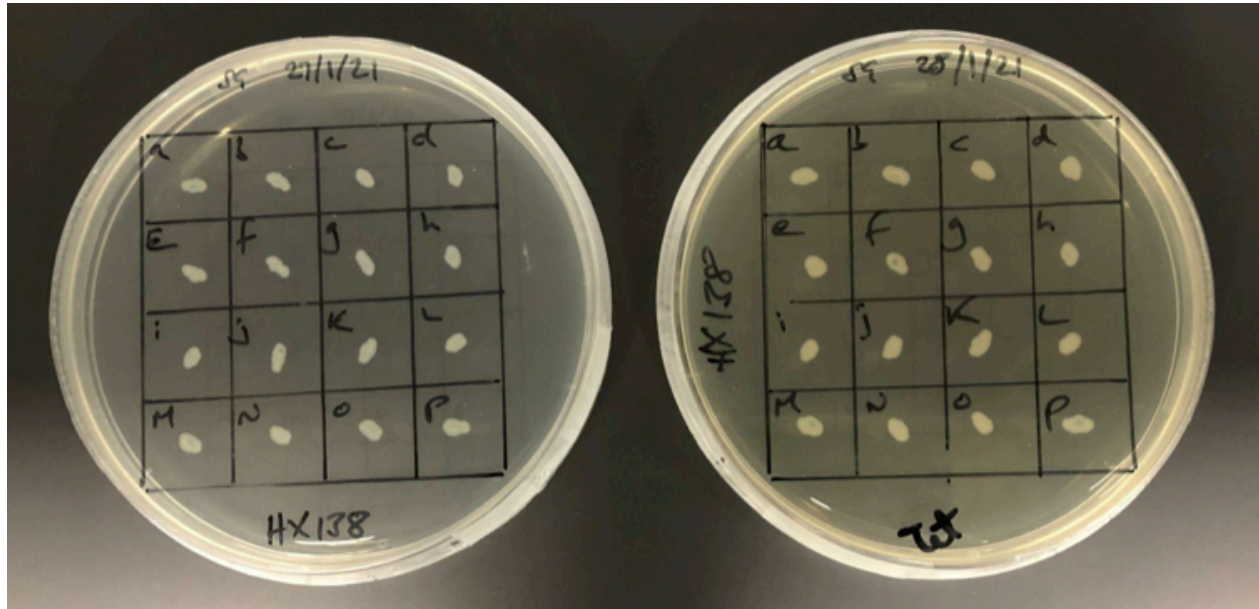


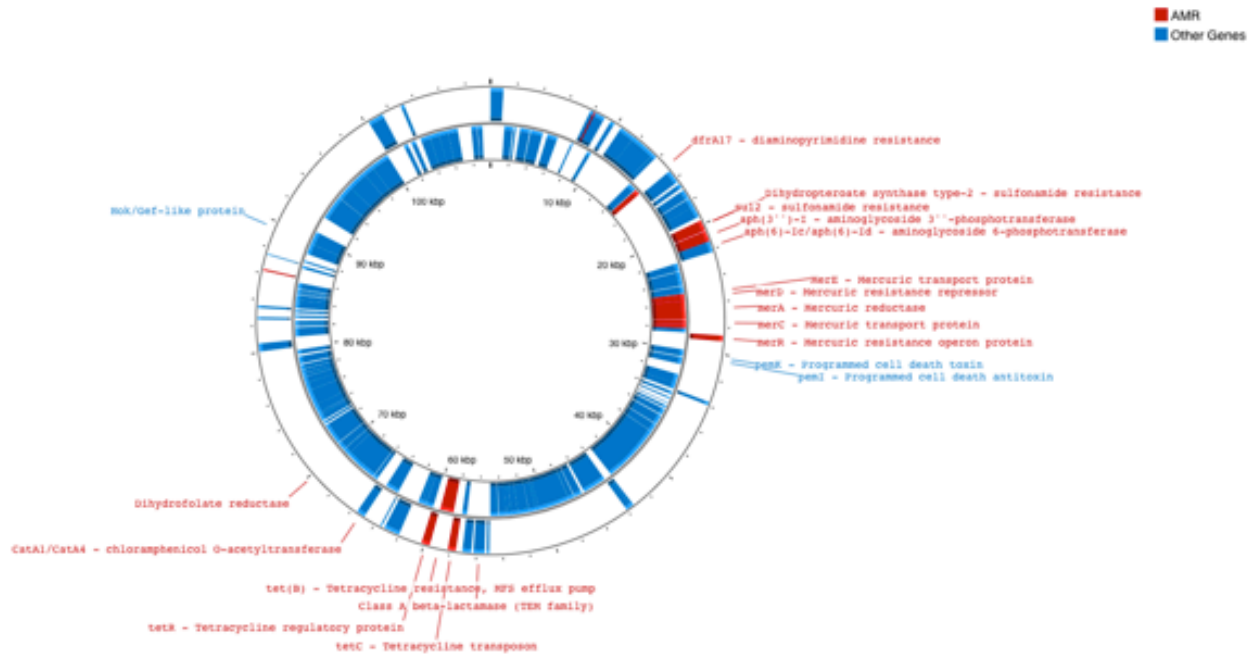
**Figure 1.** Sixteen *E. coli* isolates were recovered from the young gelding on 26 Jan. 2021, shortly after his release from quarantine. They are shown on Luria agar (left) and on Luria agar containing 0.01% w/v tetracycline (right). At this time all recovered isolates showed resistance to tetracycline.

### Plasmids

AMR-bearing plasmids are present in all three isolates. Plasmid pSWYH.B349aT (109,860 bp) carries multiple resistance genes; plasmid pHX138.261ft\_1 carries only *tetR-tetA*; and, the small 6,821 bp plasmid, carried by both HX138.261ft and HX138.33gt, contains four genes that appear to be well distributed, *sul2*, *aph(3'')-I*, *aph(6)-Id* and *dfrA17*, since they are also contained within pSWYH.B349aT.

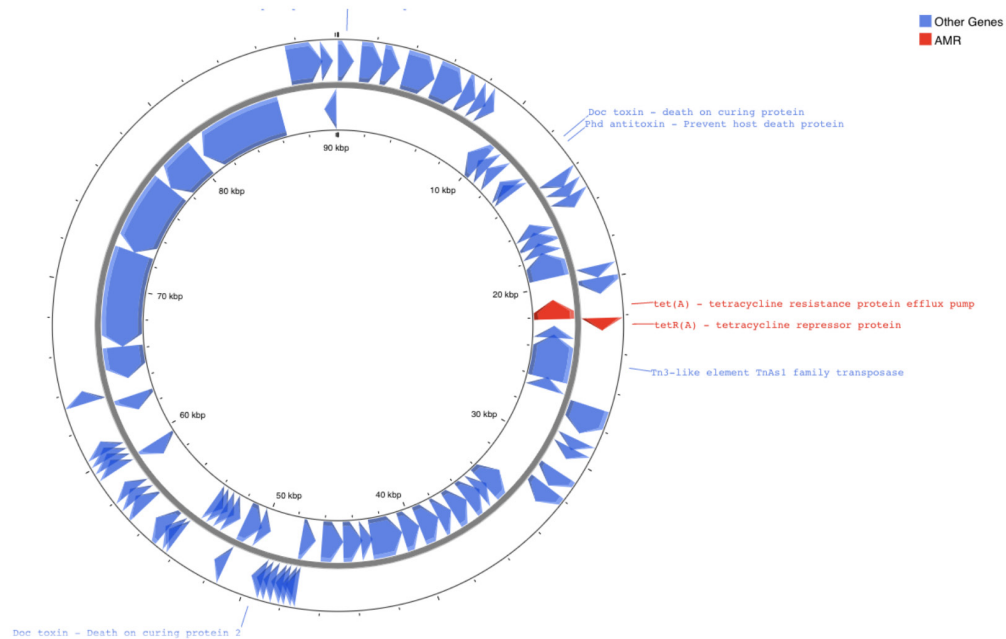
plasmid pSWYH.B349aT	plasmid pHX138.261ft_1	plasmid pHX138.261ft_2	plasmid pHX138.33gt_2
109,860 bp	90,138 bp	6,821 bp	6,821 bp
<i>macAB</i> <i>tetR-tetB</i> <i>tetC</i> <i>sul2</i> <i>aph(3'')-I</i> <i>aph(6)-Id</i> <i>dfrA17</i> <i>merRTPCADE</i> <i>bla-TEM</i> <i>catA1</i>	<i>tetR-tetA</i> <i>tetA</i>	<i>sul2</i> <i>aph(3'')-I</i> <i>aph(6)-Id</i> <i>dfrA17</i>	<i>sul2</i> <i>aph(3'')-I</i> <i>aph(6)-Id</i> <i>dfrA17</i>

**Table 2.** AMR-bearing plasmids in the three *E. coli* isolates. pHX138.261ft\_2 and pHX138.33gt\_2 are identical and pSWYH.B349aT incorporates the AMR genes of the small plasmid (shown in red).



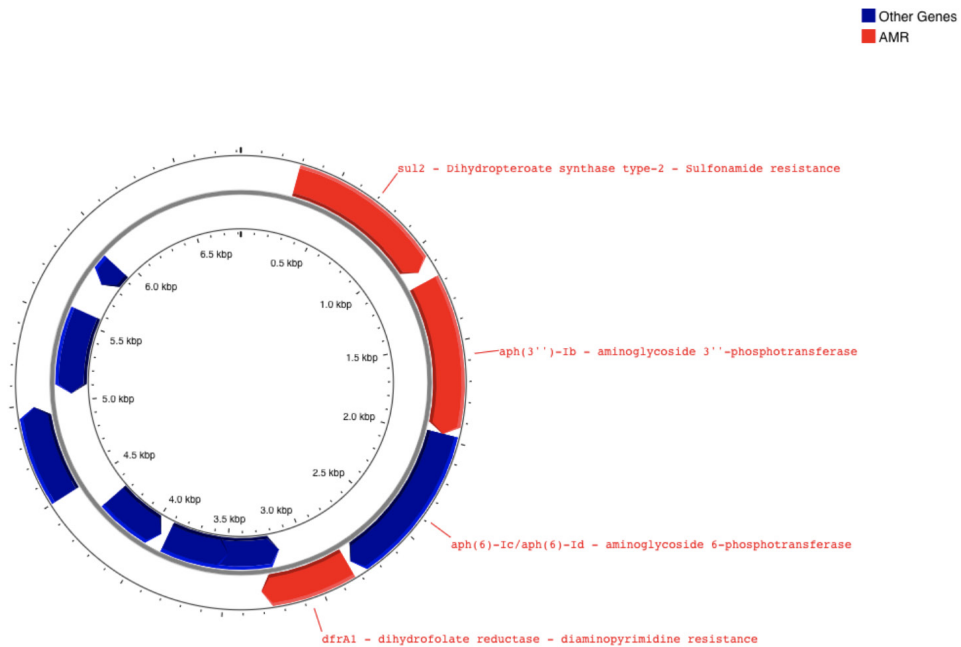
Escherichia coli strain SWYH.B349aT plasmid pB349aT\_1, complete sequence.

**Figure 2.** Map of plasmid pB329aT\_1, an IncFIB plasmid (109,860 bp) containing multiple AMR genes. The presence of *tetB-tetR-tetC* is consistent with the isolate's tetracycline resistance. In addition, dihydrofolate reductase (*dhfrA17*), dihydrodipicolinate synthase (*dhds*), beta-lactamase (*blaTEM*), and the acetyltransferase (*catA1*) allow resistance to diaminopyrimidines, sulfonamides, penicillin/cephalosporins, and chloramphenicol, respectively. Two aminoglycoside phosphotransferases (*aph(3'')*-I and *aph(6)-Id*) provide aminoglycoside resistance. The *merRTPCADE* mercuric resistance operon is also shown.



Escherichia coli strain SWYHX138.261ft plasmid pHX138.261ft\_1, complete sequence.

**Figure 3.** Map of plasmid pHX138.261ft\_1, an IncFIB plasmid (90,138 bp) bearing tetracycline resistance genes *tetA* (coding for an efflux pump protein) and the *tetR* repressor but no other AMR genes.



#### Escherichia coli strain SWYHX138.261ft plasmid pHX138.261ft\_2, complete sequence.

**Figure 4.** Map of plasmid pHX138.261ft\_2/pHX138.33gt\_2 (6,821 bp). This small plasmid contains four contiguous AMR genes: *sul2*, *aph(3'')*-*Ib*, *aph(6)-Id*, and *dfrA1*, which are also contained within pB329aT\_1 (see Fig. 2)

## Conclusion

The presence of the multi-drug resistance plasmid pB329aT\_1 in the older horse could be explained by the strong selection pressure of long-term antibiotic treatment. Meanwhile, the tetA-bearing plasmid pHX138.261ft\_1 that is present in the isolate from the younger horse following quarantine, but absent in the isolate recovered 5 weeks later seems consistent with the brief treatment with oxytetracycline he had received just before the earlier sampling.

The four contiguous AMR genes on the small 6,821 bp plasmid (pHX138.261ft\_2 and pHX138.33gt\_2) are more unexpected, however, since none of the horses had been treated with diaminopyrimidines, sulfonamides or aminoglycosides. The fact that the identical four genes also appear in plasmid pB329aT\_1 between mobile elements suggests that they are not only persistent but also highly mobile.

These *E. coli* isolates provide a useful window into resistance genes and mobile genetic elements within the gut microbiota. In horses, the prevalence of tetracycline-resistance genes is easily explained by the widespread veterinary use of oxytetracycline, which is the most common equine antibiotic prescribed. However, less easy to interpret is the presence of numerous genes

giving resistance to drugs to which the horses had never been exposed. The genes on the small 6,821 bp plasmid, which also appear in the larger InFIB plasmid pB329aT\_1 seem to be easily transmitted between isolates and between horses in the same stable. The persistence of these genes in the absence of selection pressure and also the ease by which they spread are elements that are worthy of further investigation.

## Data Availability

Complete genome sequences for *Escherichia coli* SWYH.B349aT, SWYHX138.33gt, and SWYHX138.261ft are available through NCBI under:

Strain	BioProject	BioSample	Assembly	GenBank accession	Replicon
SWYH.B349aT	PRJNA801757	SAMN25378667	GCA_022014695.1	CP091773.1	chromosome
				CP091774.1	plasmid pB349aT_1
				CP091775.1	plasmid pB349aT_2
				CP091776.1	plasmid pB349aT_3
SWYHX138.261ft	PRJNA802393	SAMN25554218	GCA_022058225.1	CP091839.1	chromosome
				CP091840.1	plasmid pHX138.261ft_1
				CP091841.1	plasmid pHX138.261ft_2
SWYHX138.33gt	PRJNA802381	SAMN25553860	GCA_022058205.1	CP091836.1	chromosome
				CP091837.1	plasmid pHX138.33gt_1
				CP091838.1	plasmid pHX138.33gt_2

## References

Alanjary, M., Steinke, K., Ziemert, N. (2019) AutoMLST: an automated web server for generating multi-locus species trees highlighting natural product potential, *Nucleic Acids Research*, 47(W1):W276–W282, doi: 10.1093/nar/gkz282 [https://automlst.ziemertlab.com/analyze]

Alcock, B. P., Raphenya, A. R., Lau, T., Tsang, K. K., Bouchard, M., Edalatmand, A., Huynh, W., Nguyen, A. V., Cheng, A. A., Liu, S., Min, S. Y., Miroshnichenko, A., Tran, H. K., Werfalli, R. E., Nasir, J. A., Oloni, M., Speicher, D. J., Florescu, A., Singh, B., Faltyn, M., ... McArthur, A. G. (2020). CARD 2020: antibiotic resistance surveillance with the comprehensive antibiotic resistance database. *Nucleic acids research*, 48(D1), D517–D525. doi: 10.1093/nar/gkz935 [https://card.mcmaster.ca]

Altschul, S. F., Gish, W., Miller, W., Myers, E. W., Lipman, D. J. (1990) Basic local alignment search tool. *Journal of Molecular Biology*, 215(3), 403-410. doi: 10.1016/s0022-2836(05)80360-2 [https://blast.ncbi.nlm.nih.gov]

Bateman, A., Martin, M., Orchard, S., Magrane, M., Agivetova, R., Ahmad, S., . . . Teodoro, D. (2020). Uniprot: The Universal Protein Knowledgebase in 2021. *Nucleic Acids Research*, 49(D1). doi:10.1093/nar/gkaa1100 [https://uniprot.org]

Chetri, S., Bhowmik, D., Paul, D., Pandey, P., Chanda, D. D., Chakravarty, A., Bora, D., & Bhattacharjee, A. (2019). AcrAB-TolC efflux pump system plays a role in carbapenem non-susceptibility in *Escherichia coli*. *BMC microbiology*, 19(1), 210. doi: 10.1186/s12866-019-1589-1

Lim, J. Y., Yoon, J., & Hovde, C. J. (2010). A brief overview of *Escherichia coli* O157:H7 and its plasmid O157. *Journal of microbiology and biotechnology*, 20(1), 5–14.

Lupindu, Athumani Msalale (2017). Isolation and Characterization of *Escherichia coli* from Animals, Humans, and Environment. In (Ed.), *Escherichia coli - Recent Advances on Physiology, Pathogenesis and Biotechnological Applications*. IntechOpen. doi: 10.5772/67390

Schoenmakers, K. (2020). How China is getting its farmers to kick their antibiotics habit. *Nature.com*. Retrieved from https://www.nature.com/articles/d41586-020-02889-y.

Ventola C. L. (2015). The antibiotic resistance crisis: part 1: causes and threats. *P & T: a peer-reviewed journal for formulary management*, 40(4), 277–283.

Wattam, A.R., Davis, J.J., Assaf, R., Boisvert, S., Brettin, T., Bun, C., Conrad, N., Dietrich, E.M., Disz, T., Gabbard, J.L., Gerdes, S., Henry, C.S., Kenyon, R.W., Machi, D., Mao, C., Nordberg, E.K., Olsen, G.J., Murphy-Olson, D.E., Olson, R., Overbeek, R., Parrello, B., Pusch, G.D., Shukla, M., Vonstein, V., Warren, A., Xia, F., Yoo, H., Stevens, R.L. (2017) Improvements to PATRIC, the all-bacterial Bioinformatics Database and Analysis Resource Center. *Nucleic Acids Res*, 45(D1): D535-D542. doi: 10.1093/nar/gkw1017 [https://patricbrc.org/]

## Bibliography

Sadikalay, S., Reynaud, Y., Guyomard-Rabenirina, S., Falord, M., Ducat, C., Fabre, L., Le Hello, S., Talarmin, A., Ferdinand, S. (2018). High genetic diversity of extended-spectrum  $\beta$ -lactamases producing *Escherichia coli* in the feces of horses. *Veterinary Microbiology*, 219, 117–122. doi: 10.1016/j.vetmic.2018.04.016

van Hoek, A. H., Mevius, D., Guerra, B., Mullany, P., Roberts, A. P., Aarts, H. J. (2011). Acquired antibiotic resistance genes: an overview. *Frontiers in Microbiology*, 2, 203. doi: 10.3389/fmicb.2011.00203

Zwanzig, M. (2021). The ecology of plasmid-coded antibiotic resistance: a basic framework for experimental research and modeling. *Computational and Structural Biotechnology Journal*, 19, 586–599. doi: 10.1016/j.csbj.2020.12.027

---

# To what extent is the diversity of mangrove stands affected by the presence of a breakwater?

Miriam M.C. Cheng

---

## Introduction

Mangrove ecosystems are wetlands that provide significant ecological and socioeconomic value (AFCD, 2021). Mangroves play an important role in the world's carbon cycle, as mangrove plants sequester atmospheric carbon underground in peat (Were, 2019). They also support a wide range of marine and terrestrial organisms, providing habitats for birds, mammals, and reptiles. According to Sandilyan (2012), 90% of marine organisms spend part of their life in mangroves, and “80% of global fish catches are dependent on mangroves”. In Hong Kong (HK), mangroves provide socio-economic value by protecting shorelines from erosion, capturing carbon, and filtering pollutants from the water (AFCD, 2021). However, mangroves increasingly face the threat of agricultural, infrastructural, industrial, and settlement development (Davidson, 2014). In HK, it was estimated that only 15% of historical mangrove stands remained in 1995 (Yip, 1995). This relates to ecology (topic 4) of the biology syllabus.

Breakwaters are man-made structures constructed to protect shorelines from erosion (Vona, 2020). The Sai Keng breakwaters, located within the Three Fathoms Cove, separate the shoreline of the nearby Sai Keng (SK) village from the sheltered Kei Ling Ha Lo Wai (KLHLW) village shoreline (Figure 1).

By studying the diversity of a hundred-meter stretch of mangroves directly behind the breakwater, then comparing it to the diversity of a hundred-meter stretch of mangroves outside the breakwater, the impact of the manmade breakwater on the diversity of mangroves in this specific case can be studied. The research question this essay seeks to explore is: To what extent is the diversity of mangroves affected by the presence of a breakwater? The question will be studied through qualitative and quantitative field research in the mangrove stands inside and outside the SK breakwater, and additional secondary research on the sites' backgrounds.



**Figure 1.** Satellite imagery of the area of study as part of greater HK (right bottom). Two HK villages: Sai Keng (SK) and Kei Ling Ha Lo Wai (KLHLW), are located on the West of the Three Fathoms Cove. The two coastal mangrove stands (named after their respective village) (in green) are separated by the Sai Keng breakwater (in red).

---

The above article was written as an Extended Essay in Biology, in partial fulfillment of the IB Diploma Programme, 2022.



# 1. Background Research

## 1.1 Mangrove ecosystems: general overview

Mangroves refer to several species of trees or shrubs with specialized adaptations for the harsh conditions of their habitat, including high salinity, fluctuating oxygen, intermittent tides, high temperatures, and unstable soils (AFCD, 2021). They form ecosystems that are found in the intertidal zones of shores, estuaries, creeks, and marshes (Sandilyan, 2012). Despite occupying less than 0.5% of the global coastal area, they contribute 10-15% of the world's coastal sediment carbon storage (Alongi, 2014). The destruction of mangrove ecosystems has the potential to release 90-970 million tons of carbon each year from biomass, soil, and peat, irreversibly disrupting the global carbon cycle, as organic soil carbon stock cannot be replenished in a short length of time (de Jong Cleyndert, 2020). This makes the immediate conservation of mangrove ecosystems crucial.

There has been a global loss of 2% of the world's mangrove land area between 2000 and 2016 according to NASA's satellite data, 62% of which has been attributed to human causes (Merzdorf, 2020). The loss is especially severe in Southeast Asia (Figure 2). HK is a group of islands in Southeast Asia that has experienced a large amount of loss over the past century: Mai Po (Figure 3) lost 85% of its mangroves

to shrimp and fish farming ponds, Tolo Harbor lost 42% of its mangroves to coastal development, and the construction of the international airport destroyed an additional 50 hectares of mangroves (Tam, 1997). Conservation and rehabilitation efforts over the past decades have successfully reduced the rate of mangrove loss through the implementation of zoning laws such as wetland conservation and buffer areas (AFCD, 2021). A successful example is the HK Wetland Park that has been developed into a tourist attraction and education center (Anderson, 2017). In comparison, smaller rural stands, such as the ones near the SK breakwater, remain vulnerable to human activity, such as housing development from nearby villages (Morton, 2016).



**Figure 3.** The HK Wetland Park has now been redeveloped into a tourist attraction and education center and is now under protection. However, many lesser sites are still under threat.

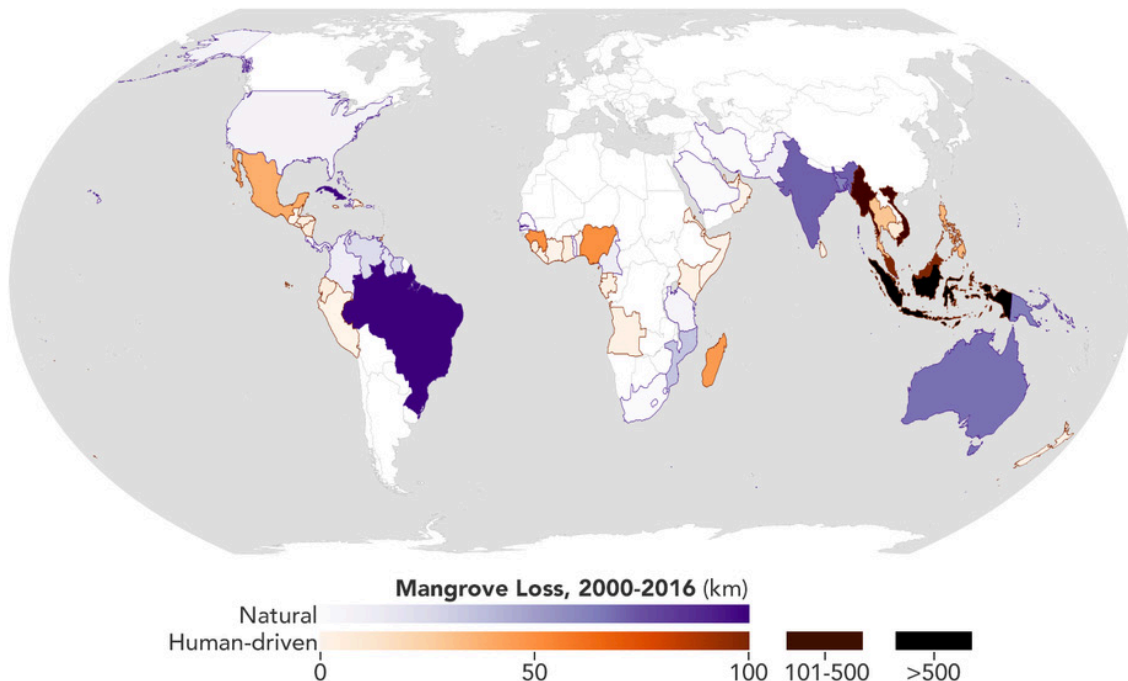


**Figure 2.** Global mangrove loss severity, cause, and location from 2000-2016 (Image Credit: NASA Earth Observatory images by Joshua Stevens)

## 1.2 The Sai Keng (SK) breakwaters

Breakwaters are man-made coastal structures created to “transform, alter and armor shorelines” by reducing wave intensity and shoreline erosion (Vona, 2020). The SK breakwaters shelter the KLHLW village, although their original purpose of construction is unclear. Reviewing past HK maps, the breakwaters were already present on a British map from 1904 (Figure 4).



**Figure 4.** Sai Keng breakwaters were featured on fragments of a British map of HK from 1904, however, their purpose of construction is not entirely clear (Image credits: HK Map Viewer).

Breakwaters actively affect nearby ecosystems by altering currents, sedimentation patterns, and nutrient distribution: Masucci (2019) showed that breakwaters decreased nearby water depth, and while the inner site experienced less erosion and accumulated finer sediments, the outer site experienced greater erosion and accumulated coarser sediments. Vona (2020) estimates that breakwaters dampen wave height by 10-50%, which is associated with less sediment transport and suspension. These examples of changes to abiotic factors in the seaward zone ecosystem (Figure 6) could have an effect on mangrove diversity.

## 1.3 Mangroves in the context of Hong Kong

HK is north of the warm South China Sea, east of the nutrient-rich outflow of the Pearl River, and west of the “thickly turbid” oceanic waters of the Taiwan current. Its coastal mangroves are characterized by their diverse growth conditions. Northeastern mangroves are shorter variants that grow in more salty oceanic water, volcanic stone or sandy mud (Morton, 2016).

HK’s Agriculture, Fisheries and Conservation Department (AFCD) has identified 63 mangrove stands

over an area of 510 hectares (Figure 5). The mangrove stands under investigation are two adjacent stands in the Northeast New Territories (numbers 11 and 30, KLHLW and SK respectively).

The most recent, thorough study of HK’s mangrove stands reports that SK features the mangrove species of *Kandelia obovata*, *Aegiceras corniculatum*, *Avicennia marina*, *Bruguiera gymnorrhiza*, *Excoecaria agallocha*, and *Lumnitzera racemosa*, with codominance of *K.obovata* and *A.corniculatum*. KLHLW features the same species except for *B.gymnorrhiza*, and *K.obovata* is dominant over *A.corniculatum* (Tam, 1997).

HK mangroves form landward to seaward zones. *Heritiera littoralis* grows in very landward zones, *E.agallocha* dominates landward zones, *K.obovata* and *A.corniculatum* survive in intertidal muddy zones, and *A.marina* colonize the seaward edge with seagrass (Figure 6). This study will focus on the mangroves only in the seaward zone, as this is most immediately affected by the breakwater. Therefore, deviations from the typical zoning pattern may be indicative of human impact.

### Mangrove species and characteristics

*K.obovata* is a fast-growing, cold-resistant pioneer species that is highly productive in the carbon cycle, with one stand yielding a biomass of 172 Mg ha<sup>-1</sup> over 10 years (Khan, 2017). *A.marina* is highly dominant in highly salty environments and highly tolerant to aridity, water temperature, and frost, but grows poorly in freshwater conditions (Nguyen, 2015). *A.corniculatum* are common in HK and present in almost every mangrove stand (Tam, 1997). *E.agallocha* are larger, more branched landward mangroves (Department of Agriculture and Fisheries, 2013). Images of mangroves typically present in the SK and KLHLW stands are shown in Figure 7, featuring their important characteristics.

1. Chek Keng
2. Chi Ma Wan
3. Fung Wong Wat
4. Ha Pak Nai
5. Ham Tin
6. Ho Chung
7. Hoi Ha Wan
8. Kai Kuk Shue Ha
9. Kau Sai Chau
10. Kei Ling Ha Hoi
11. Kei Ling Ha Lo Wai
12. Kuk Po
13. Lai Chi Chong
14. Lai Chi Wo
15. Lau Fau Shan
16. Lo Fu Wat
17. Luk Keng
18. Lut Chau
19. Ma Wan
20. Mai Po
21. Nai Chung
22. Nam Chung Yeung Uk
23. Nga Yiu Tau
24. Ngau Shi Wu Wan
25. Pak Kok Wan
26. Pak Nai
27. Sak Sha Wan
28. Pak Tam Chung
29. Pui O Wan
30. Sai Keng
31. Sam A Chung
32. Sam A Tsuen
33. Sam Mun Tsai
34. San Tau
35. Sha Kong Tsuen
36. Sham Chung
37. Sham Wat
38. Sheung Pak Nai
39. Sheun Wan
40. Shui Hau
41. Siu Tan
42. So Lo Pun
43. Tai Ho Wan
44. Tai O
45. Tai Sham Chung
46. Tai Tam
47. Tai Tan
48. Tai Wan
49. Ting Kok
50. To Kwa Peng
51. Tolo Pond
52. Tsam Chuk Wan
53. Tsim Bei Tsui
54. Tung Chung
55. Tung Wan
56. Wetland Park
57. Wong Yi Chau
58. Wu Shek Kok
59. Yam O
60. Yi O
61. Yim Tso Ha
62. Yuen Long Industrial Estate
63. Yung Shue Au

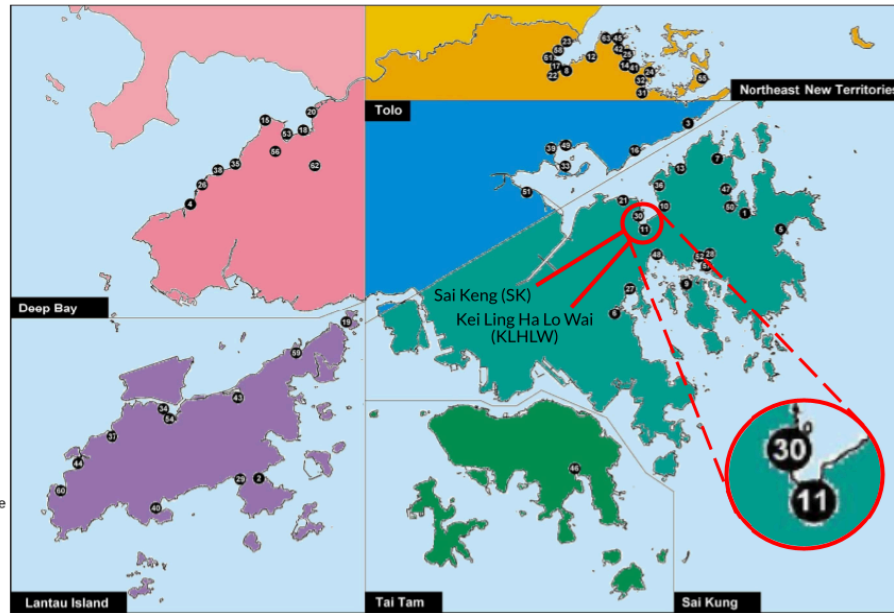


Figure 5. The mangrove stand distribution across HK (Image credits: AFCD)

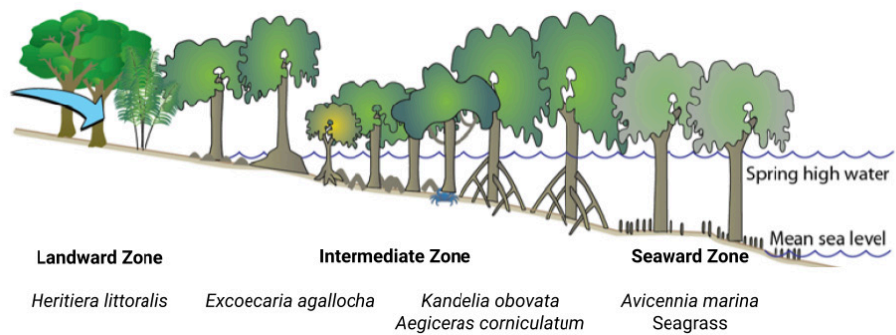


Figure 6. Diagrammatic illustration of the zonation of mangrove. Seaward zone experiences saltier water, more unstable soil, more sedimentation, and more flooding. (Image modified from Waycott, 2011)



Figure 7. Characteristics of important HK's true mangrove species, including leaves, flowers, and propagules/seedlings (Image Credits: AFCD and Bendel, M.)

## Sai Keng (SK) and Kei Ling Ha Lo Wai (KLHLW) mangroves

According to Morton (2016), HK's mangroves face the threat of human development, partially from the Small House Policy (SHP) - a policy that allows male villagers of certain recognized villages to build themselves a house within their lifetime (Lands Department, 2014). The government has attempted to address the issue of rapid mangrove loss through conservation measures. Currently, seven mangrove stands in HK are designated as Sites of Special Scientific Interest (SSSIs) and are protected by zoning plans.

However, although both KLHLW and SK are recognized-SHP villages, they are not SSSIs. Encroachment of human civilization is apparent at both sites: Figure 8 shows the footpath and buildings limiting the growth of landward mangroves (Morton, 2016).

The largest difference between the two mangrove stands is their position in relation to the SK breakwaters. A comparison of the two sites could therefore provide insight into how the SK breakwaters directly affect neighboring mangrove ecosystems.

## 2. Methodology

Transects involve taking regular observations of vegetation along a linear path in a habitat (FSC Biology Fieldwork, 2021). They can be used to form comparisons between the diversity of KLHLW and SK's mangrove stands, and are thus chosen as the primary method of data collection. Two one-hundred-meter transects of mangrove species were conducted along the KLHLW and SK coastlines (Figure 9). At each 1m interval, the species of the mangrove, its circumference at the base (cm), and its height (cm) were recorded. Other qualitative observations regarding the mangrove or its surrounding habitat were noted (raw data in Appendix II and III).

Water samples from streams within the transect and the sea adjacent to the transect were collected (Figure 9). Water quality can heavily affect an ecosystem's health (Pawar, 2013), so water measurements are important in understanding the breakwater's potential impact on its surrounding abiotic ecosystem and could possibly be used to explain variations between the diversity of the two stands. As mentioned in section 1.2, breakwaters can have a major impact on nearby water, from wave



**Figure 8.** Human development, such as the stone broadwalk (yellow dashed line) and marked villages encroach on the KLHLW and SK mangrove stands (Image credits: Google Earth).

energy, depth, and erosion (Masucci, 2019), to water quality, flushing time, and dissolved oxygen levels (Hashish, 2012). Using a Colombo 6-in-1 water quality kit, nitrite, nitrate, chlorine, general hardness, and carbonate hardness were recorded. Salinity levels and dissolved oxygen levels were measured using Vernier probes.

Qualitative observations of the nearby coastal wildlife were noted. Mangroves support a wide range of marine and terrestrial species, making the presence of greater biodiversity in an ecosystem an indirect indicator of mangrove diversity (AFCD, 2021).

## 2.1 Transect plan

Transects were chosen as the primary method, as they are not harmful to the ecosystem, and provide data to measure biodiversity. Due to safety and environmental concerns, unnecessary contact with wildlife was avoided, and mangroves were handled with caution. For safety reasons, I was accompanied by my supervisor, and a first-aid kit was brought in case of emergencies.

Pre-fieldwork planning and preparation were completed through Google maps to understand the location, estimate the extent of the transect, and identify any disturbances in the stand (Figure 9) (Ellison, 2012). The chosen date and time - the afternoon of June 26th, 2021 - was chosen for its fine weather and extremely low tides that exposed many abiotic and biotic factors in the intertidal ecosystem, such as sedimentation patterns and coastal wildlife.

## 2.2 Limitations of study

This study can only provide a snapshot of the current conditions at both mangrove sites through transects, as further studies are not within the scope of the research question. It cannot provide a causal relationship between the breakwater and the mangrove ecosystems, although many such relationships can be postulated through the research findings of others. It is also difficult to ascertain other variations between the two sites, for example, the degree of direct human impact, or the impact of differences in geography.



**Figure 9.** Planning and preparation of the mangrove transects. White dotted line shows the broadwalk; white arrows show access points to coastline or disturbances in mangrove stands; both transects and their respective directions are marked; water samples from the sea and streams are marked. Note that tides were much lower during the transect than displayed in this image. (Image Credits: Google Earth)

## 2.3 Evaluation of sources

The sources chosen to support the arguments presented within this extended essay have been carefully chosen to be relevant and accurate. They are mostly information from government sources and peer-reviewed sources. There were only three sources that were not published or updated in the past decade, and these were chosen either because they provide a snapshot of the state of mangroves from a previous decade (Tam, 1997; Yipp, 1995), or present a compelling argument that was relevant to the discussion (Martins, 2009). A limitation of the sources is that the SK breakwater's initial purpose of construction is still unknown, resulting in less meaningful discussion of mangrove conservation measures.

## 3. Data Collection

A hundred-meter tape measure was laid over the coastal mangroves. At every 1-meter interval, the measurements of the mangrove directly above or below the transect line were tabulated (Appendix II and III).

- A species identification chart (Appendix I) (AFCD, 2018) with images of trees, flowers, and propagules was used for easier on-site identification of mangroves.
- A string and ruler were used to measure the circumference at the base (cm).
- A tape measure was used to measure the height (cm) of the tree from its base. If the height exceeded 200cm, 200cm was used to calculate averages.
- Any additional observations about mangroves or surroundings were noted.

For raw data of transects and water samples, refer to Appendix II, III, and IV.



**Figure 10.** Sample transect recording at 50m inside the breakwater. The species is identified as *K.obovata* based on flowers and leaves (Figure 7); the height and its circumference at its base were measured and recorded (107 and 21cm respectively); the presence of nearby oyster shells (likely fishing waste) was noted (Appendix II).

## 4. Data Summary

Table 1 displays a summary of the data collected from both transects. Over 100m, roughly the same amount of mangroves were sampled:

Summary of Transects		
	Inside Breakwater (Area IB) (KLHLW)	Outside Breakwater (Area OB) (SK)
Transect Length	100 m	100 m
No. of Mangroves	66	67
No. of Species Present	1 ( <i>K.obovata</i> )	4 ( <i>K.obovata</i> , <i>E.agallocha</i> , <i>A.marina</i> , <i>A.corniculatum</i> ,)
Average Circumference	27 cm	40 cm
Average Height	142 cm	180 cm

**Table 1.** A comparative summary of the transects. The average circumference and heights listed above are underestimations, as heights above 2m were calculated as 2m, and circumference measurements of larger, thicker trees with intertwining branches were skipped to avoid damaging the plant.

Analysis of Water from Water Streams								
Distance (m)	Chlorine (mg/L)	pH	KH (°dH)	GH - total hardness (°H)	Nitrite (mg/L)	Nitrate (mg/L)	Conductivity (µS)	Dissolved Oxygen (mg/L)
Inside the Breakwater (Area IB): KLHLW								
26-28	1.5	7.2	10-15	>21	0-0-5	0-10	27500	9.22
76-79	3	6.4	10	>21	0	0	560	8.33
Outside the Breakwater (Area OB): SK								
67-69	0.8	8	10-15	>14	2-5	5	450	8.72
78-79	1.5	7.2-7.6	15	>21	0	0	25000	8.71

**Table 2.** Water samples from streams within the mangrove stands. The stream at SK at 67-69m shows possible signs of SK village runoff, including higher nitrite and nitrate levels. Water samples from the ocean can be found in Appendix IV, though the only noteworthy observation was the slightly higher pH and conductivity outside the breakwater at SK, indicating higher salinity levels.

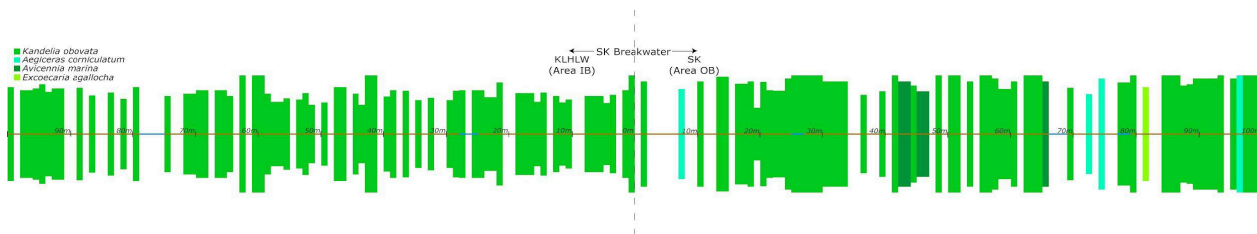


**Figure 11.** Comparative unannotated overviews of SK and KLHLW transects show greater diversity of mangrove species in Area OB, and generally taller trees (shown by the length of the green bars.)

The surveyed KLHLW mangrove stand Inside the Breakwater (IB) consisted entirely of *K.obovata* that were mostly shorter and thinner (Figure 11), and propagules were also present in abundance on the nearby beach (Figure 13). There were few disturbances, most notably one at 13m from the breakwater that shined with oil, possibly caused by water pollutants (Pawar, 2013). In addition, human fishing waste was noted, including piles of oyster shells and ropes on trees (Figure 10). The soil was muddy with rocks, as opposed to the more rocky terrain outside the breakwater.

The SK mangrove stand Outside the Breakwater (OB) was also primarily (86%) *K.obovata*, though other species were observed. The mangroves were taller and thicker, and there were fewer propagules on the beach (Figure 15). The disturbances that led to the broadwalk and SK village were larger, as they were access points for the nearby resort. There was also man-made waste, including plastic bags and a vehicle chassis (Figure 19) at 79m from the breakwater.

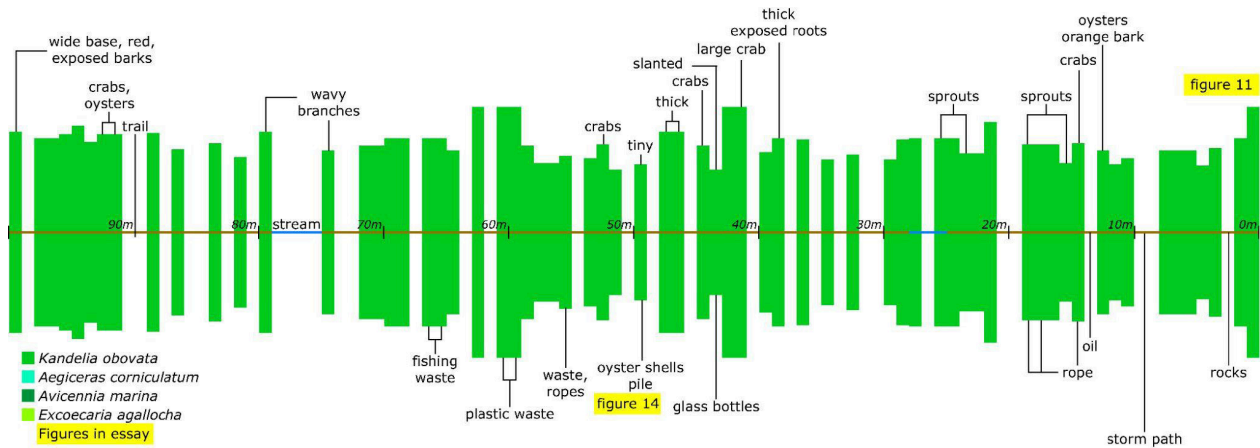


**Figure 12.** An annotated overview of KLHLW (Area IB) transect. Length of rectangles represent mangrove height; transect direction is leftwards, distance from the start of the transect is marked; biotic annotations written above and abiotic annotations below diagram; figures present in paper highlighted in yellow.

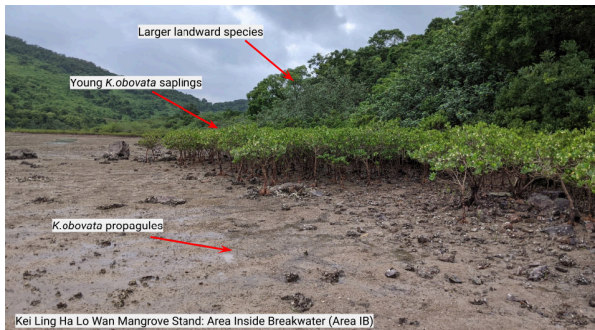


**Figure 13.** KLHLW mangrove stand, inside breakwater (IB). The coastal mangroves were all relatively young *K.obovata*. Behind them, larger landward species could be observed; on the beach, small propagules were growing



**Figure 15.** SK mangrove stand, outside breakwater (OB). Mangroves were generally taller and more diverse. Obvious human impacts were observed, such as the chair and car chassis in the background. (Image Credits: *lokface lokface* on Google Maps)

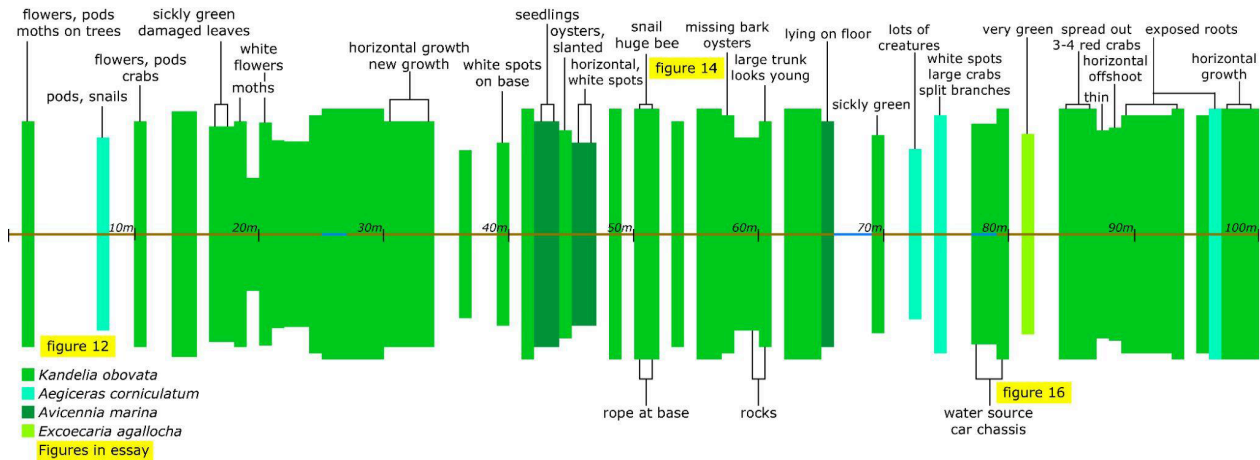


**Figure 14.** An annotated overview of SK transect (Area OB). Colors of rectangles represent corresponding species of mangrove (shown in legend in bottom left); note greater abundance of other organisms (i.e. moths, crabs, snails, etc.) (above diagram).



## 5. Data Analysis

### 5.1 Inside the breakwater (IB): the Kei Ling Ha Lo Wai transect

**Mangrove Composition:** The transect of area IB revealed more homogenous coastal mangroves. Normal HK mangrove zonation would see *A.corniculatum* and seagrass along the coast (section 1.3), so the observation of only the pioneer species *K.obovata* indicates there is a constant, unimpeded growth of new propagules, perhaps due to the protection of the breakwater or differences in the habitat.

**Water:** Using the Vernier conductivity probe as a measurement of salinity, the seawater from within the breakwater was less salty, averaging a conductivity level of 22mS compared to 29mS outside the breakwater (Appendix IV). This may be because *A.corniculatum* are hardy salt-resistant species that are accustomed to living on the seaward fringe of mangrove stands, and therefore were less dominant inside of breakwaters.

**Diversity:** as quantified by Simpson’s reciprocal index of diversity:

$$D = 1 - \frac{\sum n(n-1)}{N(N-1)}$$

(Formula taken from Barcelona Field Studies Centre, 2021; Simpson’s reciprocal index of diversity (D) is an indicator for both diversity in terms of richness and evenness, and thus was chosen to measure diversity; n = number of organisms of a particular species; N = total number of organisms)

Summary of Area IB Transect		
Species	Count (n)	n(n-1)
<i>K.obovata</i>	66	4290
<i>A.corniculatum</i>	0	0
<i>A.marina</i>	0	0
<i>E.agallocha</i>	0	0
Total	N=66	4290

Table 3. Summary of Area IB Transect

The biodiversity index of the coastal mangroves IB is 0 because no other species were present except for *K.obovata*. Most trees were quite young, and many saplings and propagules were present on the beach (Figure 16). This shows that there was still fresh growth and development, and propagules were not regularly washed away by the waves. As a result of the fresh growth, there were fewer mature flowering trees on the coastline.



Figure 16. *K.obovata* propagule on the beach at KLHLW, surrounded by many shells (various types of bivalves and gastropods).

**Coastal Wildlife:** Qualitative observations showed many bivalves and gastropods exposed by the low tides, including *Batillaria zonalis*, *Gafrarium pectinatum*, and others that were not properly identified. They coexisted in similar zones as the mangrove propagules and saplings (Figure 12). The crabs inside the breakwater included a red-clawed crab (*Parasesarma bidens*), a purple-clawed crab (*Metopograpsus frontalis*), and a Fiddler crab (*Uca borealis*). According to AFCD (2021), they are classified as “Sesarmid crabs” and play an important role in the ecosystem by consuming mangrove detritus and other small animals, completing the carbon cycle. In addition, their burrowing behavior facilitates air circulation for mangrove roots. Their presence is a good indicator of ecosystem health and diversity.

**Human impact:** There was an abundance of fishing waste, such as ropes and nets, near the mangroves. There were also piles of oyster shells, presumably fishing waste. The IB mangroves sometimes had charred or missing bark. It appeared as though the oysters (*Saccostrea cucullata*) had been removed from the trees (Figure 17). This suggests direct human activity impact on the mangrove trees, another factor that influences the possible mangrove diversity variation observed between the two transect sites. Since the extent of impact is unknown, this represents a limitation to this study.



Figure 15. Left: Piles of oyster shell waste and a nearby mangrove tree with missing bark in Area IB. Right: Mangrove in Area OB with oysters growing on its stem. It is postulated that the oysters have been removed from the mangrove trees in Area IB, eaten, and fishing waste has been disposed of in piles. These indicate possible impacts of human activity on the health of mangroves ecosystems as mangroves.

## 5.2 Outside the breakwater (OB): the Sai Keng transect

**Mangrove Composition:** The transect OB showed greater coastal mangrove diversity as compared to those IB, although *K.obovata* was still the most common species (Table 4). When inquired about this, AFCD Nature Conservation Officer of Sai Kung, Mr. Mok responded in an email, “*Kandelia obovata* is the dominant true mangrove species in most of the mangrove stands in Hong Kong, including the one at [KLHLW].” These mangroves OB were noticeably more mature: many were flowering or had fruits, and 23 were 200cm or taller (Figure 12).

**Soil and Water:** The terrain included larger rocks, which coincides with Masucci’s (2019) study that found larger sedimentation and more erosion on the outer side of the breakwater (see section 1.2). Unlike the younger saplings IB, the mangroves grew to be more intertwined. Some had many meters of horizontal branches (which presumably floats during high tide) before upward growth was observed. This made circumference measurements for larger trees difficult, as the trunk was often deep within the stand. The greater maturity in mangroves may be a result of reduced protection for younger saplings, although AFCD attributes it to the “large amount of freshwater runoff and possibly high nutrient supply from mariculture operations nearby”. There were two main water sources at 67-69m and 78-79m respectively. The first was a more basic freshwater stream (pH 8, Table 2) that contained higher amounts of nitrite, possibly indicating fertilizer use and runoff from the village. This was one of the few locations where *A.marina* was observed. A further investigation into the pollutants in the village runoff would provide more detail on the potential for this aspect of human impact on mangrove diversity.

**Diversity:** There were 4 species present, and the biodiversity index is 0.27, which is greater than that of Area IB (Table 3).

Summary of Area OB Transect		
Species	Count (n)	n(n-1)
<i>K.obovata</i>	57	3192
<i>A.corniculatum</i>	4	12
<i>A.marina</i>	5	20
<i>E.agallocha</i>	1	0
Total	N=67	3224

**Table 4.** Summary of Area OB Transect

*A.corniculatum*’s presence is expected, as it is a coastal mangrove. *A.marina* is not typically observed along the coastline, but its presence shows greater diversity. The presence of *E.agallocha* is also unexpected, because they are landward growing mangroves (section 1.3). It may indicate that seaward mangroves in this region were missing or destroyed, which are possible signs of erosion or human impact.

Comparing the notes of the two transects (Diagrams 12 and 14), the mangroves OB has more wildlife: snails, moths, bees, oysters, and crabs. Mangroves are foundation species in their ecosystem that sustain other organisms. For example, *A.corniculatum*, *E.agallocha* and *B.gymnorhiza* “provide additional surfaces for attachment by sedentary organisms, such as oysters and barnacles” (AFCD, 2021). Therefore, greater overall biodiversity supports the collected data of greater mangrove diversity in OB.

$$BC_{ij} = 1 - \frac{2c_{ij}}{S_i + S_j}$$

(Formula taken from Bobbitt, 2021; Bray–Curtis dissimilarity index (BC<sub>ij</sub>) was chosen as it can compare the richness and evenness of the diversity of two sites (i and j); C<sub>ij</sub> = sum of lesser value of shared species at sites i and j, S = total specimens at each site)

The Bray–Curtis dissimilarity index was used to compare diversity between SK and KLHLW. An index of 0.14 shows relatively high similarity, mostly because both sites are predominantly *K.obovata*.

**Coastal Wildlife:** Coastal wildlife had greater diversity and more organisms present: Anemone, bivalves, and gastropods (also observed IB), and starfish were all present (Figure 18). Since mangroves protect shorelines against erosion and storms, they are important for the biodiversity of coastal and adjoining ecosystems (Sandilyan, 2012). If a healthy coastal ecosystem is indicative of healthy and mature mangrove plants, then the increased diversity of coastal wildlife in area OB is indicative of increased mangrove diversity.

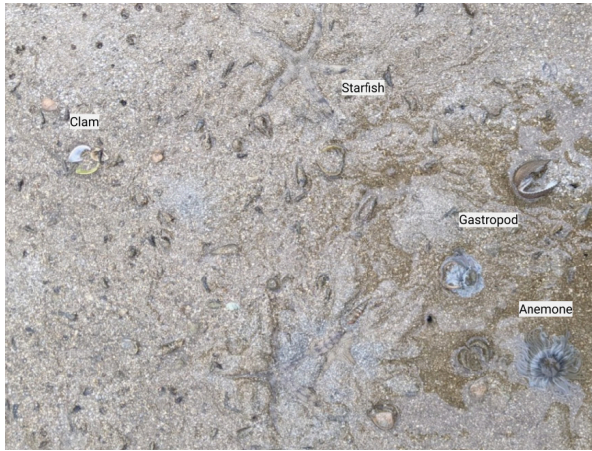


**Figure 18.** Intertidal wildlife on Sai Keng beach (Area OB) camouflaged into the sand. Though no quantitative measurements were taken, the wildlife was more diverse on the Sai Keng beach, as many more species were present (starfish, sea anemone and clams). The wildlife was closer to the sea, unlike in Area IB where they were present directly beneath the mangroves.

**Human Impact:** Apart from the aforementioned disturbances in the mangrove stand and resulting differences in nitrate levels (Figure 14), there were also bottles, plastic bags, a car chassis (Figure 19), and ropes littered amongst the stand.



**Figure 19.** 79m of the transect above a car chassis. *K.obovata* flowers are seen in the background. Note greater intertwining of branches as compared to the saplings in Figure 13.

## Conclusion

HK has experienced a rapid loss of its mangroves due to human impact in the past century (Yipp, 1995). Although the government has enacted multiple policies to save its larger sites through zoning laws and declaring them as SSSIs, many lesser stands, especially near SHP-recognized villages, are facing increasing threats from human development (Morton, 2016). The purpose of this investigation is to determine the possible impact that the SK breakwater has on the diversity of mangrove species.



**Figure 20.** displaying the SK breakwaters from within (KLHLW beach).

To answer the original research question of “*To what extent is the diversity of mangrove stands affected by the presence of a breakwater?*”, in the context of KLHLW and SK, though no direct causal relationship can be inferred through the collected data, the vast differences between the diversity of two neighboring mangrove stands with nearly identical legal status (non-SSSI, SHP-village associated stands) and similar geographical location may be partially attributed to the presence of the SK breakwater.

The diversity of the coastal mangroves inside the breakwater at KLHLW was extremely poor, with a Simpson’s diversity index of 0 (compared to 0.27 outside the breakwater). The Bray-Curtis dissimilarity index is 0.14 (relatively high similarity), as both mangroves stands are still predominantly *K.obovata*. The overall biodiversity of the mangrove ecosystem at KLHLW was also poor, as there were fewer animals (such as oysters and moths) observed as compared to SK (compare Diagrams 12 and 14). This may be partially due to human impact, or it may be indicative of poor diversity and health of mangrove plants. Aside from the mangrove ecosystems, many coastal organisms present outside the breakwater were absent within: although they had similar gastropods, bivalves, and crabs (Figure 16), the anemone, starfish, and slugs (Figure 18) were found exclusively outside the breakwater. It must be

noted that these observations are based on qualitative observations instead of quadrat sampling, so are inadequate at reliably determining intertidal coastal wildlife diversity. However, similar results of decreased diversity in ecosystems with coastal structures have been reported by Martins (2009).

The observed differences may be attributed to the breakwaters sheltering the KLHLW coastline against erosion and powerful waves, fostering the growth of mangroves by preventing waves from clearing out the young seedlings. This was apparent from the abundance of propagules and young mangroves observed on the beach (see Figures 11, 13, and 16). The pioneer species *K.obovata* is dominant in these environments, covering the entire coastline. The lack of diversity and variation of life stages places the entire stand at risk from diseases or flood events after high-intensity rainfall (Van Tang, 2020). Low diversity also decreases the carbon storage capacity of the mangrove ecosystem in the long run (Bai, 2021). The effects of the breakwater on SK's mangroves are not entirely clear, though it is possible that erosion and wave energy may be increased (Masucci, 2019).

## Discussion

Breakwaters have been built in the past to protect mangrove forests from erosion. For example, in West Kalimantan, Indonesia, the government attempted to erect a breakwater to protect the coastline and rehabilitate mangrove ecosystems, although in that case, the construction itself caused erosion and the project overall worsened the situation. On the other hand, construction and replanting efforts have been successful in Malaysia and China (Akbar, 2017). This particular case study of SK's breakwaters on its surrounding ecosystem therefore provides another perspective on the potential use of human structures for mangrove protection, or the negative impacts they may have on mangrove ecosystems.



**Figure 20.** Aerial image of Sai Keng breakwaters and nearby development of human settlements. (Image Credits: Tang on Google Maps)

Both sites showed obvious signs of degradation due to human impact, for example, missing bark on trees, or the presence of human fishing waste. As two small and remote stands, it may be necessary to better enforce protection through legislation and collaboration with nearby villagers. Enforcement of laws already in place and increased “community-based management” are both important in our efforts to protect these mangrove ecosystems from further degradation (Morton, 2016; Friess, 2020).

The SK breakwaters potentially reduces wave energy and erosion, making the coastal area of KLHLW more suitable for the rapid growth of young mangrove stands. However, based on quantitative and qualitative observations, this effect may also exact a cost on the diversity of the mangrove stand. Although a causal relationship cannot be fully determined, it can be postulated that the protection of the SK breakwater allows the growth of young saplings of the pioneer species *K.obovata*, which outcompete more salt-resistant, hardy species such as *A.corniculatum*. This ultimately forms a more homogenous mangrove stand consisting of younger trees. This lack of diversity can be harmful to the ecosystem in the long run, as it creates vulnerable, homogenous stands that are less productive and provide less socioeconomic benefits (Hai, 2020).

## Evaluation of limitations

The study presents multiple limitations, as it does not:

1. account for the differences in human impact as there is a general lack of information about the location's history and human activity;
2. account for natural differences potentially caused by the geography of the cove;
3. contain qualitative measurements of intertidal ecosystem biodiversity.

Due to these limitations, the variation in diversity between the two mangrove stands cannot be fully attributed to the presence of the breakwater. To improve upon the limitations of the methodology and to strengthen the conclusion 1) a stand in a similar geographical location unaffected by human impact may be studied; 2) a similar mangrove cove without a breakwater may be studied for comparison to understand the effect of geography on mangrove diversity; 3) quadrats could be included to quantitatively measure coastal wildlife biodiversity.

Nonetheless, the difference in the calculated diversity of mangrove species between the two stands and the observed biotic and abiotic differences of the corresponding ecosystems of the stands are supported by similar studies in literature. Future investigations are needed to further assess the effects of breakwaters on mangrove ecosystems and determine their potential use in conservation efforts.

## References

- AFCD. (2018). *Mangrove Habitats / Field Guides on True Mangroves in Marine Parks of Hong Kong*. Agriculture, Fisheries and Conservation Department The Government of the Hong Kong Special Administrative Region. [www.afcd.gov.hk/english/country/cou\\_vis/cou\\_vis\\_mar/cou\\_vis\\_mar\\_edu/files/MP\\_mangrove.pdf](http://www.afcd.gov.hk/english/country/cou_vis/cou_vis_mar/cou_vis_mar_edu/files/MP_mangrove.pdf).
- AFCD. (2021). *General Information about Wetland*. Agriculture, Fisheries and Conservation Department The Government of the Hong Kong Special Administrative Region. [https://www.afcd.gov.hk/english/conservation/con\\_wet/con\\_wet\\_abt\\_gen/con\\_wet\\_abt\\_gen.html](https://www.afcd.gov.hk/english/conservation/con_wet/con_wet_abt_gen/con_wet_abt_gen.html).
- Akbar, A. A., Sartohadi, J., Djohan, T. S., & Ritohardoyo, S. (2017). The role of breakwaters on the rehabilitation of coastal and mangrove forests in West Kalimantan, Indonesia. *Ocean & Coastal Management*, 138, 50–59. <https://doi.org/10.1016/j.ocecoaman.2017.01.004>.
- Anderson, D., Tam, C., Symonds, S., et al. (2017). *WWF-Hong Kong Annual Review 2017*. [wwf.org.hk. http://awsassets.wwf.org.panda.org/downloads/AR\\_17\\_final\\_op\\_eng.pdf](http://awsassets.wwf.org.panda.org/downloads/AR_17_final_op_eng.pdf).
- Bai, J., Meng, Y., Gou, R., Lyu, J., Dai, Z., Diao, X., Zhang, H., Luo, Y., Zhu, X., & Lin, G. (2021). Mangrove diversity enhances plant biomass production and carbon storage in Hainan island, China. *Functional Ecology*, 35(3), 774–786. <https://doi.org/10.1111/1365-2435.13753>.
- Barcelona Field Studies Centre (2021). *Simpson's Diversity Index*. All Rights Reserved Barcelona Field Studies Centre. <https://geographyfieldwork.com/Simpson'sDiversityIndex.htm>.
- Bobbitt, Z. (2021). *Bray-Curtis Dissimilarity: Definition & Examples*. <https://www.statology.org/bray-curtis-dissimilarity/>.
- Davidson, N. C. (2014). How much wetland has the world lost? Long-term and recent trends in global wetland area. *Marine and Freshwater Research*, 65(10), 934. <https://doi.org/10.1071/mf14173>.
- de Jong Cleyndert, G., Cuni-Sanchez, A., Seki, H. A., Shirima, D. D., Munishi, P. K. T., Burgess, N., Calders, K., & Marchant, R. (2020). The effects of seaward distance on above and below ground carbon stocks in estuarine mangrove ecosystems. *Carbon Balance and Management*, 15(1). <https://doi.org/10.1186/s13021-020-00161-4>.
- Department of Agriculture and Fisheries (2013). Milky mangrove. *Department of Agriculture and Fisheries, Queensland*. <https://www.daf.qld.gov.au/business-priorities/fisheries/habitats/marine-plants-including-mangroves/common-mangroves/milky-mangrove>.
- Ellison, J., Jungblut, V., Anderson, P., Slaven, C. (2012). *Manual for Mangrove Monitoring in the Pacific Islands Region*. Apia, Samoa: Secretariat of the Pacific Regional Environment Programme (SPREP).
- Friess, D. A., Yando, E. S., Abuchahla, G. M. O., Adams, J. B., Cannicci, S., Canty, S. W. J., Cavanaugh, K. C., Connolly, R. M., Cormier, N., Dahdouh-Guebas, F., Diele, K., Feller, I. C., Fratini, S., Jennerjahn, T. C., Lee, S. Y., Ogurcak, D. E., Ouyang, X., Rogers, K., Rowntree, J. K., Sharma, S. Sloey, T. M., Wee, A. K. S. (2020). Mangroves give cause for conservation optimism, for now. *Current Biology*, 30(4), R153–R154. <https://doi.org/10.1016/j.cub.2019.12.054>.
- FSC Biology Fieldwork (2021). *Transects*. Field Studies Council. <https://www.biology-fieldwork.org/a-level/fieldwork-techniques/vegetation-sampling/transects/#primary-nav>.

Hai, N. T., Dell, B., Phuong, V. T., & Harper, R. J. (2020). Towards a more robust approach for the restoration of mangroves in Vietnam. *Annals of Forest Science*, 77(1). <https://doi.org/10.1007/s13595-020-0921-0>.

Hashish, A. M., Gad, M. A., ElKamash, M. K., Gad El-Rab, M. S., and Nour El-Din, M. (2012). *Impacts of Different Breakwater Configurations on the Water Quality*; Case Study: Mandrah Beach. [https://www.researchgate.net/publication/339326516\\_IMPACTS\\_OF\\_DIFFERENT\\_BREAKWATER\\_CONFIGURATIONS\\_ON\\_THE\\_WATER\\_QUALITY\\_CASE\\_STUDY\\_MANDRAH\\_BEACH](https://www.researchgate.net/publication/339326516_IMPACTS_OF_DIFFERENT_BREAKWATER_CONFIGURATIONS_ON_THE_WATER_QUALITY_CASE_STUDY_MANDRAH_BEACH).

Khan, Md. N. I., & Kabir, Md. E. (2017). *Ecology of Kandelia obovata (S., L.) Yong: A Fast-Growing Mangrove in Okinawa, Japan*. In *Disaster Risk Reduction* (pp. 287–301). Springer Japan. [https://doi.org/10.1007/978-4-431-56481-2\\_18](https://doi.org/10.1007/978-4-431-56481-2_18).

Lands Department (2014). Small House Policy English Version. *Lands Department Hong Kong Special Administrative Region of the People's Republic of China*. [https://www.landshd.gov.hk/doc/en/small-house/NTSHP\\_E\\_text.pdf](https://www.landshd.gov.hk/doc/en/small-house/NTSHP_E_text.pdf).

Martins, G. M., Amaral, A. F., Wallenstein, F. M., & Neto, A. I. (2009). Influence of a breakwater on nearby rocky intertidal community structure. *Marine Environmental Research*, 67(4–5), 237–245. <https://doi.org/10.1016/j.marenvres.2009.03.002>.

Masucci, G. D., Acierno, A., & Reimer, J. D. (2019). Eroding diversity away: Impacts of a tetrapod breakwater on a subtropical coral reef. *Aquatic Conservation: Marine and Freshwater Ecosystems*, 30(2), 290–302. <https://doi.org/10.1002/aqc.3249>.

Merzdorf, J. (2020) NASA Study Maps the Roots of Global Mangrove Loss. *National Aeronautics and Space Administration*. <https://www.nasa.gov/feature/goddard/2020/nasa-study-maps-the-roots-of-global-mangrove-loss>.

Morton, B. (2016). Hong Kong's mangrove biodiversity and its conservation within the context of a southern Chinese megalopolis. A review and a proposal for Lai Chi Wo to be designated as a World Heritage Site. *Regional Studies in Marine Science*, 8, 382–399. <https://doi.org/10.1016/j.rsma.2016.05.001>.

Nguyen, H. T., Stanton, D. E., Schmitz, N., Farquhar, G. D., & Ball, M. C. (2015). Growth responses of the mangrove *Avicennia marina* to salinity: development and function of shoot hydraulic systems require saline conditions. *Annals of Botany*, 115(3), 397–407. <https://doi.org/10.1093/aob/mcu257>.

Pawar, P. R. (2013). Monitoring of impact of anthropogenic inputs on water quality of mangrove ecosystem of Uran, Navi Mumbai, west coast of India. *In Marine Pollution Bulletin*, 75(1–2), 291–300. Elsevier BV. <https://doi.org/10.1016/j.marpolbul.2013.06.045>.

Sandilyan, S., & Kathiresan, K. (2012). Mangrove conservation: a global perspective. *Biodiversity and Conservation*, 21(14), 3523–3542. <https://doi.org/10.1007/s10531-012-0388-x>.

Tam, N. F. Y., Wong, Y.-S., Lu, C. Y., & Berry, R. (1997). Mapping and characterization of mangrove plant communities in Hong Kong. *Asia-Pacific Conference on Science and Management of Coastal Environment*, 25–37. [https://doi.org/10.1007/978-94-011-5234-1\\_4](https://doi.org/10.1007/978-94-011-5234-1_4).

Van Tang, T., Rene, E. R., Binh, T. N., Behera, S. K., & Phong, N. T. (2020). Mangroves diversity and erosion mitigation performance in a low salinity soil area: case study of Vinh City, Vietnam. *Wetlands Ecology and Management*, 28(1), 163–176. <https://doi.org/10.1007/s11273-019-09704-0>.

Vona, I., Gray, M., & Nardin, W. (2020). *The Impact of Submerged Breakwaters on Sediment Distribution along Marsh Boundaries*. *Water*, 12(4), 1016. <https://doi.org/10.3390/w12041016>.

Were, D., Kansime, F., Fetahi, T., Cooper, A., & Jjuuko, C. (2019). Carbon Sequestration by Wetlands: A Critical Review of Enhancement Measures for Climate Change Mitigation. *Earth Systems and Environment*, 3(2), 327–340. <https://doi.org/10.1007/s41748-019-00094-0>.

Yipp, M. W., Hau, C. H., & Walthew, G. (1995). *Conservation evaluation of nine Hong Kong mangals*. In *Asia-Pacific Symposium on Mangrove Ecosystems*, 323–333. Springer Netherlands. [https://doi.org/10.1007/978-94-011-0289-6\\_36](https://doi.org/10.1007/978-94-011-0289-6_36).

## Figures and Citations

Figure 1. Google Maps (2020). Modified from Screenshots of *Google Maps Satellite View*. [Image]. [www.google.com/maps/@22.4216753,114.274535,3361m/data=!3m1!1e3](http://www.google.com/maps/@22.4216753,114.274535,3361m/data=!3m1!1e3). [www.google.com/maps/@22.3702425,114.1259256,51413m/data=!3m1!1e3!5m1!1e4](http://www.google.com/maps/@22.3702425,114.1259256,51413m/data=!3m1!1e3!5m1!1e4).

Figure 2. Stevens, J. and NASA Earth Observatory (2020). Mapping the Roots of Mangrove Loss. [Image]. Earth Observatory NASA. [earthobservatory.nasa.gov/images/147142/mapping-the-roots-of-mangrove-loss](http://earthobservatory.nasa.gov/images/147142/mapping-the-roots-of-mangrove-loss).

Figure 4. HK Map Viewer (n.d.). Screenshot from *Map 1904* overlay. [Image]. [www.hkmaps.hk/mapviewer.html](http://www.hkmaps.hk/mapviewer.html).

Figure 5. AFCD (2020). Modified from *Distribution Map*. [Image]. [www.afcd.gov.hk/english/conservation/con\\_wet/con\\_wet\\_man/con\\_wet\\_man\\_dis/images/mangomap.jpg](http://www.afcd.gov.hk/english/conservation/con_wet/con_wet_man/con_wet_man_dis/images/mangomap.jpg)

Figure 6. Waycott, M., et al. (2011). Modified from Figure 6.1 The three zones typical of mangrove habitats in the tropical Pacific, showing the differences in mangrove species typical of each zone. [Image]. [www.researchgate.net/figure/The-three-zones-typical-of-mangrove-habitats-in-the-tropical-Pacific-showing-the\\_fig1\\_259649359](http://www.researchgate.net/figure/The-three-zones-typical-of-mangrove-habitats-in-the-tropical-Pacific-showing-the_fig1_259649359).

Figure 7. AFCD (2020). Images from *Mangrove*. [Image]. [www.afcd.gov.hk/english/conservation/con\\_mar/TKPlus/m\\_h\\_org/mangrove/mangrove.html](http://www.afcd.gov.hk/english/conservation/con_mar/TKPlus/m_h_org/mangrove/mangrove.html).

Bendel, M. (2015). *Avicennia marina flowers Rangitoto NZ*. Wikimedia Commons. [Image]. [upload.wikimedia.org/wikipedia/commons/c/cc/Avicennia\\_marina\\_flowers\\_Rangitoto\\_NZ.JPG](http://upload.wikimedia.org/wikipedia/commons/c/cc/Avicennia_marina_flowers_Rangitoto_NZ.JPG).

Figure 8. Google Earth (2020). Modified from Screenshots of *Google Earth*. [Image]. [earth.google.com/web/@22.41562833,114.27244052,0.40414482a,1768.29507768d,35y,-135.87874854h,48.00940271t,0r](http://earth.google.com/web/@22.41562833,114.27244052,0.40414482a,1768.29507768d,35y,-135.87874854h,48.00940271t,0r).

Figure 9. Google Earth (2020). Modified from Screenshots of *Google Earth*. [Image]. [earth.google.com/web/@22.41853682,114.27516841,388.94339928a,15.43011883d,30y,-134.49620604h,48.99599312t,0r](http://earth.google.com/web/@22.41853682,114.27516841,388.94339928a,15.43011883d,30y,-134.49620604h,48.99599312t,0r).

Figure 15. lokface lokface (2016). Kei Ling Ha San Wan. Screenshot from *Google Maps Street View*. [Image]. [www.google.com/maps/@22.4163351,114.2708397,3a,75y,251.28h,99.1t/data=!3m8!1e1!3m6!1sAF1QipN2sD2D2CNep9--M2PIem2IKpbrd10vpUjAcVsb!2e10!3e11!6shhttps:%2F%2F1h5.googleusercontent.com%2Fp%2FAF1QipN2sD2D2CNep9--M2PIem2IKpbrd10vpUjAcVsb%3Dw203-h100-k-no-pi0-ya276.55612-ro-0-f0100!7i10240!8i5120](http://www.google.com/maps/@22.4163351,114.2708397,3a,75y,251.28h,99.1t/data=!3m8!1e1!3m6!1sAF1QipN2sD2D2CNep9--M2PIem2IKpbrd10vpUjAcVsb!2e10!3e11!6shhttps:%2F%2F1h5.googleusercontent.com%2Fp%2FAF1QipN2sD2D2CNep9--M2PIem2IKpbrd10vpUjAcVsb%3Dw203-h100-k-no-pi0-ya276.55612-ro-0-f0100!7i10240!8i5120).



---

# How can drawing a contrast between China and the United States reveal the effectiveness of their solar energy policies in addressing climate change?

*Kennice K.H. Pong*

---

## Introduction

Climate change is a concerning threat that causes detrimental impacts on the prosperity of our Earth. Specifically, global warming leads to melting glaciers, higher sea levels, and a frequency of natural disasters. In search of mitigation strategies to address climate change, many countries have developed climate policies. For example, China and the United States enforce policies to regulate the implementation of photovoltaic panels, also named solar panels to promote clean energy consumption. The policies are created with the intention to narrow down priorities, set goals for development, allocate resources for infrastructures, reduce greenhouse gas emissions and better prepare populations to adapt and address climate change.

However, even with environmental policies in place, climate change still remains a prominent issue. Thereby, current policy makers are becoming more interested in evaluating the performance of current climate policies. Public policy creation tends to take a circular process through five main stages: agenda setting, policy formulation, policy adoption, policy implementation and policy evaluation (Anderson). While placing equal emphasis on each of the five key stages is important, the last phase of policy evaluation is often overlooked. One of the main reasons is because the evaluation of environmental policy has developed at a slower pace compared to other sectors such as education and welfare (Huitema, Dave, *et al.*). The key criteria of climate change policy evaluation are still not fully understood and agreed upon, creating many challenges for policymakers around the world.

Thus, this paper aims to identify criteria for policy evaluation and use them to evaluate the climate policies of China and the United States. The renewable energy policy of each country will first be evaluated separately, then contrasted in the discussion and conclusion section. The renewable energy policy was chosen for a more in-depth, focused and nuanced analysis.

## 1. Theory: Political Systems Matter

As defined by Paleker, federalism is a form of government where sovereignty is split between the central and local government, meaning that governments are decentralized.

China, maintaining its socialist development, operates under a one-party state called the Chinese Communist Party. The practice allows a unified and multi-level legislative system to co-exist. With a centralized government, China can be more efficient at implementing and executing national policies; and require state governments to seek mandates from the central government. For example, the Chinese government required the ten cities with the worst air quality to change coal consumption patterns through transitioning to renewables. Yet, it is important to note that the “one policy fits all” strategy may not be able to address the needs of distinct communities on a local scale, making a wrong decision by the central government have a greater impact on society.

Oppositely, the federal government of the United States practices democracy which shares political power between the central government and state governments. A decentralized government may benefit from public trust, as the local population is ensured a right to have a voice in government. The build up of trust is the foundation for the legitimacy of public legislations and a functioning government in this system, thereby it is crucial to maintain public participation for social cohesion (OECD). However, Steurer and Clar stated that decentralization enhances the “fragmentation of responsibilities” across different governments, resulting in a lack of coordination and possibly contradictory policies. Moreover, having more policymakers could extend the policy-making process as state governments can have difficulties negotiating agreements.

---

The above article was written as an essay for the G10 Global Politics class, 2021.



## 2. History and Main Criteria of Policy Evaluation

Policy evaluation has gone through a series of developments ever since its introduction by Daniel Lerner and Harold Lasswell in the 1950s. The traditional approach to policy analysis was to analyze the content and process of the policy itself. However, after much state and policy development, the process of evaluating policies has become more complex and dynamic. According to CDC, policy evaluation is a process “to ask the right questions, and use an approach to gather evidence and perform analysis that will enhance the ability of policies to improve public health.” Consequently, a wide range of criteria have been formed in order to reach the vision of a credible and practical policy evaluation. Huitema, Dave, et al analyzed a series of different policy evaluation criteria in Europe, highlighting how each evaluation approach should acknowledge the complexity of climate change and exhibit reflexivity by challenging policies. At the time of writing, no other climate policy evaluation criteria could be found from Chinese or American perspectives. Hence, these European evaluation approaches will be used as the basis for evaluation.

To allow more in-depth and focused analysis, this paper will only evaluate each policy against two criteria: goal attainment and cost effectiveness.

## 3. Renewable Energy Policies

Renewable energy systems were not a mainstream energy option in China or the United States until toxic pollutants from energy emissions (33.1 Gt CO<sub>2</sub> in 2018) increased significantly (IEA). Countries have gradually adapted the use of renewable sources such as solar panels, biogas, geothermal, wind and tidal power with the intention to reduce carbon emissions. Likewise, an increasing emphasis on renewable energy sources is evident in each government’s clean energy policy.

Yet, renewable energy policies are complex as they can be delivered regionally or nationally. While regional policies focus on individual states, national policies rely on national governments to mandate policies. For a more accurate and fair comparison of China’s and the United States’ renewable energy, this paper will compare China’s 13th Five Year Plan for solar energy (2016-2020) and the United States SunShot Initiative (launched in 2011).

Criterion	Guiding Questions to Assess
Goal attainment and effectiveness	Have the policy goals have been achieved or not?
Cost effectiveness	How much economic benefit is delivered per unit of expenditure? (e.g tons of carbon dioxide emissions reduced or number of jobs produced)
Efficiency	Should certain emission reductions be achieved by one sector? Do the benefits outweigh the costs?
Fairness	Have unfair competitive advantages arise due to climate policies? (e.g profit potential from emission trading)
Legitimacy	Does the public accept and abide by the policies?
Coordination	Is the policy well coordinated with other policies?
Legal Acceptability	Are policies aligned with legal principles?

**Table 1.** Huitema, Dave, *et al.* (p183) seven criteria for evaluating environmental policies. The criteria adapts the use of questions for reflecting the policy’s empirical effectiveness; and were chosen to show reflexivity, and to acknowledge the fact that climate policies occur and impact society at all levels.

Goals of China's 13th Five Year Plan for solar energy (International Renewable Energy Agency Renewables Policies Database)

Goal 1: Increase share of non-fossil energy in total primary energy consumption to 15% by 2020

Goal 2: Facilitate research and development for key technologies and manufacturing processes for Photovoltaics

Goal 3: Increase the manufacturing of PV systems and increase installed renewable power capacity to 680 GW by 2020

Goal 4: Solar PV to become important clean energy source enabling cleaner air and lower greenhouse gas emissions

Goals of The SunShot Initiative of the United States (Solar Energy Technologies Office)

Goal 1: Reduction of the use of fossil fuels and need for conventional generation

Goal 2: Lower the costs of solar energy to make it cost-competitive with other forms of energy generation by 2020

Goal 3: Reach 50% reduction of the cost of solar energy by 2030

Goal 4: 85% increase in renewable energy investment

## 4. Evaluation of China's 13th Five Year Plan

*References to numbered goals are references to the goals of the China's 13th Five Year Plan for solar energy as listed under section 3.*

### 4.1 Goal attainment and cost effectiveness

The 13th Five Year Plan for solar energy led to rapid development in the solar industry. As part of the plan, China pledged to increase renewable energy and nuclear power consumption from 12.3% in 2015. By the end of 2020, China surpassed this target by reaching 15.9% share of non-fossil fuels in primary energy consumption (Lewis and Edwards). China also focused on accomplishing 110 gigawatts (GW) of installed solar power capacity; and managed to surpass this goal as well. Accordingly, Goal 1 of the Five Year Plan to increase the share of non-fossil energy in total primary energy consumption to 15% by 2020 was achieved.

China is well-renowned as the biggest investor in

renewable energy, investing nearly \$760 billion USD between 2010 and 2019, doubling the investment made by the U.S. Renewable energy investments to assist and accelerate the transition from power plants to renewables. Striving towards Goal 2 of the Five Year Plan led to the creation of green jobs, greater economic productivity, and economic benefits. According to a study by UC Berkeley and Tsinghua University, the current rate of clean energy transition can bring a 7.5% increase to China's GDP and its clean jobs by 5.9% to total jobs by 2030 (Jiang and Gang). More specifically, solar heating and cooling services account for two million jobs in China — ranging from sales, engineering, and finance to highly demanded on-site maintenance workers as the panels require regular cleaning. The job growth shows how China's solar energy sector has the potential to create many social benefits and improve living standards and quality of life for citizens.

With state subsidies of around 60 billion RMB per year, production costs for solar power dropped and allowed the business to be increasingly profitable (Wu). Consequently, China has 281.5 GW of installed wind generation capacity and 253.4 GW of solar generation capacity. The development of the solar energy industry made significant changes at a local level, but it is also impacting international renewable energy industries. For example, China now produces 70% of the world's solar photovoltaic panels, implying that countries that wish to reach their corresponding renewable energy goals are likely to rely on China's clean energy manufacturing power (Wu). With sufficient energy infrastructure in China and saturated local demand, Chinese companies will target international markets and technologies abroad. The situation is a valuable opportunity for China to lead the development of clean energy technologies, ultimately boosting the clean energy economy globally. This contributes to the success of Goal 3 of the Five Year Plan.

Another critical factor that facilitated success in China's transition from power plants to renewable energy is citizen participation. After the air apocalypse happened—where smog and pollution made the country uninhabitable (Seligsohn) —demand for environmental improvements in relation to Goal 4 of the Five Year Plan increased from the general public. In response to public concerns, the Chinese government committed to plans that reduce steel and coal production and consumption, accelerating the development of renewable industries. To alleviate the burdens of people who lost their jobs, the government also started a fund of RMB 100 billion. The involvement of citizens in the 13th Five Year Plan shows the Chinese government's

effective full decision-making power and capability to recognize all stakeholders to make meaningful engagements throughout the planning and practice of policies. As explained in Cattino and Reckien's study, public participation in local climate plans is of paramount importance to raise the productivity of the plans as citizens are more willing to cooperate, leading to better "transformative potential of adaptation" and more "resilient communities."

## 4.2 Arising challenges from 13th Five Year Plan

Though the rise of the solar energy industry is evident, the Chinese government is narrowing financing channels and electricity subsidies due to a budget shortfall of 112.7 billion in 2018 (Lewis and Edwards). Lack of funding and problems with distributing subsidy payments led to a 31.6% drop in solar capacity in 2019, deterring renewable energy companies from continuing the development of renewable technologies. Downsizing subsidies for solar power could cause an increase in thermal power plant production. The regression back to fossil fuels is highly concerning as carbon emissions will rise to 14.8 billion tons, causing further detrimental effects on the environment (Guo, *et al.*).

Apart from cutting subsidies, the government made an exemption to its previous shutdown policy for coal power plants, posing more challenges to the solar industry. The exemptions first happened in 2017 due to winter heating and natural gas shortages which angered Chinese citizens (Lewis and Edwards). In response, Beijing ordered local governments to prioritize energy supply and thus revert to coal-fired heating methods. The preference for coal power instead of renewables for energy infrastructure suggests that solar energy has not made enough significant contribution yet. Moreover, coal resurface was triggered after the GDP of China dropped to 6.1%, and governments increased coal plant development to 106.2 GW) to rebound economic revenue (Lewis and Edwards). In this sense, China is still relying on coal power for economic expansion, suggesting that solar energy still has a long way to go.

Another challenge that is faced will be due to solar energy curtailment. Some photovoltaic power stations with proportions of solar energy can not function properly, leading to variability in the renewable energy generation process. In 2016, the national average curtailment rate for solar energy reached 10.3% (Auffhammer, *et al.*). The curtailment poses difficulty in maintaining a balance between load and generation of the system, wasting a high number of solar electricity. China contributed efforts to combat

the issue, allowing curtailment rates to decline. Yet, it remains a concerning issue in northwestern provinces where 91.4% of rejected solar energy occurs (Tang, *et al.*). Solar energy curtailment negatively impacts the development of renewables as it takes away investment value, wastes energy, decreasing energy efficiency, shortening the lifespan of the technology. To tackle this problem, the government should motivate grid companies to build transmission channels and purchase renewable electricity so all renewables can be connected to the grid and reduce curtailment rates.

## 5. Evaluation of sunshot initiative of the United States

*References to numbered goals are references to the goals of the SunShot Initiative of the United States as listed under section 3.*

### 5.1 Goal attainment and cost effectiveness

With policies implemented from the SunShot initiative, the U.S solar industry reached a record of 19.2 GW of installed capacity, accounting for 43% of total new electricity-generating capacity in 2020. The decrease in dependence on conventional generation relating to Goal 1 of the SunShot Initiative created significant environmental and health benefits. Specifically, it was shown by Roberts that the use of renewables resulted in an annual reduction of 17 million metric tons of CO<sub>2</sub>. Simultaneously, this led to visible improvement in air quality, evident through fewer adolescents suffering from asthma attacks and fewer people dying of respiratory and circulatory diseases as well.

Contrasted to China, the U.S approach emphasizes Goal 2 and 3 of the SunShot Initiative which is to reduce the costs of individual solar panels and technologies. The policy aimed to drive the cost of solar power down to 6 cents a kilowatt-hour by 2020. To reach this goal and Goal 4 of the SunShot Initiative, the Department of Energy (DOE) provided a funding of \$46.2 million (USD) to facilitate and support innovative companies that develop solar power technologies that improve reliability and energy efficiency. Aside from collaborating with universities, laboratories and entrepreneurs, the DOE also supported small local businesses that are setting out in the early stages of research and development of new photovoltaic technologies (Clover). The funding has been successful as it allowed communication with all relevant stakeholders, enabling the solar industry to meet its solar cost target three years earlier than anticipated. The achievement in reducing solar costs creates long-

term benefits including increasing demand for solar energy, stimulating competition among companies and ultimately leading to higher solar incentives for either self-consumption or to sell renewable electricity with feed-in tariffs.

In addition to the reduction of solar costs, the industry demonstrates sustainable economic growth through the generation of new solar jobs. Whilst China is still dependent on its coal industry for economic growth, the U.S solar industry accounts for approximately 335,000 workers which is outnumbering 211,000 workers in the coal mining and fossil fuel extraction sector (Marcacci). A main reason driving the rapid increase in solar jobs is because the sector does not require high-skilled workers with advanced college degrees. Moreover, working in a clean energy profession can equal to a 8% to 19% increase in income, ultimately creating motivation for most coal-dependent communities to transition to clean energy as well (Marcacci). The promotion and adaptation of clean jobs contributes to a smooth transition to a clean economy. As new renewable energy becomes cheaper to operate than coal plants, this will increase incentives for businesses to use solar and other renewable alternatives during the production of services or goods. More specifically, it was proven in 2018 that running 74% of existing coal fired generation results in higher spending than replacing all power plants with wind or solar generation within 35 miles (Marcacci). The numbers will increase even when federal renewable energy tax credits phase out, showing how the solar industry has potential to create even more social and economic opportunities.

## **5.2 Arising challenges from the sunshot initiative**

As evaluated previously, China relies on domestic production thereby allowing it to gain a leadership position in the development of renewable technology. Oppositely, the U.S solar industry is becoming overly dependent on foreign producers for materials and products. Currently, there are no longer any silicon solar cell manufacturers in the U.S, and SolarWorld Americas — once a solar pioneer that made historical technological influence on the solar industry is now out of business due to drop in revenues (Pickerel). This resulted in U.S dependency on foreign technology, with 90% of U.S. solar panels being produced overseas (Groom). The over dependence on foreign technology makes the U.S. solar industry vulnerable to economic and political crisis. Learning from the energy crisis between Russia and Eastern Europe, it was revealed that a supply chain that is highly dependent on a country with a geopolitical adversary may increase risk

of retaliation by a foreign government (Williams and Sutton). This suggests how the U.S should rely more on domestic production to prevent unwanted security threats from external disruptions such as natural disasters, geopolitical tensions and pandemics.

The execution of the SunShot Initiative is also impacted by external factors from the former President Donald Trump's trade policies with China. The U.S administration imposed tariffs on more than \$250 billion worth of Chinese goods across various industries (Thomas), including at least hundred of megawatts of solar panels from China's Hoshine Silicon Industry Co detained at borders. Moreover, Section 201 of the Trade Act of 1974 details that the President of the U.S may impose import duties on goods entering the U.S; this has led to many solar modules being restricted at borders regardless of their country of origin. It was observed that the legislation led to a 30% tariff on all imported silicon photovoltaic modules and solar panels (Thomas). The tariffs aggravate the problem of supply shortages, creating an upward pressure on the purchase price of solar panels in the U.S. This is detrimental as it may discourage stakeholders and industries to use solar panels and other renewables for electricity, ultimately creating adverse impacts on the natural environment.

While China operates under a centralized government, the federal government of the United States is decentralized. The regime allowed dispersion of opinions within the two political parties — the Republican Party and the Democratic Party — and this may slow down the process of policy negotiation and the implementation of legislation for solar development. As written by Kennedy and Spencer, the partisan gaps on supporting solar and wind power are now larger than at any point in 2016. To illustrate, 82% of Democrats believe that generating electricity from solar panels is beneficial for the environment, while only 45% of Republicans support the same belief. Besides, Republicans are more likely to say that renewables are unreliable sources and more expensive compared with other energy providers. The divided views on renewables may interrupt the implementation of solar and renewables on a national level, and this alerts the government to take such opinions into consideration when revising policies.

## Conclusion

Climate policy is a relatively young field of study but has shown its potential to make mitigation and adaptation strategies towards climate change. This paper has drawn on an evaluation of China's 13th Five Year Plan for solar energy, and the U.S SunShot Initiative to evaluate how different policy approaches can result in contrasting outcomes.

In terms of criteria, goal attainment and cost effectiveness were used to compare the effectiveness of each country's climate policy. Specifically, it was shown that China focused on mass production of solar panels through government subsidies which increased industry incentives to use solar energy; oppositely, the U.S emphasized the importance of accelerating the process reducing costs instead. Interestingly, the two contrasting approaches were both successful as it managed to reach and exceed goals for installed solar capacity, ultimately leading a smooth energy transition from fossil fuels to renewable energy.

As a general observation, the analysis shows that relying on domestic production offers more flexibility compared to offshore manufacturing. China now produces 70% of the world's solar energy, dominating energy manufacturing power that can be used as a catalyst for a clean energy economy. Conversely, there are no longer any solar cell manufacturers in the U.S, making its renewable sector heavily dependent on foreign technology. This makes the renewable sector vulnerable to security threats, disruptions and geopolitical tensions. Consequently, it is advised that countries gain inspiration from innovative products abroad but ensure local manufacturing at the same time.

The results of this study also show that taking into account political factors such as regime types, public participation, leadership styles and political theories make a difference in policy evaluation. China operates with a centralized government, allowing it to implement national policies with full decision power. Similarly, the air apocalypse in 2013 compelled Chinese citizens to feel a sense of urgency to combat air pollution (Seligsohn), thereby facilitating cooperation and communication between the Chinese government and relevant stakeholders. Contrarily, the U.S federal government is decentralized, allowing for diversity of opinions. The split in attitudes towards solar energy may pose challenges for the government to address all of the public's concerns thus reducing the effectiveness of the policies.

The 13th Five Year Plan of China and SunShot Initiative of the United States were successful but had

limitations in their own ways. It can be concluded that there is a growing momentum around energy policy and the clean policies of the countries revealed their high efforts in addressing climate change. After revising the policies, it is predicted that the clean energy policies will continue and drive technological advancements in the solar energy sector.

Therefore, evaluating successful and unsuccessful strategies to address clean energy holds much value to improve renewable energy initiatives around the world; and this reflects how policy evaluation should be conducted. Applying criterias identified and used in this paper to other policies including water pollution, transportation, waste and resource management would enable policymakers to craft meaningful policies that better address climate change.

## References

- Anderson, James E. (1979). *Public Policymaking: An Introduction*. 2nd ed., Houghton Mifflin.
- Auffhammer, M. *et al.* (2021). Renewable Electricity Development in China: Policies, Performance, and Challenges. *Review of Environmental Economics and Policy*, 15(2), 323–339., doi:10.1086/715624.
- Cattino, M., & Diana, R. (2021). Does Public Participation Lead to More Ambitious and Transformative Local Climate Change Planning? *Current Opinion in Environmental Sustainability*, 52, 100–110., doi:10.1016/j.cosust.2021.08.004.
- CDC (2022). *CDC Policy Process*. www.cdc.gov/policy/analysis/process/index.html.
- Clover, I (2017). US Department of Energy Backs Solar with Further \$46.2m for SunShot Initiative. *Pv Magazine International*. www.pv-magazine.com/2017/07/13/us-department-of-energy-backs-solar-with-further-46-2m-for-sunshot-initiative/.
- Groom, N. (2021). Tariffs, Seizures Expose U.S. Solar Industry's Vulnerability to Imports. *Reuters*. www.reuters.com/business/environment/tariffs-seizures-expose-us-solar-industrys-vulnerability-imports-2021-09-28
- Guo, Z., *et al.* (2020). The Impacts of Reducing Renewable Energy Subsidies on China's Energy Transition by Using a Hybrid Dynamic Computable General Equilibrium Model. *Frontiers in Energy Research*, 8. doi:10.3389/fenrg.2020.00025.
- Huitema, D. *et al.* (2011). The Evaluation of Climate Policy: Theory and Emerging Practice in Europe. *Policy Sciences*, 44(2), 179–98. JSTOR, <http://www.jstor.org/stable/41486829>. Accessed 30 May 2022.
- IEA (2019). Global Energy & CO2 Status Report 2019 – Analysis - IEA. *IEA.org*. www.iea.org/reports/global-energy-co2-status-report-2019/emissions.
- IRENA Renewables Policies Database (2021). China 13th Renewable Energy Development Five Year Plan (2016-2020) – Policies. *IEA*. www.iea.org/policies/6277-china-13th-renewable-energy-development-five-year-plan-2016-2020.
- Jiang, L. & He, G. (2021). China Can Benefit from a More Ambitious 2030 Solar and Wind Target. *China Dialogue*. chinadialogue.net/en/energy/china-can-benefit-from-a-more-ambitious-2030-solar-and-wind-target/.
- Kennedy, B. & Alison, S. (2021). Most Americans Support Expanding Solar and Wind Energy, but Republican Support Has Dropped. *Pew Research Center*. www.pewresearch.org/fact-tank/2021/06/08/most-americans-support-expanding-solar-and-wind-energy-but-republican-support-has-dropped/.
- Lerner, D. *et al.* (2002). *The Policy Sciences: Recent Developments in Scope and Method*. Ann Arbor, Mi, 2002.
- Lewis, J. & Laura, E. (2021). Assessing China's Energy and Climate Goals. *Center for American Progress*. www.americanprogress.org/article/assessing-chinas-energy-climate-goals/#:~:text=China%20was%20able%20to%20meet,from%2012.3%20percent%20in%202015.
- Marcacci, S. (2022). Renewable Energy Job Boom Creates Economic Opportunity as Coal Industry Slumps. *Forbes*. www.forbes.com/sites/energyinnovation/2019/04/22/renewable-energy-job-boom-creating-economic-opportunity-as-coal-industry-slumps/?sh=115bfcdc3665.
- OECD (2022). Trust in Government - OECD. *Oecd.org*. www.oecd.org/governance/trust-in-government/.
- Paleker, S. (2006). Indian Political Science Association Federalism: A conceptual analysis. *The Indian Journal of Political Science*, 67(2), 303–10.
- Pickerel, K. (2021). The U.S. Solar Industry Has a Chinese Problem. *Solar Power World*. www.solarpowerworldonline.com/2021/08/u-s-solar-china-polysilicon-battle/.
- Roberts, D. (2016). Solar Power Is Already Saving Lives in the US. Here's How. *Vox*. www.vox.com/2016/5/19/11711040/sunshot-solar-benefits.
- Seligsohn, D. (2016). How China's 13th Five-Year Plan Addresses Energy and the Environment. *Testimony before the U.S.-China Economic and Security Review Commission Hearing on China's 13th Five-Year Plan*, 1–15.
- Solar Energy Technologies Office (2016) The SunShot Initiative. *Energy.gov*. www.energy.gov/eere/solar/sunshot-initiative.
- Steurer, R. & Clar, C. (2015). Is Decentralisation Always Good for Climate Change Mitigation? How Federalism Has Complicated the Greening of Building Policies in Austria. *Policy Sciences*, 48(1), 85–107.
- Tang, N., *et al.* (2018). Solar Energy Curtailment in China: Status Quo, Reasons and Solutions. *Renewable and Sustainable Energy Reviews*, 97, 509–528. doi:10.1016/j.rser.2018.07.021.
- Thomas, L. (2019). The US-China Trade Wars and the Solar Industry. *New Energy Solar*. www.newenergysolar.com.au/renewable-insights/renewable-energy/the-us-china-trade-wars-and-the-solar-industry.
- Williams, M. & Trevor, S. (2021). Creating a Domestic U.S. Supply Chain for Clean Energy Technology. *Creating a Domestic U.S. Supply Chain for Clean Energy Technology*. www.americanprogress.org/article/creating-domestic-u-s-supply-chain-clean-energy-technology/.
- Wu, S. (2021). These Are the Strategies behind China's Ambitious Clean Energy Transition | Greenbiz." *Greenbiz.com*, www.greenbiz.com/article/these-are-strategies-behind-chinas-ambitious-clean-energy-transition.

---

# Isolation and genomic sequencing of *Klebsiella* sp. CTHL.F3a, a cellulolytic strain isolated from Korean Kimchi

Chloe T. H. Lee

---

## Abstract

Second-generation biofuels, generated by the valorisation of ligno-cellulosic waste, are more sustainable and economically efficient than those produced from food sources. However, lignocellulose requires pretreatment in order to release fermentable sugars and a biological approach uses either purified enzymes or cultured microbes. Here the cellulolytic strain *Klebsiella* sp. CTHL.F3a was isolated from *kimchi* (Korean fermented cabbage/vegetables) and its complete genome (6,146,223 bp, GC content 55.21%), comprising a chromosome and a single plasmid, was established through hybrid assembly. Genomic analysis of CTHL.F3a presented a full cellulose degradation pathway. Moreover, the structural analysis of a CTHL.F3a beta-glucosidase via Phyre2 demonstrated similarity to Cel10, a G8-hydrolase previously isolated from *Klebsiella pneumoniae*.

---

## Introduction

First-generation biofuels, which are generated from food sources such as sugar cane or maize, are neither economically efficient nor ethical. In contrast, second-generation biofuels, made from agricultural, industrial or municipal lignocellulosic waste, are considerably more sustainable (Gabrielle, 2008). Nevertheless, plant cellulose requires pre-processing to release fermentable sugars and a biological approach – using either purified enzymes or cultured microbes – can allow this step to be both environmentally and economically viable (Chaturvedi and Verma, 2013).

*Kimchi* is a traditional Korean fermented food made from vegetables that derives its sweetness from the microbial breakdown of cellulose at relatively low temperatures (~10-15 °C). This project screened samples of *kimchi* for cellulolytic bacteria using the ability to grow on carboxymethylcellulose (CMC) agar. Subsequent genomic sequencing not only identified likely cellulose-degraders, but also enabled characterisation of the enzymes and pathways involved (which might be relevant to later cloning, purification or over-expression).

*Klebsiella* sp. CTHL.F3a, isolated from fresh *kimchi*, demonstrated significant cellulolytic activity at ambient temperatures, hence may be useful for the pre-treatment of lignocellulosic waste for biofuel production (Joshi

*et al.*, 2019). Members of the *Klebsiella oxytoca* species complex (KoSC) may be encountered as human commensals and opportunistic pathogens (Yang *et al.*, 2021), but are common plant growth-promoting endophytes (Pavlova *et al.*, 2017; Dantur *et al.*, 2018) that fix nitrogen (Li and Chen, 2020), solubilise soil-bound phosphate (Ahemad and Khan, 2012) and also metabolise cellulose (Dantur *et al.*, Korsa *et al.*, 2022).

## 1. Method

Six different samples of *kimchi* (3 freshly fermented and 3 packaged products), purchased in Hong Kong, were screened for the presence of cellulolytic bacteria using CMC (carboxymethylcellulose) agar, as previously described (Kasana *et al.*, 2008). Twelve colonies identified in this way were further assessed by their rates of growth (OD600 via BMG Labtech CLARIOstar Plus) in Bushnell-Haas medium (BHM) (Bushnell and Haas, 1941) containing either 1% CMC or 1% cellobiose as the sole carbon source. CTHL.F3a, which showed the highest growth rate on both CMC and cellobiose, was passaged for 7 generations on Luria agar before DNA extraction using Invitrogen's PureLink® Genomic DNA Mini Kit.

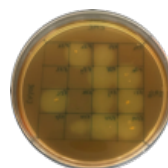


**Figure 1.** Cellulolytic activity was identified by clear zones around colonies on CMC plates stained with aqueous iodine.

---

The above article is a culmination of research undertaken at ISF's Molecular Biology Laboratory, presented at the American Society for Microbiology conference in 2021. It is also an extension of a Genome announcement: Lee, C. T. H., Lai, G. K. K., Griffin, S. D. J., Leung, F. C. C. (2022). Complete genome sequence of *Klebsiella* sp. CTHL.F3a, a cellulolytic strain isolated from Korean kimchi. Microbiology Resource Announcements, 11(8): e0037722. <https://doi.org/10.1128/mra.00377-22>

## 2. Results

### 2.1 Two *Klebsiella* isolates grow well in cellobiose and CM-cellulose

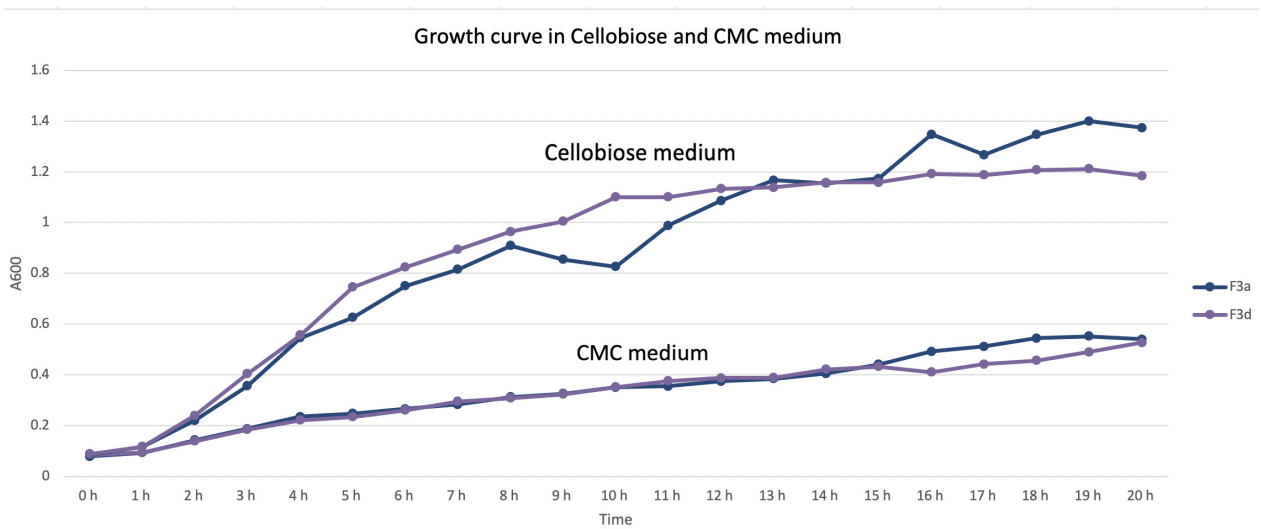


**Figure 2.** Chloe\_S3 and Chloe\_S4 are able to grow in the presence of cellobiose or CMC as their sole carbon sources and demonstrate significant cellulolytic activity at room temperature.

Two cellulose-degrading isolates, Chloe\_S3 and Chloe\_S4, were submitted for short-read sequencing (Illumina MiSeq) and both were found by phylogenetic analysis in PATRIC to be strains of *Klebsiella pasteurii/grimontii/michiganensis* with estimated genome sizes of 6.5 and 6.6 Mbp. Long-reads for Chloe\_S3 were subsequently obtained (Oxford Nanopore MinION) and the complete genome generated by hybrid assembly (see below).

### 2.2 A GH8 endoglucanase is the key enzyme in the biochemical pathway for cellulose degradation

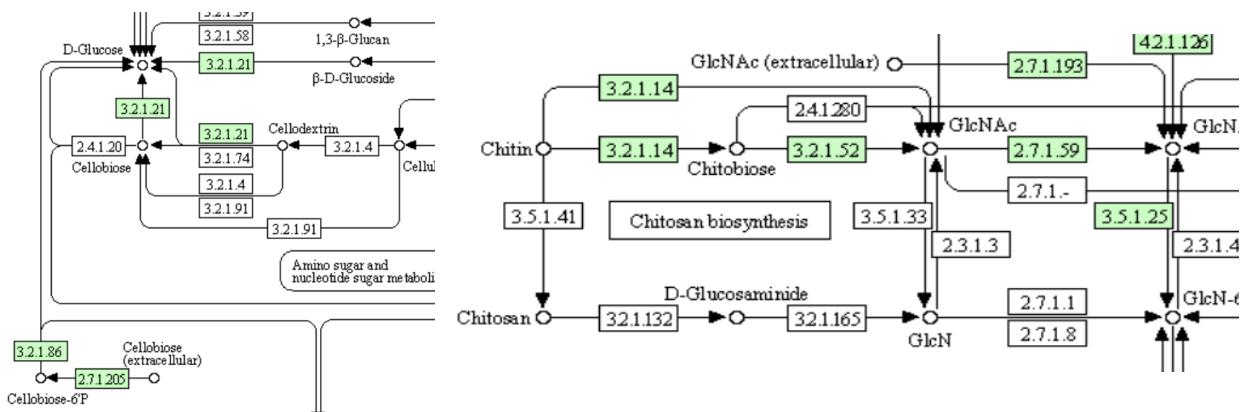


**Figure 3.** Both genomes contain a chitinase (EC 3.2.1.14), as well as a less common endoglucanase (EC 3.2.1.4) [identified by KEGG mapping in PATRIC]. Both 3.2.1.21 and 3.2.1.4 in the cellulose degradation pathway are present.



### 2.3 Phyre2 predicts close structural alignment with a GH8 hydrolase

A predicted model of the tertiary structure of the Chloe\_S3 endoglucanase was generated using Phyre2 (Kelley *et al.*, 2015) and its shape was found to be homologous with a GH8 glycosyl hydrolase, Cel10, previously-reported by Attigani (2016).

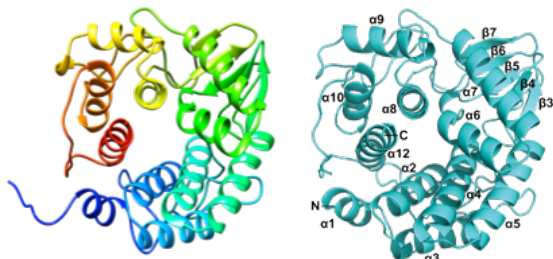


**Figure 4.** The Chloe\_S3 endoglucanase structure predicted by Phyre2 (left) is similar to Cel10 as modelled by Attigani [12] (right), but includes an N-terminal signal peptide.

### 2.4 Hybrid assembly generates the complete genome sequence for Chloe\_S3

Paired-end short-read sequencing libraries were prepared using the NexteraXT DNA Library Preparation Kit and sequenced via the Illumina MiSeq platform with v3 chemistry (2x300 bp). Adapter sequences were removed and reads quality-filtered and trimmed using Trimmomatic v0.32 (Bolger *et al.*, 2014). The resulting Illumina dataset contained 944,534 read pairs with an average length of 297 bp (approximately 263 Mbp). Long-read libraries, prepared from the same extracted DNA using a gDNA rapid barcoding kit (SQK-RBK004), were sequenced using a SpotON flow cell (vR9) and MinION sequencer, with data acquisition using MinKNOW v3.1.8 software and base-calling by Guppy v2.1.3 (all from Oxford Nanopore). The final long-read dataset, trimmed by Porechop v0.2.4 (Wick,

Chloe_S3_endoglucanase	MSLRALATVV-VTTVMMLPHAWADTAWESYKSRFMMPDGRIIDTGNVNSHTEGGGFAML	59
cel10_K_pneumoniae	-----DTAWERYKARFMMPDGRIIDTANGVNSHTEGGGFAML	37
WP_186503954.1	MPLRALVAVILTTAVMLVPRAWADTAWERYKARFMMPDGRIIDTANGVNSHTEGGGFAML	60
CtCelA	FNTKYPYGPTSIADNQSEVTAMLKAEWEDWKSKRITSNAGAGYKRVQRDASTYDVTVSEG	
	***** *:***** .*****	
Chloe_S3_endoglucanase	LAVGNDRPAPFDKLWQWTDKTLRNKENGLFYRYPNPVAPNPVADKNDA TDGDTLIAWALL	119
cel10_Klebsiella	LAVANDRPAPFDKLWQWTDSTLRDKSNGLFYRYPNPVAPDPIADKNNASDGD TLIAWALL	97
WP_186503954.1	LAVANDRPAPFDKLWQWTDSTLRDKSNGLFYRYPNPVAPDPIADKNNASDGD TLIAWALL	120
CtCelA	MGYGLLLAVCFNEQALFDDLYRYVKSHFNGLMHWHIDANNVNTSHDGDGAATDADED	
	***.*****.***.*****.***.*****.***.*****.***.*****.***.*****	
Chloe_S3_endoglucanase	RAQQQWHEKSYGSASDAITASLLKSTVVTFAGRQVMLPGA KGFYLNHDLNLPNSYFIFPA	179
cel10_Klebsiella	RAQKQWQDKRYAIASDAITASLLKYTVVTFAGRQVMLPGVKGFNLNHLNLPNSYFIFPA	157
WP_186503954.1	RAQKQWQDKRYAIASDAITASLLKYTVVTFAGRQVMLPGVKGFNLNHLNLPNSYFIFPA	180
CtCelA	IALALIFADKLWGSSGAINYGQEARTLINNLYNHCVHEGYSVVLKPGDRWGGSSVNPNSYF	
	***:***: * . ***** ***** .** *****	
Chloe_S3_endoglucanase	WQAFARHTLTAWRKLSDGQALLGKMAWGTSQLPSDWVALRADGRMEPAKEWPTRMSFD	239
cel10_Klebsiella	WRAFAERTHTLTAWRTLQTDGQALLGXGWGKSHLPSDWVALRADGKMLPAKEWPPRMSFD	217
WP_186503954.1	WRAFAERTHTLTAWRTLQTDGQALLGMGWGKSHLPSDWVALRADGKMLPAKEWPPRMSFD	240
CtCelA	APAWYKVYAQYTGDRWNQVADKCYQIVEEVKYNNGTGLVPDWC TASPASGQSYDK	
	*:*** *****.***:*****: **.***:*****: * ***** *****	

**Figure 5.** Alignment of Chloe\_S3\_endoglucanase with the GH8 endoglucanases Cel10 from *Klebsiella pneumoniae* (Attigani *et al.*, 2016) and WP\_186503954.1 from *Klebsiella variicola*. CtCelA, the endoglucanase from *Hungateiclostridium* (formerly *Clostridium*) *thermocellum* is also included.

Following Attigani *et al.* (2016), conserved catalytic residues are highlighted in yellow and the aromatic residues forming sugar-recognition subsites are shown in green. Deviations in Chloe\_S3\_endoglucanase are shown in red.

2017; Wick *et al.*, 2017), totalled 310,076 reads (2.16 Gbp) with a median length of 4,365 bp (N50 12,200 bp).

The Illumina and Nanopore datasets were combined using Unicycler v0.4.3 (Wick *et al.*, 2017) to yield a circular chromosome (5,995,415 bp, 55.34% G+C) and a circular plasmid (150,808 bp, 49.79% G+C), with genome coverage of 81x, which were submitted to the NCBI PGAP v5.0 (Haft *et al.*, 2018) and to PATRIC (Brettin *et al.*, 2015) for annotation.

## Conclusion

*Klebsiella* sp. CTHL.F3a appears well adapted to cellulose metabolism. The chromosome has an average nucleotide identity of 99.60% (Yoon *et al.*, 2017) with rice endophyte *Klebsiella* sp. BD134-6 (CP064784) (Bianco *et al.*, 2021). It contains five copies of beta-glucosidase (EC 3.2.1.21); 9 copies of 6-phospho-beta-glucosidase (EC 3.2.1.86); and, both type Ib and type IIa bcs operons (Römling and Galperin, 2015), punctuated by type I toxin-antitoxin system LdrD (Kawano *et al.*, 2002). Phyre2 (Kelley *et al.*, 2015) finds the (type 1b) endo-beta-1,4-glucanase (cellulase) (EC 3.2.1.4) structurally similar to the GH8 glycosyl hydrolase Cel10, previously characterised in a strain of *K. pneumoniae* recovered from the gut of a Chinese bamboo rat (*Rhizomys sinensis*) (Attigani *et al.*, 2016), and which has been shown capable of the hydrolysing crystalline cellulose.

Plasmid pCTHL.F3a was classified as IncFIB(K)\_30 [Clade II] by the KpVR web-based tool (<https://bioinformml.sjtu.edu.cn/KpVR/index.php>) (Tian *et al.*, 2021). It contains the RelBE and PsiAB toxin-antitoxin systems (Grønlund and Gerdes, 1999), but no antimicrobial resistance genes.

## Data Availability

Complete genome sequences and raw sequence data for *Klebsiella* sp. CTHL.F3a are available through NCBI under BioProject PRJNA758781, with GenBank accession numbers CP082360 (chromosome), CP082361 (plasmid) and SRA accessions SRX12151552 (MiSeq), SRX12151553 (MinION).

## References

- Ahemad, M., Khan, M. S. (2012) Biotoxic impact of fungicides on plant growth promoting activities of phosphate-solubilizing *Klebsiella* sp. isolated from mustard (*Brassica campestris*) rhizosphere, *Journal of Pest Science*, 100(1), 51-56. <http://dx.doi.org/10.1007/s10340-011-0402-1>
- Attigani, A., Sun, L., Wang, Q., Liu, Y., Bai, D., Li, S., Huang, X. (2016). The crystal structure of the endoglucanase Cel10, a family 8 glycosyl hydrolase from *Klebsiella pneumoniae*. *Acta Crystallographica. Section F, Structural Biology Communications*, 72(Pt 12), 870–876. doi: 10.1107/S2053230X16017891
- Bianco, C., Andreozzi, A., Romano, S., Fagorzi, C., Cangioli, L., Prieto, P., Cisse, F., Niangado, O., Sidibé, A., Pianezze, S., Perini, M., Mengoni, A., Defez, R. (2021). Endophytes from African Rice (*Oryza glaberrima* L.) Efficiently Colonize Asian Rice (*Oryza sativa* L.) Stimulating the Activity of Its Antioxidant Enzymes and Increasing the Content of Nitrogen, Carbon, and Chlorophyll. *Microorganisms*, 9(8): 1714. doi: 10.3390/microorganisms9081714
- Bolger, A. M., Lohse, M., Usadel, B. (2014). Trimmomatic: a flexible trimmer for Illumina sequence data. *Bioinformatics*, 30, 2114-2120. doi: 10.1093/bioinformatics/btu170
- Brettin, T., Davis, J. J., Disz, T., Edwards, R. A., Gerdes, S., Olsen, G. J., Olson, R., Overbeek, R., Parrello, B., Pusch, G. D., Shukla, M., Thomason, J. A. 3rd, Stevens, R., Vonstein, V., Wattam, A. R., Xia, F. (2015). RASTtk: a modular and extensible implementation of the RAST algorithm for building custom annotation pipelines and annotating batches of genomes. *Scientific Reports*, 5: 8365. doi: 10.1038/srep08365
- Bushnell, L. D., Haas, H. F. (1941). The Utilization of Certain Hydrocarbons by Microorganisms. *Journal of Bacteriology*, 41(5), 653–673. doi: 10.1128/jb.41.5.653-673.1941
- Chaturvedi, V., Verma, P. (2013). An overview of key pretreatment processes employed for bioconversion of lignocellulosic biomass into biofuels and value added products. *3 Biotech*, 3(5), 415–431. doi: 10.1007/s13205-013-0167-8
- Dantur, K. I., Chalfoun, N. R., Claps, M. P., Tórtora, M. L., Silva, C., Jure, Á., Porcel, N., Bianco, M. I., Vojnov, A., Castagnaro, A. P., Welin, B. (2018). The Endophytic Strain *Klebsiella michiganensis* Kd70 Lacks Pathogenic Island-Like Regions in Its Genome and Is Incapable of Infecting the Urinary Tract in Mice. *Frontiers in Microbiology*, 9: 1548. doi: 10.3389/fmicb.2018.01548
- Gabrielle, B. (2008). Intérêts et limites des biocarburants de première génération [Significance and limitations of first generation biofuels]. *Journal de la Société de Biologie*, 202(3), 161–165. doi: 10.1051/jbio:2008028
- Grønlund, H., Gerdes, K. (1999). Toxin-antitoxin systems homologous with relBE of *Escherichia coli* plasmid P307 are ubiquitous in prokaryotes. *Journal of Molecular Biology*, 285(4), 1401–1415. doi: 10.1006/jmbi.1998.2416
- Haft, D. H., DiCuccio, M., Badretdin, A., Brover, V., Chetvernin, V., O'Neill, K., Li, W., Chitsaz, F., Derbyshire, M. K., Gonzales, N. R., Gwadz, M., Lu, F., Marchler, G. H., Song, J. S., Thanki, N., Yamashita, R. A., Zheng, C., Thibaud-Nissen, F., Geer, L. Y., Marchler-Bauer, A., Pruitt, K. D. (2018). RefSeq: an update on prokaryotic genome annotation and curation. *Nucleic Acids Research*, 46: D851–D860. doi: 10.1093/nar/gkx1068

- Joshi, B., Joshi, J., Bhattarai, T., Sreerama, L. (2019). Currently Used Microbes and Advantages of Using Genetically Modified Microbes for Ethanol Production. In Ray, R. C., Ramachandran, S. (Eds.) *Bioethanol Production from Food Crops: Sustainable Sources, Interventions, and Challenges*, Academic Press; Ch. 15, 293–316. doi: 10.1016/b978-0-12-813766-6.00015-1
- Kasana, R. C., Salwan, R., Dhar, H., Dutt, S., Gulati, A. (2008). A rapid and easy method for the detection of microbial cellulases on agar plates using Gram's iodine. *Current Microbiology*, 57(5), 503–507. doi: 10.1007/s00284-008-9276-8
- Kawano, M., Oshima, T., Kasai, H., Mori, H. (2002). Molecular characterization of long direct repeat (LDR) sequences expressing a stable mRNA encoding for a 35-amino-acid cell-killing peptide and a cis-encoded small antisense RNA in *Escherichia coli*. *Molecular Microbiology*, 45(2), 333–349. doi: 10.1046/j.1365-2958.2002.03042.x
- Kelley, L. A., Mezulis, S., Yates, C. M., Wass, M. N., Sternberg, M. J. (2015). The Phyre2 web portal for protein modeling, prediction and analysis. *Nature Protocols*, 10(6), 845–858. doi: 10.1038/nprot.2015.053
- Korsa, G., Masi, C., Konwarh, R., Tafesse, M. (2022) Harnessing the potential use of cellulolytic *Klebsiella oxytoca* (M21WG) and *Klebsiella* sp. (Z6WG) isolated from the guts of termites (*Isoptera*). *Annals of Microbiology*, 72: 5. doi: 10.1186/s13213-021-01662-4
- Li, Q., Chen, S. (2020). Transfer of Nitrogen Fixation (*nif*) Genes to Non-diazotrophic Hosts. *ChemBioChem*, 21(12), 1717–1722. doi: 10.1002/cbic.201900784
- Pavlova, A. S., Leontieva, M. R., Smirnova, T. A., Kolomeitseva, G. L., Netrusov, A. I., Tsavkelova, E. A. (2017). Colonization strategy of the endophytic plant growth-promoting strains of *Pseudomonas fluorescens* and *Klebsiella oxytoca* on the seeds, seedlings and roots of the epiphytic orchid, *Dendrobium nobile* Lindl. *Journal of Applied Microbiology*, 123(1), 217–232. doi: 10.1111/jam.13481
- Römling, U., Galperin, M. Y. (2015). Bacterial cellulose biosynthesis: diversity of operons, subunits, products, and functions. *Trends in Microbiology*, 23(9), 545–557. doi: 10.1016/j.tim.2015.05.005
- Tian, D., Wang, M., Zhou, Y., Hu, D., Ou, H. Y., Jiang, X. (2021). Genetic diversity and evolution of the virulence plasmids encoding aerobactin and salmochelin in *Klebsiella pneumoniae*. *Virulence*, 12(1), 1323–1333. doi: 10.1080/21505594.2021.1924019
- Wick, R. R. (2017). Porechop. <https://github.com/rwick/Porechop>.
- Wick, R. R., Judd, L. M., Holt, K. E. (2018). Deepbiner: Demultiplexing barcoded Oxford Nanopore reads with deep convolutional neural networks. *PLoS Computational Biology*, 14(11): e1006583. doi: 10.1371/journal.pcbi.1006583
- Wick, R. R., Judd, L. M., Gorrie, C. L., Holt, K. E. (2017). Unicycler: Resolving bacterial genome assemblies from short and long sequencing reads. *PLoS Computational Biology*, 13(6): 97 e1005595. doi: 10.1371/journal.pcbi.1005595
- Yang, J., Long, H., Hu, Y., Feng, Y., McNally, A., Zong, Z. (2021). *Klebsiella oxytoca* Complex: Update on Taxonomy, Antimicrobial Resistance, and Virulence. *Clinical Microbiology Reviews*, 35(1): e0000621. doi: 10.1128/CMR.00006-21
- Yoon, S. H., Ha, S. M., Lim, J., Kwon, S., Chun, J. (2017) A large-scale evaluation of algorithms to calculate average nucleotide identity. *Antonie van Leeuwenhoek*, 110(10), 1281–1286. doi: 10.1007/s10482-017-0844-4

[*Klebsiella* sp. BDA134-6  
<https://www.ncbi.nlm.nih.gov/nuccore/CP064784> ]

# Lowering the impact of health risk from air pollution and improving commuter comfort in Hong Kong

Harry J. Chee

## 1. Problem Statement

Air pollution is the harsh consequence of industrial growth across the world. In Hong Kong (HK); it can be divided into roadside (street-level) pollution and regional smog. “Diesel vehicles, particularly trucks and buses, are the main source of roadside pollution” (GovHK).

For over 30% of the year, visibility is less than 8 kilometres (AirVisual). This reduction in air quality has aggravated cases of bronchial infections and asthma; it also causes irritation to many parts of the body (CHP).



Figure 1. Pedestrians waiting for the bus while covering their mouth (The Standard) \*Image has been edited

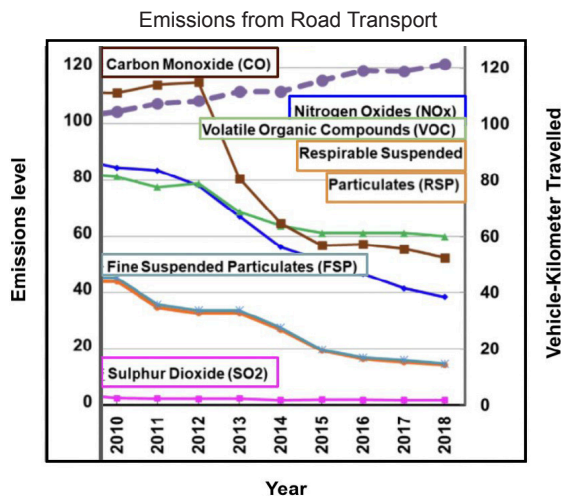


Figure 2. Road transport emissions 2010 - 2018 (“Air Pollution Control Strategies”)

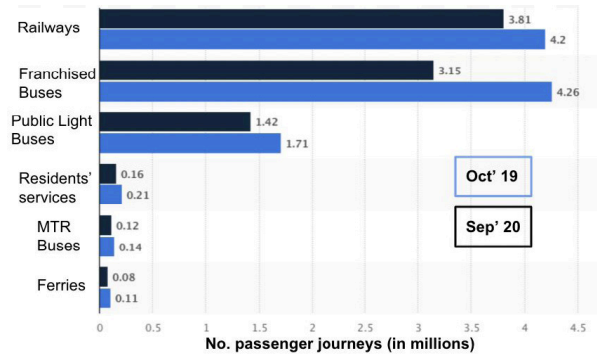


Figure 3. Average daily number of public transport passenger journeys in HK by mode of transport (Wong)

Every day, about 8.9 million passenger journeys are made on a public transport system; 3 million of which are by bus (Transport Department Q1+2)



Figure 4. Observation of South Horizons Mei Fai Court bus stop

## 2.1 Product analysis

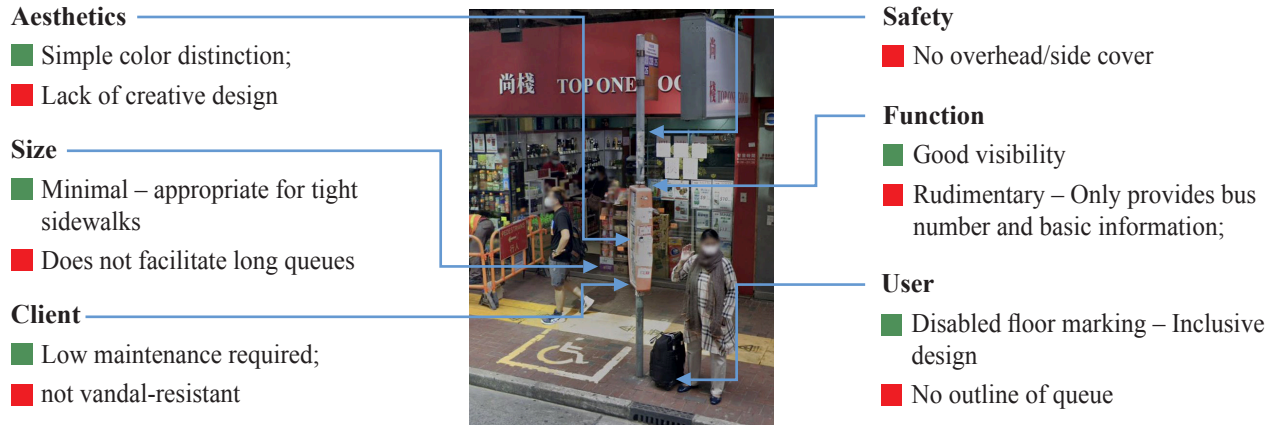
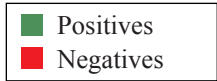


Figure 5. Cnt Tower, Henessery Road bus stop (Google Maps)

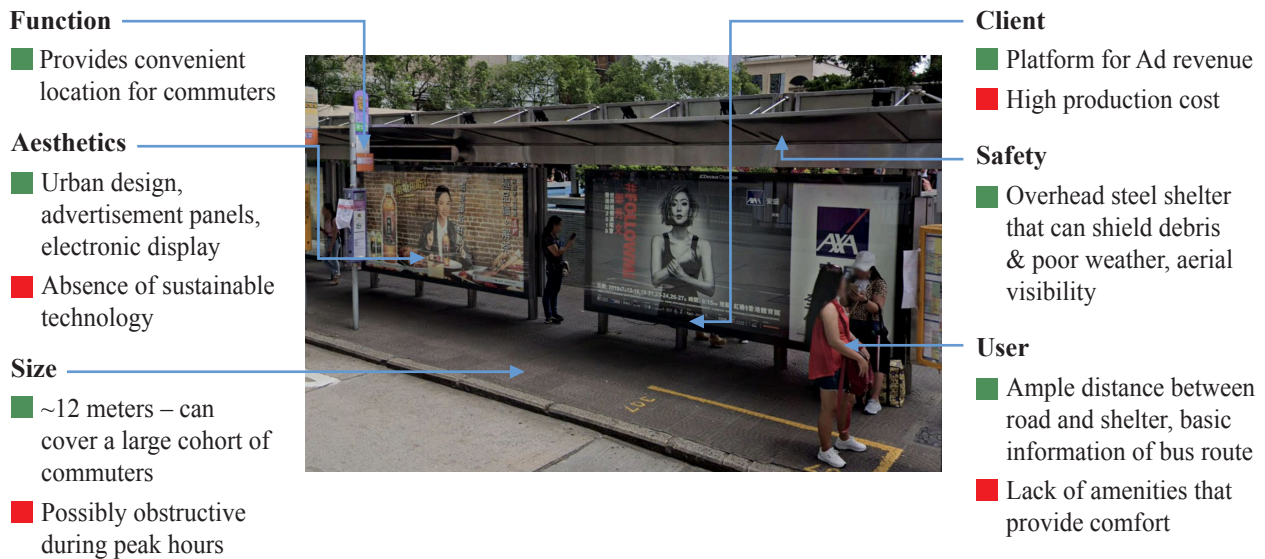


Figure 6. Statue Square, Des Voeux Road Central bus stop (Google Maps)

## 2.2 Potential technologies (solutions)

### Solar Glass

- Transparent photovoltaic glass
- \$130 per sqm; varies considerably (Snowden)
- Operates identically to conventional glass
- Thermal & Sound insulation (Onyx Solar)

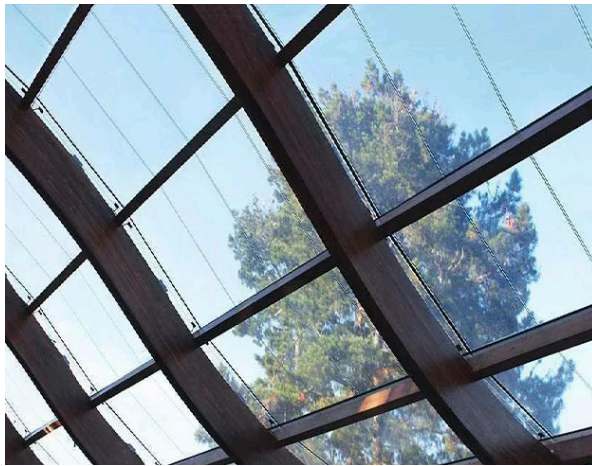


Figure 7. Solar Glass (Onyx Solar)

### HEPA Filter (“What are HEPA filters and how do they work?”)

- Generally made of fibreglass. These arbitrarily arranged fibres form a mesh-like lattice (What are HEPA filters and how do they work?)
- Removes at least 99.97% of airborne allergens & pollutants (“Pros + Cons of The 7 Main Types of Air Filters.”)
- Expensive (“GovHK: Air Quality in Hong Kong.”)

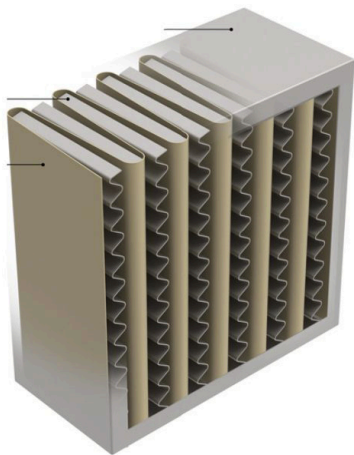


Figure 8. HEPA Filter (“What are HEPA filters and how do they work?”)

### Vertical WallGarden (“Boost Your Backyard with a Vertical garden.”)

- Plants grown on hydroponics suspended or attached to a wall (“What are Vertical Gardens?”)
- Natural clean air system; structure beautification
- \$195 – \$265 per sq ft; varies depending on project. (“Vertical Gardens & Living Walls”)



Figure 9. Vertical Wall Garden (“Boost Your Backyard with a Vertical garden.”)

### Summary

The lack of consideration in terms of commuter comfort and safety gives rise to a design opportunity. Figures 6 & 7 show the strengths and weakness of current products in Hong Kong. Figure 8, 9, 10 display various possible options capable of alleviating the problem to a certain degree. Extra research (in bibliography) also showcases a multitude of studies conducted around the globe, which have identified the needs of commuters and improvements to be made to bus stops in the future.

### 3. Design Brief

#### Objective (Solution):

- Retrofit current bus shelters for better user experience
- Sustainable technology to be implemented (E.g. Solar panels, wall gardens)
- Reduce impact of poor air quality due to existence of street canyons
- Targeting bus users of all ages
- Incorporate cradle-to-cradle design philosophy; Integrate into circular economy model. It should be sustainable for long-term use. “Made to be made – when a product is designed to be made again using the same material of the original product, once it has been disposed of” (Trumpold).

#### Constraints:

- Budget: N/A → £1,054 in UK (“Bus Shelters”), \$12,095 in CAN (Crosse), \$5,500 in US (Schmitt)
- Legal (LCQ3): Strict guidelines issued by Transport Department (“Hong Kong: The Facts - Transport”); Needs to meet requirements with other relevant government departments (E.g. Highways Department). Only franchised bus companies can apply to erect a bus shelter.
- Timescale: There will only be 10 hours to design and prototype the product
- Materials: There are only limited resources available

#### Manufacturing Processes:

- Initial prototypes to be made from cardboard and Computer-Aided-Design (“CAD”) → Based on fidelity
- Scaled mockup generated in Fusion 360, then 3D printed for feedback
- Final product completion depends on circumstances




Figure 10. Visual representation of target audience

#### Persona Mapping

Target Audience: Residents of Hong Kong who use the public bus franchise services

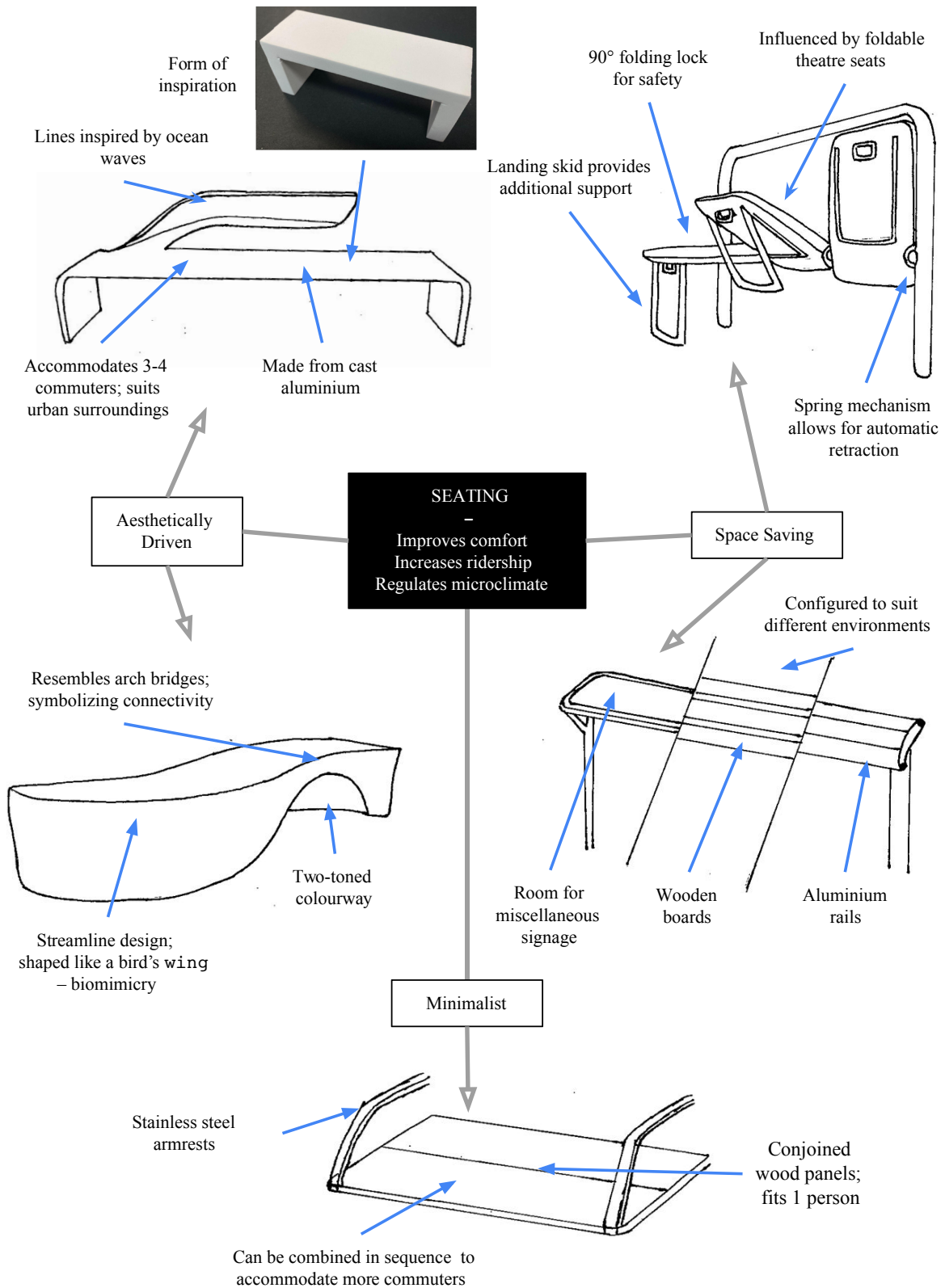
- 5 licensed bus franchises – 631 routes – Carries roughly 3,000,000 total passengers per day (“Hong Kong: The Facts - Transport”)
- Commuters wait 10 minutes at a bus stop on average, but over 29% wait for over 20 minutes (Moovit Public Transit Index)
- 58% or some 3,927,800 (Out of 6,781,100) Hong Kong residents aged 2 and above made mechanised trips on weekdays (Travel Characteristics Survey 2011)
- Buses are a common choice because they are relatively cheap, and they cover for the shortcomings of the railway system.

## 4. Design Specifications

Specification (In order of priority)		Justification
1. Function	1.A Must fulfill all basic functions of former product – A safe & convenient space for commuters; signage providing bus routes/ timings.	1.A As demonstrated by the 2 examples in A1 product analysis (“PA”), there are a set of essential aspects a bus stop must have in order to qualify as satisfactory.
	1.B Incorporate at least 1 technological device that reduces health impact of surrounding air.	1.B This incremental solution should aim to retrofit such advancements (A1 potential technologies (“PT”)), to current bus stops with intention to improve waiting environment.
	1.C Provide comfort (thermal & acoustic) and (weather/debris) protection for commuters; allows for clear visibility of oncoming buses and easy access for boarding.	1.C Increased comfort in bus shelters will reduce perceived waiting times (A1 Interview). It should also be a requirement to reduce safety/health risk of commuters.  <b>Significance:</b> Research conducted in A1 & A2 present a design opportunity that is worth refining and upgrading.
2. Safety	2.A Appropriate forms of shelter – roofs, side panels, leaning/safety rails.	2.A Not every stop can accommodate shelter (A1 PA), due to other factors such as space and location. However, equipment capable of physically protecting commuters and make them feel safe and is welcomed.
	2.B Sufficient lighting to illuminate surroundings; especially during eventide and inclement weather.	2.B Well-lit surroundings generally create a safer and visually permeable environment (A1 Research). They can also be part of a design.  <b>Significance:</b> A safe environment encourages ridership and facilitates a better bus experience.
3. User / Target Audience	3.A Comfort oriented amenities (E.g benches, leaning rails)	3.A Such items will improve waiting experience, and should match vehicle characteristic to enhance seamlessness in transition from waiting to boarding
	3.B Amenities are recommended but not necessary. (Eg. waste bins, mail boxes, art, and public phones).	 <p><b>Figure 11:</b> Modern bench (Avenezia)</p>
	3.C Full disclosure of any information appurtenant to the commuter.	3.B Installments positively influence the perceptions of public transport for the pedestrians and drivers in the surrounding area (A1 Research).  3.C Most important are schedule and arrival information. The latter needs more improving mostly in Hong Kong (A1 PA & Interview). If appropriate, community information and wayfinding indications may also be included.  <b>Significance:</b> These improvements will better customer perception and incentivise bus travel.

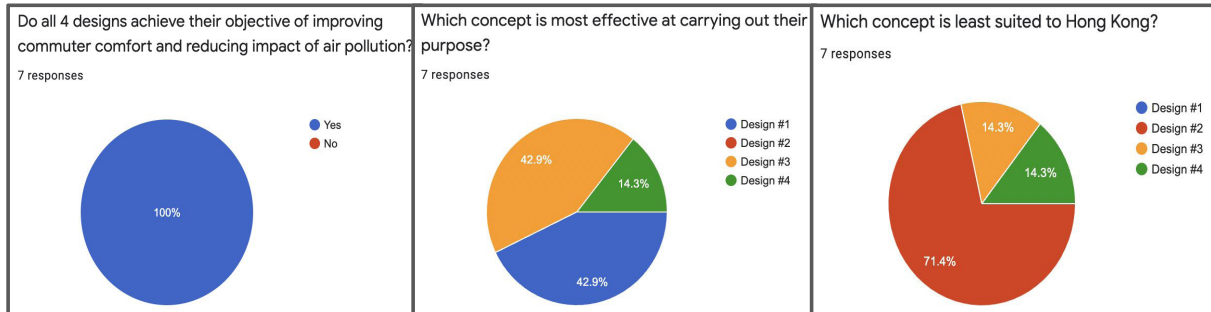


## 5. Initial Ideas



## 6. Developed Ideas and User Feedback (Benefits, Potential Improvements, Limitations)

Questionnaire results: All 7 participants of the focus group are members of the target audience; their ages range from 15 - 77.



<p><u>Design 1</u></p>	<p>Expert Appraisal</p> <ul style="list-style-type: none"> <li>- Interactive display is an interesting feature</li> <li>- 'Kerb light' is not in an optimal location</li> <li>- Production costs would be relatively high, especially due to the OLED screen.</li> </ul> <p>Synthesis: Comments are mostly favourable as it fulfills its purpose, though some parts require further development.</p>	<p>Commuter response</p> <ul style="list-style-type: none"> <li>- Joint most effective solution</li> <li>- Lots of informative components</li> <li>- Ample space for waiting</li> <li>- Feels a little claustrophobic</li> </ul>
------------------------	--	--

<p>Expert Appraisal</p> <ul style="list-style-type: none"> <li>- Simple and practical base design</li> <li>- Intelligent air filtering system</li> <li>- Audacious canopy design is unfeasible in HK</li> <li>- Concerns regarding clearance and structural integrity</li> </ul>	<p>Commuter Response</p> <ul style="list-style-type: none"> <li>- Use of leaning rails is space efficient</li> <li>- Arrival light is superfluous</li> <li>- Canopy design is creative but out-of-place</li> <li>- Least appropriate solution for HK's problem</li> </ul>	<p><u>Design 2</u></p>
<p>Synthesis: Comments are mixed. Where most criticism is attributed to the canopy design.</p>		

<p><u>Design 3</u></p>	<p>Expert Appraisal</p> <ul style="list-style-type: none"> <li>- Versatile design that incorporates many functions; perhaps the newsstand could be replaced by vending machines to automate more processes</li> <li>- Pertinent use of innovative and eco-friendly technologies</li> <li>- Size is obstructive</li> </ul>	<p>Commuter Response</p> <ul style="list-style-type: none"> <li>- Joint most effective solution</li> <li>- Aesthetic is coherent with HK's urban outlook</li> <li>- Does not offer best weather protection</li> <li>- Dot matrix display is quaint</li> <li>- Far too big for most sites within the city</li> </ul>
<p>Synthesis: Comments are mostly favourable, with praise directed towards its construction. However, compromises must be made to reduce structure size.</p>		

<p>Expert Appraisal</p> <ul style="list-style-type: none"> <li>- Safety and comfort is excellent</li> <li>- Appropriate for any climate condition and time of day</li> <li>- Colour scheme is relatively ill-chosen</li> <li>- High demand for power may worsen initial problem</li> </ul>	<p>Commuter Response</p> <ul style="list-style-type: none"> <li>- Design is luxurious and places commuter comfort as top priority</li> <li>- Ranked 3rd best overall</li> <li>- The nature of design suggests structure can be exploited for different use</li> <li>- Automatic doors are excessive</li> </ul>	<p><u>Design 4</u></p>
<p>Synthesis: Comments are generally favourable, though some components may be too lavish for a bus stop. There is certainly room for improvements.</p>		

## 7.1 Concept modelling (design 1+3+4)

**MEDIUM FIDELITY SCALE MODEL:** Made primarily out of cardboard, this physical model is the unification of design 1, 3, and 4, as they received positive reviews. Having downscaled, it lacks functionality and can only be observed for feedback.

Rogers' Characteristics: Relative advantage increased and thermal and acoustic comfort; more functionality due to new technologies

Rogers' Characteristics: Observability – placement of interactive (haptic) screens

Materials: Powder coated aluminium; durable and aesthetically pleasing

Size: Entrance is non-parallel to street; saving space

Rogers' Characteristics: (Low) complexity – simple layout that maximises available space

Function: Side glass cut out offers extra visibility of oncoming buses

Safety: Railings provide separation and support for commuters

Materials: Plastic bench; low-cost but unsustainable (FEA below)



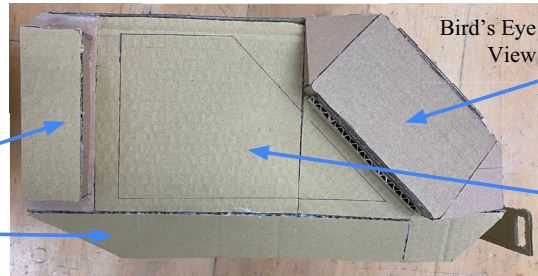
Rogers' Characteristics: Compatibility – pillar displays static information of bus service; available on both sides

User: Scaled down human figure (1.8m) relative to structure

Aesthetics: Glass panels increase visibility and allow passing of natural light

Function: Electricity storage; stores excess for night use (when there is no sunlight)

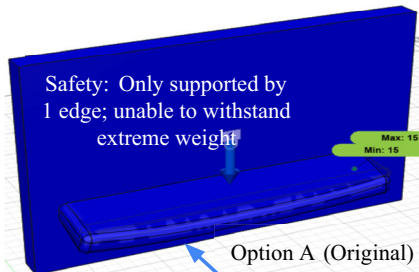
Function: Extruding canopy offers extra weather protection



Function: Air purification unit draws in polluted air from above

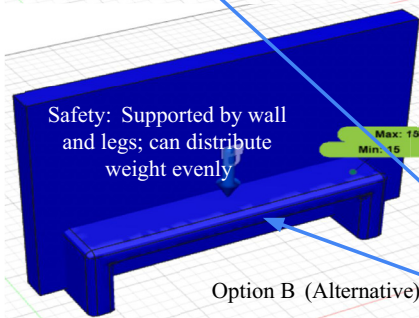
Function: Solar photovoltaic glass; covers central area of shelter (trapezoid)

Finite Element Analysis (FEA)



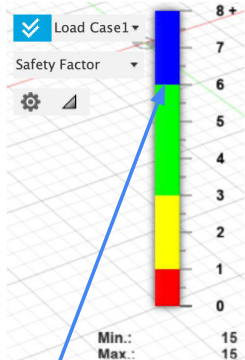
Safety: Only supported by 1 edge; unable to withstand extreme weight

Max: 15  
Min: 15



Safety: Supported by wall and legs; can distribute weight evenly

Max: 19  
Min: 15



Safety: Dark blue means both bench designs are safe  
Safety: Option A has a risk of deformation after prolonged stress/strain  
Materials: Can be reinforced by changing to composite material (e.g. Plastic lumber)

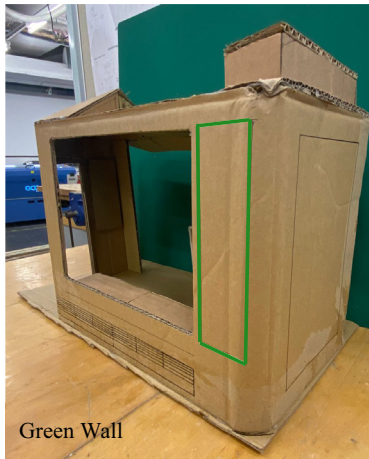


Size: Larger in relation to a 4-seater taxi

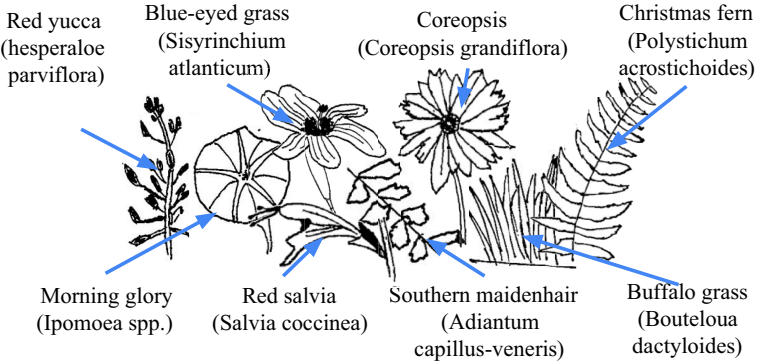
Size: 4m x 2m x 2.5m; may constrict pedestrian walkway

Rogers' Characteristics: Trialability – install at sites without existing shelter; must allow direct sunlight

## 7.2 Concept modelling



**LOW FIDELITY AESTHETIC MODELS:** Paper cutout collage of some common plants for green walls. My final design will have an exterior green wall, as stated in specification point 4B. They attract positive visual attention and naturally purify air.



**HIGH FIDELITY MOCK-UPS:** Below are 2 further developed concepts created and rendered using Fusion 360. Both designs were created with consideration of evaluation from prior models, and seek to improve in all aspects. These models will show further development of my ideas, receiving more user feedback leading up to the final design.

Function: Solar PV glass converts sunlight to energy; powers digital displays

Function: Digital displays; shows bus service information (i.e ETAs)

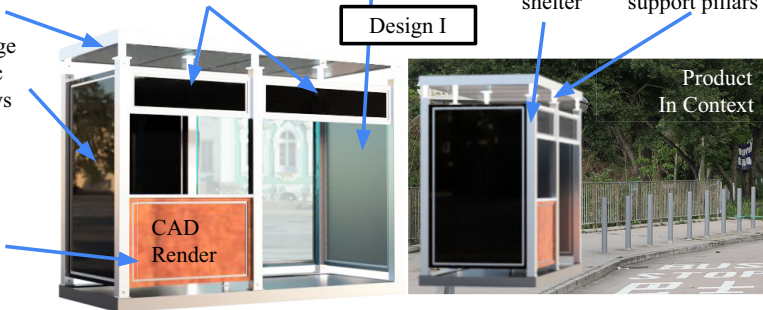
Aesthetics: Green wall (on other side)

Materials: Aluminium supports and shelter

Safety: Light rods surrounding support pillars

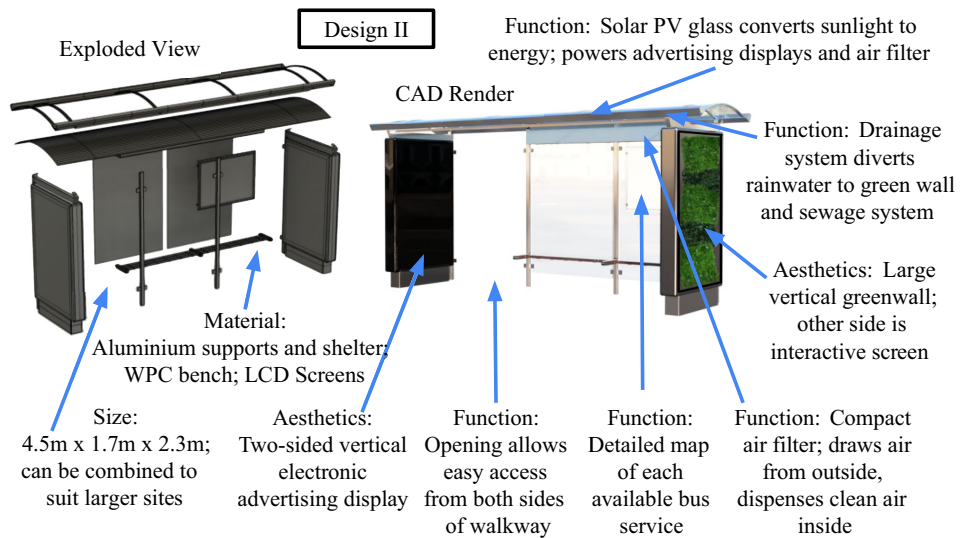
Aesthetics: 2x large vertical electronic advertising displays

Materials: Wood-plastic composite (WPC) panels; stylish, sustainable, and weather resistant



Expert Appraisal (I)  
 - Design integrates well with surroundings  
 - Good mixture of new and old technologies  
 - Aesthetics could use a bit more 'personality'  
 - Sacrificed comfort facilities (E.g. bench)

Expert Appraisal (II)  
 - Dynamic layout allows for high customizability  
 - Ample room for sites with higher commuter traffic  
 - Visibility is satisfactory; commuter comfort is prioritized  
 - Placement of bus map should be reconsidered  
 - Air filtering system seems impractical in for this design  
 - Needs more physical signage



Function: Solar PV glass converts sunlight to energy; powers advertising displays and air filter

Function: Drainage system diverts rainwater to green wall and sewage system

Aesthetics: Large vertical greenwall; other side is interactive screen

Exploded View

Design II

CAD Render

Material: Aluminium supports and shelter; WPC bench; LCD Screens

Size: 4.5m x 1.7m x 2.3m; can be combined to suit larger sites

Aesthetics: Two-sided vertical electronic advertising display

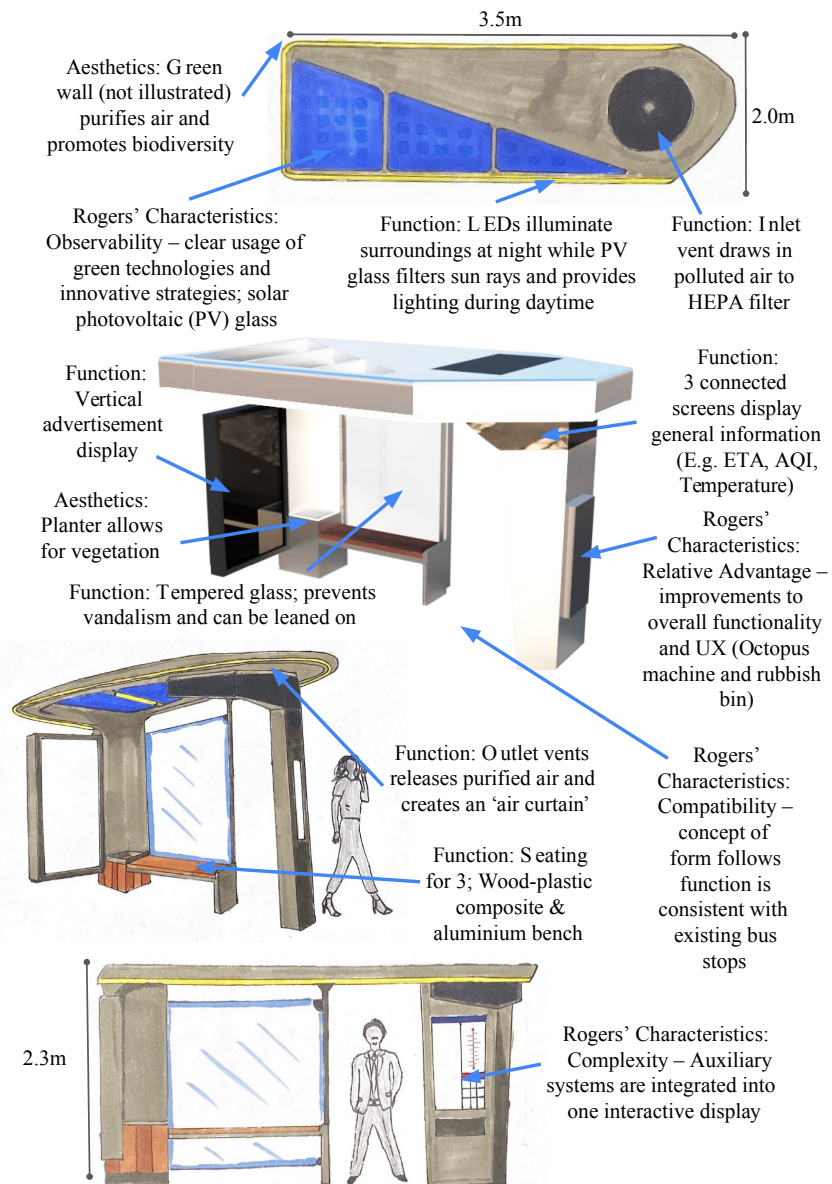
Function: Opening allows easy access from both sides of walkway

Function: Detailed map of each available bus service

Function: Compact air filter; draws air from outside, dispenses clean air inside





## 8. Final Design (Top, CAD, Perspective, Front)


Specification match: <b>High</b> , <b>Medium</b> , <b>Low</b>	
1	A: Safe and convenient space; plentiful signage B: 'Purified air curtain' C: Comfort and protection; visibility is unobstructed
2	A: Large aluminium/ PV glass roof shelter B: Lighting is sufficient
3	A: Bench for 3; supports can be leaned on B: Integrated rubbish bin and Octopus top-up machine C: Digital display
4	A: Sophisticated outlook mixed with natural elements B: Green wall (not illustrated) and planter C: Double-sided, large, vertical Ad display
5	A: 3.5m x 2m x 2.3m
6	A: Powder coated aluminium B: Side panel is tempered glass; skylight is PV glass C: High durability; non-biodegradable but recyclable



After evaluating the diverse natures of each design and their corresponding user feedback, this final design fuses the best qualities of preceding ideas and presents itself as the optimal solution to the problem in Hong Kong. This approach is able to significantly **enhance the commuter experience** across a number of facets. Its **high degree of structural integrity** provides the user with both **thermal and acoustic comfort**, alongside **physical protection**. User **visibility is unobstructed**, and is further elevated by the **use of location services and video surveillance** as integrated into the supplementary software. Other amenities such as a **rubbish bin and Octopus top-up machine** gives the product with extra functionality. Lighting can be obtained naturally through the **PV skylight**, or artificially from the **ceiling LEDs**; this will **boost the safety** of the shelter, particularly at night. The incorporation of a **green wall and planter** seek to maximise the bus stop's ability to **reduce the health risk** exposed to commuters. A **contemporary design** matched with a gray colour palette fits appropriately into the bustling streets of Hong Kong, subtly asserting itself as part of this concrete jungle. The selected **materials are durable and require minimal maintenance**, though as a compromise, they are **not the most environmentally friendly**. Also, the dimensions of 3.5m x 2m x 2.3m may prove **difficult to install** in certain locations, particularly in the city center, which prompts for a trade-off between functionality and practicality. While the **estimated cost of production is high**, the attractive **advertisement displays** serve as opportunities to **generate revenue**.

## 9. Justification of Material and Components

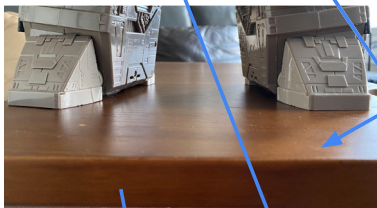
Component	Material	Justification (Advantages & Disadvantages)
<b>Structure &amp; Roof Shelter</b> 	Aluminium	<ul style="list-style-type: none"> <li>• Lightweight – specific weight of approximately 2.71 g/cm<sup>3</sup> and high strength-to-weight ratio (“6 Best Advantages”)</li> <li>• Naturally corrosion resistant; can be amplified by surface treatments such as anodizing or powder coating</li> <li>• Non toxic – odourless and impermeable</li> <li>• 100% recyclable; embodies circular economy model (“Aluminium and Aluminium Alloys”)</li> <li>• Exact material as final product</li> <li>• Conducts heat and electricity</li> <li>• Expensive to fabricate/weld</li> <li>• More expensive than steel of the the strength (Fleming)</li> </ul>
	Mediumdensity Fiberboard (MDF)	<ul style="list-style-type: none"> <li>• Decent stiffness and toughness</li> <li>• Affordable and easy to supply (Kara)</li> <li>• Dimensionally stable – does not react drastically to temperature changes or exposure to moisture (“Advantages and Disadvantages of MDF”)</li> <li>• Sustainable, biodegradable, and environmentally friendly</li> <li>• Untrue to the final product</li> <li>• While easy to paint and seal, it requires an extra cosmetic process to achieve desired appearance</li> <li>• May fracture when screwing (Mou)</li> </ul>
	<p>Although more expensive and difficult to manufacture, Aluminium has been chosen due to its strength, and more importantly – accuracy to the final product. This meets specification 6A.</p>	
<b>Seating</b> 	MDF	See above
	Bamboo Plywood	<ul style="list-style-type: none"> <li>• Sustainable and renewable source</li> <li>• More robust than most hardwood and has 22% greater tensile strength than steel (“What are the advantages and disadvantages of using Bamboo Plywood”)</li> <li>• Excellent dimensional stability; can be cut, sanded, nailed, screwed and plugged using conventional woodworking equipment (“Architecture Building and Construction Suppliers”)</li> <li>• Susceptible to deterioration if treated incorrectly (Green)</li> <li>• More expensive than MDF per sqft.</li> </ul>
	<p>While both materials possess similar properties, Bamboo plywood has been chosen as its aesthetics serve a better match to the final product.</p>	
<b>Amenities</b>  	Acrylonitrile Butadiene Styrene (ABS)	<ul style="list-style-type: none"> <li>• Low cost</li> <li>• Great heat and impact resistance (“Guide to 3D printing materials”)</li> <li>• Higher flexural strength and better elongation (Giang)</li> <li>• Does not ooze like PLA – smoother finish</li> <li>• Requires heated bed to print; unavailable at school</li> <li>• Produces pungent odour while printing (“ABS”)</li> </ul>
	Polylactic Acid (PLA)	<ul style="list-style-type: none"> <li>• Low cost</li> <li>• High stiffness and strength</li> <li>• Biodegradable (Giang)</li> <li>• Better dimensional accuracy than ABS</li> <li>• Lower heat resistance than ABS (“Guide to 3D printing materials”)</li> <li>• Not suitable to sunlight exposure (“PLA”)</li> <li>• Filament is brittle and breaks easier than ABS</li> </ul>
	<p>Despite its relative brittleness and weakness to sunlight exposure, PLA has been chosen given its stiffness and strength, in addition to its environmental benefits. ABS also isn’t accessible at school.</p>	

Component	Material	Justification (Advantages & Disadvantages)
<b>Side Window</b> 	Tempered Glass	<ul style="list-style-type: none"> <li>• Scratch resistant</li> <li>• No discoloration issues which may appear on acrylics (Wilson)</li> <li>• 4-5 times tougher than annealed glass; breaks into tiny pebbles when shattered to minimise severity of injury (Kim)</li> <li>• Heat resistant – can resist temperatures up to 243°C (“7 Advantages”)</li> <li>• Intended material of final product</li> <li>• <b>Cannot be reworked once thermally toughened</b></li> <li>• <b>Heavy and more expensive</b></li> </ul>
	Acrylic	<ul style="list-style-type: none"> <li>• Higher impact strength – does not shatter like glass under high strain</li> <li>• Lighter – density of around 1150-1190 kg/m<sup>3</sup>; less than half the density of annealed glass which ranges from 2400-2800 kg/m<sup>3</sup> (“Acrylic Windows vs. Glass Windows”)</li> <li>• Better optical transmission – Acrylic transmits more light than glass; up to 92% of visible light is transmitted</li> <li>• Much cheaper than tempered glass</li> <li>• <b>Unable to withstand extreme heat; may yellow with age if constantly exposed under direct sunlight (Sheahan)</b></li> <li>• <b>Not sustainable and hard to be recycled</b></li> </ul>
<p>Acrylic has been chosen due to its high impact resistance, lighter weight, and lower costs. That said, acrylic is not sustainable, and it isn't planned to be used in the final product.</p>		

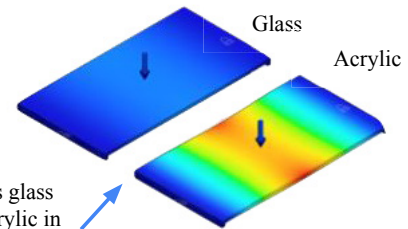
## Material testing



Aluminium is better for this context as it requires less maintenance and is more weather resistant



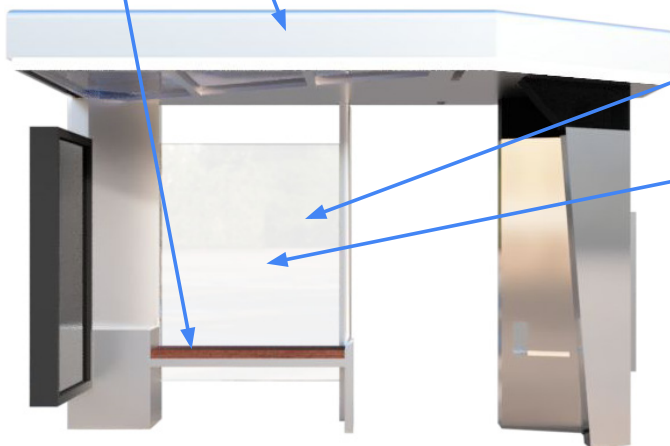
Both 5mm aluminium and MDF can easily support weights of 6 kg without bending



FEA shows glass edges out acrylic in terms of strength.



Acrylic is much lighter and more flexible than tempered glass



Tempered glass is hard to scratch and very clear



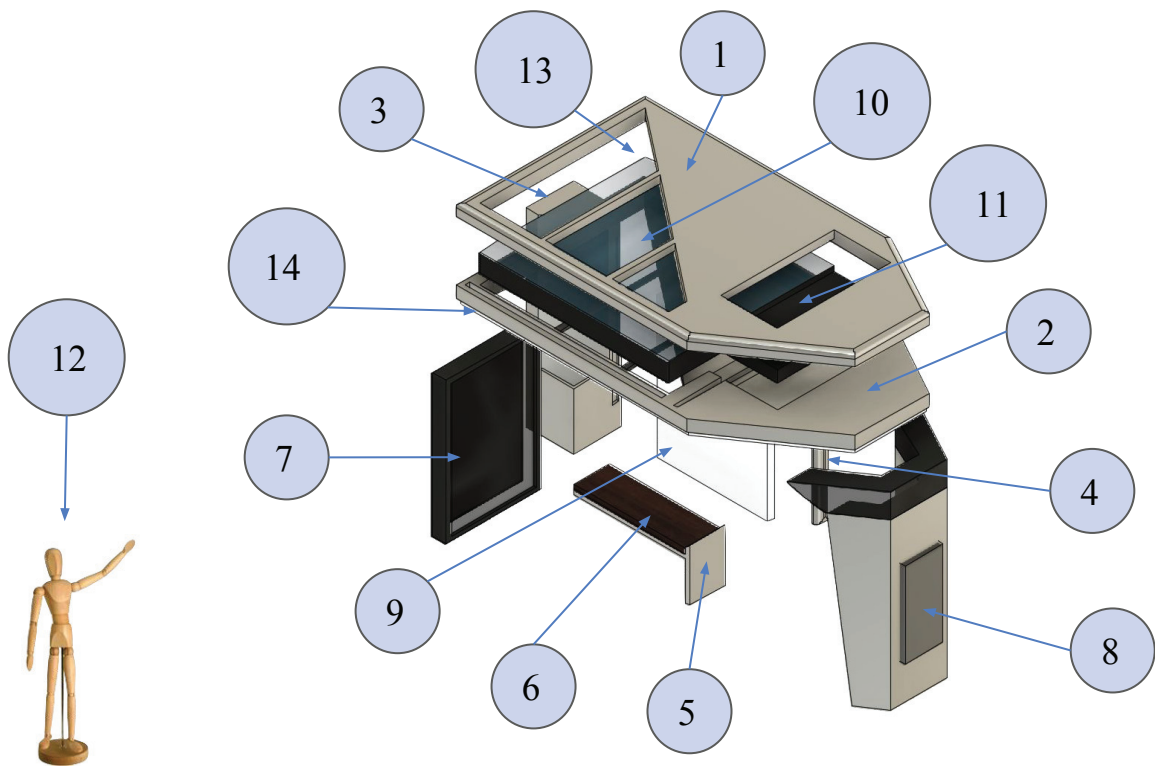
## 10.1 Isometric & orthographic drawing of final design



### Technical Drawing



## 10.2 Assembly drawing





Item #	Qty	Component	Material	Dimensions (LxWxH) (mm)	Manufacturer Cost (Any \$)	Total cost (\$USD)
11		Roof (Top)	Aluminium	700 x 400 x 25	£515.62	\$678.80
21		Roof (Bottom)		700 x 400 x 35		
31		Pillar X		100 x 100 x 400	£148.34	\$195.29
41		Pillar Y		25 x 25 x 400	£36.50	\$48.05
51		Bench Support		245 x 75 x 110	£73.78	\$97.13
61		Bench	Bamboo Plywood	235 x 75 x 10	\$4.99	\$4.99
71		Faux Advertising Display	Polylactic Acid (PLA)	300 x 180 x 30	\$22.99	\$22.99
81		Faux Auxiliary Pillar		280 x 130 x 400		
91		Side Window	Acrylic	300 x 235 x 15	£10.94	\$14.41
10	1	Solar Photovoltaic Glass	Pre-built (Purchased)	450 x 350 x 40	33.75 €	\$37.32
11	2	Intake Fans		120 x 120 x 25	\$31.9 x 2	\$63.8
12	1M	anikin		102 x 102 x 406	\$26.15	\$26.15
13	1	Diorama Plants		N/A	4.99 €	\$5.52
14	2	Lighting Strip		785 x 10 x 8	\$99.9 HKD x 2	\$25.55
<b>Total cost in USD</b>						\$1220
<b>Total cost in HKD (1 USD = 7.82 HKD)</b>						\$9540.34

## 11. Production Plan

Process	Equipment	Scheduling	Quality control	Risk assessment
<b>Prepare for manufacturing</b>				
Create 3D CAD model of final design	Computer with Fusion 360 installed	6 hours	Always refer back to specification (A3) and conceptual drawings (B3)	Work in set intervals to prevent eye fatigue from prolonged exposure to blue light
Separate files for different materials (E.g. aluminium vs bamboo plywood)	Computer with Fusion 360 installed	1 hour(s)	Ensure that each component will line up properly with one another	Save files periodically in case of application crash or lag
Export designs as DXF Files for laser and water jet cutter; Export designs as STL files for 3D Printer	Computer with Fusion 360 installed. USB	10 minutes	Do not forcefully eject USB; follow correct procedures	Use systems to making identifying files easier (E.g. Folders, custom names)
Power up water pump and water jet; turn on water and air pressure	Water jet cutting machine	5 minutes	Allow machine to run system checks before cutting	Be mindful of surroundings when starting up a large machine
Place aluminium plates into water jet cutter; Place bamboo plywood and acrylic into laser cutter;	Aluminium plates, bamboo plywood, acrylic, laser cutter, water jet cutting machine	5 minutes	Double check material dimensions with calipers	Wear gloves when handling materials as they can be sharp
<b>Manufacturing</b>				
Insert USB and begin laser cutting	Bamboo plywood, acrylic, laser cutter, USB	3 hours	Attempt a test run to ensure the laser's accuracy	Wear protective goggles and never stare the the laser or reach into tight spaces in the machine
Execute water jet cutting procedure	Aluminium, water jet cutting machine	5 hours	Make sure water jet cutting machine is fully functional and is no shortage of other resources (E.g. water)	Do a safety check before cutting and wear protective gear
Prepare filaments; insert USB into 3D Printer	PLA, 3D printer, USB	15 minutes	Verify that filaments can be extruded correctly by printing simple test files	Avoid making contact with high temperature nozzle as it will burn
Begin 3D Printing components 7 & 8	PLA, 3D printer	24 hours	Regularly check on the 3D printer to certify printing progress	Do not linger around the 3D printer for long periods as it diffuses toxic fumes
Remove completed components from each machine	Aluminium, bamboo plywood, acrylic, PLA	20 minutes	Use pliers when handling 3D printed object to prevent damage	Wear gloves when extracting components to avoid cuts or scratches

Process	Equipment	Scheduling	Quality control	Risk assessment
<b>Assembly</b>				
Install solar PV glass and fans into component 2	Solar PV glass, intake fans, component 2	10 minutes	Make sure that each component fits appropriately into their designated slot	Components 10 and 11 could be fragile and should be handled with caution
Sand down aluminium components in areas of connection	Sandpaper, components 1, 2, 3, 4	10 minutes	Sanding action must be smooth and consistent	Wear gloves and protective goggles when in contact with abrasives
Heat up components 1, 2, 3, 4; begin brazing once ready; braze 1 & 2 together first (roof), then braze 3 & 4 to 2 one after the other (structure)	Brazing rods, brazing torch, MAPP gas, vise grip, c-clamp, components 1 & 2	1 hour(s)	Minimise errors by using vise grips and c-clamps to hold components in place	Wear fireproof gloves and protective headwear; never touch the welding part or connecting part of component
Glue components 7 & 8 to aluminium structure; then glue components 5 & 6 together (bench); finally, glue bench to rest of structure	Epoxy, component 1234, components 5, 6, 7, 8	30 minutes	Clean surfaces before glueing to maximise the adhesive abilities of epoxy	Wear gloves when dealing with epoxy to avoid direct contact
Install acrylic panel into designated slot; glue diorama plants into back of structure (green wall)	Acrylic, UHU glue, rest of structure	15 minutes	Wear gloves when touching acrylic panel to avoid scratching; Hold diorama plant in place for a few second to solidify its placement	Wear disposable gloves when using UHU glue to minimise impact of potentially getting stuck. Only apply small amounts of glue to prevent overflow
Glue lighting strip to specific sections beneath and around the roof; then connect to solar PV glass	Lighting strip, UHU Glue	20 minutes	Accurately align each section of the lighting strip around the roof, especially the bending parts	
<b>Final prototype</b>				
Place component 12 (manikin) inside prototype and prepare for testing	Manikin, completed prototype	1 minute(s)	Ensure that each element of the prototype is secure and structurally stable	Be aware of the possible wood splinters on the manikin
Relocate prototype to a site of natural sunlight for testing; or present prototype to gain feedback	Completed prototype	N/A	Keep the prototype in an enclosed environment; for example, a clear box on display when not in tests	Always handle prototype carefully and transport it with both hands. Do not drop the prototype

## Bibliography

- 6 Best Advantages of Aluminium - Thyssenkrupp Materials (UK). *Materials UK*, [www.thyssenkrupp-materials.co.uk/advantages-of-aluminium.html](http://www.thyssenkrupp-materials.co.uk/advantages-of-aluminium.html).
- 7 Advantages Of Tempered Glass. (2022). *One Day Glass*. [www.onedayglass.com/7-advantages-of-tempered-glass/](http://www.onedayglass.com/7-advantages-of-tempered-glass/).
- ABS. (2019). *All-In-One 3D Printing Software*, Simplify3D Software. [www.simplify3d.com/support/materials-guide/abs/](http://www.simplify3d.com/support/materials-guide/abs/).
- Acrylic Windows vs Glass Windows. *Hydrosight*, [www.hydrosight.com/glass-vs-acrylic-a-comparison](http://www.hydrosight.com/glass-vs-acrylic-a-comparison).
- Advantages and Disadvantages of MDF: Buildingtalk: Construction News and Building Products for Specifiers.(2021). *Buildingtalk*. [www.buildingtalk.com/blog-entry/advantages-and-disadvantages-of-mdf/](http://www.buildingtalk.com/blog-entry/advantages-and-disadvantages-of-mdf/).
- Aluminium and Aluminium Alloys - Characteristic Advantages and Beneficial Properties of Aluminium Extrusions. (2008). *AZoM.com*. [www.azom.com/article.aspx?ArticleID=4192](http://www.azom.com/article.aspx?ArticleID=4192).
- Air Pollution Control Strategies. *Air Pollution Control Strategies Environmental Protection Department*, [www.epd.gov.hk/epd/english/environmentinhk/air/prob\\_solutions/strategies\\_apc.html#:~:text=The Government has been implementing,strengthening emissions control on LPG](http://www.epd.gov.hk/epd/english/environmentinhk/air/prob_solutions/strategies_apc.html#:~:text=The Government has been implementing,strengthening emissions control on LPG).
- AirVisual: Hong Kong SAR Air Quality Index (AQI) and Hong Kong SAR Air Pollution. *Hong Kong SAR Air Quality Index (AQI) and Hong Kong SAR Air Pollution | AirVisual*, [www.iqair.com/hong-kong](http://www.iqair.com/hong-kong).
- Amorphous Silicon Photovoltaic Glass* - Onyx Solar, [www.onyx-solar.com/product-services/amorphous-pv-glass](http://www.onyx-solar.com/product-services/amorphous-pv-glass).
- Architecture, Building & Construction Suppliers. *Architecture & Design (A&D)*, [www.architectureanddesign.com.au/suppliers/plywood-plastics/3-reasons-why-bamboo-plywood-is-better-than-hardwo](http://www.architectureanddesign.com.au/suppliers/plywood-plastics/3-reasons-why-bamboo-plywood-is-better-than-hardwo).
- Avenezia, and Avenezia (2017). *3D Modern Design Outdoor Bench - TurboSquid* 1217561. [www.turbosquid.com/3d-models/3d-modern-design-outdoor-bench-1217561](http://www.turbosquid.com/3d-models/3d-modern-design-outdoor-bench-1217561).
- Boost Your Backyard with a Vertical Garden. (2020). *The Garden Men*. [www.thegardenmen.com.au/blog/boost-your-backyard-with-a-vertical-garden/](http://www.thegardenmen.com.au/blog/boost-your-backyard-with-a-vertical-garden/).
- Bus Shelters. *RSS*. [www.pps.org/article/busshelters](http://www.pps.org/article/busshelters).
- Bus Shelters Supplier & Manufacturer. *Shelter Solutions*. [www.shelter-solutions.co.uk/product-category/bus-shelters/](http://www.shelter-solutions.co.uk/product-category/bus-shelters/).
- Centre for Health Protection (CHP), Department of Health - The Health Effects of Air Pollution. *Centre for Health Protection*, [www.chp.gov.hk/en/healthtopics/content/460/3557.html](http://www.chp.gov.hk/en/healthtopics/content/460/3557.html).
- Crosse, D. (2019). What Does a Bus Shelter Cost? *My Muskoka Now*. [www.mymuskokanow.com/87783/what-does-a-bus-shelter-cost/](http://www.mymuskokanow.com/87783/what-does-a-bus-shelter-cost/).
- Design Technology*, [www.ruthtrumpold.id.au/destech/](http://www.ruthtrumpold.id.au/destech/).
- Fleming, E. (2019). Home. *SidmartinBio*. [www.sidmartinbio.org/what-are-the-advantages-and-disadvantages-of-aluminium/](http://www.sidmartinbio.org/what-are-the-advantages-and-disadvantages-of-aluminium/).
- Giang, K. PLA vs. ABS: What's the Difference? *Hubs*. [www.hubs.com/knowledge-base/pla-vs-abs-whats-difference/](http://www.hubs.com/knowledge-base/pla-vs-abs-whats-difference/).
- GovHK: Air Quality in Hong Kong. (2021). GovHK 香港政府一站通. [www.gov.hk/en/residents/environment/air/airquality.htm](http://www.gov.hk/en/residents/environment/air/airquality.htm).
- Green, E. (2016). "THE PROS AND CONS OF BAMBOO IN GREEN BUILDING." *Medium*. [www.medium.com/@elementalgreen/the-pros-and-cons-of-bamboo-in-green-building-838a72e265c1](http://www.medium.com/@elementalgreen/the-pros-and-cons-of-bamboo-in-green-building-838a72e265c1).
- Guide to 3D Printing Materials: Types, Applications, and Properties. *Formlabs*, [formlabs.com/asia/blog/3d-printing-materials/](http://formlabs.com/asia/blog/3d-printing-materials/).
- HEPA Filter: What It Is, What It Does and What It Doesn't Do*, [inspiredliving.com/airpurifiers/hepa-filters.htm](http://inspiredliving.com/airpurifiers/hepa-filters.htm).
- Home. *Innovative Aluminium Profile Air Condit Bus Stop Solar Shelter Design - Buy Bus Stop Shelter Design,Bus Stop Solar Shelter,Air Condit Bus Stop Shelter Product on Alibaba.com*, [www.alibaba.com/product-detail/Innovative-aluminium-profile-air-condit-bus\\_60222747724.html](http://www.alibaba.com/product-detail/Innovative-aluminium-profile-air-condit-bus_60222747724.html).
- Hong Kong Air Pollutant Emission Inventory - Road Transport. *Hong Kong Air Pollutant Emission Inventory - Road Transport |Environmental Protection Department*, [www.epd.gov.hk/epd/english/environmentinhk/air/data/emission\\_inve\\_transport.html](http://www.epd.gov.hk/epd/english/environmentinhk/air/data/emission_inve_transport.html).
- Hong Kong: The Facts – Transport. (2020). *Transport Department*. <https://www.gov.hk/en/about/abouthk/factsheets/docs/transport.pdf>
- How Waterjet Works. *How Waterjet Technology Works - Flow Waterjet*, [www.flowwaterjet.com/Learn/How-Waterjet-Works.aspx#components](http://www.flowwaterjet.com/Learn/How-Waterjet-Works.aspx#components).
- James, D. (2022). The Best PC Fans in 2022. *Pcgamer*, PC Gamer. [www.pcgamer.com/best-pc-fans/](http://www.pcgamer.com/best-pc-fans/).
- Kara, D. (2017). MDF or Solid Wood Furniture: Advantages and Disadvantages. *Parade of Homes*. [www.paradeofhomes.org/blog/mdf-solid-wood-furniture-advantages-disadvantages/](http://www.paradeofhomes.org/blog/mdf-solid-wood-furniture-advantages-disadvantages/).
- Kim. (2012). The Advantages and Disadvantages of Tempered Glass. *Shenzhen Sun Global Glass*. [www.sggglassmanufacturer.com/news/The-advantages-and-disadvantages-of-tempered-glass.html](http://www.sggglassmanufacturer.com/news/The-advantages-and-disadvantages-of-tempered-glass.html).
- LCQ10: Erection of Bus Shelters. [www.info.gov.hk/gia/general/201903/20/P2019031900684.htm](http://www.info.gov.hk/gia/general/201903/20/P2019031900684.htm).
- LCQ3: Bus Stops. [www.info.gov.hk/gia/general/201807/11/P2018071100581.htm](http://www.info.gov.hk/gia/general/201807/11/P2018071100581.htm).
- LCQ19 (2005): *Design and Locations of Bus Shelters*. [www.info.gov.hk/gia/general/200510/26/P200510260218.htm](http://www.info.gov.hk/gia/general/200510/26/P200510260218.htm).
- LEDBERG - LED Lighting Strip, White. *IKEA Hong Kong and Macau*, [www.ikea.com.hk/en/products/integrated-lighting---electronics/multi-purpose-lighting/ledberg-art](http://www.ikea.com.hk/en/products/integrated-lighting---electronics/multi-purpose-lighting/ledberg-art).
- Limited, Alamy. "Stock Photo - People Waiting at Bus Stops, Wan Chai, Hong Kong." *Alamy*, [www.alamy.com/stock-photo-people-waiting-at-bus-stops-wan-chai-hong-kong-39496419.html](http://www.alamy.com/stock-photo-people-waiting-at-bus-stops-wan-chai-hong-kong-39496419.html)
- Moovit: Public Transit Facts & Statistics for Hong Kong. *Public Transit Facts & Statistics for Hong Kong | Moovit Public Transit Index*, [moovitapp.com/insights/en/Moovit\\_Insights\\_Public\\_Transit\\_Index\\_China\\_Hong\\_Kong-2741#](http://moovitapp.com/insights/en/Moovit_Insights_Public_Transit_Index_China_Hong_Kong-2741#).
- Mou, S.U. Shanta Urmila Mou. *Civil Engineering*, [civiltoday.com/civil-engineering-materials/timber/163-advantages-and-disadvantages-of-mdf](http://civiltoday.com/civil-engineering-materials/timber/163-advantages-and-disadvantages-of-mdf).

NF-A12x25 PWM. Noctua.at - *Premium Cooling Components Designed in Austria*, noctua.at/en/products/fan/nf-a12x25-pwm.

*Onyx Solar - Photovoltaic Glass for Buildings*, www.onyx solar.com/.

PLA (2019). *All-In-One 3D Printing Software*, Simplify3D Software, www.simplify3d.com/support/materials-guide/pla/.

Professional Plant with Green Leaves. *Diorama-World*, www.diorama-world.com/en/p/professional-plant-with-leaves-for-diorama-dioramapresepe-fm004.

Pros & Cons of The 7 Main Types of Air Filters. (2020). *Home Climates*, homeclimates.com/blog/air-filter-types.

Sheahan, K. (2020). The Disadvantages of Acrylic Plastic. *EHow UK*. www.ehow.co.uk/list\_7392243\_disadvantages-acrylic-plastic.html.

Schmitt, A., et al. (2018). Why We Need a Bus Shelter at Every Stop. *Streetsblog USA*, usa.streetsblog.org/2018/10/01/opinion-we-should-put-a-bus-shelter-at-every-stop-in-america/.

Snowden, S. (2020). Solar Glass Could Convert The Windows Of Every Building Into Power-Generating Panels. *Forbes*. www.forbes.com/sites/scottsnowden/2020/07/29/solar-glass-windows/.

So, H. K., et al. (2008) Secular Changes in Height, Weight and Body Mass Index in Hong Kong Children. *BMC Public Health*, BioMed Central. www.ncbi.nlm.nih.gov/pmc/articles/PMC2572616/.

The Standard. Uni Team Calls for Electric Bus Switch.” *The Standard*, www.thestandard.com.hk/section-news/section/4/178899/Uni-team-calls-for-electric-bus-switch.

Travel Characteristics Survey 2011 Final Report. (2014). *Transport Department*, ARUP. https://www.td.gov.hk/filemanager/en/content\_4652/tcs2011\_eng.pdf

Vertical Gardens & Living Walls: Vancouver, Toronto, Montreal. (2021). *Architek*. architek.com/products/vertical-gardens/.

What are HEPA filters and how do they work? (2021) *Airtecnic*. https://www.airtecnic.com/news/what-are-hepa-filters-and-how-do-they-work.

What Are the Advantages and Disadvantages of Using Bamboo Plywood? (2021). *July Bambu*. www.julybambu.com/what-are-the-advantages-and-disadvantages-of-using-bamboo-plywood-2/.

What Are Vertical Gardens? *Ambius*, www.ambius.com/green-walls/what-are-vertical-gardens/.

Wilson, B. (2021). PC Cases: Tempered Glass Side Panels vs Acrylic Side Panels. *Appuals.com*. appuals.com/pc-cases-tempered-glass-side-panels-vs-acrylic-side-panels/.

Wooden Manikins. *Jack Richeson & Co.*, products.richesonart.com/collections/manikins/products/manikin?variant=5619125649435

Wong, S. (2021). Hong Kong: Average Daily Public Transport Passenger Journey Number by Mode 2020. *Statista*. www.statista.com/statistics/960577/hong-kong-average-daily-passenger-journey-number-on-public-transport-by-mode/.

---

# Generating fire and water through the sun and moon: the mechanism and philosophy behind *yangsui* 陽燧 and *fangzhu* 方諸

Ronnie L.C. Cheung

---

## Introduction

The ancient Eastern Zhou dynasty Chinese technologies *yangsui* 陽燧 and *fangzhu* 方諸 were designed to generate fire from the sun and water from the moon respectively.

*Yangsui* is often translated as “burning mirror”. While *yangsui* was an ancient Chinese technology, other cultures, such as the ancient Greeks, also had their own versions of a ‘burning mirror’. *Yangsui* is a bronze mirror used to generate fire through the reflection of light onto a surface for a certain period of time until the temperature rises. Although this mechanism has been developed in different time periods and cultures, each of these prototypes revolved around the use of a mirror that reflects light.

Compared with *yangsui*, *fangzhu* is not as well understood. *Fangzhu* is to collect dew from the moon through the process of water condensation. The term *fangzhu* was first recorded in the *Huainanzi*. Based on historical documents, it is understood that *fangzhu* is a natural mechanism that was used in Chinese culture in a more religious context (Blanc 120). Unlike *yangsui*, and until the discovery of an artefact, there were many different beliefs as to what the physical properties of *fangzhu* were: was it a clam shell, a polished bowl, or a bronze plate?

There are several different perspectives to better understand *yangsui* and *fangzhu*, each with its own distinct religious purposes. For instance, *yangsui*, a symbol of yang 陽, was used for ceremonial purposes. *Yang* represents “heaven, maleness, light, activity, and penetration” (Encyclopedia Britannica). *Fangzhu* was used for traditional rituals, representing belief in immortality, and a symbol of yin 陰. In Chinese culture, *yin* symbolises “earth, femaleness, darkness, passivity, and absorption” (Encyclopedia Britannica).

Another perspective to view the two tools is through the science behind nanotechnology, condensation,

and reflection/refraction. The scientific significance of these two tools were well understood in recent research by He *et al.* and Qiu. Overall, this research paper analyses *yangsui* and *fangzhu* through their properties, representations, and religious beliefs by including ancient and contemporary perspectives.

## 1. *Yangsui*

The fire generating mechanism *yangsui* (Figure 1) has numerous names given from different time periods or cultures, such as *yangsui* 陽燧 or *fusui* 夫燧 translated as “sun collector” (Blanc 120). In *yangsui*, *yang* 陽 literally translates as “sun” or “sunlight”. *Sui* 燧 can be translated as “flintstone” or “torch”. Thus, the two Chinese characters combined form “sun torch”. Despite the different names of *yangsui*, the properties of the tools were similar, all sharing the same concept of using bronze mirrors to reflect sunlight to a certain point, focusing high temperatures until the point catches fire.

Side View



Back View



Figure 1. *Yangsui* from Bronze Age (Perlin 38)

---

The above article was written as a culminating essay for the Shuyuan NRI Scholar’s Summer Retreat, 2021.

As mentioned above, understandings of *yangsui* differed through time. *Huainanzi* 淮南子 was a compendium of Daoist, Legalist and Confucian thought compiled under the patronage of Liu An in 139 BC. Liu An (179 BCE - 122 BCE) was a Han dynasty prince that ruled the Huainan 淮南 kingdom. In *Huainanzi*, Liu explains that

故陽燧見日則燃而為火 (*huainanzi* 21)

When the burning-mirror sees the sun, it ignites tinder and produces fire (trans. Major 65).

The description above was translated by John Major in his book *Heaven and earth in early Han thought*, a present study of *Huainanzi* chapters three, four, and five.

Liu's description of *yangsui* was then reinterpreted by Gao You 高誘, an Eastern Han dynasty commentator on *Huainanzi*,

陽燧，金也。取金杯無緣者，熟摩令熱，日中時以當日下，以艾承之，則燃得火也。

*Yangsui* is made of metal. If one takes a metal bowl without a rim (a slightly concave mirror), polishes it vigorously so that it becomes hot, places it directly below the sun at noon and puts mugwort before it, the mugwort will then catch fire (trans. Blanc 120).

The description above was translated by Charles Le Blanc in his *Huai-nan Tzu: Philosophical Synthesis in Early Han Thought*, a present study on the sixth chapter of *Huainanzi*.

Mugwort, or in Chinese known as *aiye* 艾葉, is a plant that is sometimes used dry. As a dry plant, there is no water in the leaves, which increases the speed of ignition. Blanc also exemplifies that, "If the bowl and mugwort are placed too far apart, it will fail from producing fire." The distance between the mugwort and the reflection of the sunlight plays an important role in the process of ignition. This is because the further the distance, the weaker the strength of the sunlight, and the heat will not be able to ignite the mugwort. Simultaneously, the mugwort cannot be placed too close to the metal concave mirror as a lack of adequate distance will impact the focal point.

*Yangsui* is also mentioned in *Lunheng* 論衡, a work written in 88 CE by the Eastern Han thinker Wang Chong 王充 (self-translation in quotations below):

陽燧取火

*Yangsui* collects fire.

陽燧若偃月

*Yangsui* is shaped like a half moon.

鑄陽燧用五月丙午日午時，鍊五色石為之，形如圓鏡，向日即得火

*Yangsui* is used during the fifth month at the third noon of the month. It is made of five-colored stones smelted together, shaped like a circular mirror, which creates fire immediately when facing the sun. (Wang 378)

Tang dynasty Daoist priest and writer Du Guangting 杜光庭 also mentions *yangsui* in the *Daode zhenjing guangsheng* 道德真經廣聖, a 5-volume book that outlines the purpose of the scriptures, introduces the life and deeds of Laozi 老子, and explains the preface to the imperial annotations of Emperor Ming of the Tang Dynasty. Du describes *yangsui* as,

陽燧者，範金為器，其形若杯，或類鏡焉，以玄繪潔之，以日照之，以艾承之，則得火焉。

As for *yangsui*, the metal is used as a vessel, its shape is like a cup, or a mirror. Clean it and reflect sunlight onto the mugwort, then it will catch fire (*Daode zhenjing guangsheng*, Volume 20).

The above describes when the sun reflects on the *yangsui* to the mugwort inside, the cleaned, concave, mirror-like device will ignite fire. This is different from Wang Chong's perspective because instead of five-colored stones smelted together, the material is reported to be a type of metal.

Throughout Chinese literary history, works such as *Huainanzi* and its commentaries, *Lunheng*, and *Daode zhenjing guangsheng* each had their own views towards the properties of *yangsui*. There are some variations between the different sources, but all include the same basic properties: *yangsui* is a stone/metal that ignites fire through reflection of sunlight. Metal is an effective material because of its high reflectivity due to the large number of electrons. When the light is in contact with the electrons, it gives the electrons more energy causing it to move around more. Thus, the increase of movement in the electrons reflects more light.

## 2. Fangzhu

*Fangzhu* 方諸 ('square receptacle') or *fangzhu* 方渚 ('water in isolated lands') had far fewer references or mentions in Chinese literature (He *et al.* 2). Due to limited evidence and artefacts available throughout the years, even in ancient times, several theories about the properties of *fangzhu* emerged. For instance, *fangzhu* was believed to be either a large clam or a square receptacle. There were far less scientific details or understanding of how the tool was used in ancient China. From Liu An's *Huainanzi*, he indicates,

方諸見月則津而為水 (*Huainanzi* 21)

When the square receptacle sees the moon, it moistens and produces water (trans. Major 65).

This was one of the attempts to comprehend the workings of this tool.

In addition, three main distinct interpretations of *fangzhu*'s physical properties were noted:

1. A large clam shell (Needham 87-89)
2. A jade cup (Li 248-429)
3. A square receptacle (Major 65)

The argument was that these three properties could produce water when *fangzhu* was placed under the moon. By vigorously polishing the *fangzhu* and with a surface cooler than humid air, the device is able to collect the dew from the atmosphere (Blanc 120). This is due to condensation: when the humid water vapour is in contact with the low temperature *fangzhu*, the heat loss causes the water vapour to cool down. This leads to the molecules losing energy and slowing down until the movement shifts from gas like molecules to liquid like molecules. Liquefying on the cooler surface of the *fangzhu*.

Joseph Needham, a science historian, biochemist, and publication initiator of the book series: Science and Civilisation in China suggests that *fangzhu* is known as a *yin* mirror, a large, polished clam shell. When it is held under the moonlight, water will condensate onto the shell: "When the Fang Zhu sees the moon, there is a dampness (or secretion) and water is produced" (Needham 87-89). From another source, according to Li Xiangguang, apart from clams, some believed that *fangzhu* was made of bronze or crystal. Recently, archaeologists have found real dragonflies whose eyes were replaced with soda-lime glass inside the Qing 清 Dynasty tombs. This low temperature soda-lime glass

from the West was also used as the material to make the *fangzhu* (Li 428-429).

Certain conjectures exist for the development of *fangzhu*'s material. Li argues that at first, copper was used to manufacture *fangzhu* (Li 248-429). However, due to its strong thermal conductivity, it was difficult to form dew on the *fangzhu*, since it required a cool surface to collect the dew. Due to the issue with thermal conductivity, the material was then altered to pottery clay. Although clay was easily accessible and cheap, it did not look aesthetically pleasing. A further evolution of *fangzhu* was the use of actual sea clam and jade to increase its value, along with its lower thermal conductivity. The function and appearance attracted more consumers. Hence, jade (Figure 2) and clam became a popular *fangzhu* material (Li 248-429).



Figure 2. *Fangzhu* made out of jade (Gao and Lei, 67)

Nonetheless, a simple description of *fangzhu* is that it is a low thermal conductivity clam or jade shell, or a square receptacle that is polished vigorously to be able to collect water through the humidity and process of condensation during the night (Blanc 120).

## 3. Representations

In the ancient sources, *yangsui* and *fangzhu* are often mentioned together, acting as symbols of the ancient Chinese philosophical concepts *yin* and *yang*. The concepts revolve around the idea of dualism, meaning that a bond can be created between two opposites. Cartwright, a history writer, indicates that the opposites can also balance each other out to create a perfect match (qtd. in World History Encyclopedia).

*Yangsui* with its fire-ignition property was believed to be a representation of *yang*; *fangzhu* with its water-generating property was believed to be a representation of *yin*. The two tools demonstrated qualities of *yin* and *yang*. *Yang* is fast, hard, solid, focused, hot, dry, and active; associated with fire, sky, the sun, masculinity



and day time. *Yin* is characterised as slow, soft, yielding, diffuse, cold, wet, and passive; associated with water, earth, moon, femininity, and night. The attributes of *yin* and *yang* establish correlations between *yin* and *fangzhu*; *yang* and *yangsui*. Through the use of both *yangsui* and *fangzhu*, it creates a balance between the *yin* and *yang* to the user.

## 4. Religious Beliefs

*Yangsui* and *fangzhu* had several purposes. From a practicality perspective, it was to generate fire and collect dew respectively, but they were also important for religious and cultural practices.

### 4.1 Fangzhu

Li Xiangguang discusses the beliefs of immortality from consuming jade scraps, jade ointments, and jade fluids. This relates to the book *mucaojingkaozhu* 本草經考注 written by Sen Lin Zhi 森立之 about Chinese medicine (self-translation in quotations below),

長肌肉，益氣，久服耐寒暑，不飢渴，不老神仙。  
(Li 428).

Softening tendons and strengthening bones, soothing the soul, nourishing breathing, growing muscles, enduring cold and heat for a long time, no hunger and thirst, and immortality.

However such consumption can also lead to side effects such as a rise in body temperature. It was believed that this rise in body temperature was a result of consuming the *yang* within the jade (Li 428). Therefore, to eliminate the heat and bring the body back to a balanced temperature, one must drink dew, which is known as an extreme form of *yin*. In order to remove the *yang* and the excess heat, *fangzhu* is used to collect dew (Li 428) from under the moon during the midnight of November, which is believed to be the month when *yin* is strongest (Li 429).

Aside from collecting dew to balance body temperature, *fangzhu* was also used for ceremonial traditions, whereby the Chinese would extract the dew from *fangzhu* and sterilise their wheat harvests as a form of respect. After sterilisation with the dew from the *fangzhu*, the food was then used to worship the gods (Liu 428).

Other cultures had practices similar to the concept of *fangzhu* and consuming *yin* and *yang*. For example, the Afghans had an idea that consuming a balance between sunlight and moonlight would make them healthier (Li 432). This concept has connections with *fangzhu*,

where consuming *yin* through the dew would make human bodies healthier.

Finally, the most crucial factor of combining nature with *yin* and *yang* into the human body through the exertion of *fangzhu* dew (*yin*) is that it creates a sense of balance and combines the powers of nature into the human body (self-translation in quotations below):

掌握之中，引類於太極之上，而水火可立致者，陰陽同氣相動也

If you use what is in your hands and draw sorts above the Supreme Extremity, fire and water can be summoned because the *yin* and *yang* are moved by the same *qi*. (huainanzi 52)

### 4.2 Yangsui

Similar to *fangzhu*, *yangsui* also had religious and ceremonial associations. According to Needham, the “[Directors of Sun Fire] have the duty of receiving, with the mirror, brilliant fire from the sun... They carry out these operations in order to prepare brilliant rice, brilliant torches for sacrifices” (Needham 87). The ceremonial association of *yangsui* was also mentioned in *Lunheng*. The sons and daughters in law of the family wore belts that held utilities including the metal fire starters. This implies that the mirrors were used frequently amongst households at the time (Forke *et al.* 497). Another example is that the fire is drawn from the sun for sacramental purposes during the summer solstice. It is done in the fifth month of the year, where the solstice falls in (Bodde 301). This is believed to be the month that most exemplifies *yang*.

## 5. Contemporary Perspectives

The properties, attributes, representations of *yin* and *yang*, and religious beliefs shaped the ancient perspectives of *fangzhu* and *yangsui*. However, new contemporary perspectives have provided alternative views in light of modern science.

### 5.1 Does the moon really matter?

According to modern science, the moon does not in fact have a direct correlation with the dew forming on a device like the *fangzhu*. When the night sky is filled with clouds, the heat in the atmosphere is trapped by the clouds. The heat/radiation waves encounter the clouds and refract back into the earth’s ground, which prevents dew from forming on the *fangzhu* (Gao and Lei 67).

On the other hand, when the night sky is clear without clouds, the heat in the air will travel up into the atmosphere without refracting off the clouds. Therefore,

no heat will be bouncing back into the earth's ground, allowing the *fangzhu* to form dew (Evers, an editor from National Geographic explains as the process of condensation: materials undergoing change from gas to liquid), and the dew is a result of water vapour transforming into liquid (qtd. in National Geographic).

This explains why the ancient Chinese thought when the night sky was clear, by allowing the *fangzhu* to be exposed to the moon, dew would be formed. However, the true scientific reasoning behind this lies in the clouds that cause a refraction of heat.

## 5.2 Reflection and refraction to a focal point

In terms of contemporary scientific views of *yangsui*, Qiu discusses the four different forms of reflection and refraction towards a focal point illustrated in Figure 3.

- A. When the shape of the *yangsui* is a concave mirror, the parallel sunlight shone against the concave *yangsui* will have a focal point in the centre. If the mugwort was placed at the point of intersections of the sunlight reflections, fire will be ignited.

- B. If the material of *yangsui* was transparent, the parallel sunlight shone would refract like a glass of water refracting light. The refraction will lead to another focal point (intersection of the sunlight).
- C. When the mirror of the *yangsui* is concave and the light is shone in a non-parallel line, the mirror will refract the light into different directions and users should place the mugwort in the intersection of the light that bounces off the mirror.
- D. When the glass of *yangsui* is convexed, it acts the same way as B. The parallel sunlight is shone through the transparent glass creating a focal point for the mugwort.

Aside from the use of mirrors reflecting the sunlight and concentrating it onto a focal point, another related concept is the use of a magnifying glass. Sunrays contact the magnifying glass. They are then converged and focused onto a certain point (usually dead or dry plants or paper).

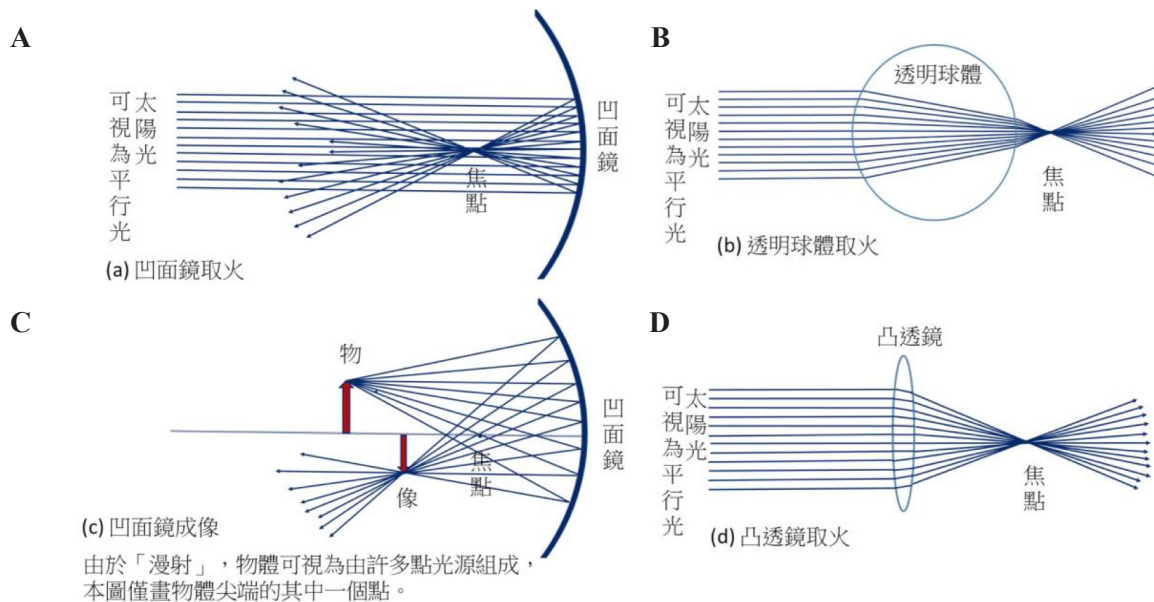
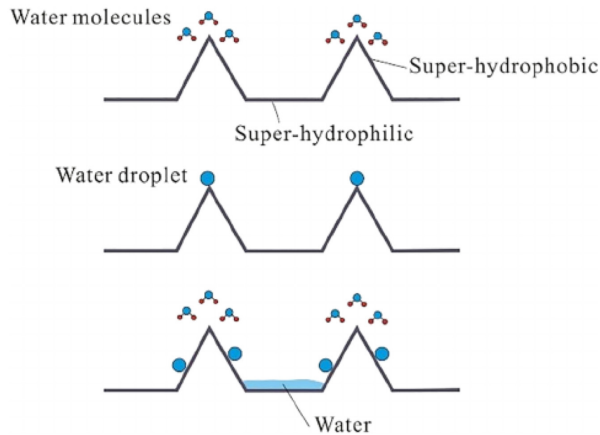


Figure 3. The light path diagram of *yangsui* igniting fire and illuminating objects (Qiu 76)

### 5.3 How can nanotechnology be implemented into *fangzhu*?

Nanotechnology could be applied to *fangzhu*. From a modern nanotechnology point of view, *fangzhu* water harvesting ability is through the “hydrophilic-hydrophobic hierarchy of the surface”. The concept is similar to the spider webs harvesting water droplets illustrated in Figure 4 (He *et al.* 4).



**Figure 4.** Diagram of the hydrophobic surface and hydrophilic surfaces presenting the possible tools behind *fangzhu* (He *et al.* 4)

The convex-concave shape and the low wettability of the *fangzhu* attracts the water molecules from the air, which can then successfully harvest dew droplets into the device shown by Figure 5.

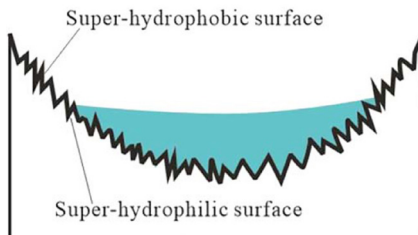


**Figure 5.** Surface of the *fangzhu* and its low wettability (Wang 2)

Nanotechnology is a highly advanced science that officially started development in 1981. The ancient Chinese did not understand the nanotechnological aspect of the *fangzhu* but simply believed that *fangzhu* harvested water merely from the moon when the night sky was clear. It is important to understand the ancient perspectives of how *fangzhu* worked and compare it to contemporary scientific views because it portrays how *fangzhu* worked in the past.

## Conclusion

In conclusion, *yangsui* is an ancient Chinese technology that could generate fire when exposed to the sun, while *fangzhu* could generate water when exposed to the moon. This paper discussed the properties of *yangsui* and *fangzhu* and the different attributes that allowed these two devices to collect fire and water. The mechanisms *yangsui* and *fangzhu* have a number of cultural and religious beliefs behind them, including *yin* and *yang*, and feminine and masculine representations, respectively. By incorporating new scientific and contemporary perspectives into these ancient tools, this paper compared the ancient beliefs of how the two tools worked in comparison to the contemporary scientific perspectives.

## References

Bodde, Derek. *Festivals in Classical China*. Princeton UP and The Chinese University of Hong Kong, 1975.

Cartwright, Mark. "Yin and Yang." *World History Encyclopaedia*, 16 May 2018, [https://www.worldhistory.org/Yin\\_and\\_Yang/](https://www.worldhistory.org/Yin_and_Yang/). Accessed 31 May 2022.

"Chinese Sun and Moon Mirrors." *Wikipedia*, Wikimedia Foundation, 15 Mar. 2022, [https://en.wikipedia.org/wiki/Chinese\\_sun\\_and\\_moon\\_mirrors](https://en.wikipedia.org/wiki/Chinese_sun_and_moon_mirrors). Accessed 18 April 2022.

Encyclopaedia Britannica, "yinyang". 7 May. 2021, <https://www.britannica.com/topic/yinyang>. Accessed 31 May 2022.

Evers, Jeanie. "Dew." *National Geographic Society*, 9 Oct. 2012, [www.nationalgeographic.org/encyclopedia/dew/](http://www.nationalgeographic.org/encyclopedia/dew/). Accessed 31 May 2022.

Forke, Alfred, translator. *Lunheng, Part 2, Philosophical Essays of Wang Chung*. Otto Harrassowitz. 1991.

He, Chun-Hui, et al. "Fangzhu (方諸): An Ancient Chinese Nanotechnology for Water Collection from Air: History, Mathematical Insight, Promises, and Challenges." *Mathematical Methods in the Applied Sciences*, Special Issue, 2020.

Le Blanc, Charles, translator. *Huai-nan Tzu: Philosophical Synthesis in Early Han Thought, The Idea of Resonance (Kan-Ying), with a Translation and Analysis of Chapter Six*. Hong Kong UP, 1985.

Lozano, Carey. "Nanotechnology." *National Geographic Society*, <https://education.nationalgeographic.org/resource/nanotechnology>. Accessed 18th March 2022.

Major, John. S, translator. *Heaven and Earth in Early Han Thought, Chapters Three, Four, and Five of the Huainanzi*. State University of New York Press, 1993.

Needham, Joseph, et al. *Science and Civilisation in China*. Vol. IV. pt. 1 Cambridge UP, 1976.

Perlin, John. *Let It Shine: The 6,000-Year Story of Solar Energy*. 2013

Wang, Kang-Le. "Effect of Fangzhu's Nanoscale Surface Morphology on Water Collection." *Mathematical Methods in the Applied Sciences*, Special Issue, 2020.

李顯光。“從陽遂與方諸看天人合一”。第二屆中華文化與天人合一國際研討會。(2015/1/9~11), 南投。

邱韻如。“陽燧與方諸：名詞演變及其物理概念發展”。《中華科技史學會》，2020。

劉安。“淮南子”。[chinaschool.org](http://chinaschool.org), 2013。

高策, 雷志華。“中国古代‘方諸’研究”。《科學技術哲學研究》，第26卷, 第4期, 2009。

---

# **Cognitive Behavioural Therapy as a treatment for Social Anxiety Disorder (SAD): an analysis of its effectiveness in addressing the etiology of SAD**

*Marsha C.Y. Lau*

---

## **Introduction**

Abnormal psychology is “devoted to the study, assessment, treatment, and prevention of maladaptive behaviour” (American Psychological Association). It intends to identify the causes and symptoms of various psychological disorders, then develop interventions to treat them. However, this is challenging because causes and treatment often display a bidirectional relationship; it is difficult to determine the usefulness of a treatment if the causes of a disorder are unknown, but causes are often informed by the outcomes of treatment.

A mental disorder studied in abnormal psychology is Social Anxiety Disorder (SAD)—the “significant anxiety and discomfort about being embarrassed, humiliated, rejected or looked down on in social situations” (Parakh). It is the most common anxiety disorder, with a lifetime prevalence of 5% in adults, thus raising the question of whether existing treatment is effective (Thomas). As a pre-science, Psychology does not have a single universally accepted paradigm, hence presents challenges in establishing a single cause for SAD. With various factors that could cause one’s social anxiety, the effectiveness of treatment in addressing those causes may be difficult to determine.

Existing research on SAD suggests biological, cognitive and sociocultural causes. According to Clark and Wells, social anxiety may be developed cognitively when one perceives the social world as threatening and thus fears it (Clark and Wells 69). Meanwhile, research in neuroscience suggests biological explanations, that SAD may be localized in certain areas of the brain and triggered by abnormalities in neurotransmission. Moreover, as a disorder closely associated with one’s social life, sociocultural research understands SAD as being a mixture of cultural upbringing and exposure to social constructs. This complexity generates challenges in designing treatment that can account for such individual and sociocultural differences.

Cognitive behavioural therapy (CBT) is a common treatment for social anxiety, thus its effectiveness is valuable to study (Priyamvada 60). CBT merges the techniques derived from behavioural and cognitive sciences (Cameron). It attempts to reframe errors in thinking, allowing patients to exert healthier control over their behaviour by separating the actions of others from their own interpretation of the world (Greenwood). Although CBT is centered around the cognitive aspects of SAD, the question remains whether the biological and sociocultural factors can also be treated by adjusting thinking. Therefore, the research question arises, “How effective is cognitive behavioural therapy in treating social anxiety disorder?”

This topic is significant not only to patients suffering SAD but to Psychology in general. Evaluating the effectiveness of CBT can provide insight into how successful the field of abnormal psychology is in achieving its goal of identifying and treating maladaptive behaviour. By breaking down the strengths and limitations of CBT, treatment for social anxiety can be improved upon and better adapted to the demands of the specific patient.

With support from psychological studies, the research question will be answered by discussing the effectiveness of CBT in determining whether reframing thinking and behaviour are sufficient in addressing the cognitive, biological and sociocultural etiologies of SAD. The first part of the essay evaluates whether the procedures of CBT can successfully reduce patients’ fear of the social world. Part two analyses biological explanations and the efficacy of pharmacological interventions as a complementary treatment option. Lastly, the third part explores whether CBT is effective for SAD patients from collectivist cultures, whereby their interpretation of the disorder and approach to seeking treatment may be different from those in individualist cultures in which CBT was developed. This essay ultimately proposes that if supplemented with medication, CBT can treat the

cognitive and biological symptoms of SAD, but may be ineffective in addressing the sociocultural causes. Pharmacological interventions may be utilised in combination with CBT to provide a more well-rounded and desirable treatment for SAD.

## 1. Reframing Thinking - Addressing Cognitive Causes and Symptoms

CBT is effective in addressing the cognitive factors of SAD because it challenges patients' distorted appraisals of themselves in social situations and replaces them with more realistic interpretations (Cameron). Patients learn to gauge control over their social performance without resorting to fear and avoidance. The first component of CBT in treating SAD is psychoeducation, where the clinician facilitates the cognitive awareness of the patient that they are no less socially skilled than others (Simos and Hofmann 114). It is the first step to opening the patient's mind and encouraging them to embrace cognitive change. The patient will learn that SAD will decrease over time in the absence of avoidance behaviour and thus reduce the use of such strategies (Simos and Hofmann 115).

The second component in CBT is attention and situation modification. The anticipation of an anxiety-provoking situation produces an attentional shift in SAD patients toward the self. Such intense self-monitoring monopolises the patient's attentional resource that would otherwise facilitate successful social performance (Simos and Hofmann 115). Hence, the clinician will teach the patient to divert their attention from anxiety symptoms, such as sweating and facial flushing, to the social situation, such as making eye contact and asking questions (Simos and Hofmann 116).

Prior to entering a social event, SAD patients often imagine it in great detail and anticipate poor performance. This leads to an overestimation of the social standards that others may evaluate them against. After the event, the patient may reflect on the experience with a distorted perception that they behaved awkwardly. These exceptionally high and unrealistic standards that patients place on themselves result in a lack of confidence in their own social skills. Hence, the third component of CBT, cognitive restructuring, allows the therapist to understand and challenge the factual basis of such beliefs, thereby assisting the patient in generating more rational predictions and interpretations of their social experiences (Simos and Hofmann 116).

According to research, the above treatment procedures can effectively modify a patient's distorted perceptions of themselves in social events, thereby decreasing their fear of social interactions. The study conducted

by Pinjarkar *et al.* (2015) aimed to investigate the effectiveness of CBT in reducing self-consciousness and fear of social situations in patients with SAD. Seven patients with a DSM-IV diagnosis of SAD engaged in 16 weekly sessions of individual CBT. Participants were assessed at baseline, post-intervention and one month follow up using the Liebowitz Social Anxiety Scale and Social Phobia Scale, which assess the participant's fear, avoidance, self-consciousness, and other negative beliefs in recent anxiety provoking social situations (Pinjarkar *et al.* 22). The results showed that clinically significant improvement of 56% to 95% was seen in four patients on all social anxiety measures at post-treatment, meaning the intervention was successful in replacing distorted evaluations with more realistic interpretations of their social performance, thereby reducing fear. At the follow up assessment, the improvements observed at post-treatment were maintained, indicating a long term benefit of CBT (Pinjarkar *et al.* 23). Therefore, this study demonstrates the effectiveness of CBT in addressing the cognitive etiologies of SAD because it shows that participants were less self-conscious and fearful of social interactions after receiving the treatment.

The use of two SAD scales which account for a comprehensive variety of symptoms provides a holistic assessment of participants' SAD throughout the course of the study and reflects the complexity of the disorder. However, both scales rely on self-reported data, whereby patients rate their level of fear in different scenarios. This decreases the credibility of the assessments because participants may have low introspective ability, meaning they are unable to assess themselves objectively and accurately, especially when their anxiety further distorts their thoughts. Moreover, questionnaires are prone to demand characteristics because participants may realise they are being tested on their SAD based on the questions on the surveys. Response bias may occur, where participants' responses are influenced by previous questions that may have stimulated certain memories of social experiences, thus affecting their fear rating of the later scenarios. These factors may reduce the trustworthiness of the findings, causing them to not fully reflect the actual impact that CBT had on participants' SAD.

Moreover, an in-depth analysis of seven participants provides a deep understanding of each patient's response to treatment, despite limiting the study's transferability. Although all participants had a proper clinical diagnosis of SAD, the small sample size means that their treatment outcomes may not be representative of individuals who developed SAD under different contexts. Therefore, it is questionable whether similar results would occur with the wider SAD population.

## 2. Pharmacological Intervention - Addressing Biological Causes and Symptoms

One of the fundamental elements of SAD may be biological in nature. Regarding brain structure, it has been found that overactivation of the amygdala and hippocampus are features of SAD. The study conducted by Machado-de-Sousa *et al.* (2014) aimed to investigate whether there are structural abnormalities in the amygdala and hippocampus of individuals with SAD (Machado-de-Sousa *et al.* 3). Thirteen participants with a DSM-IV diagnosis of SAD and fourteen healthy non-anxious participants underwent MRI brain scans (Machado-de-Sousa *et al.* 2). The images were then compared to identify differences in brain structure as a result of social anxiety. The results showed that participants suffering from SAD had greater amygdala and hippocampus volumes compared to the healthy controls. That was because the amygdala is responsible for processing threatening stimuli and activating fear-related behaviours in response as an evolutionary defense mechanism (Baxter and Croxson 21180). The amygdala of SAD patients recognise social stimuli as potentially threatening and thus employ fear to overcome it, resulting in hyperresponsiveness (Machado-de-Sousa *et al.* 1). Meanwhile, the hippocampus is part of the neural anxiety network associated with encoding and retrieving past traumatic memories of social events (Furmark *et al.* 425). SAD patients enter social situations with heightened memory of themselves performing poorly in a previous similar context, even if such memories were reconstructed by an insistence on their lack of social skills (Khetrapal). Therefore, this study demonstrates the biological implications of SAD because it shows that participants with this disorder had larger amygdala and hippocampal volumes. These findings hence suggest that CBT may not be conclusive in addressing such structural biological abnormalities.

However, due to neuroplasticity, the amygdala and hippocampus may actually change as one practices the skills required to overcome social fears from CBT. In this case, CBT may be effective in addressing the biological causes of SAD. The study conducted by Furmark *et al.* (2002) aimed to investigate how alleviation of social anxiety changes the structure of the brain. Eighteen patients who fulfilled the DSM-IV criteria for SAD received eight weekly sessions of CBT. Before and after treatment, they received a brain Positron Emission Tomography (PET) scan while engaging in a public speaking task and completed various questionnaires to assess their disorder (Furmark *et al.* 426). The brain images and questionnaire responses were compared

to identify correlations between changes to the brain and alleviation of SAD after treatment. The results showed that 67% of participants exhibited reduction in symptoms after receiving CBT, which was accompanied by a decrease in amygdala and hippocampal density (Furmark *et al.* 428). That was because as participants learned to reframe thinking, these brain structures changed in size to facilitate this skill through neuroplasticity (Goldin *et al.* 1049). Therefore, this study demonstrates the effectiveness of CBT in treating the biological causes of SAD because it shows that neural activity in the amygdala and hippocampal regions were successfully suppressed after treatment, thereby alleviating social anxiety symptoms such as fear of public speaking (Furmark *et al.* 430).

The biological approach in psychology attempts to identify causal relationships, but Furmark *et al.*'s study is limited in that it is correlational in nature. Although results show a relationship between reduction in SAD symptoms and brain density, there is insufficient evidence to suggest that changes in brain structure were direct products of symptom alleviation by CBT. In addition, brain structure and symptom alleviation may display a bidirectional relationship. It is unknown whether CBT reduced amygdala and hippocampal density which led to decreased fear of social interactions or that treatment reduced symptoms which led to changes in the brain. Hence, although this study suggests neuroplasticity as an explanation to the effectiveness of CBT in addressing the biological factors of SAD, this relationship may only be correlational and indirect.

Assessments of participants' social anxiety were conducted through self-report questionnaires, which may be prone to subjectivity and inaccuracy. Demand characteristics may lead to dishonest responses in an attempt to meet researcher demands. This limitation would affect the correlation identified between changes in the brain and alleviation of SAD. Consequently, conclusions on whether CBT can actually address the neurobiological element of SAD may lack credibility.

In terms of the neurochemical elements of SAD, the neurotransmission of serotonin, norepinephrine and dopamine may also be involved (Starcevic 167). To address these factors, pharmacological interventions can be utilized, which provide immediate and temporary relief to SAD symptoms (Starcevic 177). Together with CBT, the two interventions can exert greater levels of success in treating SAD. Common first line pharmacological treatment options for SAD include Selective Serotonin Reuptake Inhibitors (SSRIs), which increase serotonin levels in the synapses, thereby improving the regulation of emotion.

MonoAmine Oxidase Inhibitors (MAOIs) reduce the amount of monoamine oxidase in the brain—an enzyme responsible for removing norepinephrine, serotonin and dopamine, hence boosting the patient’s mood (Starcevic 179). The study conducted by Heimberg *et al.* (1998) aimed to compare the effects of CBT and MAOIs on SAD. A hundred and thirty-three American patients with a DSM-III diagnosis of SAD were allocated to one of three groups: CBT, MAOI and placebo. Patients in the MAOI and placebo groups were administered the corresponding medication everyday, while the remaining participants engaged in 12 weekly sessions of CBT. A range of scales, including the Liebowitz Social Anxiety Scale and Fear Questionnaire were used to assess the participants’ conditions before, mid, and post intervention (Heimberg *et al.* 1134). The results showed that compared to the placebo group, both CBT and MAOI led to higher rates of response post-treatment, indicating the effectiveness of both interventions in treating SAD. At mid-intervention, 52% of MAOI patients and only 28% of CBT patients were classified as responders, meaning the effects of MAOI were exerted quicker than CBT (Heimberg *et al.* 1140). Therefore, this study demonstrates a limitation of CBT being time lags because it shows that participants who received this treatment experienced improvements later than those who received pharmacological intervention.

Assessments of SAD may be unreliable in Heimberg *et al.*’s study because participants’ conditions were determined through self-reported questionnaires. Demand characteristics and social desirability may hinder the study’s credibility in arguing that CBT is not the most effective treatment option in the short run. However, by comparing participants’ outcomes after receiving medicine and CBT, it can be validly concluded that both interventions are successful despite different approaches in treating the disorder. Medication can offer an immediate but temporary relief to symptoms during urgent situations by increasing the essential chemicals in the brain responsible for regulating emotion (Schneier *et al.* 530). This is useful for contexts where one has to meet the demands of a social event immediately (Starcevic 175). CBT goes beyond this and tackles the root cause of one’s social anxiety by reframing the patient’s cognitive interpretations of their social experiences and suppressing the biological mechanisms that sustain the disorder. Unlike pharmacological therapy, CBT can potentially treat one’s SAD in the long run (Yoshinaga *et al.* 2). Therefore, combining both treatment methods may be the most effective (Schneier *et al.* 538).

### **3. Culturally Specific SAD - Addressing Sociocultural Causes and Symptoms**

As a treatment developed in the West, CBT focuses on the Western manifestation of SAD. However, when considering the success of treatment, one must acknowledge that although cross-national research has confirmed that this disorder occurs worldwide, the classification and symptomatic indicators of it may vary. For instance, Taijin Kyofusho (TKS) is a culture-specific type of SAD from Japan referring to the fear of offending others in social situations rather than the concern of one’s own embarrassment (Kleinknecht *et al.* 160). Thus, CBT that attempts to help TKS patients understand that they are not as negatively evaluated as they believe may not be effective in treating their cultural-specific fear of embarrassing others. This shows that the cultural context of one’s SAD is significant in directing the approach of treatment. This raises the issue of whether CBT would be effective if the patient’s causes, symptoms and attitudes toward treatment do not align with the Western context in which CBT was developed.

The causes of social anxiety may be shaped by societal values embedded in one’s upbringing, thus CBT may not be successful in addressing non-Western societal factors that are integral in one’s SAD. In a collectivist country like Japan, the etiology of TKS is founded on the concern of hindering the well-being of others in social events, as this implies failing to meet the norms of the group. Contrastingly, SAD in an individualistic context tends to be centered around the fear of being negatively evaluated by others and seeming undesirable (Hofmann *et al.* 1122). Although TKS and SAD are both associated with the avoidance of social interactions, the underlying social factors that result in symptoms are different. Hence, it is questionable whether the framework for CBT can successfully address the collectivist norms that cause one’s SAD.

Furthermore, differences in the causes of SAD across cultures result in varied symptomatology. As treatment is designed based on the patient’s symptoms, a problem arises of whether CBT is the desired form of treatment when patients display symptoms different from a Western understanding of SAD found in the DSM-V. The study conducted by Fan and Chang (2015) aimed to investigate whether there are culture-specific symptoms in SAD patients from the collectivist country of China which are absent in the West. Twenty-five Chinese undergraduate students were asked to speak about their experiences when they felt anxious, nervous or



awkward in social situations, such as public speaking. A list of social anxiety indicators were generated from the interview responses, which was then compared with the Western measures of SAD: the Social Interaction Anxiety Scale and Social Phobia Scale (Fan and Chang 9). The results showed that 10 new indicators of SAD were raised by the Chinese participants that were not recognised in the Western measuring scales, including physical symptoms when interacting with others, fear of making others uncomfortable, and worries about maintaining their family's image. These new items are unique to China as a collectivist society because the culture promotes the interdependent self and obligations to family (Fan and Chang 9). Therefore, this study demonstrates cultural factors in SAD because it shows that the symptoms experienced by Chinese participants were different from those listed in Western SAD indicators. Hence, CBT may be ineffective in addressing these culture-unique symptoms.

However, findings from Fan and Chang's study are based on the assumption that participants have SAD despite not being formally diagnosed, hence it is unsure whether the new symptoms identified in the study are reflective of the experiences of diagnosed SAD patients in China. This decreases the credibility of the study's comparison between SAD in the East and West. If the differences in symptomatology between these two cultures are not validly identified, there may be difficulties in evaluating the effectiveness of CBT in addressing the sociocultural factors of SAD for patients outside of Western individualistic cultures.

Since mental disorders are not viewed as valid reasons to receive treatment in Eastern societies, patients somatize their psychological symptoms to conform to societal norms (Kirmayer 23). As treatment is guided by symptoms and CBT focuses on the cognitive aspect of mental disorders, this treatment may not be recommended nor effective to address physical symptoms. The study conducted by Kirmayer (2001) aimed to investigate somatization of SAD symptoms in patients from different ethnocultural groups. Seven hundred SAD patients from Eastern ethnicities of Afro-Caribbean, Vietnamese and Filipino were observed as they presented their condition to their physicians. The results showed that the vast majority of patients made exclusively somatic presentations to their physicians, such as musculoskeletal pain and fatigue, and only 15% presented any psychological complaint. When participants were asked what caused their somatic symptoms, 20% of participants were persistent on their somatic symptoms and rejected any connection with their anxiety disorder. This was because patients in these cultures may be ashamed to seek professional help about

their SAD due to stigmas in society surrounding mental health. Hence, they express somatic complaints, which are more socially appropriate and non-stigmatized reasons to receive treatment (Kirmayer 24). This study demonstrates the impact of sociocultural factors on patients' interpretation of their SAD because it shows that participants from Eastern cultures tend to report physical symptoms, which may lead to ineffective CBT in addressing the underlying fear of social interactions.

The criteria for SAD in the DSM-V only indicates psychological symptoms, such as fear and avoidance (CBHSQ 41). Therefore, conclusions from Kirmayer's study can be compared with it to show that somatization of SAD may be unique to Eastern cultures and not accounted for in the Western framework. This offers an indication that CBT may not be successful in treating SAD when the patient's reporting of symptoms are not compatible with the Western framework. However, Kirmayer does not mention how participants' SAD were assessed. Without a formal diagnosis, researchers may have assumed an underlying psychological disorder when participants presented their somatic symptoms, when in reality their symptoms may have been purely physiological. Furthermore, the questions regarding participants' beliefs on the causes of their symptoms may have implied the idea that anxiety was involved. For instance, researchers directly suggested a psychological cause and recorded whether participants would reject this idea. The phrasing of such questions may have influenced participants to answer a certain way, thus decreasing the credibility of the responses. Consequently, the extent to which somatization of symptoms in Eastern cultures impacts the effectiveness of CBT remains uncertain.

As a result of the above reasons, CBT may be ineffective in treating collectivist Eastern SAD. The study conducted by Kroll *et al.* (1990) aimed to investigate the effectiveness of CBT on Southeast Asian SAD patients. Thirty-two patients from Southeast Asia, including Hmong, Cambodia and Laos participated in 17 weeks of CBT and were assessed on the severity of their disorder against a range of measures before and after treatment. The results showed that 80% of Hmong, 25% of Cambodia and 40% of Laotian patients displayed minimal improvements in the post-CBT assessment (Kroll *et al.* 280). Therefore, this study demonstrates the ineffectiveness of CBT in treating non-Western individualistic SAD patients because it shows that Southeast Asian patients experienced minor reduction in anxiety after intervention.

A limitation in Kroll *et al.*'s study is that Western diagnostic tools for SAD were used, which does not

take into account somatic indicators and other culture-unique symptoms. Nonetheless, this study suggests that CBT being a treatment that originated from the West, may not be effective in treating SAD that developed from other cultures.

## Conclusion

This investigation into the effectiveness of CBT in treating SAD shows that the disorder is complex in which etiological roots could be cognitive, biological and sociocultural. It is evident from research that CBT is effective in treating the cognitive symptoms of SAD because it deals with patients' fear of being negatively evaluated and facilitates reframing of thoughts, as indicated by Pinjarkar *et al.* Overactivation of the amygdala and hippocampus are physiological features of SAD that CBT may not be able to address. However, research conducted by Furmark *et al.* shows that repeated practice of skills learnt from CBT can treat such abnormalities through neuroplasticity. Since treatment takes relatively long, medication can be utilized in combination with CBT to offer immediate relief to SAD symptoms. As a Western intervention developed in an individualistic context, CBT may be ineffective in addressing the sociocultural factors of SAD unique to Eastern collectivist societies because the causes and symptoms from these cultural dimensions may be incompatible.

Studies examined in this essay are reliable because they use the scientific method to make comparisons between participants' conditions before and after treatment. This enables researchers to identify the effect of CBT on participants' SAD, hence arriving at a credible conclusion about whether such intervention is effective. However, such research relies on self-reported measures in questionnaires to assess participants' symptoms because anxiety may not always be observable. These methods may yield less trustworthy results due to participants' biases and demand characteristics, leading to unreliable knowledge on the effectiveness of CBT in treating SAD.

From the above analysis, it may be concluded that CBT is effective in explicitly addressing the cognitive symptoms of SAD and implicitly the biological causes with medication. Socioculturally, initial research in this paper indicates that CBT may be ineffective in treating collectivist Eastern SAD. The application of CBT in etic studies examining culturally specific symptoms is an area for further research.

## References

- American Psychological Association. Abnormal Psychology. *APA Dictionary of Psychology*, American Psychological Association. <https://dictionary.apa.org/abnormal-psychology>.
- Baxter, M. G. & Crosson, P. L. (2012). Facing the role of the amygdala in emotional information processing. *PNAS*, 109(52), 21180-21181. <https://doi.org/10.1073/pnas.1219167110>.
- Cameron, A. Y. (2019). *Cognitive Behavioural Therapy*. AccessScience, McGraw-Hill Education. <https://doi.org/10.1036/1097-8542.146850>.
- CBHSQ. (2016). Table 16. DSM-IV to DSM-5 Social Phobia/Social Anxiety Disorder Comparison. *DSM-5 Changes: Implications for Child Serious Emotional Disturbance, Substance Abuse and Mental Health Services Administration*. <https://www.ncbi.nlm.nih.gov/books/NBK519712/table/ch3.t12/>.
- Clark & Wells. (1995). A Cognitive Model of Social Phobia. *Social Phobia: Diagnosis, Assessment, and Treatment*, edited by Richard G. Heimberg, Michael R. Liebowitz, Debra A. Hope, & Franklin R. Schneier, The Guilford Press. 69-93.
- Fan, Q. & Weining C. C. (2015). Social Anxiety among Chinese People. *The Scientific World Journal*, 1-12. <https://doi.org/10.1155/2015/743147>.
- Furmark, T., *et al.* (2002). Common Changes in Cerebral Blood Flow in Patients with Social Phobia Treated with Citalopram or Cognitive Behavioural Therapy. *Archives of General Psychiatry*, 59(5), 425-433. <https://doi.org/10.1001/archpsyc.59.5.425>.
- Goldin, P. R., *et al.* (2013). Impact of Cognitive-Behavioral Therapy for Social Anxiety Disorder on the Neural Dynamics of Cognitive Reappraisal of Negative Self-Beliefs. *JAMA Psychiatry*, 70(10), 1048-1056. <https://doi.org/10.1001/jamapsychiatry.2013.234>.
- Greenwood, V. (2014) Goals of Cognitive Therapy. *The Washington Center for Cognitive Therapy*, DC Web Design. <https://washingtoncenterforcognitivetherapy.com/treatment-models/cognitive-therapy/goals-of-cognitive-therapy/>.
- Heimberg, R. G., *et al.* (1998). Cognitive Behavioural Group Therapy vs Phenelzine Therapy for Social Phobia. *Archives of General Psychiatry*, 55(12), 1133-1141. <https://doi.org/10.1001/archpsyc.55.12.1133>.
- Hofmann, S. G., *et al.* (2010). Cultural Aspects in Social Anxiety and Social Anxiety Disorder. *Depression and Anxiety*, 27(12), 1117-1127. <https://doi.org/10.1002/da.20759>.
- Khetrpal, A. (2019). Neural Mechanisms of Social Anxiety Disorder. *News Medical Life Sciences*, AZoNetwork. <https://www.news-medical.net/health/Neural-Mechanisms-of-Social-Anxiety-Disorder.aspx>.
- Kirmayer, L. J. (2001) Cultural Variations in the Clinical Presentation of Depression and Anxiety: Implications for Diagnosis and Treatment. *J Clin Psychiatry*, 62(13), 22-30. <https://pubmed.ncbi.nlm.nih.gov/11434415/>.
- Kleinknecht, R. A., *et al.* (1997) Cultural Factors in Social Anxiety: A Comparison of Social Phobia Symptoms and *Taijin Kyofusho*. *Journal of Anxiety Disorders*, 11(2), 157-177. [https://doi.org/10.1016/S0887-6185\(97\)00004-2](https://doi.org/10.1016/S0887-6185(97)00004-2).

Kroll, J. *et al.* (1990). Medication Compliance, Antidepressant Blood Levels, and Side Effects in Southeast Asian Patients. *Journal of Clinical Psychopharmacology*, 10(4), 279-283. <https://doi.org/10.1097/00004714-199008000-00007>.

Machado-de-Sousa, João Paulo, *et al.* (2014). Increased Amygdalar and Hippocampal Volumes in Young Adults with Social Anxiety. *PLoS ONE*, 9(2), 1-5. <https://doi.org/10.1371/journal.pone.0088523>.

Parakh, R. (2017). What Are Anxiety Disorders? *American Psychiatric Association*. <https://www.psychiatry.org/patients-families/anxiety-disorders/what-are-anxiety-disorders>.

Pinjarkar, R. G., *et al.* (2015). Brief Cognitive Behavioural Therapy in Patients with Social Anxiety Disorder: A Preliminary Investigation. *Indian Journal of Psychological Medicine*, 37(1), 20-26. <https://doi.org/10.4103/0253-7176.150808>.

Priyamvada, R. *et al.* (2009). Cognitive behavioral therapy in the treatment of social phobia. *Industrial Psychiatry Journal*, 18(1), 60-63. <https://doi.org/10.4103/0972-6748.57863>.

Schneier, F.R., *et al.* (2014). Pharmacological Treatment for Social Anxiety Disorder. *The Wiley Blackwell Handbook of Society Anxiety Disorder*, edited by Justin W. Weeks, John Wiley & Sons Ltd, 521-546.

Simos, G. & Stefan G. H. (2013). Social Anxiety Disorder: Treatment Targets and Strategies. *CBT for Anxiety Disorders: A Practitioner Book*, John Wiley & Sons Ltd, 104-123.

Starcevic, V. (2005). Social Anxiety Disorder (Social Phobia). *Anxiety Disorder in Adults: A Clinical Guide*, Oxford University Press, 141-190.

Thomas, L. (2021). Social Anxiety Epidemiology. *News Medical Life Sciences*, AZoNetwork. <https://www.news-medical.net/health/Social-Anxiety-Epidemiology.aspx>.

Wong, J. *et al.* (2014). Cognitive-Behavioural Models of Social Anxiety Disorder. *The Wiley Blackwell Handbook of Society Anxiety Disorder*, edited by Justin W. Weeks, John Wiley & Sons Ltd, 3-23.

Yoshinaga, N., *et al.* (2013). A preliminary study of individual cognitive behavior therapy for social anxiety disorder in Japanese clinical settings: a single-arm, uncontrolled trial. *BMC Research Notes*, 6(74), 1-8. <https://doi.org/10.1186/1756-0500-6-74>.

---

# What is the relationship between the different types of terrace fields of the same total height and the volume of water needed to fully fill the terrace fields?

Franklin S. Ke

---

## Introduction

Food is imperative to human life. In many countries, terrace cultivation, an approach of growing crops on the slope of the mountains (Encyclopædia Britannica), is used to control soil erosion on sloping farmlands. It significantly affects water storage, soil conservation, and yields. Through the use of terrace fields, better ventilation and light conditions can be provided, increasing crop growth and nutrient accumulation efficiency for plants such as rice and trees. In China, a huge proportion of rice is planted in terraces. If an incoming drought causes all the water stored in the terraces to dry out, farmers will receive no revenue. Because rice is unable to survive without water, people living in China may suffer from hunger due to the scarce supply of rice. As a compassionate citizen, where most of my family members live in China, it is unfathomable to realise that my home country could experience such a disaster. Therefore, there is a suggestion that the government calculate the amount of water needed to fully refill the terrace fields to mitigate the effects of a potential drought.

## 1. Methodology

Since mountains have different slopes at different altitudes, the type of terrace field used in different altitudes will differ. Table 1 shows the angle of mountain where each type of terrace field is preferred.

Type of terrace field	Level terrace field	Level terrace field (sloping onward)	Bench terrace field (sloping inward)
Angle (°)	Mostly less than 15.0°, some can be more than 15.0°	Less than 10.0°	15.0° to 25.0°

Table 1. Types of terrace fields and their angle used

I will consider an ideal situation where a mountain has constant slopes at different altitudes for each of the three types of terrace field listed above. As the height of each layer of terrace field and the amount of water stored in each layer of terrace field is different for the three types of terrace fields, to investigate the aggregate volume of water required to fulfill each type of terrace field on a mountain, the height of the mountain will be considered constant. Therefore, I will take an additional step to calculate the number of layers that each type of terrace field can have on the same mountain of height 1000 meters. Integration will be used to find the volume of water required for each layer of terrace field, and sequences and series will be used to sum up the total volume needed.

The degree of accuracy I will use for the volume of water will be accurate to the nearest 1000 meters cubed. The degree of accuracy I will use for measurements in degrees will be accurate to 1 decimal place.

## 2. Level Terrace Field

A level terrace field is a type of terrace field that is built on mountains that has a gentle slope (the angle between the mountain and the ground is less than 15.0°) as shown in Figure 1. The shape of this type of terrace field is similar to staircases, with regular height, width, and slope for each layer of terrace field as shown in Figure 2. Also, the barrier between two consecutive layers of terrace field has the same width and slope. Normally, the width of each layer of level terrace field is between 7 and 8 meters; the height of the barrier between two layers of terrace field is 1.2 to 2.2 meters; the slope of the barrier is 75.0 to 85.0°; the height of the water level of each layer of terrace is between 0.03 to 0.05 meters (Dabie, 2020).

The average of the range of values is used to model the volume of water stored in each layer of the level terrace field to enhance the accuracy of the result calculated.

Width of each layer of terrace field	Height of the water level of each layer of terrace field	Height of outer barrier	Slope of barrier
7.5 meters	0.04 meters	1.7 meters	80°

**Table 2.** Design standards for level terrace field (Jz, 2012)

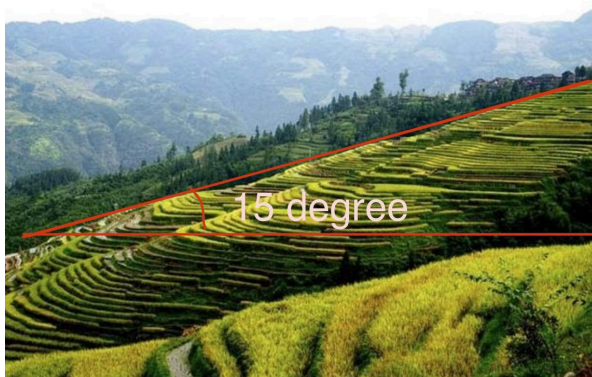


**Figure 1.** Level Terrace Field

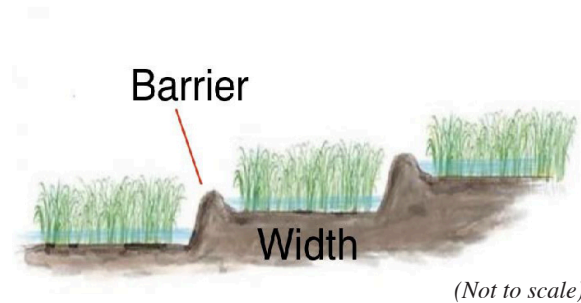


**Figure 2.** Cross-sectional View of Level Terrace Field (Didao, 2020)

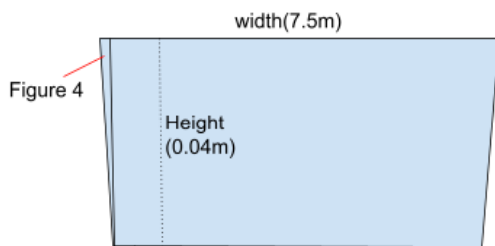


**Figure 3.** Cross-sectional View of Level Terrace Field from side

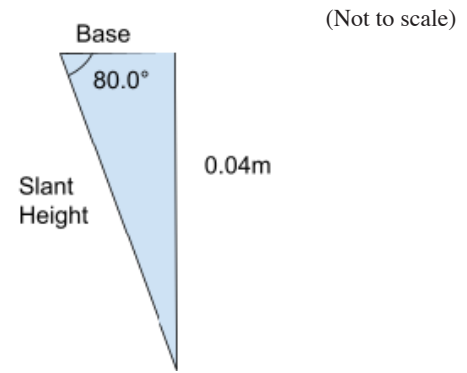


**Figure 4.** Triangle for Calculation

The cross sectional area of each layer of terrace field is the same, which is a trapezium (the blue area presented in Figure 3). The upper base of the trapezium is the width of each layer of terrace field, 7.5 meters. The base of the right angle triangle in Figure 4 and the lower base of the trapezium can be calculated using the height of the water level and the slope of the barrier:

$$\tan(80.0) = \frac{0.04}{\text{base of triangle}}$$

$$\text{base of triangle} = \frac{0.04}{\tan(80.0)} \approx 0.007m$$

$$\text{Lower base} = 7.5 - 2 \times 0.007053 = 7.486m$$

To calculate the total number of layers in the terrace field, the height difference between two consecutive layers of terrace field needs to be known. The height difference can be calculated by finding the difference between the height of the top of two consecutive barriers. Although the height of the barrier is a fixed number, 1.7 meters, the inner height of the barrier must be higher than the water level to prevent water spillage, 0.4 meters, is needed to be subtracted from the height of the outer barrier. Therefore, 1.2 meters will be used as the height difference between two layers of terrace fields ( $1.7 - (0.4 + 0.1) = 1.2m$ , 0.1 meters is the additional height that is used to prevent water spillage). Consequently, the number of layers of the level terrace field can be found: *number of layers*

$$= \frac{1000}{1.2} \approx 833 \text{ layers.}$$

Calculations for table 3:

$$Volume = \pi \int_0^{0.04} (\text{function of the left slant height})^2 dy - \pi \int_0^{0.04} (\text{function of the right slant height})^2 dy$$

If the four vertices of the trapezium are plotted first in Desmos, the line of best fit of the function of the left slant height and function of right slant height can be found. Note that these functions will be expressed in terms of  $y$ , not  $x$ , in the form of  $x = my + c$ .

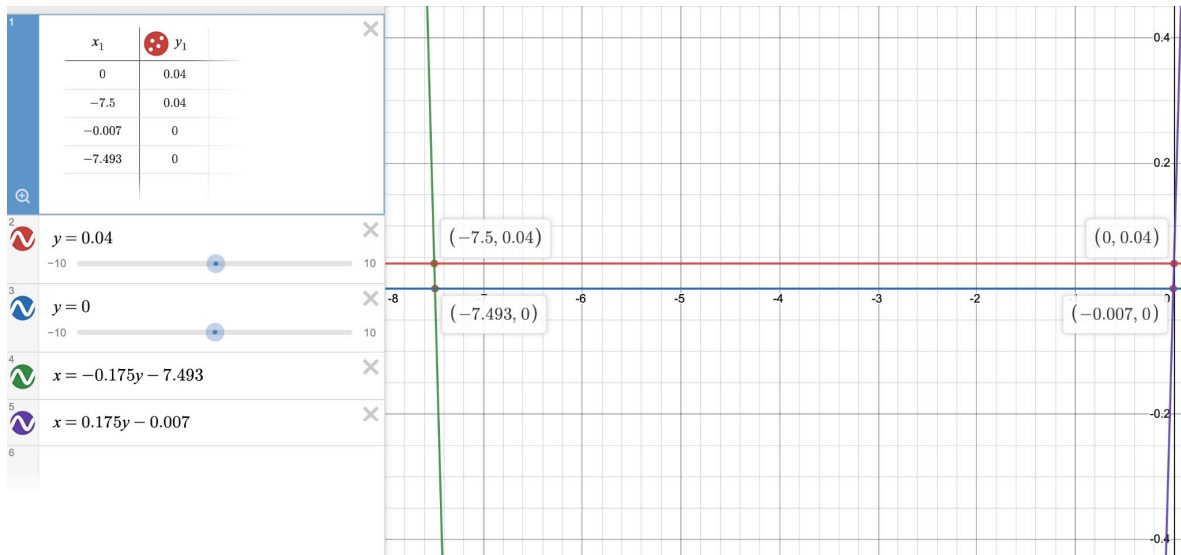


Figure 5 . The cross-sectional area of the first layer of the terrace field and the formula of the two slant heights of the trapezium shown by Desmos)

Sample Calculation (using the first layer of the level terrace field(the top layer)):

$$\begin{aligned}
 Volume &= \pi \int_0^{0.04} (-0.175y - 7.4973)^2 dy - \pi \int_0^{0.04} (0.175y - 0.007)^2 dy \\
 &= \int_0^{0.04} \pi \left( -\frac{7y}{40} - \frac{7493}{1000} \right)^2 dy - \int_0^{0.04} \pi \left( \frac{7y}{40} - \frac{7}{1000} \right)^2 dy \\
 &= \frac{\pi}{1000000} \int_0^{0.04} (175y + 7493)^2 dy - \frac{49\pi}{1000000} \int_0^{0.04} (25y - 1)^2 dy \leftarrow \text{Linearity} \\
 &= \frac{0.04}{0} \left( \frac{\pi(175y + 7493)^3}{525000000} - \frac{49\pi(25y - 1)^3}{75000000} \right) \\
 &= \frac{0.04}{0} \left( \frac{3\pi y(175y + 7486)}{400} \right) \\
 &= \frac{22479\pi}{10000} m^3
 \end{aligned}$$

$$\text{substitute } u = 175y + 7493 \rightarrow dy = \frac{1}{175} du$$

$$\text{substitute } w = 25y - 1 \rightarrow dy = \frac{1}{25} dw$$

$$\frac{1}{175} \int u^2 du - \frac{1}{25} \int w^2 dw$$

$$= \frac{u^3}{525} - \frac{w^3}{75}$$

$$= \frac{(175y + 7493)^3}{525} - \frac{(25y - 1)^3}{75}$$

As the width of a layer of the terrace field is 7.5 meters, the four vertices of the nth layer of terrace field will experience a horizontal shift to the left by 7.5 (n - 1) meters, and the equation of the left and right slant height of the nth layer of terrace field can be found by using the following formula:

$$\text{function of the left slant height} = -0.175y - (7.493 + 7.5(n - 1))$$

$$\text{function of the left slant height} = 0.175y - (0.007 + 7.5(n - 1))$$

Sample Calculation (using the second layer of the level terrace field):

$$\begin{aligned} \text{function of the left slant height} &= -0.175y - (7.493 + 7.5(2 - 1)) \\ &= -0.175y - 14.993 \end{aligned}$$

$$\begin{aligned} \text{function of the left slant height} &= 0.175y - (0.007 + 7.5(2 - 1)) \\ &= 0.175y - 7.507 \end{aligned}$$

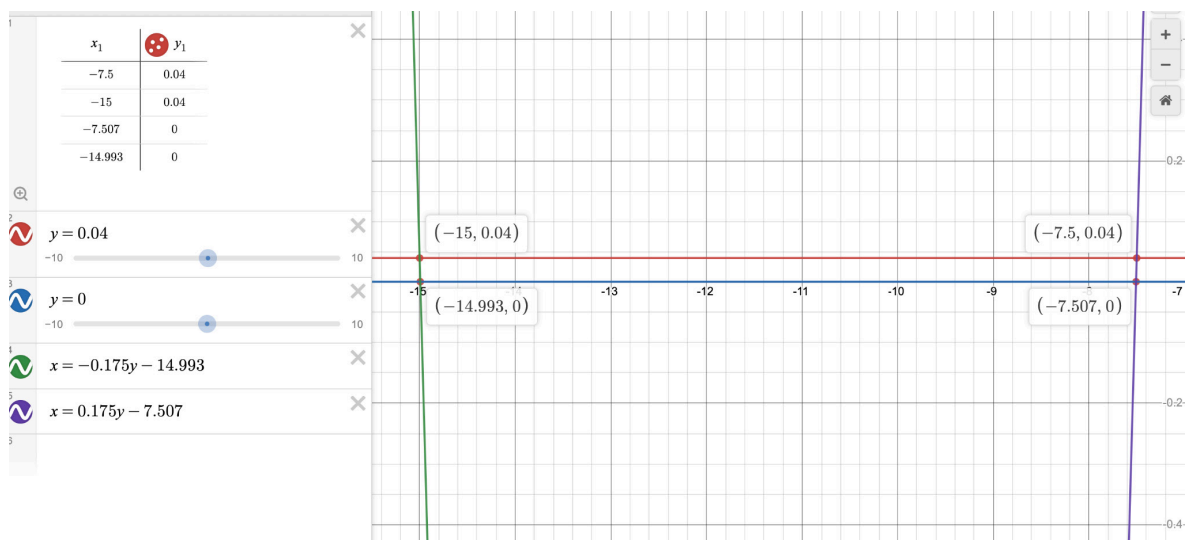


**Figure 6 .** The cross-sectional area of the second layer of the terrace field and the formula of the two slant heights of the trapezium shown by Desmos

Desmos graphing calculator can prove the reliability of the formula used as the cross-sectional areas shown in Figure 5 and Figure 6 are equivalent (the cross-sectional area of the level terrace field is the area surrounded by the four curves).

The number of layer	Function of the left slant height	Function of the right slant height	Volume (m <sup>3</sup> )
1	$x = -0.175y - 7.493$	$x = 0.175y - 0.007$	$\frac{22479\pi}{10000}$
2	$x = -0.175y - 14.993$	$x = 0.175y - 7.507$	$\frac{67437\pi}{10000} = 3 \times \frac{22479\pi}{10000}$
3	$x = -0.175y - 22.993$	$x = 0.175y - 15.007$	$\frac{112395\pi}{10000} = 5 \times \frac{22479\pi}{10000}$
4	$x = -0.175y - 29.993$	$x = 0.175y - 22.507$	$\frac{157353\pi}{10000} = 7 \times \frac{22479\pi}{10000}$
...	...	...	...
832	$x = -0.175y - 6239.993$	$x = 0.175y - 6232.507$	$\frac{37382577\pi}{10000} = 1663 \times \frac{22479\pi}{10000}$
833	$x = -0.175y - 6247.993$	$x = 0.175y - 6240.007$	$\frac{37427535\pi}{10000} = 1665 \times \frac{22479\pi}{10000}$

**Table 3.** the number of layer, the functions of its left and right slant height, and its volume

In table 3, consecutive layers of the terrace field from the top and the bottom of the mountain are presented, and it is noticeable that the volume of water in the layers of the level terrace field forms an arithmetic sequence that has a common difference of  $\frac{22479\pi}{5000}$ . Therefore, the total amount of water stored in the level terrace (height of 1000 meters) can be calculated:

$$\begin{aligned}
 \text{total volume} &= \left( \frac{22479\pi}{10000} + 1665 \times \frac{22479\pi}{10000} \right) \times \frac{833}{2} \\
 &= 693889 \times \frac{22479\pi}{10000} \\
 &= 1559793\pi \\
 &\approx 4,900,000\text{m}^3
 \end{aligned}$$

### 3. Bench Terrace Field (sloping outward)

An outward sloping bench terrace field is built on mountains that have a slope of less than 10.0°. In the same layer of terrace field, the height of the outer section (section on the left of Figure 7) is lower than the height of the inner section (section on the right of Figure 7). Apart from the outward sloping base of the terrace field, all other designs are the same as the scale of a level terrace built on a mountain that has a slope of less than 10.0°, which means that the width of each layer of level terrace field is between 8 and 10 meters; the height of the water level of each layer of terrace is between 0.03 to 0.05 meters; the height of the barrier between two layers of terrace field is between 0.7 and 1.8 meters; the slope of the barrier is 80.0 to 90.0°.

Width of each layer of terrace field	Height of the water level of each layer of terrace field	Height of outer barrier	Slope of barrier
9 meters	0.03 - 0.05 meters	1.25 meters	85°

**Table 4.** Design standards for level terrace field (Jz, 2012)

The average of the range of values is used to model the volume of water stored in each layer of the outward sloping bench terrace field. (The height of water level is not constant so the range of values is kept for that column.)



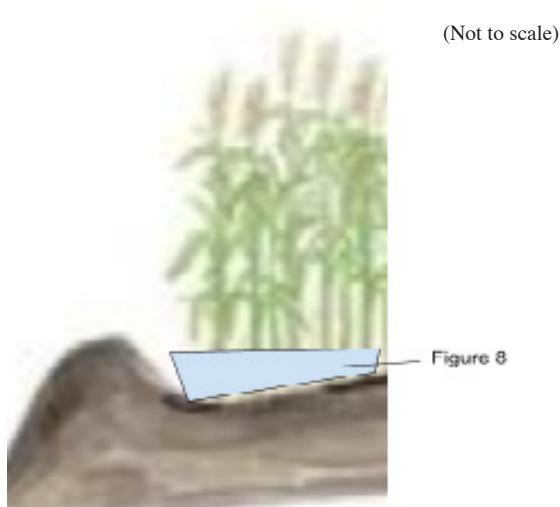


**Figure 7.** Cross-sectional view of an outward sloping bench terrace field (Didao, 2020)

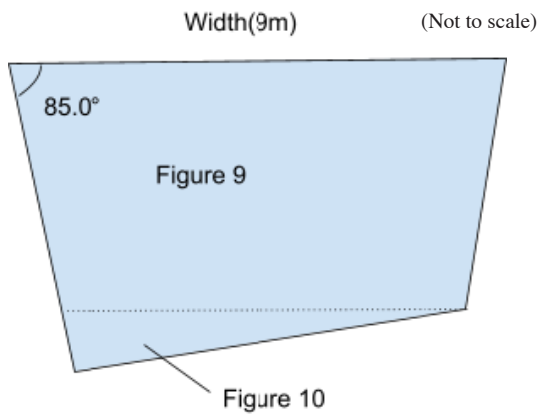


**Figure 8.** Cross-sectional view of the water level in an outward sloping bench terrace field

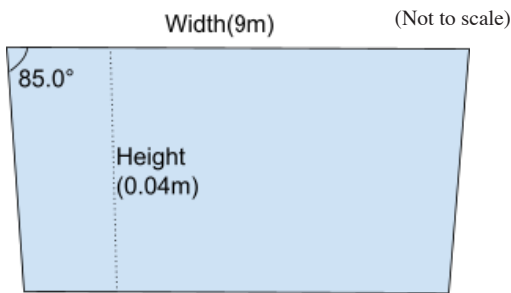


**Figure 9.** Upper section of Figure 8

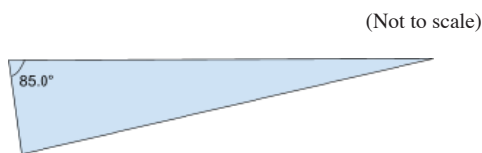


**Figure 10.** Lower section of Figure 8

The water stored in each layer of outward sloping bench terrace field can be approximated to the quadrilateral shape shown in Figure 8, and this shape can be separated into a trapezium (Figure 9) and a triangle (Figure 10). The height of Figure 9 will be 0.04 meters because it is in the range of the average water level required for crops to grow, and the water level in the outer section of the layer will be deeper.

Using a similar approach as used before, the number of layers of terrace field can be calculated:

$$\frac{1000}{1.25 - 0.5} = \frac{1000}{0.75} = 1333 \text{ layers}$$

The width can also be calculated:

$$\text{width} = 9 - 2 \times \frac{0.04}{\tan(85.0)} \approx 8.993 \text{ m}$$

The volume of the trapezium section can be calculated using the same method as the level terrace field by using integration and arithmetic sequence.

*Total volume (trapezium region)*

$$\begin{aligned} &= \left( \frac{81\pi}{25} + 2665 \times \frac{81\pi}{25} \right) \times \frac{1333}{2} \\ &= 1776889 \times \frac{81\pi}{25} \\ &\approx 18,087,999 \text{ m}^3 \end{aligned}$$

As shown in Figure 10 above, the top left angle is 85.0°. Also, the height of the triangle is expected to be less than 0.01 meter (The sum of height of trapezium and triangle should be less than 0.05 meters for rice to survive). Hence, I will set the height of the triangle to 0.005 meters to enable the growth of rice. The volume of the triangular section can also be calculated using integration and arithmetic sequence.

*Total volume (triangle region)*

$$\begin{aligned} &= (0.8472 + 1695.69) \cdot \frac{1333}{2} \\ &\approx 1130742 \text{ m}^3 \\ &\approx 1,131,000 \text{ m}^3 \end{aligned}$$

Consequently, the total (combined the trapezium and triangular region) volume of the bench terrace field can be calculated:

*Total volume*

$$= 18,087,000 + 1,131,000 = 19,218,000 \text{ m}^3$$

#### 4. Bench terrace field (sloping inward)

Most inward sloping bench terrace fields are built on mountains that have a slope between 20.0 and 25.0°. In the same layer of terrace field, the height of the outer section (section on the left of Figure 11) is higher than the height of the inner section (section on the right of Figure 11). All other designs of inward sloping bench terrace fields are the same as the scale of a level terrace built on a mountain that has a slope between 20.0 to 25.0° except the inward sloping base. The width of each layer of level terrace field is between 5 and 6 meters; the height of the water level of each layer of terrace is between 0.03 to 0.05 meters; the height of the barrier between two layers of terrace field is between 1.8 and 2.8 meters; the slope of the barrier is 65.0 to 70.0°. Also, the inward sloping base needs to have an inward sloping angle between 3.0 and 5.0° to prevent soil erosion.

The average of the range of values is used to model the volume of water stored in each layer of the inward sloping bench terrace field. (The height of water level is not constant so the range of value is kept for that column.)

Width of each layer of terrace field	Height of the water level of each layer of terrace field	Height of outer barrier	Slope of barrier	Inward sloping angle
5.5 meters	0.03 - 0.05 meters	2.3 meters	67.5°	4.0°

**Table 5.** Design standards for inward sloping bench terrace fields (Jz, 2012)

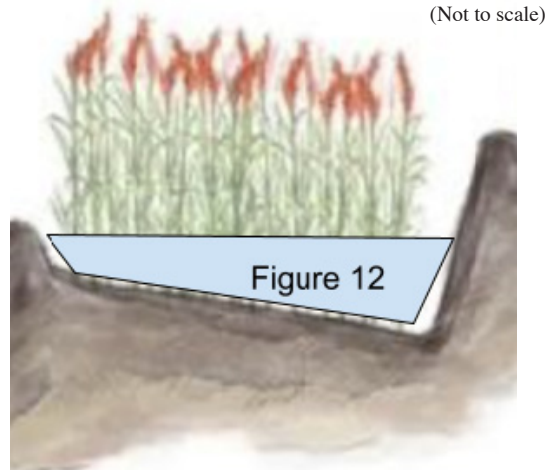


**Figure 11.** Cross-sectional view of the inward sloping bench terrace field (Didao, 2020)

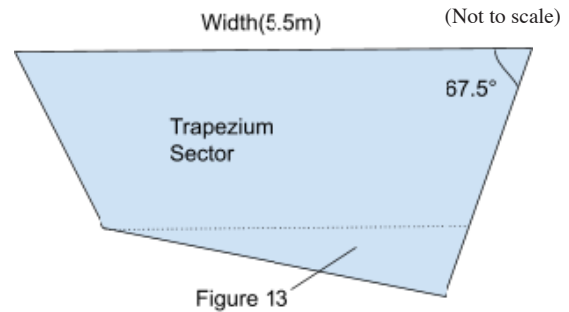


**Figure 12.** Cross-sectional view of the water level in an inward sloping bench terrace field using Table 5

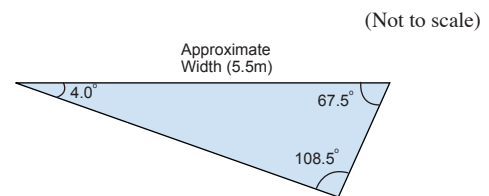


**Figure 13.** Lower section of Figure 12 using data from Table 5

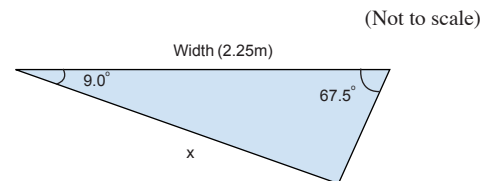


**Figure 14.** Lower section of Figure 12 using data from Table 6

The cross sectional area of a layer of inward sloping bench terrace field can be approximated to a quadrilateral (Figure 12), which can be split into a trapezium and a triangle (Figure 13).

As the inward slope must be between 3.0 and 5.0°, the height of the triangle is estimated to be  $\frac{5.5\sin(4.0)}{\sin(108.5)} = 0.405m$ , which has already exceeded

the suggested water level for z. Therefore, further research about inward sloping bench terrace field suggests that it can also be used for planting trees, which means the water level does not need to be kept below 0.05 meters in all cases, but the width of the layer of terrace needs to be between 1.5 and 3 meters (Shui Zhishi, 2020), and the inward slope needs to be between 3.0 and 15.0°.

Width of each layer of terrace field	Height of the water level of each layer of terrace field	Height of outer barrier	Slope of barrier	Inward sloping angle
2.25 meters	No specific requirement	2.3 meters	67.5°	9.0°

**Table 6.** Design standards for afforestation inward sloping bench terrace field

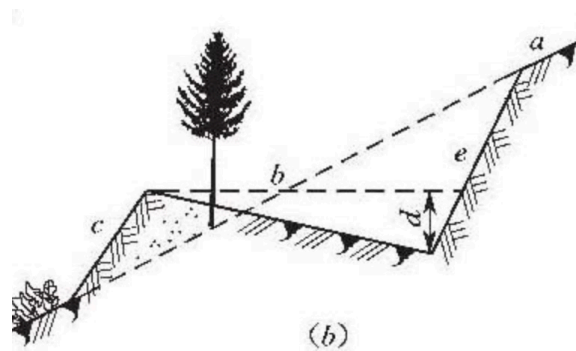


**Figure 15.** Cross-Sectional View of an Inward Sloping Bench Terrace (Shui Zhishi, 2020)

As shown in the Figure 15, the afforestation inward sloping bench terrace field does not have an inner barrier, which means the trapezium section of the terrace is no longer present (only left with the triangle section (Figure 14)) In the Figure, (a) is the general slope of the mountain, (b) is the width of a layer of the terrace field (2.25 meters), (c) is the outer barrier, (d) is the depth of a layer of the terrace field, which means the water level cannot exceed (d). Hence, the average value table is moderated.

Using the width of each layer of the terrace field, the slope of barrier, and the inward slope, (d) can be calculated:

$$180 - 9 - 67.5 = 103.5^\circ \text{ (referring to Figure 14)}$$

Let x be the length of the bottom left side in Figure 14, and d is referenced to Figure 15:

$$\frac{x}{\sin(67.5)} = \frac{2.25}{\sin(103.5)}$$

$$x = 2.14 \text{ meters}$$

$$\frac{d}{2.14} = \sin(9.0)$$

$$d \approx 0.335 \text{ meters}$$

Therefore, to prevent water spilling out from the terrace, the water level will be set to 0.3 meters. The height difference two consecutive layer of terrace will be Hence, the number of layers that can be built on a mountain with altitude of 1000 meters can be found:

$$\frac{1000}{1.965} \approx 509 \text{ layers}$$

The horizontal distance between the top right and the bottom right end point is

$$\frac{0.335}{\tan(67.0)} \approx 0.14 \text{ meters}$$

Therefore, the volume of water needed for the terrace field can be calculated by using the same method above:

$$(1.6749 + 2415.7969) \times \frac{509}{2} \approx 615,000m^3$$

## 5. Conclusion and Evaluation

Type of terrace field	Level terrace field	Bench terrace field	
		Outward sloping	Inward sloping
Volume of water ( $m^3$ )	4,900,000	19,218,000	615,000

**Table 7.** Comparison of different types of terrace fields

According to the volume of water needed for the three different types of terrace field with the same total height 1000 meters, the volume of water needed in the inward sloping bench terrace field is least, and the volume of water needed in the outward sloping terrace field is most. There are two possible reasons for this result.

### 5.1 The height difference between two consecutive layers

Type of terrace field	Level terrace field	Bench terrace field	
		Outward sloping	Inward sloping
Height between two consecutive layers ( $m$ )	1.2	0.75	1.965
Number of layers	833	1333	509

**Table 8.** Height of each type of terrace fields and the number of layers in a 1000 meter mountain

As shown in Table 8, the height difference of the inward sloping bench terrace field is almost three times that of the outward sloping bench terrace field. Hence, in the same total height of 1000 meters, the outward sloping bench terrace field will have more layers, which may explain the volume difference between different types of terrace fields.

### 5.2 The width of each level of terrace field

Type of terrace field	Level terrace field	Bench terrace field	
		Outward sloping	Inward sloping
Width of each layer of terrace field ( $m$ )	7.5	9	2.25

**Table 9.** Width of each level of terrace field

As shown in Table 9, the width of each layer of terrace field of the outward sloping bench terrace field is the largest among the three types of terrace fields, which means more water can be stored in each layer of terrace field, leading to a higher total volume of water needed for the whole terrace field.

However, extending from the second reason, a restriction of the methodology can be noticed: the height of the mountain is considered but not the width. Nevertheless, if both height and width are controlled, the slope of the mountain will be a fixed number (the hypothesis states the mountain has a constant slope), so only one type of terrace field can be used. Therefore, the width of the mountain cannot be controlled in order to investigate all three types of terrace fields separately, causing inaccuracies. Also, the slope of the mountain will not be constant in real life situations; instead, the slope of the mountain may increase or decrease with altitude. For simplicity, the following investigation assumes that the slope of the mountain may increase, but not decrease. I will separate the 1000 meter mountain into three sections, each of height 333.3 meters. The outward sloping bench terrace field will be used in the lower section; the level terrace field will be used in the middle section; the inward sloping bench terrace field will be used in the upper section. The number of layers of each type of terrace field will be shown in the Table 10 - 14 below.

Type of terrace field	Level terrace field	Bench terrace field	
		Outward sloping	Inward sloping
Range of number of layers	278-555	889-1333	1-170
Number of layers	278	445	170

Table 10. Number of Layers of Each Terrace

Number of layers	Function of the left side	Function of the right side	Volume ( $m^3$ )
1	$x = -7y - 0.14$	$x = 0.47y - 0.14$	1.675
170	$x = -7y - 380.39$	$x = 0.47y - 380.39$	804.798

Table 11.

$$Volume = (1.675 + 804.798) \times \frac{170}{2} \approx 69,000m^3$$

Number of layers	Function of the left side	Function of the right side	Volume ( $m^3$ )
278	$x = -0.175y - 2084.993$	$x = 0.175y - 2077.507$	$\frac{2495169\pi}{2000}$
555	$x = -0.175y - 4162.493$	$x = 0.175y - 4155.007$	$\frac{24929211\pi}{10000}$

Table 12. Level Terrace Field Section

$$Volume = \left( \frac{2495169\pi}{2000} + \frac{24929211\pi}{10000} \right) \times \frac{278}{2} \approx 1,633,000m^3$$

Number of layers	Function of the left side	Function of the right side	Volume ( $m^3$ )
889	$x = -0.175y - 8000.9965$	$x = 0.175y - 7992.0035$	$\frac{81\pi}{25} \times 177$
1333	$x = -0.175y - 11996.9965$	$x = 0.175y - 11988.0035$	$\frac{81\pi}{25} \times 266$

Table 13. Outward Sloping Bench Terrace Section - Trapezoid Region

$$\left( 1777 \times \frac{81\pi}{25} + 2665 \times \frac{81\pi}{25} \right) \times \frac{445}{2} = 3202237.8\pi$$

$$\approx 10,060,000m^3$$

Number of layers	Function of the left side	Function of the right side	Volume ( $m^3$ )
889	$x = -0.088y - 8000.99256$	$x = 1800y - 8000.99256$	1130.74
1333	$x = -0.088y - 11996.99256$	$x = 1800y - 11996.99256$	1695.69

Table 14. Outward Sloping Bench Terrace Section - Triangular Region

$$(1130.74 + 1695.69) \times \frac{445}{2} \approx 629,000m^3$$

$$Volume = 10,060,000 + 629,000 = 10,689,000m^3$$

Therefore, the total volume of water needed for combined terrace field is:

$$69,000 + 1,633,000 + 10,689,000 = 12,391,000m^3$$

This volume is lower than that required for merely using outward sloping bench terrace field and higher than that required for merely using inward sloping bench terrace field, suggesting that the result is reliable. Although the mountains in real life situations may not only have three sections with constant slopes, this volume is a more accurate reflection of the volume of water needed for the terrace fields built on a mountain of 1000 meters height than the volume calculated using a constant slope for the whole mountain. Therefore, if further research is done to divide the mountain into smaller sections with different slopes, the result calculated for the volume of water needed should be even more accurate.

Moreover, as the total volume of water is accurate to the nearest 1000 meters cubed, which is relatively accurate, this investigation is able to model the water present in each type of terrace fields. Hence, I would be able to calculate the volume of water required for mountains that have decreasing slopes with increasing altitudes if the research is continued in the future. The volume of water at the apex is relatively smaller than at the bottom due to the smaller radius. In this situation, the outward sloping bench terrace will be placed on the top section of the mountain, and the inward sloping bench terrace will be placed on the bottom section of the mountain. Therefore, I predict that the volume of the water needed for this situation will be less than that of the previous investigation (slope of the mountain increases with altitude) given the same height.

A final note on restrictions created when using mathematical notation software is relevant. Multiple programs were employed to help with formatting, but difficulties in achieving parity with the text could not be fully resolved, leading to some lack of consistency

## References

Dabie, S. (2020). What should be paid attention to in the irrigation method of high yield cultivation of rice? Retrieved November 30, 2021, from <https://www.juduo.cc/club/817756.html>.

Didao, F. (2020). Where are the most beautiful terraced fields in China? *China on WeChat*. Retrieved November 30, 2021, from <https://chinaqna.com/a/109764>.

Encyclopædia Britannica. (n.d.). *Terrace cultivation*. Encyclopædia Britannica. Retrieved August 10, 2021, from <https://www.britannica.com/topic/terrace-cultivation>.

Jz, S. (2012). *The Design Standards for Terrace Fields*. Retrieved August 11, 2021, from <https://wenku.baidu.com/view/f314b1224b35eefdc8d333c9>.

Shui, Z. (2020). *Inward Sloping Bench Terrace*. Shui Zhishi. Retrieved August 11, 2021, from [http://xxfb.mwr.cn/slbk/stbc/stbccs/202004/t20200409\\_1466648.html](http://xxfb.mwr.cn/slbk/stbc/stbccs/202004/t20200409_1466648.html).

---

# Tracking COVID-19's genomic and structural evolution

Valerie C.W.D. Huang

---

## Introduction

Coronaviruses in general have high genetic plasticity, meaning that they are inclined to mutate in behavior, morphology, phenology and physiology as a result of environmental changes. Similarly, the SARS-CoV-2 virus has exhibited significant genetic diversity since its discovery. Researchers have identified more than 13,000 mutations in SARS-CoV-2 genomes, constantly mutating and experiencing (random) genetic changes. Most mutations do not affect the virus's ability to spread or cause disease, but those that do usually alter the shape of its proteins. However, despite RNA virus replication typically having a high error rate, the frequency of mutations has been reduced in this virus by the presence of Nsp14 and cofactor Nsp10, proofreading the nascent RNA strand and correcting misincorporated (errored) nucleotides (Naqvi, *et al.*, 2020).

This publication will investigate the evolution and variations of SARS-CoV-2.

## 1. SARS-CoV-2

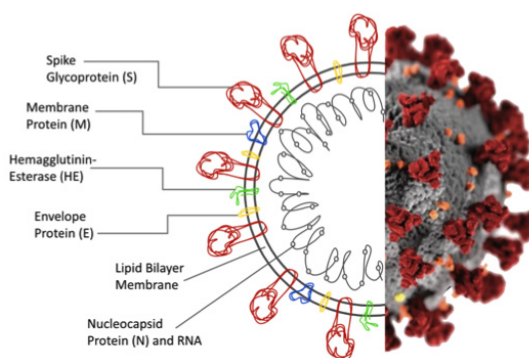
### 1.1 Origin

The first case of the virus was identified in Wuhan, Hubei, China. The original source of the virus is unclear and remains under investigation by intelligence agencies. Experts suspect that the virus originated from the Huanan Seafood Market, since many infected victims were workers of the place ("SARS-CoV-2-Delta Variant"). Others suggest that it could be a transmission from visitors that used the market as a medium for rapid expansion (through the food supply chain).

Bats have become an infamous natural reservoir for the virus. Scientists have discovered that a virus (RaTG13), collected from *Rhinolophus affinis* in Yunnan, had a 96% similarity to SARS-CoV-2 (Hu, *et al.*, 2021). The studies formulate the conclusion that bats are a pathway of zoonotic transmission, likely transmitted to humans through an intermediate host. History has shown that bats have hosted versions of MERS and

viruses of the same family as SARS-CoV-1 (SARS) and SARS-CoV-2 (COVID-19) (Briggs, 2021).

### 1.2 Structure



The SARS-CoV-2 virion is 50–200 nanometres in diameter. The coronavirus has four structural proteins: spike protein (S), membrane protein (M), envelope protein and nucleocapsid protein (N), along with sixteen non-structural proteins and numerous other accessory proteins.

The spike glycoprotein plays a critical part in viral entry into host cells by mediating receptor recognition, cell attachment, and fusion. The 1,160 to 1,400 amino-acid protein is highly glycosylated, forming homotrimers attached to the viral surface. The S protein can be divided into two primary functional subunits: S1 and S2. S1 consists of an amino terminus (N-terminal domain) and a receptor binding domain (RBD). S2 consists of the fusion peptide, heptapeptide repeat sequence 1, heptapeptide repeat sequence 2, transmembrane domain, and cytoplasm domain. There is also a short intracellular carboxyl terminus (C-terminal segment). Together, S1 and S2 form the bulbous head and stalk region of the protein; S1 catalyzes attachment while S2 initiates fusion (Duan *et al.*, 2020). The cleavage site between S1 and S2 is called the S1/S2 protease cleavage site. The spikes are covered in polysaccharide molecules for camouflaging purposes, therefore eluding cytotoxic T lymphocytes detection from the host cell's immune system during entry. In the prefusion

conformation, S1 and S2 are non-covalently bonded (Cuffari, 2021). When interactions are made with the host cell, S proteins undergo structural rearrangements, which allows the virus to fuse its membrane with that of the host cell (Huang *et al.*, 2021).

Membrane glycoproteins are the most abundant structural proteins in SARS-CoV-2, located on the membrane bilayer with an extracellular NH<sub>2</sub>-terminal domain and an intracellular C-terminus (cytoplasmic domain). The M protein functions to maintain structural integrity and shape to the virion. They are capable of binding to all structural proteins, acting as an assembler during the budding process by stabilizing the N protein RNA complex. M protein interacts with S protein for retention of S in the ER-Golgi intermediate compartment and during cell entry, thus making it a vital facilitator for viral infection ; M protein binds with E protein to create the viral envelope and produce virus-like particles ; M protein binds with N protein to stabilize the nucleocapsid, therefore promoting viral assembly (Mahtarin *et al.*, 2020). It is also a dominant immunogen for both humoral responses and cellular immune responses.

The envelope protein is the smallest in size compared to other structural proteins of SARS-CoV-2. It is an integral membrane protein with a size of 8.4 to 12 kDa and 76–109 amino acids. The E protein is made up of three main parts: a (short) hydrophilic N-terminus domain, a (large) hydrophobic transmembrane domain, and a (long) hydrophilic C-terminus. The E protein structurally induces membrane curvature for viral assembly with M protein (Javorsky *et al.*, 2021). It also controls host immune responses of the NLRP3 inflammasome and interferes with cell polarity and cell-cell adhesion, communication or junction integrity by binding to the PALS1 PDZ domain in human epithelial cells via the C-terminus (Schoeman and Fielding, 2019).

The nucleocapsid protein is a RNA-binding protein, critical for viral life cycle procedures. It is made up of 5 domains: two intrinsically disordered regions (N-terminus domain and C-terminus domain), an RNA-binding domain, a disordered central linker, and a dimerization domain (McBride *et al.*, 2014). The three dynamic disordered regions house transiently-helical binding motifs, while the two folded domains interact minimally, making the protein flexible and multivalent (“Human Coronavirus 2019-nCoV Nucleocapsid”, 2020). It also undertakes liquid-liquid phase separation when in contact with RNA. All of these domains have been predicted with the ability to bind with RNA, but due to the protein’s high sensitivity to proteolysis,

its complete structure, interaction mechanisms and functions remain elusive (Cubuk *et al.*, 2021). However, from what we know so far, the N protein performs viral RNA genome packaging, interacts with the viral membrane protein during virion assembly and enhances transcription and assembly efficiency.

## 2. Mutations and Variants

### 2.1 $\alpha$ variant (B.1.1.7)

In September 2020, the B.1.1.7 lineage emerged in the United Kingdom and quickly became one of the dominant circulating SARS-CoV-2 variants in England. Its prevalence started low, but due to its comparably high transmissibility, it exhibited rapid growth in early 2021, becoming the predominant variant in March. B.1.1.7 was detected in over 30 countries, including the United States. It defines the presence of 23 nucleotide mutations-14 encode amino acid changes and three are deletions, including amino acid substitutions in the spike protein (N501Y, A570D, P681H, T716I, S982A and D1118H) and two NTD deletions ( $\Delta$ H69–V70 and  $\Delta$ Y144). The lineage has rapidly increased in SARS-CoV-2 cases, and a study by COG-UK found that its transmissibility was 50-100% higher than pre-existing variants. B.1.1.7 has an increased viral load, and both N501Y and  $\Delta$ Y144 have antigenic effects to reduce neutralization by RBD antibodies.  $\Delta$ Y144 alters the conformation of the N3 NTD loop (amino acid positions 140–156) and may have the ability to abolish neutralization by a range of neutralizing antibodies. The mutations reduce convalescent sera neutralizing activity against B.1.1.7, making host cells more vulnerable to the variant (“SARS-CoV-2-variants of concern”)

Regarding its clinical impact, the variant does not show increased lethality or risk of hospitalization and death in all age groups. B.1.1.7 also shows no increase in reinfection rates, but is susceptible to antibodies produced by both mRNA (Pfizer and Moderna) and non-replicating recombinant viral vector (AstraZeneca, Janssen) vaccines.

### 2.2 $\beta$ variant (B.1.351)

The beta variant, professionally known as the B.1.351, was announced in December 2020 from South Africa. Most prominent in South Africa and its neighboring countries, as well as European countries like France, Austria, Belgium and Germany, the variant has the ability to bind more readily to human cells due to three primary mutations in the RBD in the S-protein of the virus spicule- K417N, E484K and N501Y (Roberts, 2021). Similar to the other variants, this variant carries the N501Y mutation, making it more contagious and



easily spread. It has also been observed that these mutations have reduced titers of RBD antibodies and neutralizing antibodies compared to other variants, though acute and convalescent patient sera neutralize this variant, retaining protective immunity induced by vaccines (Cantón *et al.*, 2021).

In terms of its clinical impacts, statistics have shown in clinical trials that the protective efficacies of vaccines AstraZeneca, Novartis, and Janssen have significantly diminished in countries and locations where this variant was also prevalent, being only 10% effective towards the beta variant. This variant is considered the one with the highest risk of hospitalization, 3.6 times higher than others, and intensive care unit admission being 3.3 times higher than other variants.

### 2.3 $\gamma$ variant (P.1)

Lineage P.1, otherwise referred to as the gamma variant, was first detected in Brazil in January 2021. Cases of the P.1 variant were reported among travelers arriving in Japan from Brazil, therefore spreading the virus to Japan as well. It is nearly twice as contagious than its ancestors and may amplify the severity of symptoms. P.1 is a descendant of the B.1.1.28.1 lineage, with approximately 17 amino acid substitutions, 3 deletions, 4 synonymous mutations, 4 nucleotide insertions, and 12 mutations encoding the S protein (considered the most among all SARS-CoV-2 variants). The gamma variant carries mutations that are shared with other VOCs and strains, such as N501Y, L18F, K417T, E484K, D614G etc, which are important for transmissibility, reinfection rates and evasion of antibody-mediated immunity. Studies have shown that this variant has an increased transmissibility of 1.4 and 2.2 times compared to previous variants, a 1.1-1.8 times higher mortality rate, a 2.6 times higher hospitalization risk, and ICU admission risk of 2.2 times higher than other variants. P.1 is also resistant to neutralization by various RBD-directed monoclonal antibodies (mAbs), caused by possession of the E484K mutation. Sera and convalescent plasma show notable losses in neutralizing activity against P.1 (not as significant as beta variant).

### 2.4 $\delta$ variant (B.1.617.2)

The delta variant, or B.1.617.2 strain, first emerged in India in October 2020, spreading to over 163 countries as of 24 August 2021. The WHO indicated that this variant was the dominant strain globally, especially in the U.K where the Delta variant accounted for over 91% of cases. The B.1.617.2 genome has 13-17 mutations (depending on study), with four of particular concern- D614G, T478K, L452R and P681R and 2 deletions

(“SARs-CoV-2 Delta variant”). According to studies, B.1.617.2 is sixfold less sensitive to serum neutralizing antibodies from recovered individuals, and eightfold less sensitive to vaccine-elicited antibodies, than the original variation of SARS-CoV-2. While the delta variant exhibited compromised sensitivity to monoclonal antibodies to the receptor-binding domain and the amino-terminal domain, it also demonstrated higher replication efficiency than other variants in both airway organoid and human airway epithelial systems, a result of its spike being in an already cleaved state- it was able to mediate highly efficient syncytium formation that was less sensitive to inhibition by a neutralizing antibody. In other words, it is more transmissible, continuously spreading at a higher rate within the country and across the world, while indicating that previously infected individuals are susceptible to reinfection. U.K scientists claim that the variant is 40%-60% more transmissible than the Alpha variant or any previous variant, with a R0 value of 5-9 (very high). A preprint shows that the viral load with the variant is on average around 1000x higher than infections during 2020, which is shocking (Scudellari, 2021). A mutation of the delta variant- AY.4.2- was discovered in the U.K and at the time this article was written was under investigation (Burn-Murdoch, 2021). There were worries that it would make the virus yet more transmissible, and possibly undermine COVID-19 vaccines further.

## 2.5 Key mutations

### D614G

The first widely distributed mutation was D614G, which first emerged from China in late January and has a substitution in the gene encoding the S protein. Occurring in over 74% of all published sequences of COVID-19 patients by June 2020, the D614G substitution, according to a study from Nature Portfolio, “was accompanied by three other mutations: a C-to-T mutation in the 5' untranslated region at position 241, a synonymous C-to-T mutation at position 3037, and a nonsynonymous C-to-T mutation at position 14408 in the RNA-dependent RNA polymerase gene” (Volz *et al.*, 2021). The mutations describes the replacement of amino acid aspartate (D) with glycine (G) in the 614th amino-acid position of the spike protein, due to a replication fault that altered a single nucleotide in the virus's 29,903-letter RNA code. D614G mutation has a “moderate effect on transmissibility”, and does not escape neutralization but is instead neutralized at a higher degree by vaccination serum, D614G increases infectivity, alters receptor binding conformations (increasing ACE2 binding affinity), increases viral load,

as well as enhances transmission and replication in the upper respiratory tract (Laguipo, 2021).

### **ΔH69–V70**

The loss/deletion of two amino acids at positions 69 and 70 causes S-gene target failure in RT-PCR-based diagnostic assays, meaning that transmissibility is increased as a result. Although ΔH69-V70 itself does not have antibody neutralising effects or mechanisms, it has the ability to increase infectivity associated with enhanced incorporation of cleaved spikes into virions (Thomas, 2020). Specifically, it compensates for immune escape mutations that impair infectivity, surveils deletions, and mediates faster kinetics of cell-cell fusion. This deletion is only found in the Alpha variant (thus far), and leads to spike gene target failure and false negative results in polymerase chain reaction tests (Lokman *et al.*, 2020).

### **N501Y**

N501Y, nicknamed “Nelly”, denotes an alteration from asparagine (N) to tyrosine (Y) in amino-acid position 501 (Burgess, 2021). It is an important mutation that increases transmissibility significantly. The change happens in the S protein RBD, more specifically the RB motif, which binds to ACE2 in the host cell membrane (Harvey *et al.*, 2021). Mutations in the RBD can change antibody recognition and binding specificity, leading to increased infectivity in the virus. In other words, the N501Y mutation allows for greater ACE2 receptor binding affinity (Luan *et al.*, 2021).

### **E484K**

This mutation refers to an exchange whereby the glutamic acid (E) is replaced by lysine (K) at position 484. E484K is a mutation that can improve the virus’s ability to evade host immune responses, making it an escape mutation. It also increases the stability of the RBD-hACE2 complex, enhancing the binding affinity as a result. It has been calculated that monoclonal and serum-derived antibodies are 10-60x less effective in neutralising the virus bearing the E484K mutation.

### **L452R**

This mutation refers to an exchange whereby the amino acid leucine (L) is replaced by arginine (R) at position 452. Since leucine of the amino acid sequence is non-charged, the replacement of it with a high-charged arginine or glutamine in the RBD creates a stronger attachment to the ACE2 while avoiding interfering neutralising antibodies (MDPI, 2021).

### **K417N**

K417N, refers to an exchange whereby lysine (K) is replaced by asparagine (N) at position 417. The mutation may contribute to immune escape, risk of reinfection, and reduced effectiveness of vaccines, but its impact is unclear and remains under investigation. This mutation is present in variants beta, gamma and delta-plus.

## **2.6 Impact on vaccines**

Vaccine development faces difficulties such as timeliness and ineffectiveness. Despite the exceptional speed of vaccine development along with implemented global mass vaccination efforts, the constant emergence of new SARS-CoV-2 variants and its ever changing mutations threatens to overturn the significant progress made so far in limiting the spread of the disease and mitigating symptoms. Variants of concern possess the ability to decrease susceptibility to vaccine-induced or infection-induced immune responses, thus being able to reinfect previously infected and recovered individuals (Marian, 2021). For example, the effectiveness of the Pfizer-BioNTech vaccine was 86.5% for B.1.1.7, and 75.0% for B.1.1.351 (Ahaley, Cuffari, 2021).

At the time that this article was written, the WHO had approved 12 vaccines (Heng, Au, Hinterseer, 2021). Such development is only possible due to the efforts of scientists, researchers and politicians, as well as massive financial resources and government funding for vaccine projects. Therapies include utilizing antibodies to prevent virus entry, nucleotide analogues to prevent viral replication, and proteases inhibitors that prevent virion formation (Tang *et al.*, 2020).

Many of them are directed at eliciting neutralizing antibodies against the S protein to inhibit entry. However, since mutations have diminished neutralizing attempts, our approaches in vaccine development and formulation require immediate updates to prevent further aggravation of the problem. Persistent efforts in finding new technological alternatives or biological routes must be continued, and perhaps prioritizing diversity in vaccines (not just S protein targeting) is the way to go.

### **3. Personal Response**

#### **3.1 Lessons COVID-19 has taught us**

##### **Being resilient and adaptable**

The pandemic is a stark demonstration that in a globalized world, everything is system-based. Economies, industries and businesses have had to adopt new systems and ways of continuation businesses who fail to do so will suffer greatly from financial losses. Communities have also learned to quickly adapt to new lifestyles. People have practiced self-care in a multitude of strategies as they are forced to adjust to new schedules, routines, and cut backs on socializing. Those who are versatile or adjustable to change will experience difficulty in sustaining their mental composure and original lives.

##### **Society's interconnectedness**

The pandemic has proven that despite the disparities and distances between people and places, we are all collaborating to fight the same virus. Local and international collaboration has driven cure development and mitigation efforts, all following the concept that "No one is safe until everyone is safe". There is no doubt that community, family and friends have assisted people through difficult times, encouraging each other to persevere. With no one left unaffected, people have recognized that they themselves aren't experiencing this in solitary; we are all in this together. In order to move forward, we must embrace it ("COVID-19 showed how interconnected we are", 2021).

##### **Importance of technology and science**

Human interactions have decreased significantly greatly as a result of quarantine and social distancing. During isolation, education, learning and meetings have been shifted online and are remote. Without technology, this would not be possible- applications such as Zoom, Google Meet, Facetime etc have allowed more efficient and accessible communication. Netflix, YouTube and various social media platforms have slowly turned into places to which we can resort when stress and anxiety caused by loneliness becomes increasingly consuming. Science is also equally as important- without knowledge on immunization, viruses, antibodies, or vaccines, the situation would have been unimaginably more serious. Scientific literacy must be emphasized in future generations. Educating the next generation about these concepts will allow our world to become more prepared for the next pandemic. While scientific and

technological knowledge has been reshaped to being more advanced, it has been proven to be more important than ever.

##### **Vaccine dose? More like humility dose**

Through the pandemic, scientists and nonscientists alike learned that humans are insignificant in comparison to tiny creatures like viruses. Anti-vaxxers, "freedom" enthusiasts (rebels of containment measures), and those who deny Science and choose to spread vicious lies suffer from the virus eventually. Less than 50% of US citizens heed health recommendations and wear masks in public; while only 4% of the world's population resides in the US, the country has accounted for more than 20% of global deaths and handled the pandemic significantly worse than other nations (Miller, 2020). Antiscience rhetoric has consequences. We all need to be humble, accept reality and be disciplined on our part, contributing to global collaboration.

#### **3.2 Future of COVID-19**

##### **Emergence of variants**

While different organisations and sources have tried to predict what the future of the pandemic holds, it is still highly unpredictable. The frequency and dispersion of new variants, the number of cases, and the sanitary situation of each country is highly influenced by epidemiological strategies and vaccination regulations. If we want to avoid the emergence of new variants that may be more transmissible or severe, we must increase vaccinated populations in all countries as soon as possible by strengthening and tightening epidemiological surveillance and containment measures. Otherwise, no matter how quickly vaccines are advanced, the possibility of mutations will be infinite, and there will be no end to the global health crisis.

##### **Diversity in vaccination approaches**

Scientists must acknowledge that conventional vaccine approaches may not be applicable to future COVID-19 variants. A diversified vaccination strategy needs to be our Plan A. SARS-CoV-2 may be an asymptomatic infection, meaning that eradication of it without a combination vaccine and therapeutics will be quite unlikely. We can do this by having different "waves" of vaccines that are responsible for their own type of immunity. First wave vaccines are for "rapid response", which includes first generation mRNA vaccines. Second wave vaccines are next-generation mRNA vaccines that are more refined, effective, elicit longer immunity,

and updated to combat mutations (“CSU to implement COVID-19 vaccination requirement”, 2021). Given that current vaccines do not provide 100% protection, a more varied vaccination strategy with new therapeutics needs to be implemented.

### Healthcare responses

Quality improvement training for healthcare professionals is vital in future development. We must continue to work towards localizing aid by building organizations, establishing new ones, delegating more land, and investing more money into health worker training. This is because they will be the ones on the front lines of the next pandemic, who will respond to future outbreaks, who will have to handle nature’s largest problems. Governments need to realise the importance of empowering responders, reinstating trust in science and promoting facts (“Aiding First Responders”, 2021). We also need to create new systems or healthcare plans that are more methodical, coherent and consistent in order to ensure best treatment towards patients.

### Relief, rehabilitation, recovery

Governments must provide and impose integrated recovery plans towards those who are vulnerable to viruses or are in difficult situations. This will assist them in resuming normal activities and lifestyles. Countries and political systems also require recovery plans to rebuild a stable, durable and well-developed economy.

### Conclusion

No matter when the pandemic ends, once it does, we will have a choice: to return to the way things were, or accept that we can and must do better by improving ourselves. We can continue to prioritize personal benefits and success over other things in life, or we can collaborate and connect to solve global problems.

By choosing the latter in both cases, and working towards a global community that is prepared for a pandemic, a group of healthcare workers who are equipped to tackle global crises, the world will be more powerful, more resilient and more impenetrable against future challenges.

### References

- 2002–2004 SARS Outbreak (2021). Wikipedia, Wikimedia Foundation. [https://en.wikipedia.org/wiki/2002%E2%80%932004\\_SARS\\_outbreak](https://en.wikipedia.org/wiki/2002%E2%80%932004_SARS_outbreak).
- 2021, Burgess, Michael. (2011) N501Y Mutation in SARS-COV-2 Responsible for Increased Viral Transmission. *News-Medical.Net*, <https://www.news-medical.net/news/20210311/N501Y-mutation-in-SARS-CoV-2-responsible-for-increased-viral-transmission.aspx>.
- Ahaley, S.S. (2021) A Review of Covid-19 Vaccine Effectiveness. *New-medical.net*, <https://www.news-medical.net/news/20210929/A-review-of-COVID-19-vaccine-effectiveness.aspx>.
- Aiding First Responders: Front Lines Need to Know of Covid-19 Encounters. (2020). *The Pittsburgh Post-Gazette*. <https://www.post-gazette.com/opinion/editorials/2020/04/23/Aiding-first-responders-Front-lines-need-to-know-of-COVID-19-encounters/stories/202004020053>.
- Briggs, H. (2021). Coronavirus: Bat Scientists Find New Evidence. *BBC News, BBC*. <https://www.bbc.com/news/science-environment-55998157>.
- Burn-Murdoch, J. (2021). New Delta Descendant May Be More Infectious than Its Ancestor. *Financial Times*. <https://www.ft.com/content/f1ec9d5d-9e02-4cc4-95e7-1dcb1844d43>.
- Cantón, R., De Lucas Ramos, P., García-Botella, A., García-Lledó, A., Gómez-Pavón, J., González Del Castillo, J., Hernández-Sampelayo, T., Martín-Delgado, M.C., Martín Sánchez, F.J., Martínez-Sellés, M., Molero García, J.M., Moreno Guillén, S., Rodríguez-Artalejo, F.J., Ruiz-Galiana, J., Bouza, E. (2021). New Variants of SARS-COV-2. *Revista Espanola De Quimioterapia: Publicacion Oficial De La Sociedad Espanola De Quimioterapia, U.S. National Library of Medicine*, <https://pubmed.ncbi.nlm.nih.gov/34076402/>.
- Cherian, S., Varsha, P., Santosh, J., Pragya, Y., Nivedita, G., Mousumi, D., Partha, R., Sujeet, S., Priya, A., Samiran, P. & NIC Team. (2021). “SARS-CoV-2 Spike Mutations, L452R, T478K, E484Q and P681R, in the Second Wave of COVID-19 in Maharashtra, India” *Microorganisms* 9(7), 1542. <https://doi.org/10.3390/microorganisms9071542>
- CSU to Implement COVID-19 Vaccination Requirement upon FDA Approval. (2021). *SSU News*. <https://news.sonoma.edu/article/csu-implement-covid-19-vaccination-requirement-upon-fda-approval>.
- Cubuk, J. *et al.*, (2021). The SARS-COV-2 Nucleocapsid Protein Is Dynamic, Disordered, and Phase Separates with RNA. *Nature News*, <https://www.nature.com/articles/s41467-021-21953-3>.
- Cuffari, B. (2021). What Are Spike Proteins? *News-medical.net*, <https://www.news-medical.net/health/What-are-Spike-Proteins.aspx>.
- Duan, L., *et al.*, (2020). The Sars-COV-2 Spike Glycoprotein Biosynthesis, Structure, Function, and Antigenicity: Implications for the Design of Spike-Based Vaccine Immunogens. *Frontiers in Immunology*, 20. <https://www.frontiersin.org/article/10.3389/fimmu.2020.576622/full>.
- Harvey, W. T., *et al.*, (2021). SARS-COV-2 Variants, Spike Mutations and Immune Escape. *Nature News*, <https://www.nature.com/articles/s41579-021-00573-0>.

- Hu, B. *et al.*, (2020) Characteristics of SARS-COV-2 and COVID-19. *Nature News*, <https://www.nature.com/articles/s41579-020-00459-7>.
- Huang, Y. *et al.*, (2020). Structural and Functional Properties of SARS-COV-2 Spike Protein: Potential Antivirus Drug Development for Covid-19. *Nature News*, <https://www.nature.com/articles/s41401-020-0485-4>.
- Human Coronavirus 2019-Ncov Nucleocapsid.(2021) *InvivoGen*. <https://www.invivogen.com/sars2-nucleocapsid>.
- Javorsky, A., *et al.*, (2021). Structural Basis of Coronavirus E Protein Interactions with Human PALS1 PDZ Domain. *Nature News*, <https://www.nature.com/articles/s42003-021-02250-7>.
- Laguipo, A. B. B. (2021) Mutations in the Spike Proteins of SARS-COV-2 Select for Amino Acid Changes, Increasing Protein Stability. *News-medical.net*, <https://www.news-medical.net/news/20210701/Mutations-in-the-spike-proteins-of-SARS-CoV-2-select-for-amino-acid-changes-increasing-protein-stability.aspx>.
- Lokman, S. M., *et al.*, (2020) Exploring the Genomic and Proteomic Variations of SARS-COV-2 Spike Glycoprotein: A Computational Biology Approach. *BioRxiv*, Cold Spring Harbor Laboratory, <https://www.biorxiv.org/content/10.1101/2020.04.07.030924v1>.
- Luan, B., *et al.*, (2021) Enhanced Binding of the N501Y-Mutated SARS-COV-2 Spike Protein to the Human ACE2 Receptor: Insights from Molecular Dynamics Simulations. *FEBS Press*, <https://febs.onlinelibrary.wiley.com/doi/10.1002/1873-3468.14076>.
- Mahtarin R., *et al.*, Structure and Dynamics of Membrane Protein in SARS-COV-2. *Journal of Biomolecular Structure & Dynamics*, 40(10), 4725-4738, <https://www.tandfonline.com/doi/abs/10.1080/07391102.2020.1861983>.
- Marian, A. J. (2021) Current State of Vaccine Development and Targeted Therapies for Covid-19: Impact of Basic Science Discoveries. *Cardiovascular Pathology*, <https://www.ncbi.nlm.nih.gov/pmc/articles/PMC7462898/>.
- McBride, R. (2014). The Coronavirus Nucleocapsid Is a Multifunctional Protein. *Viruses*, <https://www.ncbi.nlm.nih.gov/pmc/articles/PMC4147684>.
- Miller, B. L. (2020). Science Denial and COVID Conspiracy Theories-Lessons from Clinical Disease about Possible Neurophysiological Mechanisms. *JAMA*, <https://jamanetwork.com/journals/jama/fullarticle/2772693>.
- Naqvi, A. A. T, *et al.*, (2020). Insights into SARS-COV-2 Genome, Structure, Evolution, Pathogenesis and Therapies: Structural Genomics Approach. *Biochimica Et Biophysica Acta (BBA)*, <https://www.sciencedirect.com/science/article/pii/S092544392030226X>.
- Roberts, M. (2021). Beta Coronavirus Variant: What Is the Risk? *BBC News*, BBC, <https://www.bbc.com/news/health-55534727>.
- SARS-COV-2 Delta Variant. (2021). Wikipedia, Wikimedia Foundation. [https://en.wikipedia.org/wiki/SARS-CoV-2\\_Delta\\_variant#Epidemiology](https://en.wikipedia.org/wiki/SARS-CoV-2_Delta_variant#Epidemiology).
- SARS-CoV-2 Variants of Concern - UpToDate. *UpToDate*. <https://www.uptodate.com/contents/image?imageKey=ID%2F131216>.
- Schoeman, D., & Burtram C. (2019). Coronavirus Envelope Protein: Current Knowledge. *Virology Journal*, 16(69), <https://virologyj.biomedcentral.com/articles/10.1186/s12985-019-1182-0>.
- Scudellari, M. (2021). How the Coronavirus Infects Cells - and Why Delta Is so Dangerous. *Nature News*, <https://www.nature.com/articles/d41586-021-02039-y>.
- Tang, T. *et al.* (2020). Coronavirus Membrane Fusion Mechanism Offers a Potential Target for Antiviral Development. *Antiviral Research*, <https://www.ncbi.nlm.nih.gov/pmc/articles/PMC7194977/>.
- Thomas, D. L. (2020). SARS-COV-2 Spike Deletion ΔH69/ΔV70 Shows Repeated Emergence and Spread. *News*, <https://www.news-medical.net/news/20201217/SARS-CoV-2-spike-deletion-ce94H69ce94V70-shows-repeated-emergence-and-spread.aspx>.
- Torbay, R. (2020). Covid-19 Showed How Interconnected We Are, to Move Forward, We Must Embrace It. *Project HOPE*, <https://www.projecthope.org/covid-19-showed-how-interconnected-we-are-to-move-forward-wemust-embrace-it/12/2020/>.
- Volz, E., *et al.*, (2021). Evaluating the Effects of SARS-COV-2 Spike Mutation D614G on Transmissibility and Pathogenicity. *Cell, Cell Press*, <https://www.ncbi.nlm.nih.gov/pmc/articles/PMC7674007/>.
- What Are Covid-19 Vaccines Made of? *South China Morning Post*, <https://www.scmp.com/video/coronavirus/3128139/scmp-explains-whats-covid-19-vaccine>.

---

# Complete genome sequence of *Kluyvera* sp. CRP, a cellulolytic strain isolated from Red Panda faeces (*Ailurus fulgens*)

Angus C.H. Wai

---

## Abstract

The enterobacterium genus *Kluyvera* is widely-distributed in the environment and a rare source of infection in humans. *Kluyvera* sp. CRP was isolated from faeces of a healthy, captive Chinese Red Panda (*Ailurus fulgens*) and its complete genome (5,157,963 bp, 54.80% GC content) established through hybrid assembly.

---

## 1. Greener Biofuels

Biofuels generated from food sources may be ‘carbon neutral’ but they also have negative consequences for economies and the environment. In contrast, second-generation biofuels from lignocellulosic biomass, such as industrial, agricultural and municipal waste, are more sustainable but require pre-treatment in order to release fermentable sugars.

Biological pre-treatment with isolated enzymes or whole cells is cheap and energy-efficient, so that this project has looked for strongly cellulolytic bacteria in faeces of the Chinese red panda (*Ailurus fulgens*). This species uses bamboo as its major food source, and previous characterisation of its gut microbiota has indicated the presence of extensive carbohydrate metabolism, including cellulose-degrading pathways consistent with a mainly bamboo diet (Kong *et al.*, 2014).

## 2. Genus *Kluyvera*

*Kluyvera* species are coliforms widely distributed in the environment. Previous studies have isolated *Kluyvera* from freshwater (Gesew *et al.*, 2021), seawater (Paschoal *et al.*, 2017), sewage (Li *et al.*, 2019) and soil (López *et al.*, 2019; Tanaka *et al.*, 1990); from insects such as synanthropic spiders (Dunbar *et al.*, 2020) and flies (Cadavid-Sanchez *et al.*, 2015); from animals such as cows (Sawant *et al.*, 2007), Egyptian fruit-bats (Han *et al.*, 2010), and sea turtles (Trotta *et al.*, 2021);

and, from the rhizosphere (Chung *et al.*, 2005) and as endophytes (Singha *et al.*, 2021), where they may be acting to promote plant growth (Backer *et al.*, 2018; Burd *et al.*, 2000) and protect against disease (Crales *et al.*, 2017). In humans, *Kluyvera* bacterial infections are uncommon but often persistent and even fatal (Lee *et al.*, 2019; Metoyer *et al.*, 2019; Nicolosi *et al.*, 2009; Sarria *et al.*, 2001).

*Kluyvera* sp. CRP was isolated from the faeces of a healthy Chinese red panda (*Ailurus fulgens*) housed at Ocean Park, Hong Kong.

## 3. *Kluyvera* sp. CRP

### 3.1 Methodology

Fresh faeces (1g) was vortexed in 9 mL of 0.9% w:v NaCl and briefly allowed to settle before serial-dilution. 100 µL of the 1000x extract was spread onto carboxymethylcellulose (CMC) agar (Kim *et al.*, 2012) and incubated at 27 °C for 48 hours. Colonies displaying strong growth were picked and passaged to purity on Luria agar. Cellulolytic activity was confirmed by incubation on CMC agar followed by staining with Gram’s iodine (Kasana *et al.*, 2008). Isolate CRP, which showed the greatest activity, was passaged on Luria agar nine times before a single colony was incubated in Luria broth for 24 hours prior to DNA extraction (Invitrogen: PureLink® Genomic DNA Mini Kit).

### 3.2 Assembly statistics

Paired-end short-read sequencing libraries were prepared using the NexteraXT DNA Library Preparation Kit and sequenced via the Illumina MiSeq platform using v3 chemistry (2x300 bp). Adapter sequences were removed using Trimmomatic v0.32 (Bolger *et al.*, 2014) and reads were quality-filtered and trimmed, producing 1,204,982 read pairs (mean length 297bp) totalling ~358 Mbp. Long-read libraries, prepared from the same extracted DNA using the Rapid Barcoding Kit SQK-RBK004, were sequenced via Oxford Nanopore's Spot-ON Flow Cell (vR9), MinION sequencer and MinKNOW v3.1.8 software, with base-calling by Guppy v2.1.3. The final long-read dataset, trimmed by Porechop v0.2.4 (Wick, 2017; Wick *et al.*, 2018), totalled 40,127 reads (494 Mbp) with median length 15,833 bp (N50 60,789). Default parameters were used for all software unless otherwise specified.

The complete genome sequence combined Illumina and MinION datasets using Unicycler v0.4.3 (Wick *et al.*, 2017). The sequence was submitted to PATRIC (PATRIC; Haft *et al.*, 2018) and to NCBI PGAP v5.0 (Brettin *et al.*, 2015) for annotation. GenBank accession no. CP082841.

### 3.3 Genomic analysis

Mash/MinHash using PATRIC (Ondov *et al.*, 2016) found CRP closest to *Kluyvera* genomsp. 3 strain PO2S7 (CP050321) with an average nucleotide identity of 98.83% (Goris *et al.*, 2007; Yoon *et al.*, 2017). Ten copies of 6-phospho-beta-glucosidase (EC 3.2.1.86) are present, together with multiple copies of cellobiose phosphotransferase (EC 2.7.1.205) and the bcs operon (Figure 1) (Römling & Galperin, 2015). In susceptibility testing (Liofilchem discs), CRP showed resistance to ampicillin (10 µg) consistent with the presence of a CTX-M-40 beta-lactamase (Hemlata *et al.*, 2021; Zhao & Hu, 2013) identified by CARD (Alcock *et al.*, 2020).

The complete genomic sequence of CRP totals 5.16 Mbp and Mash/MinHash using PATRIC (Ondov *et al.*, 2016) found it closest to *Kluyvera* genomsp. 3 strain PO2S7 (CP050321) with an average nucleotide identity of 98.83% (Goris *et al.*, 2007; Yoon *et al.*, 2017).

Cellulolytic pathways are strongly represented with four copies of beta-glucosidase, 10 copies of 6-phospho-beta-glucosidase (chbF/celF), together with multiple copies of cellobiose phosphotransferase and the bcs operon.

A complete cellulose degradation pathway (Figure 2) was identified in CRP. A cellulase (bcsZ) in CRP sequence is nested within the bcs operon. This is consistent with activity on CMC plates (Figure 3).

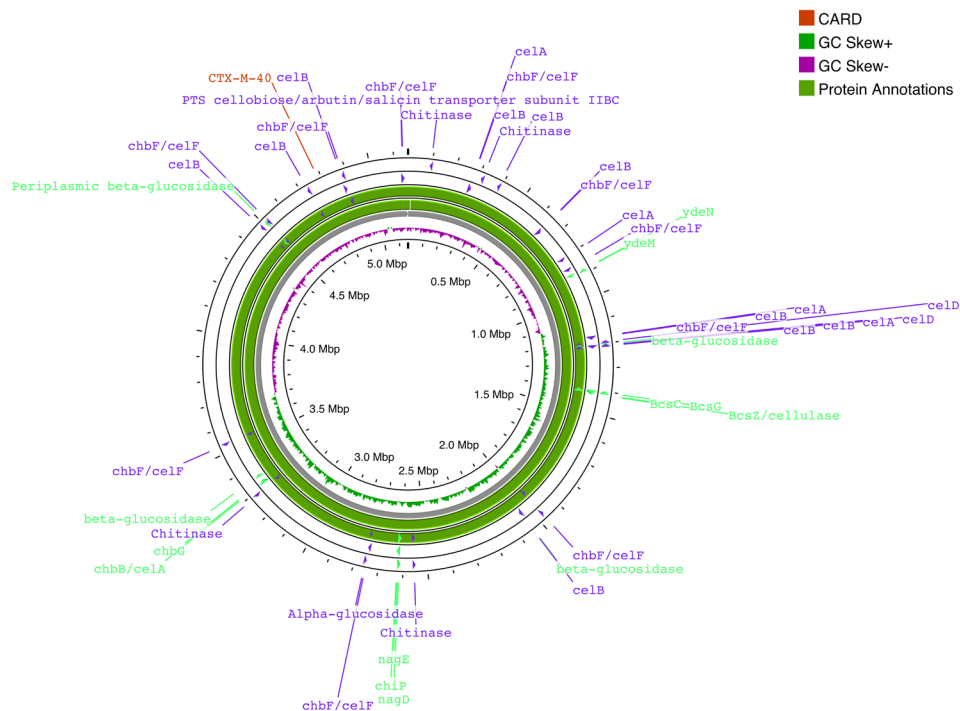


**Figure 1.** Circular genome diagram of CRP, with labels highlighting important genes. To save space, only the start and ends of a sequence of proteins are labeled, full sequence can be seen in the pathway diagrams.

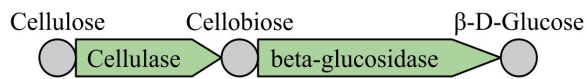


Figure 2. Cellulose degradation pathway as identified in CRP

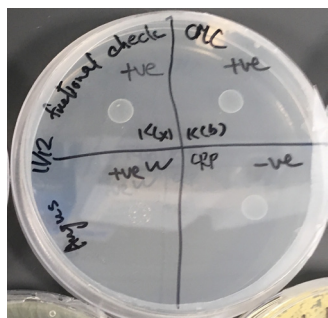


Figure 3. CRP on a CMC plate

Four copies of beta-glucosidase in CRP are spread around the genome and each have completely different sequences with no conserved regions. Protein models by Phyre2 (Kelley *et al.*, 2015) also show different structures for each beta-glucosidase (Figure 4). This suggests the four copies might come from different origins.

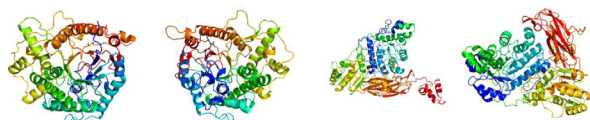


Figure 4. Model of each of the four beta-glucosidase in CRP left to right in order of appearance

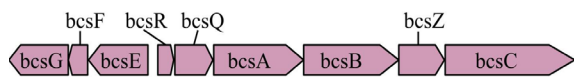


Figure 5. bcs operon as identified in CRP

A nine-enzyme long bcs operon (Römling & Galperin, 2015) is present in the sequence. The presence of the bcs operon in CRP is consistent with activity shown on CMC agar plates (Figure 5). Sequence alignment of the bcs operon present in genomosp. 3 strain PO2S7 showed a 99% identity (4534/4560 aligned) between the two.

```

2281 YRHLAEFAPPVAKEIFRSLTLLVAVVASFVPRRPERDAVVEHPLSALAQQM----- 2331
2281 .....KRNLSWICA..... 2340
2332 -AVGMGSLPLLTTHSETTPEVSVTPTVQQDATAPTDAAPVVVEDAPSRDVKLSFAQIAP 2390
2341 v..... 2400

```

Figure 6. Sequence alignment of CRP and genomosp. 3 strain PO2S7 between *bcsA* and *bcsB* by NCBI BLAST (Altschul *et al.*, 1990). M indicates the start of *bcsB*



Figure 8. Chitin and GlcNAc utilization pathway from Yang *et al.* (2006) identified in CRP

The most significant discrepancy is a gap of 10 acids at the start of *bcsB* in CRP, compared to genomosp. 3 strain PO2S7 (Figure 6).

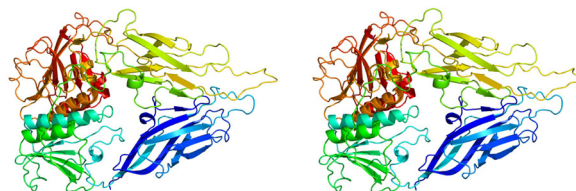


Figure 7. Model of *bcsB* protein in CRP and in genomosp. 3 strain PO2S7, left and right respectively

Protein structure modeled by Phyre2 (Kelley *et al.*, 2015) shows no significant difference in structure between the two proteins (Figure 7).

A complete chitin and GlcNAc utilization pathway (Figure 8)(Yang *et al.*, 2006), including a *chb* operon, was identified around the genome. Compared to the pathway in Yang *et al.* (2006), *ydeN* and *ydeM* are in opposite strands in the genome.

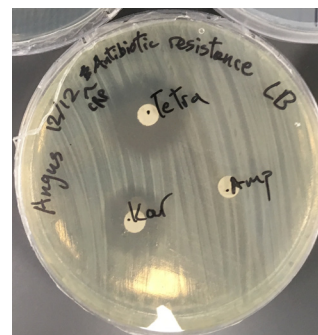


Figure 9. Disk diffusion (Liofilchem discs) assay of CRP on ampicillin

CRP shows resistance to ampicillin (Figure 9) consistent with the presence of a CTX-M-40 beta-lactamase (Figure 1)(Hemlata *et al.*, 2021; Zhao & Hu, 2013) identified by CARD (Alcock *et al.*, 2020).



## Conclusion

*Kluyvera* sp. CRP shows strong activity with chitin and cellulose. Genomic analysis shows prominent chitin and cellulolytic pathways. These could give CRP an advantage in breaking down lignocellulosic waste.

## Data Availability

The complete genome sequence and raw sequence data for *Kluyvera* sp. CRP are available through NCBI under BioProject PRJNA758164 and GenBank accession number CP082841.

*Kluyvera* genomsp. 3 strain PO2S7 [CP050321]  
<https://www.ncbi.nlm.nih.gov/nucleotide/CP050321>  
<https://www.ncbi.nlm.nih.gov/bioproject/758164>  
<https://www.ncbi.nlm.nih.gov/nucleotide/CP082841.1>

## Supplementary Data



## References

- Alcock, B. P., Raphenya, A. R., Lau, T. T. Y., Tsang, K. K., Bouchard, M., Edalatmand, A., Huynh, W., Nguyen, A.-L. V., Cheng, A. A., Liu, S., Min, S. Y., Miroshnichenko, A., Tran, H.-K., Werfalli, R. E., Nasir, J. A., Oloni, M., Speicher, D. J., Florescu, A., Singh, B., ... McArthur, A. G. (2020). CARD 2020: Antibiotic resistance surveillance with the comprehensive antibiotic resistance database. *Nucleic Acids Research*, 48(D1), D517–D525. <https://doi.org/10.1093/nar/gkz935>
- Backer, R., Rokem, J. S., Ilangumaran, G., Lamont, J., Praslickova, D., Ricci, E., Subramanian, S., & Smith, D. L. (2018). Plant Growth-Promoting Rhizobacteria: Context, Mechanisms of Action, and Roadmap to Commercialization of Biostimulants for Sustainable Agriculture. *Frontiers in Plant Science*, 9. <https://www.frontiersin.org/article/10.3389/fpls.2018.01473>
- Bolger, A. M., Lohse, M., & Usadel, B. (2014). Trimmomatic: A flexible trimmer for Illumina sequence data. *Bioinformatics (Oxford, England)*, 30(15), 2114–2120. <https://doi.org/10.1093/bioinformatics/btu170>
- Brettin, T., Davis, J. J., Disz, T., Edwards, R. A., Gerdes, S., Olsen, G. J., Olson, R., Overbeek, R., Parrello, B., Pusch, G. D., Shukla, M., Thomason, J. A., Stevens, R., Vonstein, V., Wattam, A. R., & Xia, F. (2015). RASTtk: A modular and extensible implementation of the RAST algorithm for building custom annotation pipelines and annotating batches of genomes. *Scientific Reports*, 5(1), 8365. <https://doi.org/10.1038/srep08365>
- Burd, G. I., Dixon, D. G., & Glick, B. R. (2000). Plant growth-promoting bacteria that decrease heavy metal toxicity in plants. *Canadian Journal of Microbiology*, 46(3), 237–245. <https://doi.org/10.1139/w99-143>
- Cadavid-Sanchez, I. C., Amat, E., & Gomez-Piñerez, L. M. (2015). Enterobacteria Isolated From Synanthropic Flies (Diptera, Calyptratae) In Medellín, Colombia. *Caldasia*, 37(2), 319–332. <https://doi.org/10.15446/caldasia.v37n2.53594>
- Chung, H., Park, M., Madhaiyan, M., Seshadri, S., Song, J., Cho, H., & Sa, T. (2005). Isolation and characterization of phosphate solubilizing bacteria from the rhizosphere of crop plants of Korea. *Soil Biology and Biochemistry*, 37(10), 1970–1974. <https://doi.org/10.1016/j.soilbio.2005.02.025>
- Crialesi, P. C. B., Thuler, R. T., Filho, F. H. I., Thuler, A. M. G., Lemos, M. V. F., & Bortoli, S. A. de. (2017). Plant Growth Promoting Rhizobacteria (PGPR) and *Plutella xylostella* (L.) (Lepidoptera: Plutellidae) interaction as a resistance inductor factor in *Brassica oleracea* var. capitata. *Plant Science Today*, 4(3), 121–132. <https://doi.org/10.14719/pst.2017.4.3.305>
- Dunbar, J. P., Khan, N. A., Abberton, C. L., Brosnan, P., Murphy, J., Afoullouss, S., O'Flaherty, V., Dugon, M. M., & Boyd, A. (2020). Synanthropic spiders, including the global invasive noble false widow *Steatoda nobilis*, are reservoirs for medically important and antibiotic resistant bacteria. *Scientific Reports*, 10(1), 20916. <https://doi.org/10.1038/s41598-020-77839-9>
- Gessew, G. T., Desta, A. F., & Adamu, E. (2022). High burden of multidrug resistant bacteria detected in Little Akaki River. *Comparative Immunology, Microbiology and Infectious Diseases*, 80, 101723. <https://doi.org/10.1016/j.cimid.2021.101723>

- Goris, J., Konstantinidis, K. T., Klappenbach, J. A., Coenye, T., Vandamme, P., & Tiedje, J. M. Y. (2007). (n.d.). DNA–DNA hybridization values and their relationship to whole-genome sequence similarities. *International Journal of Systematic and Evolutionary Microbiology*, 57(1), 81–91. <https://doi.org/10.1099/ijs.0.64483-0>
- Haft, D. H., DiCuccio, M., Badretidin, A., Brover, V., Chetvermin, V., O'Neill, K., Li, W., Chitsaz, F., Derbyshire, M. K., Gonzales, N. R., Gwadz, M., Lu, F., Marchler, G. H., Song, J. S., Thanki, N., Yamashita, R. A., Zheng, C., Thibaud-Nissen, F., Geer, L. Y., ... Pruitt, K. D. (2018). RefSeq: An update on prokaryotic genome annotation and curation. *Nucleic Acids Research*, 46(D1), D851–D860. <https://doi.org/10.1093/nar/gkx1068>
- Han, J. E., Gomez, D. K., Kim, J. H., Jr, C. H. C., Shin, S. P., & Park, S. C. (2010). Isolation of a Zoonotic Pathogen *Kluyvera ascorbata* from Egyptian Fruit-Bat *Rousettus aegyptiacus*. *Journal of Veterinary Medical Science*, 72(1), 85–87. <https://doi.org/10.1292/jvms.08-0342>
- Hemlata, Bhat, M. A., Kumar, V., Ahmed, M. Z., Alqahtani, A. S., Alqahtani, M. S., Jan, A. T., Rahman, S., & Tiwari, A. (2021). Screening of natural compounds for identification of novel inhibitors against  $\beta$ -lactamase CTX-M-152 reported among *Kluyvera georgiana* isolates: An *in vitro* and *in silico* study. *Microbial Pathogenesis*, 150, 104688. <https://doi.org/10.1016/j.micpath.2020.104688>
- Kasana, R. C., Salwan, R., Dhar, H., Dutt, S., & Gulati, A. (2008). A Rapid and Easy Method for the Detection of Microbial Cellulases on Agar Plates Using Gram's Iodine. *Current Microbiology*, 57(5), 503–507. <https://doi.org/10.1007/s00284-008-9276-8>
- Kim, Y.-K., Lee, S.-C., Cho, Y.-Y., Oh, H.-J., & Ko, Y. H. (2012). Isolation of Cellulolytic *Bacillus subtilis* Strains from Agricultural Environments. *ISRN Microbiology*, 2012, e650563. <https://doi.org/10.5402/2012/650563>
- Kong, F., Zhao, J., Han, S., Zeng, B., Yang, J., Si, X., Yang, B., Yang, M., Xu, H., & Li, Y. (2014). Characterization of the Gut Microbiota in the Red Panda (*Ailurus fulgens*). *PLOS ONE*, 9(2), e87885. <https://doi.org/10.1371/journal.pone.0087885>
- Lee, J., Hwang, J.-H., Jo, D. S., Lee, H. S., & Hwang, J.-H. (2019). *Kluyvera ascorbata* as a Pathogen in Adults and Children: Clinical Features and Antibiotic Susceptibilities in a Single Center Study. *Japanese Journal of Infectious Diseases*, 72(3), 142–148. <https://doi.org/10.7883/yoken.JJID.2018.375>
- Li, Y., Luo, L., Xiao, Z., Wang, G., Li, C., Zhang, Z., Zhou, Y., & Zhang, L. (2019). Characterization of a Carbapenem-Resistant *Kluyvera Cryocrescens* Isolate Carrying *Bla<sub>ndm-1</sub>* from Hospital Sewage. *Antibiotics*, 8(3), 149. <https://doi.org/10.3390/antibiotics8030149>
- López, S., Pastorino, G., Malbran, I., & Balatti, P. (2019). Enterobacteria isolated from an agricultural soil of Argentina promote plant growth and biocontrol activity of plant pathogens. *Revista de La Facultad de Agronomía*, 118(2), 022–022. <https://doi.org/10.24215/16699513e022>
- Metoyer, G. T., Huff, S., & Johnson, R. M. (2019). Polymicrobial infection with *Kluyvera* species secondary to pressure necrosis of the hand, a case report. *Journal of Surgical Case Reports*, 2019(11), rjz262. <https://doi.org/10.1093/jscr/rjz262>
- Nicolosi, D., Nicolosi, V. M., Cappellani, A., Nicoletti, G., & Blandino, G. (2009). Antibiotic Susceptibility Profiles of Uncommon Bacterial Species Causing Severe Infections in Italy. *Journal of Chemotherapy*, 21(3), 253–260. <https://doi.org/10.1179/joc.2009.21.3.253>
- Ondov, B. D., Treangen, T. J., Melsted, P., Mallonee, A. B., Bergman, N. H., Koren, S., & Phillippy, A. M. (2016). Mash: Fast genome and metagenome distance estimation using MinHash. *Genome Biology*, 17(1), 132. <https://doi.org/10.1186/s13059-016-0997-x>
- Paschoal, R. P., Campana, E. H., Corrêa, L. L., Montezzi, L. F., Barrueto, L. R. L., da Silva, I. R., Bonelli, R. R., Castro, L. de S., & Picão, R. C. (2017). Concentration and Variety of Carbapenemase Producers in Recreational Coastal Waters Showing Distinct Levels of Pollution. *Antimicrobial Agents and Chemotherapy*, 61(12), e01963-17. <https://doi.org/10.1128/AAC.01963-17>
- Römling, U., & Galperin, M. Y. (2015). Bacterial cellulose biosynthesis: Diversity of operons, subunits, products, and functions. *Trends in Microbiology*, 23(9), 545–557. <https://doi.org/10.1016/j.tim.2015.05.005>
- Sarria, J. C., Vidal, A. M., & Kimbrough, R. C., III. (2001). Infections Caused by *Kluyvera* Species in Humans. *Clinical Infectious Diseases*, 33(7), e69–e74. <https://doi.org/10.1086/322686>
- Sawant, A. A., Hegde, N. V., Straley, B. A., Donaldson, S. C., Love, B. C., Knabel, S. J., & Jayarao, B. M. (2007). Antimicrobial-Resistant Enteric Bacteria from Dairy Cattle. *Applied and Environmental Microbiology*, 73(1), 156–163. <https://doi.org/10.1128/AEM.01551-06>
- Singha, K. M., Singh, B., & Pandey, P. (2021). Host specific endophytic microbiome diversity and associated functions in three varieties of scented black rice are dependent on growth stage. *Scientific Reports*, 11(1), 12259. <https://doi.org/10.1038/s41598-021-91452-4>
- Tanaka, M., Anzai, Y., Kato, F., & Koyama, Y. (1990). Isolation of Bacterial Strains, Which Hydrolyze Glycyrrhizin and Produce Glycyrrhetic Acid, from Soil. *Journal of Pharmacobio-Dynamics*, 13(6), 361–366. <https://doi.org/10.1248/bpb1978.13.361>
- Trotta, A., Marinaro, M., Sposato, A., Galgano, M., Ciccarelli, S., Paci, S., & Corrente, M. (2021). Antimicrobial Resistance in Loggerhead Sea Turtles (*Caretta caretta*): A Comparison between Clinical and Commensal Bacterial Isolates. *Animals*, 11(8), 2435. <https://doi.org/10.3390/ani11082435>
- Wick, R. R., Judd, L. M., Gorrie, C. L., & Holt, K. E. (2017). Unicycler: Resolving bacterial genome assemblies from short and long sequencing reads. *PLOS Computational Biology*, 13(6), e1005595. <https://doi.org/10.1371/journal.pcbi.1005595>
- Wick, R. R., Judd, L. M., & Holt, K. E. (2018). Deepbinner: Demultiplexing barcoded Oxford Nanopore reads with deep convolutional neural networks. *PLOS Computational Biology*, 14(11), e1006583. <https://doi.org/10.1371/journal.pcbi.1006583>
- Wick RR. 2017. Porechop. <https://github.com/rwick/Porechop>.

Yang, C., Rodionov, D. A., Li, X., Laikova, O. N., Gelfand, M. S., Zagnitko, O. P., Romine, M. F., Obratsova, A. Y., Nealson, K. H., Osterman, A. L. (2006). Comparative Genomics and Experimental Characterization of N-Acetylglucosamine Utilization Pathway of *Shewanella oneidensis*\*. *Journal of Biological Chemistry*, 281(40), 29872–29885. doi: 10.1074/jbc.M605052200

Yoon, S.-H., Ha, S., Lim, J., Kwon, S., & Chun, J. (2017). A large-scale evaluation of algorithms to calculate average nucleotide identity. *Antonie van Leeuwenhoek*, 110(10), 1281–1286. <https://doi.org/10.1007/s10482-017-0844-4>

Zhao, W.-H., & Hu, Z.-Q. (2013). Epidemiology and genetics of CTX-M extended-spectrum  $\beta$ -lactamases in Gram-negative bacteria. *Critical Reviews in Microbiology*, 39(1), 79–101. <https://doi.org/10.3109/1040841X.2012.691460>

---

# The impact of urbanisation on the frequency and length of bat echoes recorded in Hong Kong

Allison C.Y. Cheung

---

## Abstract

The COVID-19 pandemic has brought attention towards bats as transmitters of the coronavirus. Under rapid urbanization, these mammals are now found in urban parks, trees or even households in areas in Hong Kong with high population densities. Previous research has attempted to identify bat species in the city through mist-net capturing techniques and direct roost censuses, but the current local distribution of bats is unknown. In this study an acoustic survey using bat echo detectors is conducted in Southern Hong Kong using transect lines to investigate the impact of urbanisation on bat visitations. Results suggest the influential impact of street lights on the frequency and length of bat echoes recorded – more bat calls with higher frequency were recorded at transect sites with more and brighter light sources. The time length of the calls is also longer at these sites, suggesting that the street lights are providing a source of food for insect-eating bats. Bat acoustic data collected in this study sheds light on the adaptability of bat species under urbanisation and provides insight on potential measures that could be taken to reduce urban bat visitations.

*Key words: Hong Kong, bats, horseshoe bats, COVID-19, bat visitation, urban areas, village areas, countryside.*

---

## Introduction

### Bats and urbanisation

Covering only 427 square miles (1,110 square kilometers) of area, Hong Kong's high pace of development accounts for its high population density of 17,311 people per square mile (6,659 people per square kilometer) (World Population Review, 2021). Rural-to-urban migration and spatial expansion under the rapid process of urbanisation leads to the loss of natural habitats, including those for the local bat population. Though most animals are affected negatively, a minority of species have been reported to adjust their communication and foraging in order to adjust to a life in the city (Egert-Berg *et al.*, 2021). More bats are now found in trees, buildings or under bridges in the urban areas of the city, suggesting that urban environments can actually provide suitable habitats for the species (Agriculture, Fisheries and Conservation Department, n.d., Jung & Threlfall, 2015).

Bats, a diverse group of mammals under the order *Chiroptera*, are the most abundant and widely distributed mammalian group after rodents, making up 20% of the total number of mammalian species (Woo

& Lau, 2019). They are nocturnal animals that are active during the night, living in caves, trees, mines and water tunnels in colonies. With fruit, nectar, pollen and insects as their main food sources, bats play important ecological roles like pollination and dispersal of seeds, as well as the predation of insects, and thus bear great significance in the biodiversity of an ecosystem.

However, their capability to fly in addition to their highly diversified cell types and receptors also facilitates the dissemination of the viruses, increasing the chances of both interspecies and intraspecies transmission (Woo & Lau, 2019). Thus, the increased human-bat interactions due to urbanisation may bring serious consequences to public health because bats are also well recognized to be the hosts of a number of highly pathogenic viruses, such as rabies virus, Hendra virus, Nipah virus and Ebola virus (Woo & Lau, 2019). This issue is especially prominent under the COVID-19 pandemic, given that at least 30 bat coronaviruses have been discovered after the SARS epidemic in 2003, and the species is now recognised as the gene source of *Alphacoronavirus* and *Betacoronavirus* that are known to infect humans (Woo & Lau, 2019).

---

The above article was written as a culmination of research presented at Hong Kong's Young Engineers (IEEE) conference, 2021.

## Significance and goal of study

Previous research in 2006 attempted to assess species diversity using techniques such as direct roost censuses and mist-net capturing surveys, and found ten species of non-cave-dwelling bats in Hong Kong (Yang *et al.*, 2006). An acoustic survey in 2017 explored the distribution of bats only in urban parks to show a wide distribution and high population of insectivorous bats, but the current distribution of the species are unknown (Tong, 2016, Yu, 2016).

Therefore, the aim of this study is to understand the distribution of bats in Hong Kong under impacts of urbanisation, and to find out whether human activity affects the way the species live. The acoustic surveillance of bat calls in the urbanised areas of southern Hong Kong allows for the comparison of bat visitations along transect lines extending from a school campus in Pok Fu Lam, potentially providing insight into the distribution or living patterns of bats.

## 1. Methodology

To collect data for analysis, 3 transects were designed (labelled T1, T2, T3), each with 3 sites (labelled A, B, C). All 3 transects extend from a biodiversity rooftop garden in a school campus in Cyberport, Pok Fu Lam, Hong Kong (labelled site A), so there are a total of 7 different locations involved in the study. The three transects cover a fan-like area extending from the school campus (Figure 1). T1B is on a slope opposite to a riding school, where T1C is right off a walking trail in the Pok Fu Lam Country Park. T2B and C are two schools which gave permission to set up a detector in their rooftop gardens. T3B is also on a slope behind a school, whereas T3C is on a rooftop garden of a pre-school campus. These sites are areas with different levels of urbanisation and population densities, and were classified into high, medium, and low according to their relative levels of urbanisation and population densities.

After arriving at the site, a stand with a cement base is placed on the ground, and a labelled detector (with a battery which can last for a month) is placed on top and locked in place with zip ties (Figure 2). The sides of the device are sealed with plastic tape to prevent rainwater from leaking in and the device is tilted slightly upwards to record bat calls. The device is directed towards a light source nearby, which is usually a street light - this is because bats are more inclined to fly towards light.



**Figure 1.** Annotated map showing the 3 transects involved in the study.



**Figure 2.** Photo of bat detector device setup.

The ultrasonic bat detector device counted the bursts of bat sonar signals the animal uses for echolocation. Two groups of signals were detected; one that included high ultrasonic frequencies (>40kHz) and a second that did not have high ultrasonic frequencies (<40kHz). This allowed for the broad separation of large and small bats, as well as mixtures of both. The detectors were equipped with a Murator ultrasonic acoustic sensor.

The data collection period for each transect lasted for 16 days, across a span of six months from January to June as only six detectors were available. Acoustic data such as the maximum, minimum and average streams of bat pulses, times of detected echoes and time length of calls were collected and transferred onto Microsoft Excel for analysis.

## 2. Results and Discussion

### 2.1 Number of echoes

The highest number of bat echoes were recorded at sites with highest levels of population densities and urbanisation. As seen from table 1, for each transect, the site with the highest level of urbanisation and population density had the highest total number of bat echoes - T1A had 3367, T2B had 9360 and T3C had 8981. Although T1 and T2 reflect an increasing trend of bat calls in relation to increasing population density, sites with the lowest level of urbanisation in T1 and T3 have higher total number of bat calls than that of the medium level.

Directly looking at urbanisation and population density in relation to the number of bat calls recorded suggests that there is not a direct relationship between the two sets of data. However, attention was drawn to the presence of street lights, as there was an abundance of light sources near the garden at site A. Among the 3 transects, the 3 sites with the highest numbers of bat calls were T2B (9360), followed by T3C (8981) and T2A (8646) (Table 1). These three sites are all schools with street lights turned on at night. When examining all the sites, locations with more street lights had higher recorded numbers of bat calls. Because insects, a main food source for many bats, fly towards light, higher light intensities might be the cause of increased bat calls, suggesting that there could have been increased bat visitations.

This is consistent with other studies reporting that fast-flying bats, such as the *Eptesicus nilssonii* are attracted to white light due to higher insect populations, but contrasting results are observed for slow-flying bats such as the *Rhinolophus hipposideros* (Rich & Longcore, 2013, pp. 48–51, Stone et al., 2009). This highlights the importance of adopting a species-specific approach to assess whether the impact of urbanisation of bat populations are positive or negative. In addition, there is also evidence showing that bats approach streetlights because they are primarily attracted to the light source directly (Rich & Longcore, 2013, pp. 48–51).

Transect / Site	A	B	C
1	T1A: School Base LU = High PD = High NoC = 3367	T1B: Riding School LU = Medium PD = Medium NoC = 244	T1C: Country Park LU = Low PD = Low NoC = 438
2	T2A: School Base LU = Low PD = Medium NoC = 8646	T2B: Local School LU = High PD = High NoC = 9360	T2C: Local School LU = Medium PD = Low NoC = 4514
3	T3A: School Base LU = Low PD = Low NoC = 5194	T3B: Slope behind Local School LU = Medium PD = Medium NoC = 1873	T3C: Rooftop in Community Area LU = High PD = High NoC = 8981

**Table 1.** Number of bat calls (NoC) at 7 sites, which are classified into high, medium and low Levels of Urbanisation (LU) and population density (PD).

### 2.2 Frequency of bat echoes

To look at whether prey attracted by the street lights are causing the high bat visitations, bat echoes were then examined (Figure 4). Sites with the highest maximum number of bat echoes, recorded at 0.5 second intervals, were T3A (193), T1A (115) and T2B (112), two of which are the school base of the study, where large amounts of insects are seen in the garden. T2B is also a school garden. As bats use echolocation to navigate and forage during hunting, the data here supports the hypothesis that bat visitations and hunting are more common at sites with more street lights due to a more abundant food source. Another hypothesis is that the size of average insects caught at lights, which may be moths, are larger than insects that they feed on in their natural habitats, such as flies or beetles (Rich & Longcore, 2013, pp. 48–51). From the bats' point of view, food supply will also be more predictable both temporally and spatially, which benefits their hunting and feeding processes (Rich & Longcore, 2013, pp. 48–51). Hence, feeding efficiency of bats could be concluded to have increased due to the various advantages of streetlights and which led to their increased detected density and frequency of echoes. However, it is important to note that findings of this study could also be accounted for by various factors such as the species of bats being detected, type of prey they catch or the relatively lower population density of Southern Hong Kong when compared to city centres like Central or Mong Kok.

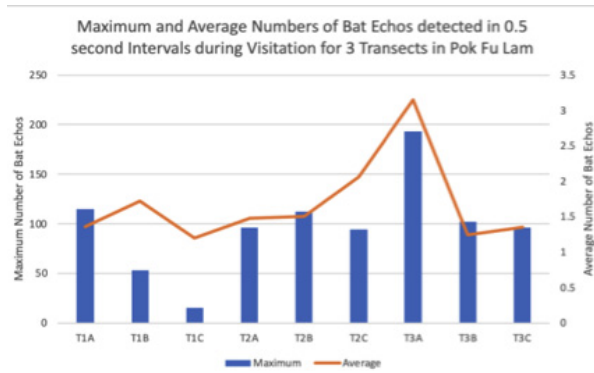


**Figure 3.** Graph showing the maximum and average numbers of bat echoes detected in 0.5 second intervals for 3 transects involved in this study.

### 2.3 Timing of recorded bat echoes

This finding would give insight perhaps into the timing of bat visitations as well, as the number of bat calls at different hours of the day could also reflect the impact of urbanisation on bats. The time range within which bat calls were detected were from 5pm to 6am. Hours with peak numbers of detected calls vary among sites and transects, but there are generally more detected calls from 5pm to 12 am, eventually decreasing towards 6am.

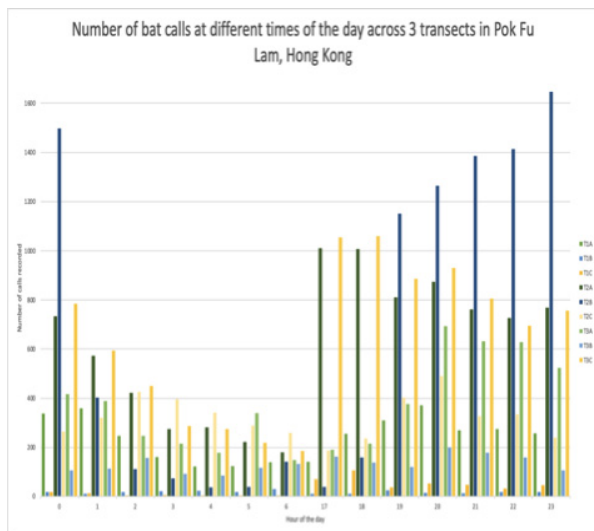


**Figure 4.** Graph showing the number of bat calls at different times of the day for 3 transects involved in this study.

To identify a clearer trend, the total number of calls detected at each hour for each site was averaged to create the figure 5. The peak hour of bat call detection is at around 8pm, which is not during midnight when lights are turned off - this might be due to the bright light from urbanised buildings and areas, where insects gather near and get eaten by bats. Another hypothesis is that insects common in households, like cockroaches, mosquitoes and flies, are major diets of bats like the

Japanese pipistrelle, which might attract them to visit the area, resulting in increased numbers of recorded calls. This suggests that urbanised areas actually increase bat visitations with their rich food source and light attraction for the species.

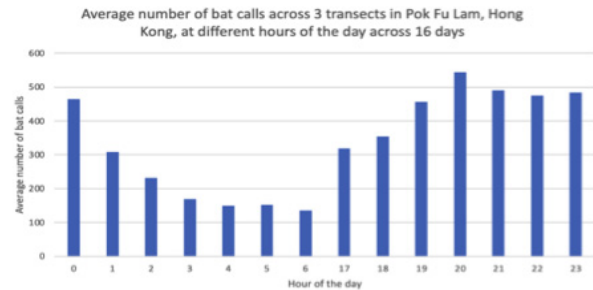


**Figure 5.** Graph showing the average number of bat calls at different hours of the day for 3 transects involved in this study.

### 2.4 Length of bat echoes

Looking at the length of bat echoes might give insight into the duration of bat visitations. Regarding duration and timing, the duration of bat visits was also considered to find out how long the species would stay around the sites. Adding up the total number of seconds that bats have stayed in the area, the 4 sites with significantly longer total durations of visitation are T1A, T2A, T3A and T3C. Considering these 4 sites contain bright street lights and are rooftop gardens, it is hypothesised that bats spend longer each visit to forage and hunt for insects near the light sources. A reason for this could be that larger prey such as moths can be found near the street lights, which require more time for prey handling (Rich & Longcore, 2013, pp. 48–51).

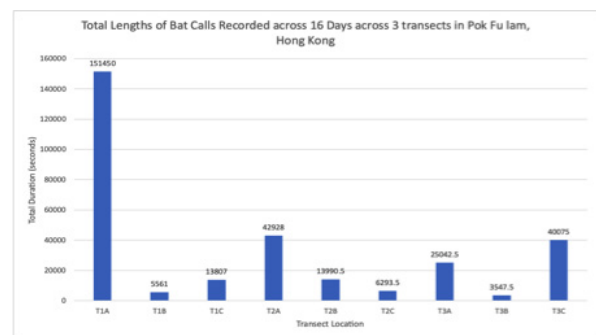


**Figure 6.** Graph showing the total time length of bat calls recorded across 16 days across 3 transects in Pok Fu Lam, Hong Kong.

## Conclusion

In conclusion, results of this study contain several aspects regarding recorded bat calls under the impact of urbanisation, including their frequency, timing and duration. Findings suggest that urbanisation increases the frequency and density of bat visitation possibly due to increased light sources, which allow bats to hunt more effectively as there are more abundant food sources.

With bat activity peaking during the night (7-11pm), attempts to reduce bat visitations should focus on dimming the intensity or amount of street lights to decrease sources of attraction. Since high bat activity was also recorded at different schools, turning off unnecessary light sources or averting the direction to which lights are pointing to would also help reduce visitations. An extension of the project would be to identify the bat species which have been foraging around street lights, and finding out their distribution patterns across the entire city, which could contribute to the further investigations regarding interspecies transmission of bat viruses, and better management of bat populations in urban areas.

## Appendix I

Follow the QR code for the data.



## Acknowledgements

This work is funded under the ISF Academy. Many thanks also to Oceanway Corporation Limited and Mr Paul Hodgson for the technical support and guidance in this project, and local school sites which have allowed the detector set-ups.

## References

- Egert-Berg, K., Handel, M., Goldshtein, A., Eitan, O., Borissov, I., & Yovel, Y. (2021). Fruit bats adjust their foraging strategies to urban environments to diversify their diet. *BMC Biology*, *19*(1). <https://doi.org/10.1186/s12915-021-01060-x>
- Jung K., Threlfall C.G. (2016). Urbanisation and Its Effects on Bats—A Global Meta-Analysis. In: Voigt C., Kingston T. (eds) *Bats in the Anthropocene: Conservation of Bats in a Changing World*. Springer, Cham. [https://doi.org/10.1007/978-3-319-25220-9\\_2](https://doi.org/10.1007/978-3-319-25220-9_2)
- Rich, C., & Longcore, T. (2013). *Ecological Consequences of Artificial Night Lighting*. In Google Books (pp. 48–51). Island Press.
- Stone, E. L., Jones, G., & Harris, S. (2009). Street Lighting Disturbs Commuting Bats. *Current Biology*, *19*(13), 1123–1127. <https://doi.org/10.1016/j.cub.2009.05.058>
- World Population Review. (2021). Hong Kong Population 2020 (Demographics, Maps, Graphs). [worldpopulationreview.com](https://worldpopulationreview.com/countries/hong-kong-population). <https://worldpopulationreview.com/countries/hong-kong-population>
- Woo, P. C. Y., & Lau, S. K. P. (2019). Viruses and Bats. *Viruses*, *11*(10), 884. <https://doi.org/10.3390/v11100884>
- Yang, K., Kong, H., Shek, C.-T., & Chan, C. (2006). Mist Net Survey of Bats with Three New Bat Species Records for Mist Net Survey of Bats with Three New Bat Species Records for Hong Kong (pp. 1–7). *Agriculture, Fisheries and Conservation Department Newsletter*.



---

# A study into the antibacterial properties of Chinese herbal medicine herb *Coptis chinensis*

Aidan Tam

---

## Introduction

The focus of this investigation was to evaluate the efficiency of Traditional Chinese Medicine (TCM) herb *Huanglian* as an antibacterial agent. I chose to investigate the antibacterial properties of TCM as I have personally experienced the therapeutic effects of herbal medicine as a treatment for various ailments, ranging from fevers to food poisoning. I was first exposed to the medicinal effects of TCM through watching my dad apply brewed *Huanglian* (*Coptis chinensis*) extracts around his eyes to help treat eye infections. Further research led me to discover that eye infections are commonly caused by pathogenic bacteria (O'Callaghan, 2018). Normally, antibiotics are used to treat such bacterial infections, but observing my father use *Huanglian* as an alternative treatment piqued my interest to investigate the antibacterial properties of *Huanglian*.

Antibiotics are used by man to treat bacterial infections. Antibiotics are classified into two categories, bactericidal and bacteriostatic. Bactericidal antibiotics kill the bacteria by interfering with the synthesis of the bacterial cell wall or inhibit the process of synthesizing genetic material (Kohanski *et al.*, 2010). Bacteriostatic antibiotics prevent the multiplying of bacteria by inhibiting bacterial growth but do not kill the bacteria. However, over-reliance or incorrect usage of antibiotics leads to the life-threatening problem of antibiotic resistance (Kohanski *et al.*, 2010).

Antibiotic resistance may develop in bacteria colonies over generations due to genetic mutations. Antibiotics provide selective pressure, whereby bacteria that have developed resistance mechanisms against the antibiotic are able to survive and multiply (Zhang *et al.*, 2015). This antibiotic-induced selection process causes bacteria with antibiotic resistance phenotypes to have a survival benefit and continue to produce more resistant bacteria (NHS Choices., 2021). One example of an antimicrobial-resistant bacteria is Methicillin-resistant *Staphylococcus aureus* (MRSA), an ongoing

issue affecting people with weak immune systems *e.g* hospitals and healthcare centers (MRSA - Minnesota Dept. of Health, 2011). MRSA is multi resistant to various antibiotics and requires advanced medical treatment, which has its complicated side effects (The Background And Significance Of MRSA Infection, 2020).

The prevalence of resistance to pharmaceutical antibiotics among pathogenic bacteria in healthcare areas and hospital environments is becoming a bigger concern as resistant organisms can resist medical treatment (World Health Organization: WHO, 2020). Therefore, the lack of availability and variability of new antibiotics prompts for the search for alternative sources of antimicrobial treatments. One such alternative is TCM, which has gained more attention in the medical field as a complementary therapy to antibiotic treatments, which may provide an effective solution for antibiotic resistance.

## 1. Background

### 1.1 *Huanglian*

TCM has been used to treat diseases for more than 2000 years in eastern Asian countries (Liu *et al.*, 2020). One such Medicinal herb, *Huanglian* (黃連) is the dried rhizome of a *Coptis chinensis* plant, belonging to the *Ranunculaceae* family. It is native to Asia and North America and is traditionally used to treat viral and bacterial infectious diseases of the digestive tract, respiratory tract and facial organs (Lau & Plotkin, 2013). *Huanglian* is prescribed as a herbal tea, or directly applied onto skin as an aqueous extract to treat skin infections (Jian-Ling *et al.*, 2010). The main active constituents of *Huanglian* are alkaloids such as Berberine and Coptisine.

### 1.2 Antibacterial mechanisms

Antibacterial mechanisms of *Coptis chinensis* include the alkaloid molecules causing changes to the nucleotide chain structures, interfering with the DNA replication process, as well as inhibiting RNA transcription and

---

The above article was written as an Extended Essay in Biology, in partial fulfillment of the IB Diploma Programme, 2022.

translation in bacterial cells (Jian-Ling *et al.*, 2010). Therefore the parent DNA strand cannot act as a normal DNA template, causing lethal mutation in the daughter bacteria cells. Additionally, alkaloids interact with the bacteria's plasma membrane, causing morphological changes to the bacteria cell surface, preventing the cell from performing homeostatic functions and thus killing the bacteria (Tseng *et al.*, 2020).

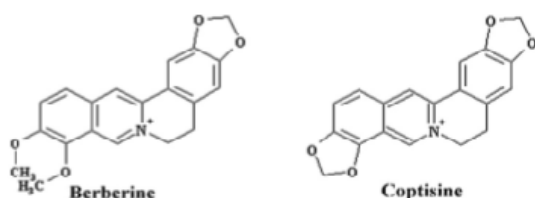


**Figure 1.** Chemical composition of Berberine and Coptisine, the active constituents found in *Huanglian*. Alkaloids are organic compounds with at least one nitrogen atom (Gröger, 1988)

### 1.3 Bacteria

The bacteria that was tested against *Huanglian* was *Staphylococcus aureus*. Some strains of *S.aureus* cause eye infections, and thus investigating this microbe was relevant to my personal understanding of how *Huanglian* treats eye infections (Jian-Ling *et al.*, 2010). It was also mentioned above that antibiotic resistant strains of *S.aureus* (MRSA) can also be extremely difficult to treat as it is resistant to many types of antibiotics. Biosafety level 1 strain of *S. aureus* ATCC 14990 was used in this experiment, to prevent possible contamination of pathogens and cause infections among students.

To investigate the antibacterial properties of *Huanglian* on *S. aureus*, two variables was tested, the effect of concentration (experiment A) and contact time (experiment B) on the zone of inhibition around the disc. Inhibition zone was determined through the Kirby Bauer Disc Diffusion Method, and antibacterial activity measured includes bacteriostatic (inhibiting growth of bacteria) and bactericidal (killing bacteria) activity, as they are hard to differentiate with disc diffusion assay.

#### **Experiment A: Investigation on the effect of concentration of *Huanglian* to inhibit growth of *S.aureus* bacteria colonies**

In experiment A, *Huanglian*'s ability to inhibit *S.aureus* growth at different concentrations was tested, and controlled through serial dilutions. Studies have demonstrated the correlation between antibiotic concentration and bacterial response, as well as the concentration dependent activity of antibiotics (Bernier & Surette, 2013). An increased concentration of *Huanglian* could cause increased interferences in

the DNA replication, RNA transcription and protein synthesis process resulting in the death of more mutated cells. Thus, as the aim of this investigation was to evaluate the efficacy of *Huanglian* as an antibacterial agent, the activity of *Huanglian* at different concentrations was investigated.

#### **Experiment B: Investigation on the effect of contact time of paper discs to inhibit growth of *S.aureus* bacteria colonies**

In experiment B, *Huanglian*'s ability to inhibit *S.aureus* growth when applied for different periods of time was measured. Whenever my father would use *Huanglian*, he would apply the extracts to his eyes using cotton balls and allowing the extract to evaporate before rinsing it off. As the herbal solution is topically applied onto skin and mucosal areas, solutions need time to diffuse into targeted areas to allow for active compounds to interact with bacteria. Wiping off the solution too early may result in minimal active compounds being able to penetrate the target areas and produce minimal antibacterial activity, whilst leaving the solution for an extended period of time may not continuously increase the effectiveness of *Huanglian*. Thus to investigate the efficacy of *Huanglian* as an antibacterial agent, the effect of contact time of paper discs to inhibit growth of *S.aureus* bacteria colonies was also investigated.

### 1.4 Preliminary tests

During the preliminary testing, I had the initial idea to compare the antibacterial activity of *Huanglian* on Gram positive versus Gram negative bacteria. I selected *E.coli* (Gram negative) alongside *S.aureus* (Gram positive) to be tested against *Huanglian*. Preliminary results showed that *Huanglian* exhibited no activity against *E.coli*, but did demonstrate inhibition against *S.aureus*. The ineffectiveness of *Huanglian* against *E.coli* could be justified due to the extra outer membrane of Gram negative bacteria not allowing for the active constituents to penetrate the cell (Tseng *et al.*, 2020). Therefore, instead of focusing on two types of bacteria, I focused my Extended Essay on various variables (concentration of herbal extracts and contact time) and its effect on *Huanglian*'s antibacterial activity against *S.aureus*. Furthermore, *Huanglian*'s antibacterial activity against *E.coli* will be further discussed in the evaluation.

## 2. Investigation

<p><b>RQ:</b> How does changing the concentration and contact time of the Chinese herbal medicine <i>Huanglian</i> (<i>Coptis chinensis</i>) inhibit the growth of <i>Staphylococcus aureus</i> bacteria colonies as measured by the zone of inhibition?</p>	
<p><b>Experiment A:</b> To investigate the effect of concentration of <i>Huanglian</i> extracts on width of inhibition zone after 48 hours</p>	<p><b>H<sub>0</sub>:</b> Different concentrations of <i>Huanglian</i> extract does not affect width of the inhibition zone</p>
	<p><b>H<sub>1</sub>:</b> I hypothesize that as the concentration of <i>Huanglian</i> extract increases, the area of inhibition also increases due to the increased concentration of alkaloids causing increased interferences in the DNA replication, RNA transcription and protein synthesis process thus the death of more disrupted cells.</p>
<p><b>Experiment B:</b> To investigate the effect of contact time of <i>Huanglian</i> loaded paper discs on width of inhibition zone after 48 hours of incubation</p>	<p><b>H<sub>0</sub>:</b> Different contact times of <i>Huanglian</i>-loaded paper discs placed onto each plate does not affect the width of inhibition zone</p>
	<p><b>H<sub>1</sub>:</b> I hypothesize that as the paper disc contact time increases, the diameter of the inhibition zone also increases due to the aqueous herbal extract having more time to diffuse into the surrounding agar, thus increasing the concentration of alkaloids to inhibit the growth of bacteria cells.</p>

### 2.1 Variables

<p><b>Independent Variable:</b></p>
<p><b>Experiment A:</b> Concentration of <i>Coptis chinensis</i> herbal extract (0.0%,12.5%,25.0%,50.0%,100.0%), was controlled through serial dilution. As my herbal extract is water soluble, a set amount of the original extract is diluted using sterile water by a dilution factor of 2, reducing the concentration.</p>
<p><b>Experiment B:</b> Paper discs loaded with <i>Coptis chinensis</i> herbal extract are placed onto the agar plate for 1, 3, 5,7 &amp; 9 minutes. Paper discs loaded with herb extract were removed from the agar plates after the different contact times set by a timer. Inhibitory zone diameter was measured after 48 hours post initial contact</p>
<p><b>Dependent Variable:</b></p>
<p>Diameter of the inhibition zone in the disc diffusion assay (mm). The minimum diameter of the inhibition zone is measured using a caliper, as according to the Kirby Bauer Method.</p>

## 2.2 Control variables

Control variable	Why it is controlled	Manipulation of variable
Incubation time	Time allowed for bacteria to grow directly influences the amount of bacteria. A difference in the amount of bacteria influences the significance of the antibacterial properties of <i>Huanglian</i> .	All plates were incubated for 48 hours to allow for sufficient bacteria growth. Time frame was determined in the pre-tests as it allowed bacteria to grow, showing the influences of variables on inhibition zones.
Incubation temperature	Increasing temperature also increases the growth rate of bacteria. As metabolic processes in bacteria are enzyme mediated, changing the temperature thus has an effect on the growth of bacterial colonies (Marajan <i>et al.</i> , 2018).	Temperature of 25°C was chosen according to the IB lab safety guidelines, to prevent students being exposed to any form of pathogenic risks. All plates were incubated in the same incubator to ensure the same consistent temperature.
Type of nutrient agar & pH of agar	Different growth mediums contain different nutrients which at the same time also affect the pH of the agar plate. A difference in nutrients would affect the growth of bacteria, impacting the significance of the antibacterial properties of <i>Huanglian</i> .	LB agar plates were used in all trials, and were all produced in the same batch to ensure the same amount of nutrients and volume of agar to be consistent on every plate, and to maintain the same pH of 7.8.
Volume of herbal extract loaded into paper disc	Different volumes of herbal extract loaded into each disc would result in different diffusion rates and different concentrations of the herbal active ingredients, influencing the diameter of inhibition zones.	10.00 ±0.01µl of <i>Coptis chinensis</i> herbal extract is loaded onto each paper disc using a 20.00 ±0.01µl automatic pipette. A volume of 10 microliters was chosen following the original standardized disc diffusion assay method as published by Bauer <i>et al.</i> (1959)
Size of paper disc	Different brands of paper discs would have varying diameters and would result in a difference in inhibition zones as the starting diameter would be different. Furthermore, the material of the paper disc would influence the diffusion rates of the herbal extract.	All paper discs used in the exploration are 6 mm in diameter, and all produced by JC LAB.
Volume of bacteria suspension used	A varying volume of bacteria suspension would result in a difference in bacteria cell count, thus affecting time bacteria colonies take to grow and number of bacteria cells on the plate.	100.00 ±0.01µL of bacteria suspension was placed onto each plate. This was controlled by having the school lab technician prepare the bacteria suspension the day before testing. All testing was also conducted on the same day to ensure constant bacteria cell count throughout the investigation.
Strain of bacteria used	Different strains of bacteria would each have different growth rates, and the degree to which <i>Huanglian</i> have antibacterial effects on the bacteria would also differ. Some strains of bacteria may potentially be more resistant against the active ingredients in the herbal extract, vice versa some may be more susceptible.	The same species and strain of bacteria <i>Staphylococcus aureus</i> ATCC 14990 was used in all trials.

### 2.3 Preparation of herb and extraction of water soluble products from *Huanglian*

Samples of dried *Coptis chinensis* roots were purchased at a local TCM store in North Point, Hong Kong on May 26, 2021. Herbs were stored in the microbiology lab refrigerator at 7°C before testing.

Herbal infusions were prepared fresh the day of testing, whereby 50.00±0.01g of dried *Coptis chinensis* roots were blended into powder using a kitchen herb grinder. *Huanglian* powder and 200ml of sterilized water was added into a 500 ml beaker, placed onto a heating magnetic stirrer plate and boiled at 100°C for 30 minutes. The boiled contents were filtered using a syringe filter, removing potential bacteria that remains in the boiled solution. The remaining sample was stored in a 50ml centrifuge tube for later use.

### 2.4 Procedure for Kirby Bauer method/disc diffusion assay:

The antibiotic properties of *Coptis chinensis* under various application methods were compared using the disc diffusion assay (aka the Kirby Bauer method). This test uses discs loaded with various *Huanglian* herbal infusions to assess effectiveness of the samples to inhibit the growth of *S.aureus*. The Kirby Bauer Method as mentioned in Bauer *et al.* (1959) was selected because of its simplicity, affordability and its ability to be replicated in the future as materials used in the test are common laboratory items. Instead of using the Mueller Hinton agar detailed in Bauer’s method, LB agar was used as it was the only medium available in school. Agar plates used in this experiment were prepared by the school technicians.

On each agar plate, a 3x3 grid was drawn to separate 9 boxes [Figure 3], each box allowing for one trial. It was determined during preliminary testing that the average zones of inhibition were approximately 10mm (including paper discs). The width of each box was 16mm thus avoiding any overlap of inhibition zones. The agar plates were inoculated with *S.aureus*, and evenly spread using an L-shaped spreader to grow a bacterial lawn. Sterile paper discs were placed in the center of each box, then 10.00±0.01µl of selected extract was loaded onto the paper discs using a 20±0.01µl autopipette. Plates were taken out of the incubator after 48 hours, and the zone of inhibition was measured using a caliper recording the diameter. The diameter of the paper disc was subtracted from the total inhibition diameter to determine the width of the kill zone. The mean kill zone width of all 5 trials and standard

deviation of the kill zone width were calculated, which was later used for comparisons against inhibition zones from other treatments.

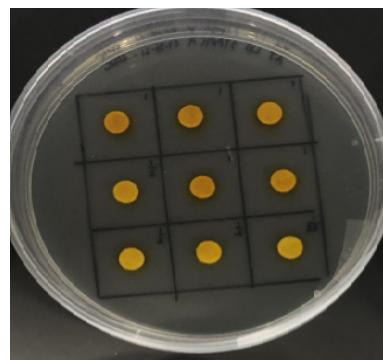


Figure 3. Agar plate showing 3x3 grid each filled with an extract-loaded paper disc

### 2.5 Procedure for Experiment A: serial dilution to determine appropriate infusion concentration of *Coptis Chinensis* extract

In order to investigate the effect of different herbal infusion concentrations on the antibacterial effects of *Coptis chinensis*, a serial dilution by a factor of 2 was performed. The full-strength herbal infusion was collected from the extraction mentioned in the “preparation of herbs” section 2.4, where 1000.0±0.1µl of solution was added in a microcentrifuge tube and used to conduct a 2 fold dilution series [Figure 4]. 500.0±0.1µl of saline solution was added into the second and third and fourth microcentrifuge tubes. The differently concentrated samples (100.0%, 50.0%, 25.0%, 12.5%, 0.0% of the original infusion concentration) were then tested for their antibacterial activity using the disc diffusion method. All concentrations were repeated in pentacate in order to remove any outliers.

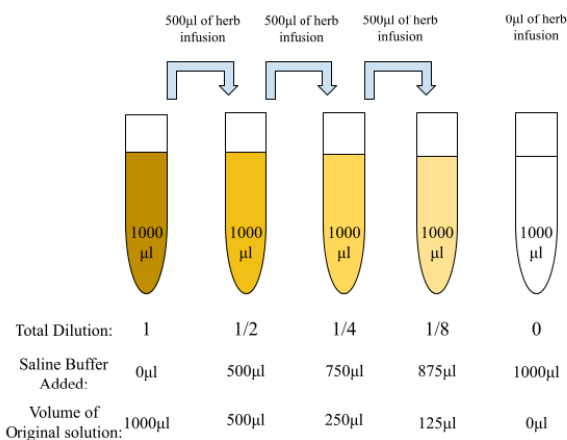


Figure 4. Diagram demonstrating serial dilution series by the factor of 2

## 2.6 Procedure for Experiment B: investigation of the effect of contact time of paper discs

The effect of different contact times between *Huanglian* loaded paper discs and agar plate was controlled through removing paper discs from agar plates after different periods of time. Agar plates were inoculated with *S.aureus*, and paper discs were placed into individual grids on the plate. Concentration of *Huanglian* extract was controlled through only using stock solution of *Huanglian* extract (50g *Huanglian* and 200 ml sterile water). Upon pipetting extract onto paper discs, a timer was started, and paper discs were removed and disposed after 1, 3, 5,7, 9 minutes.

## 2.7 Ethical and safety issues

To eliminate the possibility of contamination of bacteria, agar plates were autoclaved after experimentation. Additionally, agar plates were sealed using parafilm to prevent growing bacteria from contaminating the external environment. Personal protective equipment (PPE) were worn whenever inside the microbiology lab, and disposed of or left inside the lab before exiting to prevent contamination. Though bacteria used in the experiment are non-pathogenic bacteria, bacteria will still be handled with care, and all equipment used in handling bacteria were either disposed of, or sanitized using alcohol and an alcohol burner as according to the ASM Biosafety Guidelines. Finally, bacteria was incubated at room temperature to ensure a controlled and safe rate of bacteria growth. The optimal temperature for bacterial growth for is 37°C. However the rapid rate of bacterial growth at such temperature may have led to potential dangers of contamination, and harm to human health.

## 3. Results

### 3.1 Qualitative observations

- *S.aureus* colonies grew uniformly to form a bacteria lawn covering the agar plates, with no perceivable difference in growth.
- The diffusion of *Huanglian* extract was visible, seen through the yellow staining of agar surrounding the paper discs [Figure 6].
- At weaker concentrations, inhibition zones were barely visible [Figure 6].
- On one plate, external microbes contaminated the plate [Figure 7]
- Inhibition zones were mostly circular, but there were also irregular inhibition zones shapes [Figure 8, Figure 9].

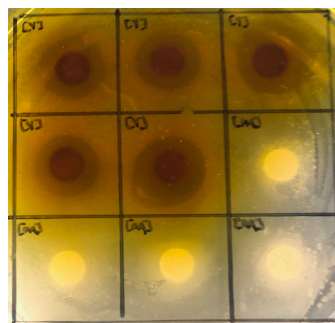


**Figure 6.** Coloured image showing the inhibition zones of 100% vs 0% *Huanglian*. Inhibition zones of 100% *Huanglian* can be seen, and the diffusion zone of *Huanglian* seen in the dark brown colouration.

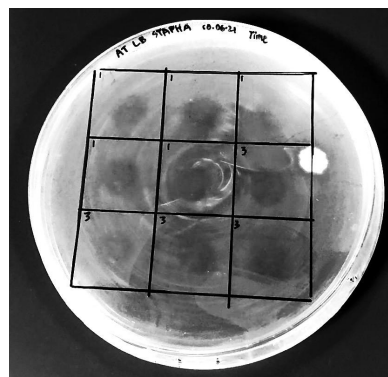


**Figure 7.** Photo of a contaminated agar plate, with an unknown microbial colony growing alongside *Staphylococcus aureus*. The contamination did not interfere with any inhibition zones.

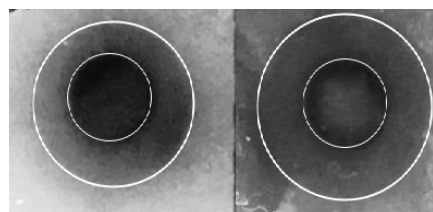


**Figure 8.** Inhibition zones of 100% *Huanglian* extract. Inhibition zones and paper discs are highlighted, and image contrast was increased for better visibility of bacteria lawn and inhibition zone.

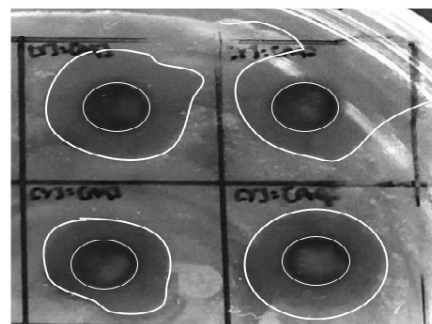


**Figure 9.** Asymmetrical inhibition zones of 50.0% *Huanglian* extract. Inhibition zones demonstrated are irregular, and not the circular shape as expected. Inhibition zone of the circular disc on the top right grid did not have a closed inhibition zone presumably due to inconsistencies in bacteria spreading.

## 3.2 Statistical tests and analysis

### Experiment A

Graph 1: Concentration of Huanglian extract (%) vs width of inhibition zone produced

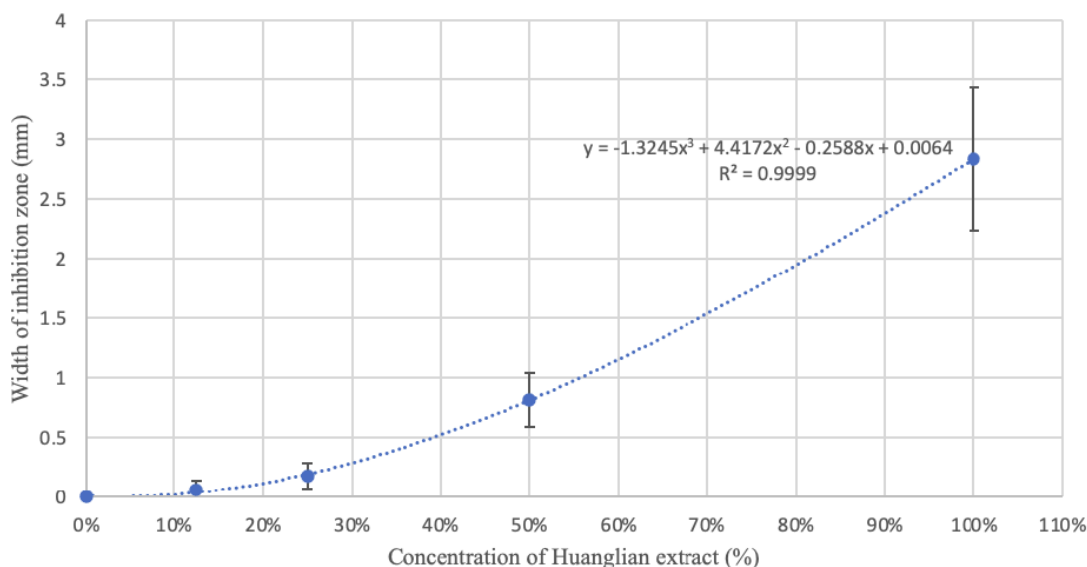


**Figure 10.** Concentration of *Huanglian* extract (%) vs width of inhibition zone produced (mm).

All concentrations but 0% *Huanglian* extract formed a zone of inhibition against *Staphylococcus aureus*. The graph shows a strong positive correlation: as the concentration of the *Huanglian* extract increases, the width of the inhibition zone also increases. A polynomial trendline was plotted, and it was observed that the trendline was very close to every data point and within all error bars. However, large standard deviations of the inhibition width of 100.0% *Huanglian* resulted in large error bars, indicating the large variability, reflecting a degree of uncertainty. Such results were taken into consideration when evaluating the data.

One-tailed t-tests with a significance level of 0.05 were conducted using an online calculator tool (“Single Sample T-Test Calculator”) to determine the statistical significance between adjacent *Huanglian* concentration values and their respective inhibition zone widths. A t-test was used due to the trend of data not being linear, hence not using a Pearson’s correlation coefficient test. A p-value lower than 0.05 indicates that there is a low probability data has occurred by chance, thus rejecting the null hypothesis.

$H_0$ : Different concentrations of *Huanglian* extract does not affect diameter of the inhibition zone

$H_1$ : As concentration of *Huanglian* extract increases, the width of the inhibition also increases

Variable pairs	t-value	p-value	Null Hypothesis
0.0% vs 12.5%	-2.13809	0.032485	Rejected
12.5% vs 25.0%	-1.62221	0.071707	Accepted
25.0% vs 50.0%	-5.65685	0.000239	Rejected
50.0% vs 100.0%	-7.05415	0.000053	Rejected

**Table 1.** t-test results of data in Experiment A

All p-values except for concentrations 12.5%-25.0% were less than 0.05. Therefore, the null hypothesis is rejected and the alternate hypothesis is accepted, suggesting a difference in the width of inhibition between each *Huanglian* concentration is statistically significant. However, it should be noted during analyzing results of the t-test that data points in this experiment were not spread apart evenly, but were rather spread by a scale factor of 2. Thus, the difference in antibacterial efficacy may be different and not linearly distributed. It can be biologically assumed that as *Huanglian* concentration increases, the concentration of Berberine, Coptisine and other alkaloids also increase. Hence there are more active constituents that can cause disruptions in the usual bacterial DNA replication, RNA transcription and protein synthesis process, causing the mutation of the bacterial daughter cell and thus the death of bacteria (Jian-Ling *et al.*, 2010).

## Experience B

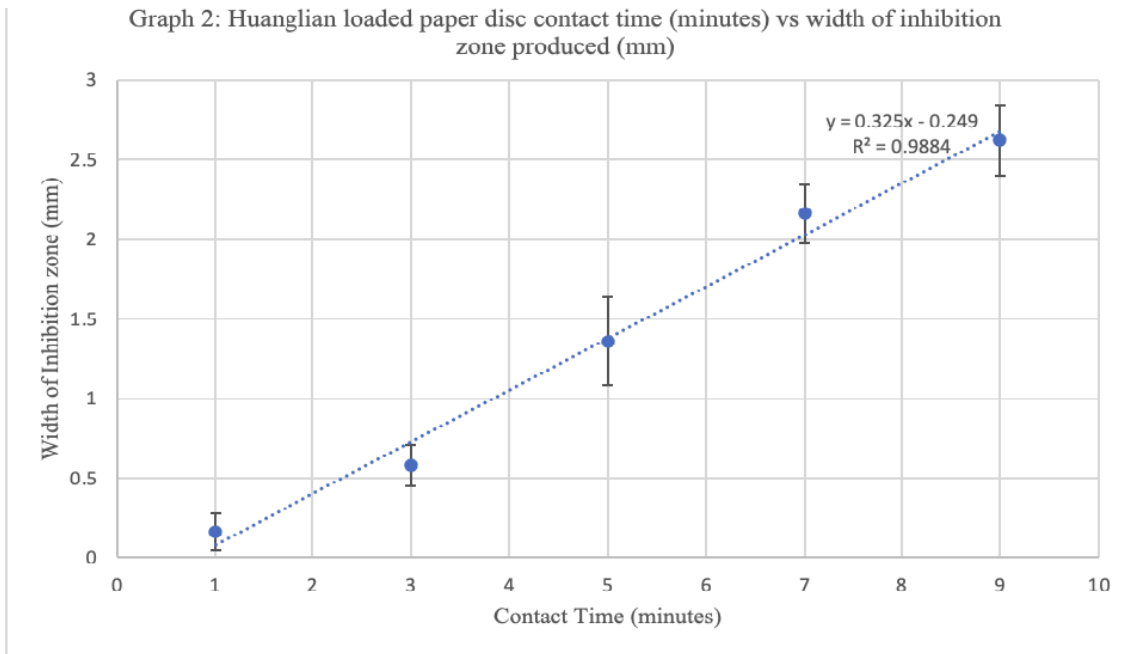


**Figure 11.** Huanglian loaded paper disc contact time (minutes) vs width of inhibition zone (mm).

All contact times tested formed a zone of inhibition and a strong positive correlation was demonstrated as increasing contact time increased the width of the inhibition zone (Graph 2). A linear trendline was plotted to demonstrate the trend of data points, with the trendline fitting within data points and their error bars. A Pearson's correlation coefficient test was conducted to determine the statistical significance of the data points. A Pearson's correlation coefficient test was used instead of a t-test as the data exhibited a linear relationship. R-value could range from +1 to -1, and a greater absolute value indicates a stronger linear relationship where a change in one variable is accompanied by a consistent change in the other. Similarly, a coefficient of zero represents no linear relationship. Thus a correlation coefficient test could be used as a hypothesis test.

$H_0$ : Different paper disc contact times do not affect the width of inhibition zone ( $r = 0$ )

$H_1$ : As the paper disc contact time increases, the width of inhibition also increases ( $r \neq 0$ )

An r-value of 0.9923 was calculated, demonstrating that data points exhibit a strong positive correlation, where data points fit closely to the linear line and differences are statistically significant. Consequently, the null hypothesis is rejected as the r value was greater than 0.05, and the alternate hypothesis that different contact times influences the width of the inhibition zone is accepted.

## 4. Evaluation

### 4.1 Method evaluation

The disc diffusion method used in this extended essay allowed for a large number of trials to be conducted in a short period of time, and for trials to be conducted under similar conditions. Internal variabilities between different plates were reduced through conducting multiple trials on the same plate, controlling the difference in agar composition and Huanglian's rate of diffusion etc. Any difference in inhibition width demonstrated in the disc diffusion method could be attributed to the variables investigated, thus also allowing results to be internally compared to each other.

However the Mcfarland standard, a solution used to adjust the turbidity of bacterial suspensions as detailed in Bauer's standard disc diffusion method was not used due to limitation in school resources. This influences the ability for experimental results to be compared with literature values as my agar plates would have a different quantity of bacteria, affecting the inhibition zones produced. This also potentially explains the non circular inhibition zones noticed in the qualitative observations [Figure 8, Figure 9]. Without using the Mcfarland standard to control the "concentration" of the bacteria suspension potentially resulted in insufficient amount of bacteria growing on the agar plates, causing unclear zones of inhibitions. Low clarity of the inhibition zones



boundaries could cause the recorded inhibition width values to be inaccurate. To eliminate this systematic error, the Mcfarland standard should be followed, alongside using the computer program ImageJ to more accurately measure the width of inhibition zones through increasing contrast of images. Furthermore, testing of *Huanglian*'s antibacterial activity was conducted in an in-vitro environment, removed from all real life biological context of *S.aureus* infections on the human body, reducing the results generalisability to a real life context.

## 4.2 Source evaluation and comparison

Literature values were compared against the experimental results of Experiment A and B. For experiment A, the positive correlation between the concentration of *Huanglian* and its ability to inhibit or kill *S.aureus* is supported by Leach *et al.* (2011). Leach demonstrated *Huanglian*'s antibacterial efficiency using the disc diffusion method, showing that as *Huanglian* concentration increases, the zone of inhibition on gram positive bacteria increases.

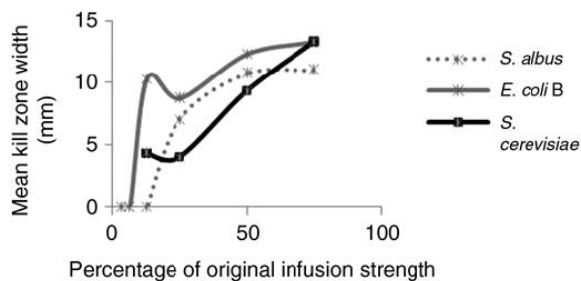


**Figure 12.** Effect of different *Coptis chinensis* concentrations on mean zone of inhibition of *S.albus*, *E.coli* and *S.cerevisiae* (Leach *et al.*, 2011)

Though a different species of bacteria was used compared to my investigation, the bacteria were both gram positive bacteria from the same genus and share similarities. The trends observed from the literature graph are also similar to my results, seen through the significantly greater antimicrobial effect as concentration of *Huanglian* increases. Even though the standardized Kirby Bauer Method was followed in both my extended essay and Leach *et al.* study, it is observed that the mean inhibition zone widths were significantly greater in the literature findings. Such variation in results could be attributed to the limitations in the investigation methodology as mentioned in the "Method Evaluation" section, as the concentration of the bacterial suspension may have potentially affected the inhibition zones produced. Furthermore, the source and extraction method of *Coptis chinensis* may also have been a major factor affecting the potency of *Huanglian*.

Experiment B's results were compared with the literature results in Leach's article testing the effect of contact time on coagulase negative *Staphylococcus* (Leach *et al.*, 2011). Leach documented a fluctuating trend, where mean inhibition widths decreased between 15s and 1 minute, but plateaued after reaching maximum inhibition at 3 minutes. However, literature results contradicted the linear relationship demonstrated by my experimental values, as literature results did not demonstrate the trend that as contact time increases, the width of inhibition (directly correlated to the number of bacteria killed or inhibited) increases proportionally.

However, as the range of contact times tested in Leach's study was different to contact times tested in my extended essay, it is not possible to critically evaluate whether the observed trend is the most representative of the impact of contact time on antibacterial activity, and may require further research to verify results.

Online sources used in this essay were reliable because they come from a range of academic databases that are subject to peer review. Credible articles were selected through reviewing their date of publication as well as the presentation of information. Most recent sources were selected, as it contains the most updated information. Furthermore, sources were also selected if they had an appropriate structure (Introduction, Method, Results, Discussion).

## Conclusion

This exploration aimed to investigate the antibacterial properties of TCM Herb *Huanglian* against *Staphylococcus aureus*. Results show that *Huanglian* exhibits antibacterial activity against *S.aureus*, seen through the zone of inhibition around *Huanglian* loaded paper plates.

Experiment A demonstrated that as concentration of *Huanglian* extract increases, the antibacterial activity also increases, seen in the increased inhibition width (Figure 10; 100% conc. = 2.80 ±0.60mm, 50% conc. = 0.80mm ±0.23mm). However even at 100% concentration, inhibition zones were still small at only 2.8mm, indicating weak antibacterial activity against *S.aureus*. A t-test concluded that the inhibition widths of different herbal extract concentrations were significantly different. Therefore the results of this experiment demonstrate the potential of *Huanglian* antibacterial activity at high concentrations, justifying the use of *Huanglian* extracts to help treat and prevent eye infections as well as for future research to potentially develop novel antibiotics from the active constituents of *Huanglian*.

Experiment B demonstrates that increasing the contact time *Huanglian* infused paper discs have with agar plates increases antibacterial activity, seen through the increased inhibition width (Figure 11). A Pearson correlation coefficient calculated had a R value of 0.9923, indicating a strong positive correlation. However, literature values contradict with experimental results, not showing the proportional increase in antibacterial activity instead a fluctuating trend. Thus making it difficult to evaluate the relative effectiveness of *Huanglian* at different contact times. Further research would need to be conducted in order to understand how various application times affect *Huanglian* antibacterial activity, and whether an optimal contact time of *Huanglian* solution for which antibacterial effects are maximized.

## Further Investigations

Further investigations that could extend the understandings gained from this investigation could be investigating a wider range of IV values for both concentration and contact time, to possibly determine the optimal *Huanglian* concentration and contact time that would maximize the antibacterial effects. This would provide insight regarding the potential use of *Huanglian* as a source for future antibiotic drug development, whereby results could inform the dosage of the potential drug. Furthermore, determining the effects of a wide range of contact times on the antibacterial effects of *Huanglian* would allow for better understanding of the applications of *Huanglian* for eye infections.

Finally, as some active compounds within *Huanglian* are not water soluble, the use of other solvent such as methanol to optimize the extraction of *Huanglian* may be investigated. I have begun preliminary testing for this extended investigation, and have demonstrated an increase in antibacterial properties with methanol extracted *Huanglian*. However, such extraction methods have low applicability as common households do not have easy access to chemicals such as methanol.

## References

- Bauer, A. W. (1959). Single-Disk Antibiotic-Sensitivity Testing of Staphylococci. A.M.A. *Archives of Internal Medicine*, 104(2), 208.
- Bernier, S. P., & Surette, M. G. (2013). Concentration-dependent activity in natural environments. *Frontiers in Microbiology*, 4. <https://doi.org/10.3389/fmicb.2013.00020>
- Cowan, M. M. (1999). Plant Products as Antimicrobial Agents. *Clinical Microbiology Reviews*, 12(4), 564–582. <https://doi.org/10.1128/cmr.12.4.564>
- Githeng'u, S. K., Nyalala, S., & Gaoqiong, L. (2016). Antibacterial Activity of *Coptis chinensis* Extract Against *Pectobacterium carotovorum* subsp. *carotovorum*. *International Journal of Phytopathology*, 5(2), 61–66. <https://doi.org/10.33687/phytopath.005.02.1159>
- Gopalasatheeskumar Kasiramar. (2019, April 14). *Significant Role Of Soxhlet Extraction Process In Phytochemical Research*. ResearchGate; unknown. [https://www.researchgate.net/publication/332407655\\_SIGNIFICANT\\_ROLE\\_OF\\_SOXHLET\\_EXTRACTION\\_PROCESS\\_IN\\_PHYTOCHEMICAL\\_RESEARCH](https://www.researchgate.net/publication/332407655_SIGNIFICANT_ROLE_OF_SOXHLET_EXTRACTION_PROCESS_IN_PHYTOCHEMICAL_RESEARCH)
- Gröger, D. (1988). Terpenoid and Steroid Alkaloids. *Phytochemicals in Plant Cell Cultures*, 435–448. <https://doi.org/10.1016/b978-0-12-715005-5.50032-7>
- Kohanski, M. A., Dwyer, D. J., & Collins, J. J. (2010). How antibiotics kill bacteria: from targets to networks. *Nature Reviews Microbiology*, 8(6), 423–435. <https://doi.org/10.1038/nrmicro2333>
- Jian-Ling, J., Guo-Qiang, H., Zhen, M., & Gao, P.-J. (2010). Antibacterial Mechanisms of Berberine and Reasons for Little Resistance of Bacteria. *Chinese Herbal Medicines*, 3(1), 27–35. <https://doi.org/10.3969/j.issn.1674-6384.2011.01.007>
- Lau, D., & Plotkin, B. J. (2013). Antimicrobial and Biofilm Effects of Herbs Used in Traditional Chinese Medicine. *Natural Product Communications*, 8(11), 1934578X1300801. <https://doi.org/10.1177/1934578x1300801129>
- Leach, F. S. (2011). Anti-microbial properties of *Scutellaria baicalensis* and *Coptis chinensis*, two traditional Chinese medicines. *Bioscience Horizons*, 4(2), 119–127. <https://doi.org/10.1093/biohorizons/hzr014>
- Liu, R., Li, X., Huang, N., Fan, M., & Sun, R. (2020). Toxicity of traditional Chinese medicine herbal and mineral products. *Pharmacological Advances in Natural Product Drug Discovery*, 301–346. <https://doi.org/10.1016/bs.apha.2019.08.001>
- Marajan, C., Alias, S., Ramasamy, K., & Abdul-Talib, S. (2018). *The effect of incubation time, temperature and pH variations on the surface tension of biosurfactant produced by Bacillus spp.* <https://doi.org/10.1063/1.5062673>
- Methicillin-resistant Staphylococcus aureus* (MRSA) - Minnesota Dept. of Health. (2011). State.mn.us. <https://www.health.state.mn.us/diseases/staph/mrsa/index.html>
- NHS Choices. (2021). Antibiotic resistance - Antibiotics. <https://www.nhs.uk/conditions/antibiotics/antibiotic-antimicrobial-resistance/>
- O'Callaghan, R. (2018). The Pathogenesis of *Staphylococcus aureus* Eye Infections. *Pathogens*, 7(1), 9. <https://doi.org/10.3390/pathogens7010009>

Soxhlet extraction. (2016). RSC Education. <https://edu.rsc.org/resources/soxhlet-extraction/2256.article>

Tseng, C.-Y., Sun, M.-F., Li, T.-C., & Lin, C.-T. (2020). Effect of *Coptis chinensis* on Biofilm Formation and Antibiotic Susceptibility in *Mycobacterium abscessus*. *Evidence-Based Complementary and Alternative Medicine*, 2020, 1–9. <https://doi.org/10.1155/2020/9754357>

World Health Organization: WHO. (2020). Antibiotic resistance. Who int; World Health Organization: WHO. <https://www.who.int/news-room/fact-sheets/detail/antibiotic-resistance>

Zhang, L., Levy, K., Trueba, G., Cevallos, W., Trostle, J., Foxman, B., Marrs, C. F., & Eisenberg, J. N. S. (2015). Effects of Selection Pressure and Genetic Association on the Relationship between Antibiotic Resistance and Virulence in *Escherichia coli*. *Antimicrobial Agents and Chemotherapy*, 59(11), 6733–6740. <https://doi.org/10.1128/aac.01094-15>

Zhang, Q.-W., Lin, L.-G., & Ye, W.-C. (2018). Techniques for extraction and isolation of natural products: a comprehensive review. *Chinese Medicine*, 13(1). <https://doi.org/10.1186/s13020-018-0177-x>

## Appendix I. Raw Data Tables



## Appendix II. Example of One Tailed T-test Calculation



## Appendix III. Example of Pearson's Correlation Coefficient Statistical Test



---

# Genomic analysis of the airborne *Micrococcus luteus* strain CW.Ay reveals extensive versatility and resilience

Charlotte A.C.M. Wong

---

## Abstract

*Micrococcus luteus* is a Gram-positive, non-motile, obligate aerobe found in a remarkable range of habitats. *M. luteus* strain CW.Ay strain was isolated from indoor air in a school classroom in Hong Kong. The complete genome (2,543,764 bp; GC content 72.93%) was established by hybrid assembly, comprising a linear plasmid and single chromosome. The chromosome features many genes to account for its broad distribution in very diverse habitats, including those allowing tolerance of heavy and ionising radiation.

---

## Introduction

*Micrococcus luteus* (formerly *M. lysodeikticus*) is a Gram-positive, non-motile, obligate aerobe found in a remarkable range of habitats, including soil (Sims *et al.*, 1986; Ghosh *et al.*, 2013), seawater (Mohanrasu *et al.*, 2018; Ferrari *et al.*, 2019), freshwater (López *et al.*, 2005; Min *et al.*, 2010), and on surfaces including clothing and human skin (Chierighin *et al.*, 2020; Khayyira *et al.*, 2020). It is also airborne in dust and bioaerosols and has been recovered from samples of indoor air (Kookan *et al.*, 2012; Kutmutia *et al.*, 2019) and urban air (Fang *et al.*, 2007). *Micrococcus* spp. even comprise a major proportion of bacteria recovered from the lower stratosphere (Smith *et al.*, 2018). Given its mobility and the variety of conditions *M. luteus* may encounter, the features encoded by its small genome (~2.5 Mbp) enable impressive versatility and resilience.

## 1. Methods

CW.Ay was isolated from indoor air in a school classroom in Cyberport, Hong Kong using the IUL Spin Air Basic sampler passing 100 L/min onto the surface of Luria agar for 5 minutes. After incubation for 48 hours at 27 °C, selected yellow colonies were passaged 10 times on Luria agar. A single colony was incubated in Luria broth for 24 hours before DNA extraction using a PureLink® Genomic DNA Mini Kit (Invitrogen). Paired-end short-read sequencing libraries were prepared using the NexteraXT DNA

Library Preparation Kit and sequenced via the Illumina MiSeq platform using v3 chemistry (2x300 bp). Adapter sequences were removed using Trimmomatic v0.32 (Bolger *et al.*, 2014) and reads quality-filtered and trimmed, producing 703,669 read pairs with an average length of 278 bp (~196 Mbp). Long-read libraries, prepared from the same extracted DNA using the Rapid Barcoding Kit SQK-RBK004, were sequenced using Oxford Nanopore's Spot-ON Flow Cell (vR9), MinION sequencer and MinKNOW v3.1.8 software with base-calling by Guppy v2.1.3. The final long-read dataset, trimmed by Porechop v0.2.4 (Wick, 2017; Wick *et al.*, 2018), totalled 182,541 reads (2.21 Gbp) with a mean length of 12,121 bp (N50 20,668). Default parameters were used for all software unless otherwise specified.

## 2. Results and Discussion

Assembly of short-reads by Newbler 2.7 (Roche Diagnostics) suggested a draft genome of ~2.5 Mbp, based on 411 contigs (mean length 6,202 bp). However, Unicycler v0.4.3 (Wick *et al.*, 2017) combined the Illumina and MinION datasets to render a circular chromosome of 2,449,847 bp and a linear plasmid of 93,917 bp, with mean coverage of 194x, which were submitted to NCBI PGAP v5.0 (Haft *et al.*, 2018) and to PATRIC (Brettin *et al.*, 2015) for annotation.

Mash/MinHash using PATRIC (Ondov *et al.*, 2016) found the CW.Ay chromosome and plasmid close to *Micrococcus luteus* strain SA211 and *Micrococcus sp.*

---

The above article is a culmination of research undertaken at ISF's Molecular Biology Laboratory, and is an extension of a Genome announcement: Wong, C. A. C. M., Lai, G. K. K., Griffin, S. D. J., Leung, F. C. C. (2022). Complete genome sequence of *Micrococcus luteus* strain CW.Ay, isolated from indoor air in a Hong Kong school. *Microbiology Resource Announcements*, 11(2): e0119421. <https://doi.org/10.1128/mra.01194-21>

A7 plasmid pLMA7, with average nucleotide identities of 97.11% and 97.09% respectively (Yoon *et al.*, 2017).

In antimicrobial susceptibility tests (discs from Liofilchem), CW.Ay exhibited resistance to ampicillin (10 µg), chloramphenicol (30 µg), colistin (10 µg), erythromycin (15 µg) and sulfanilamide (30 µg), with relevant genes chromosomally encoded (Alcock *et al.*, 2020). A CRISPR array was also identified in the plasmid exclusively, with CRISPR repeats aligning closest to that of the *Micrococcus* sp. A1 plasmid pLMA1 (Biswas *et al.*, 2016). The annotated genome also reveals a diversity of genes directed towards environmental versatility and resilience, including UV tolerance, thermoregulation, heavy metal resistance etc. A selection of these genes are given in table 1.

A CRISPR array contains a record of specific bacteriophages against which a bacterium maintains a defence. So, for this very mobile bacterium, the presence of the CRISPR array in the plasmid may suggest a mechanism for the prompt integration into new environments by rapid conjugation with local strains. The possible sharing of the array, together with the functions of the many unidentified plasmid genes, should certainly be explored in future investigations.

## Data Availability

The complete genome sequence and raw sequence data for *Micrococcus luteus* CW.Ay are available through NCBI under BioProject PRJNA758605 with GenBank accession numbers CP082331 (chromosome) and CP082332 (plasmid), and SRA accession numbers SRX11980019 (MinIon) and SRX11980018 (Illumina MiSeq).

## References

- Abriata, L. A., Banci, L., Bertini, I., Ciofi-Baffoni, S., Gkazonis, P., Spyroulias, G. A., Vila, A. J., Wang, S. (2008). Mechanism of Cu(A) assembly. *Nature Chemical Biology*, 4(10), 599–601. doi: 10.1038/nchembio.110
- Achour-Rokbani, A., Cordi, A., Poupin, P., Bauda, P., Billard, P. (2010). Characterization of the ars gene cluster from extremely arsenic-resistant *Microbacterium* sp. strain A33. *Applied and Environmental Microbiology*, 76(3), 948–955. doi: 10.1128/AEM.01738-09
- Alcock, B. P., Raphenya, A. R., Lau, T., Tsang, K. K., Bouchard, M., Edalatmand, A., Huynh, W., Nguyen, A. V., Cheng, A. A., Liu, S., Min, S. Y., Miroshnichenko, A., Tran, H. K., Werfalli, R. E., Nasir, J. A., Oloni, M., Speicher, D. J., Florescu, A., Singh, B., Faltny, M., ... McArthur, A. G. (2020). CARD 2020: antibiotic resistance surveillance with the comprehensive antibiotic resistance database. *Nucleic Acids Research*, 48(D1), D517–D525. doi: 10.1093/nar/gkz935
- Angelov, A., Bergen, P., Nadler, F., Hornburg, P., Lichev, A., Übelacker, M., Pachel, F., Kuster, B., & Liebl, W. (2015). Novel FliP pilus biogenesis-dependent natural transformation. *Frontiers in microbiology*, 6(84). <https://doi.org/10.3389/fmicb.2015.00084>
- Antelmann, H., Scharf, C., & Hecker, M. (2000). Phosphate starvation-inducible proteins of *Bacillus subtilis*: proteomics and transcriptional analysis. *Journal of bacteriology*, 182(16), 4478–4490. <https://doi.org/10.1128/JB.182.16.4478-4490.2000>
- Biswas, A., Staals, R. H., Morales, S. E., Fineran, P. C., & Brown, C. M. (2016). CRISPRDetect: A flexible algorithm to define CRISPR arrays. *BMC genomics*, 17(356). <https://doi.org/10.1186/s12864-016-2627-0>
- Bolger AM, Lohse M, Usadel B. (2014). Trimmomatic: a flexible trimmer for Illumina sequence data. *Bioinformatics*, 30, 2114–2120. doi: 10.1093/bioinformatics/btu170
- Bonilla C. Y. (2020). Generally Stressed Out Bacteria: Environmental Stress Response Mechanisms in Gram-Positive Bacteria. *Integrative and comparative biology*, 60(1), 126–133. <https://doi.org/10.1093/icb/icaa002>
- Brettin T, Davis JJ, Disz T, Edwards RA, Gerdes S, Olsen GJ, Olson R, Overbeek R, Parrello B, Pusch GD, Shukla M, Thomason JA 3rd, Stevens R, Vonstein V, Wattam AR, Xia F. (2015). RASTtk: a modular and extensible implementation of the RAST algorithm for building custom annotation pipelines and annotating batches of genomes. *Scientific Reports*, 5(8365). doi: 10.1038/srep08365
- Bucca, G., Hindle, Z., & Smith, C. P. (1997). Regulation of the dnaK operon of *Streptomyces coelicolor* A3(2) is governed by HspR, an autoregulatory repressor protein. *Journal of bacteriology*, 179(19), 5999–6004. <https://doi.org/10.1128/jb.179.19.5999-6004.1997>
- Chaplin, A. K., Tan, B. G., Vijgenboom, E., Worrall, J. A. (2015). Copper trafficking in the CsoR regulon of *Streptomyces lividans*. *Metallomics : Integrated Biometal Science*, 7(1), 145–155. doi: 10.1039/c4mt00250d
- Chiereghin, A., Felici, S., Gibertoni, D., Foschi, C., Turello, G., Piccirilli, G., Gabrielli, L., Clerici, P., Landini, M. P., Lazzarotto, T. (2020). Microbial Contamination of Medical Staff Clothing During Patient Care Activities: Performance of Decontamination of Domestic Versus Industrial Laundering Procedures. *Current Microbiology*, 77(7), 1159–1166. doi: 10.1007/s00284-020-01919-2

- Christakis, C. A., Barkay, T., Boyd, E. S. (2021). Expanded Diversity and Phylogeny of *mer* Genes Broadens Mercury Resistance Paradigms and Reveals an Origin for MerA Among Thermophilic Archaea. *Frontiers in Microbiology*, 12: 682605. doi: 10.3389/fmicb.2021.682605
- Crupper, S. S., Worrell, V., Stewart, G. C., Iandolo, J. J. (1999). Cloning and expression of *cadD*, a new cadmium resistance gene of *Staphylococcus aureus*. *Journal of Bacteriology*, 181(13), 4071–4075. doi: 10.1128/JB.181.13.4071-4075.1999
- Fang, Z., Ouyang, Z., Zheng, H., Wang, X., Hu, L. (2007). Culturable airborne bacteria in outdoor environments in Beijing, China. *Microbial Ecology*, 54(3), 487–496. doi: 10.1007/s00248-007-9216-3
- Ferrari, V. B., Cesar, A., Cayô, R., Choueri, R. B., Okamoto, D. N., Freitas, J. G., Favero, M., Gales, A. C., Niero, C. V., Saia, F. T., de Vasconcellos, S. P. (2019). Hexadecane biodegradation of high efficiency by bacterial isolates from Santos Basin sediments. *Marine Pollution Bulletin*, 142, 309–314. doi: 10.1016/j.marpolbul.2019.03.050
- Fierros-Romero, G., Gómez-Ramírez, M., Sharma, A., Pless, R. C., Rojas-Avelizapa, N. G. (2020). *czcD* gene from *Bacillus megaterium* and *Microbacterium liquefaciens* as a potential nickel-vanadium soil pollution biomarker. *Journal of Basic Microbiology*, 60(1), 22–26. doi: 10.1002/jobm.201900323
- Gasperotti, A., Göing, S., Fajardo-Ruiz, E., Forné, I., & Jung, K. (2020). Function and Regulation of the Pyruvate Transporter CstA in *Escherichia coli*. *International journal of molecular sciences*, 21(23), 9068. <https://doi.org/10.3390/ijms21239068>
- Ghosh, A., Chaudhary, S. A., Apurva, S. R., Tiwari, T., Gupta, S., Singh, A. K., Katudia, K. H., Patel, M. P., Chikara, S. K. (2013). Whole-Genome Sequencing of *Micrococcus luteus* Strain Modasa, of Indian Origin. *Genome Announcements*, 1(2): e0007613. doi: 10.1128/genomeA.00076-13
- Haft DH, DiCuccio M, Badretdin A, Brover V, Chetvermin V, O'Neill K, Li W, Chitsaz F, Derbyshire MK, Gonzales NR, Gwadz M, Lu F, Marchler GH, Song JS, Thanki N, Yamashita RA, Zheng C, Thibaud-Nissen F, Geer LY, Marchler-Bauer A, Pruitt KD. (2018). RefSeq: an update on prokaryotic genome annotation and curation. *Nucleic Acids Research*, 46: D851–D860. doi: 10.1093/nar/gkx1068
- Hołowka, J., & Zakrzewska-Czerwińska, J. (2020). Nucleoid Associated Proteins: The Small Organizers That Help to Cope With Stress. *Frontiers in microbiology*, 11, 590. <https://doi.org/10.3389/fmicb.2020.00590>
- Illigmann, A., Thoma, Y., Pan, S., Reinhardt, L., & Brötz-Oesterhelt, H. (2021). Contribution of the Clp Protease to Bacterial Survival and Mitochondrial Homeostasis. *Microbial physiology*, 31(3), 260–279. <https://doi.org/10.1159/000517718>
- Jung, C. J., Hsu, C. C., Chen, J. W., Cheng, H. W., Yuan, C. T., Kuo, Y. M., Hsu, R. B., & Chia, J. S. (2021). PspC domain-containing protein (PCP) determines *Streptococcus mutans* biofilm formation through bacterial extracellular DNA release and platelet adhesion in experimental endocarditis. *PLoS pathogens*, 17(2), e1009289. <https://doi.org/10.1371/journal.ppat.1009289>
- Keto-Timonen, R., Hietala, N., Palonen, E., Hakakorpi, A., Lindström, M., & Korkeala, H. (2016). Cold Shock Proteins: A Minireview with Special Emphasis on Csp-family of Enteropathogenic *Yersinia*. *Frontiers in microbiology*, 7, 1151. <https://doi.org/10.3389/fmicb.2016.01151>
- Khayyira, A. S., Rosdina, A. E., Irianti, M. I., Malik, A. (2020). Simultaneous profiling and cultivation of the skin microbiome of healthy young adult skin for the development of therapeutic agents. *Heliyon*, 6(4), e03700. doi: 10.1016/j.heliyon.2020.e03700
- Kooken, J. M., Fox, K. F., Fox, A. (2012). Characterization of *Micrococcus* strains isolated from indoor air. *Molecular and Cellular Probes*, 26(1), 1–5. doi: 10.1016/j.mcp.2011.09.003
- Kutmutia, S. K., Drautz-Moses, D. I., Uchida, A., Purbojati, R. W., Wong, A., Kushwaha, K. K., Putra, A., Premkrishnan, B., Heinle, C. E., Vettath, V. K., Junqueira, A., Schuster, S. C. (2019). Complete Genome Sequence of *Micrococcus luteus* Strain SGAir0127, Isolated from Indoor Air Samples from Singapore. *Microbiology Resource Announcements*, 8(41), e00646-19. doi: 10.1128/MRA.00646-19
- Lawton, T. J., Kenney, G. E., Hurley, J. D., Rosenzweig, A. C. (2016). The CopC Family: Structural and Bioinformatic Insights into a Diverse Group of Periplasmic Copper Binding Proteins. *Biochemistry*, 55(15), 2278–2290. doi: 10.1021/acs.biochem.6b00175
- López, L., Pozo, C., Rodelas, B., Calvo, C., Juárez, B., Martínez-Toledo, M. V., González-López, J. (2005). Identification of bacteria isolated from an oligotrophic lake with pesticide removal capacities. *Ecotoxicology*, 14(3), 299–312. doi: 10.1007/s10646-003-6367-y
- Min, K. R., Zimmer, M. N., Rickard, A. H. (2010). Physicochemical parameters influencing coaggregation between the freshwater bacteria *Sphingomonas natatoria* 2.1 and *Micrococcus luteus* 2.13. *Biofouling*, 26(8), 931–940. doi: 10.1080/08927014.2010.531128
- Mohanrasu, K., Premnath, N., Siva Prakash, G., Sudhakar, M., Boobalan, T., Arun, A. (2018). Exploring multi potential uses of marine bacteria; an integrated approach for PHB production, PAHs and polyethylene biodegradation. *Journal of Photochemistry and Photobiology. B, Biology*, 185, 55–65. doi: 10.1016/j.jphotobiol.2018.05.014
- Nguyen, H. T., Wolff, K. A., Cartabuke, R. H., Ogowang, S., & Nguyen, L. (2010). A lipoprotein modulates activity of the MtrAB two-component system to provide intrinsic multidrug resistance, cytokinetic control and cell wall homeostasis in *Mycobacterium*. *Molecular microbiology*, 76(2), 348–364. <https://doi.org/10.1111/j.1365-2958.2010.07110.x>
- Ondov, B. D., Treangen, T. J., Melsted, P., Mallonee, A. B., Bergman, N. H., Koren, S., Phillippy, A. M. (2016). Mash: fast genome and metagenome distance estimation using MinHash. *Genome Biology*, 17(1), 132. doi: 10.1186/s13059-016-0997-x
- Radhakrishnan, S. K., Pritchard, S., & Viollier, P. H. (2010). Coupling prokaryotic cell fate and division control with a bifunctional and oscillating oxidoreductase homolog. *Developmental cell*, 18(1), 90–101. <https://doi.org/10.1016/j.devcel.2009.10.024>
- Sher, S., Hussain, S. Z., Rehman, A. (2020). Phenotypic and genomic analysis of multiple heavy metal-resistant *Micrococcus luteus* strain AS2 isolated from industrial waste water and its potential use in arsenic bioremediation. *Applied Microbiology and Biotechnology*, 104(5), 2243–2254. doi: 10.1007/s00253-020-10351-2
- Shiota, S., & Nakayama, H. (1997). UV endonuclease of *Micrococcus luteus*, a cyclobutane pyrimidine dimer-DNA glycosylase/abasic lyase: cloning and characterization of the gene. *Proceedings of the National Academy of Sciences of the United States of America*, 94(2), 593–598. <https://doi.org/10.1073/pnas.94.2.593>

Sims, G. K., Sommers, L. E., Konopka, A. (1986). Degradation of Pyridine by *Micrococcus luteus* Isolated from Soil. *Applied and Environmental Microbiology*, 51(5), 963–968. doi: 0.1128/aem.51.5.963-968.1986

Smith, D. J., Ravichandar, J. D., Jain, S., Griffin, D. W., Yu, H., Tan, Q., Thissen, J., Lusby, T., Nicoll, P., Shedler, S., Martinez, P., Osorio, A., Lechniak, J., Choi, S., Sabino, K., Iverson, K., Chan, L., Jaing, C., McGrath, J. (2018). Airborne Bacteria in Earth's Lower Stratosphere Resemble Taxa Detected in the Troposphere: Results From a New NASA Aircraft Bioaerosol Collector (ABC). *Frontiers in Microbiology*, 9:1752. doi: 10.3389/fmicb.2018.01752

Szollósi, A., Vieira-Pires, R. S., Teixeira-Duarte, C. M., Rocha, R., & Morais-Cabral, J. H. (2016). Dissecting the Molecular Mechanism of Nucleotide-Dependent Activation of the KtrAB K<sup>+</sup> Transporter. *PLoS biology*, 14(1), e1002356. <https://doi.org/10.1371/journal.pbio.1002356>

Truglio, J. J., Croteau, D. L., Van Houten, B., & Kisker, C. (2006). Prokaryotic nucleotide excision repair: the UvrABC system. *Chemical reviews*, 106(2), 233–252. <https://doi.org/10.1021/cr040471u>

von Rosen, T., Keller, L. M., & Weber-Ban, E. (2021). Survival in Hostile Conditions: Pupylation and the Proteasome in Actinobacterial Stress Response Pathways. *Frontiers in molecular biosciences*, 8, 685757. <https://doi.org/10.3389/fmolb.2021.685757>

Wang, L., Chen, S., Xiao, X., Huang, X., You, D., Zhou, X., Deng, Z. (2006). arsRBOCT arsenic resistance system encoded by linear plasmid pHZ227 in *Streptomyces* sp. strain FR-008. *Applied and Environmental Microbiology*, 72(5), 3738–3742. doi: 10.1128/AEM.72.5.3738-3742.2006

Wick, R.R., Judd, L.M., Gorrie, C.L., Holt, K.E. (2017). Unicycler: Resolving bacterial genome assemblies from short and long sequencing reads. *PLoS Computational Biology*, 13(6): 97 e1005595. doi: 10.1371/journal.pcbi.1005595

Wick, R.R., Judd, L.M., Holt, K.E. (2018). Deepbiner: Demultiplexing barcoded Oxford Nanopore reads with deep convolutional neural networks. *PLoS Computational Biology*, 14(11): e1006583. doi: 10.1371/journal.pcbi.1006583

Wick, R.R. (2017). Porechop. <https://github.com/rrwick/Porechop>.

Yoon, S.H., Ha, S.M., Lim, J., Kwon, S., Chun, J. (2017). A large-scale evaluation of algorithms to calculate average nucleotide identity. *Antonie van Leeuwenhoek*, 110(10), 1281–1286. doi: 10.1007/s10482-017-0844-4

**Table 1.** lists a selection of CW.Ay genes directed towards environmental versatility

Function	Gene(s) <sup>1</sup>	Protein(s)	CW.Ay Locus <sup>2</sup>	Reference
UV tolerance	<i>uvrABC</i>	excinuclease ABC subunits UvrA, UvrB, UvrC	05545, 05500, 05555	Shiota and Nakayama, 1997; Truglio <i>et al.</i> , 2006
Non-Replicative Persistence (NRP)	<i>sulA</i>	Cell division inhibitor SulA	02010	Radhakrishnan <i>et al.</i> , 2010
Osmotic Stress Response	<i>lpqB, mtrAB</i>	Lipoprotein modulator LpqB and two-component system sensor histidine kinase MtrAB	07205-07215	Nguyen <i>et al.</i> , 2010
	<i>ktrAB</i>	KtrAB K <sup>+</sup> Transporter	08790, 08795	Szollosi <i>et al.</i> , 2016
Thermoregulation	<i>dnaK-grpE-dnaJ-hspR operon</i>	Heat shock protein GrpE	09195-09210,	Bucca <i>et al.</i> , 1997
Cold Shock Protein Heat Shock Protein	<i>dnaJ-hrcA</i>	Chaperone protein DnaJ with heat-inducible transcription repressor HrcA	06090-06095	von Rosen <i>et al.</i> , 2021
	<i>Cold Shock Protein</i>	Cold shock protein of CSP family	09455	Keto-Timonen <i>et al.</i> , 2016
	<i>Heat Shock Protein</i>	Cold shock protein of CSP family => SCO4325	01830	Keto-Timonen <i>et al.</i> , 2016
	<i>Mlut_17360</i>	phage shock protein C, PspC	08455	Jung <i>et al.</i> , 2021
Oxidative Stress Protection	<i>clpC, clpS</i>	ATP-dependent Clp protease, ATP-binding subunit ClpC	00465, 04055	Bonilla, 2020
	<i>clpP, clpX</i>	ATP-dependent Clp protease proteolytic subunit ClpP (EC 3.4.21.92)	04805-04815	Illigmann <i>et al.</i> , 2021
	<i>clpB</i>	Chaperone protein ClpB (ATP-dependent unfoldase)	09140	Illigmann <i>et al.</i> , 2021
Natural Transformation (assists adaptation and survival)	<i>tadABC, cpaF</i>	Type II/IV secretion system and Flp pilus assembly	03660-03670, 08960	Angelov <i>et al.</i> , 2015
Starvation	<i>ybeZ_1, ybeZ_2</i>	Phosphate starvation-inducible protein PhoH	02335, 06080	Antelmann <i>et al.</i> , 2000
	<i>dps</i>	DNA protection during starvation protein	09215	Hołowka and Zakrzewska-Czerwińska, 2020
	<i>cstA</i>	Carbon starvation protein A	04190	Gasperotti <i>et al.</i> , 2020
Heavy Metal Resistance	<i>arsC1-acr3-arsR-arsC-arsC</i>	Arsenic resistance operon, including arsenate-mycotoxin transferase (EC 2.8.4.2) and arsenate efflux Acr3	05330-05350	Sher <i>et al.</i> , 2020
	<i>trxB-trxA</i>	Thioredoxin reductase (EC 1.8.1.9)-thioredoxin [reported as <i>arsT-arsX</i> in an arsenic-resistant <i>Microbacterium</i> ]	11190-11195	Achour-Rokbani <i>et al.</i> , 2010; Sher <i>et al.</i> , 2020
	<i>czcD</i>	Cobalt/zinc/cadmium resistance protein	00780, 02990, 10120, 03020	Fierros-Romero <i>et al.</i> , 2020
	<i>csoR, copZ</i>	Copper(I) chaperone CopZ	10385-10390, 06440	Chaplin <i>et al.</i> , 2015
	<i>cadA</i>	Lead, cadmium, zinc and mercury transporting ATPase (EC 7.2.2.21)	10150, 10175, 10395, 06435	Nucifora <i>et al.</i> , 1989

<sup>1</sup> Gene assignments by NCBI PGAP v5.0 and via UniProt

<sup>2</sup> NCBI Locus prefix: K7G68\_



---

## 論孫思邈的養生養性觀對中國醫學、養生學的影響

Jamee B.Y. Tsai 蔡寶瑤

---

### 引言

孫思邈是(581年-682年)隋唐時期的著名的醫學家。他被譽為「藥王」,是中國道家、佛家、儒家、易學的集大成者,與華佗、扁鵲同為「中國三大神醫」。為了促成醫學的普遍化,孫思邈編寫了簡化、標準化的醫書供學生、百姓參考。孫思邈以「人命至重,有貴千金。一方濟之,德逾於此。」的理念,分別在公元652年與682年創作出《備急千金要方》(簡稱《千金要方》)和《千金翼方》。前者共30卷,記載了5300條醫方,而後者同為30卷,記錄了2571條藥方。千金二方結合了《黃帝內經》的臟腑學說和張仲景的《傷寒論》的臨床學問,首創多個方劑合一的「複方」,達到「一方多用」的效果,為百姓提供了涉及疾病、解毒、急救、養生、草藥、針灸、按摩等方面的基礎食療配方或藥方。該書內容豐富,是繼張仲景《傷寒雜病論》後中國醫學的又一次總結,被譽為中國歷史上最的臨床醫學百科全書。

本文將從養生學的發展、以及「藥王」孫思邈的在《備急千金要方》中的養生思想為切入點,探討孫思邈養生養性觀對當代中國醫學、養生學的影響。

### 一、 養生思想的發展與孫思邈的道醫養生

養生,是指通過各種方法頤養生命、增強體質、預防疾病,達到延年益壽的中醫學理論。「養生」理論由《莊子·養生主》(前3世紀)提出,是馬王堆漢墓醫術(西元前169年)以及中國最早中醫學著作《黃帝內經》中重要的醫學理念,提倡配合天地、陰陽之道、以及自然規律的理念,維持身體健康。

孫思邈養生養性之道含有儒家、道家哲學以及宇宙學的思想,從個人身體健康上升到社會,甚至整個宇宙的正常運轉與和諧。

孫思邈的養生觀繼承了孔子「仁者壽」的儒家思想,表示「道德日全,不祈善而有福,不求壽而自延,此養生之大旨也。」「仁者不憂」。孫思邈認為道德行為可以使人獲得積極的心理感受,從而增進健康。

「道法自然好養生」為道家以及孫思邈養生觀中的重要理論,以協調人與人、社會、自然之間的關係,使身體與環境形成和諧相融的關係。《黃帝內經》其中也提倡與陰陽五行以及自然、宇宙法則形成平衡,把人類身體視為社會以及宇宙的縮影,而人類的健康亦能對社會與自然環境產生一定影響。

## 二、《備急千金要方》中的養生思想

孫思邈在《千金要方》以及《千金翼方》等著作中探討了養生思想。孫思邈提出：「一曰嗇神，二曰愛氣，三曰養形，四曰導引，五曰言論，六曰飲食，七曰房室，八曰反俗，九曰醫藥，十曰禁忌。」十種養生的具體方法，涵蓋人們思想、運動、飲食、居住以及性生活各方面的生活習慣。

### 2.1、「依時攝養」、「治未病」的養生思想

孫思邈曰：「善養性者，則治未病之病，是其義也。」在孫思邈的養生思想中，養生與治病相結合，其中繼承了《黃帝內經 素問》中的「治未病」的思想去達到養生「延年益壽」的終極目標。「治未病」即是採取相應的措施，未病先防，「防衰於未然」。孫思邈在《千金要方論診候第四》中論述道：「上醫醫未病之病，中醫醫欲病之病，下醫醫已病之病。」可見，此思想不只限於病人，指導病人去調理並確保身心健全是對與醫者來說尤為重要。

「治未病」的思想源於《黃帝內經 素問 四氣調神大論》，表示世間萬物的四時陰陽變化是生老病死之根，對人體有利也有害處，逆則有害，順則有利且防止疾病的產生。孫思邈在《千金要方：卷二十七養性 養性序第一》中提出的「天地合氣，命之曰人」、「依時攝養」的道家養生理念。其重點在於「順應四時」、「陰陽得宜」，具體方法為：「春養生氣，夏養長氣，秋養收氣，冬養藏氣。」其核心在於判斷每個季節的特點和規律，依照身體在不同季節下的變化，做出相應的行為。如春天，萬物復甦，「氣」集於肝，通過夜臥早起，在晨曦散步，能夠促進氣血的循環，避免感染風寒。相反，冬天萬物潛藏，「

人氣在腎」，為了保暖，要減少身體能量的消耗，應該早臥晚起，避免過度勞累。孫思邈曰：「人能依時攝養，故得免其妖枉也。」

### 2.2、「養性」、「嗇神」的養生思想

在《千金要方：卷二十七養性》當中，孫思邈在序章《養性第一》中論述了「養性」對「養生」的重要性。養性是通過培養高尚的道德品質，淡化對名利的追求，做到「於名於利，若存若亡，於非名非利，亦若存若亡」，故曰：「善養性者，則治未病之病，是其義也。」孫思邈引用了嵇康養生之說，定義名利、喜怒、聲色、滋味、思慮為消耗人體精神氣血的「五難」，表示若五難並存，便「德行不克，縱服玉液金丹，未能延壽」，如若五難並存於人體中，便「性既自善，內外百病悉皆不生，禍亂災害亦無由作，此養性之大經也」。

《道林養性第二》含有道家觀念養生觀念，涉及起居飲食、運動、視聽言行、思想意識、喜怒情志、道德修養等方面。文中提到的「十要」原則論述了有益於健康的思想意識與行為：「一曰嗇神，二曰愛氣，三曰養形，四曰導引，五曰言論，六曰飲食，七曰房室，八曰反俗，九曰醫藥，十曰禁忌。」此原則提倡減少神氣消耗、運動吐納、謹慎言語、控制飲食、節制性生活、淡泊名利、服用保健藥品、遠離有害於健康的環境和事物並且「習以成性」，養成健康的生活規律，調理精神與生理狀態。「十二少」在於節約身體能量，做到少消耗，多養身，曰：「故善攝生者，常少思、少念、少欲、少事、少語、少笑、少愁、少樂、少喜、少怒、少好、少惡。」「多思則神殆，多念則志散，多欲則志昏，多事則形勞，多語則氣乏，多笑則麟傷，多愁則心攝，多樂則意溢，多喜則忘錯昏亂，多怒則百脈不定，多好則專迷不理，多惡則憔悴無歡。」

### 2.3、「動靜結合」的養生思想

除了精神上的修養，孫思邈也提出了鍛煉身體的方法，其中強調了「動靜相宜」的要旨。孫思邈認為氣血「不得安於其處，以致壅滯」，所以需通過適當的運動來讓氣血運行。然而，凡事都需要適量，因此孫思邈曰：「常欲小勞，但莫大疲及強所不能堪耳。且流水不腐，戶樞不蠹，以其運動故也。」，常活動則讓身體不易被侵蝕破壞，卻不能「大疲」，挑戰身體的極限。為了達到適當的運動量，孫思邈在《千金要方》禮陸輪了以「動」為本的按摩、導引，和以「精」為關鍵的調氣與導引之法。

孫思邈在《千金要方：按摩法第四》裡論述了天竺、老子按摩法等促進人體氣血循環、增加身體精華能量的肢體活動。天竺按摩法源於印度，有養生保健和醫療作用，全套共18節動作。孫思邈說，即使老年人，如果能每天練習三遍，不出一月，有病盡除，身輕腿健，「行及奔馬」，並且補益延壽，不復疲勞。老子按摩法是一套相傳為老子所編寫的養生方法，全套動作49節，能與天竺按摩達到異曲同工之妙。如若在不超過人體正常的生理負荷下堅持做這種運動，能夠「使人精和、血脈流通、風氣不入、行之不病」，恰恰達到了養生祛病、延年的目的。

動靜與人體的健康相輔相成，而「精」的關鍵在於調理氣血。在中醫學中，「氣」是身體的三寶之一，氣與精同為物質基礎，氣是人類活動的動力，而神則是精神，是生命活動的表現。孫思邈引用了抱樸子之說：「夫愛民所以全其國，惜氣所以全其神，民散則國亡，氣竭則身死」，如若把人體當做一個國家，神為國家君主，氣為子民，人民就需

如君主愛惜一般愛惜氣。其中「惜氣」的方法包括調氣，此章開頭寫道：「彭祖曰：心無煩，形勿極，而兼之以導引，行氣不已，亦可得長年，千歲不死。凡人不可無思，當以漸遣除之」，凡人無法做到「無思」，但應逐漸消除對衣食、聲色、勝負、得失、榮辱顧慮，如若配合調氣、導引之法，便可達到修身養性、延年益壽的效果。書中記載了一種名為「六字訣」的吐納法，又名「踵息法」，通過唇齒喉舌用力不同的噓、呵、呼、咽、吹、嘻六種發音，牽動不同臟腑經絡氣血運行，使自身寒熱平和，順應季節更替，避免生病，確保體內的氣和諧充沛。

### 2.4、「飲食居住」的養生思想

《居處法第三》記載了日常生活起居應採取的保健措施和養生之法。此章提醒人們及早就醫，發現病情，避免病入膏肓，提高對疾病的警覺性。對於居住環境，孫氏表示房屋必須建造周密不能留下許多縫隙，否則容易受到風寒。倘若勉強忍受而不及時避風，會產生中風病。此章也提到，夏天的住處一定要防潮、隔熱，每天上下午開窗透風；秋天儘量避免長期處於陰暗、孤獨的環境中，對人的健康心理都有影響。

《服食法第六》以飲食、藥品方面調理身體，通過養成良好習慣預防疾病，延年益壽。孫思邈在《千金要方：卷二十六食治》中探討飲食對治療調養身體的重要性。食物被視為提供精氣神的主要來源，如果得到了正確的供應與補充，身體便能維持健康的機能，協調有序，方能延年益壽。《服食法第六》結合了《卷二十六食治》當中「先饑而食，先渴而飲」，「莫強食，莫強飲」，「過饑傷氣，過飽傷肺，過酸傷骨，過鹹傷筋」的飲食養性理念，並提供了具體的飲食醫藥調

配方法。其中服地黃方、黃精膏方、服烏麻法、服枸杞根方等有「無病延年」、「久服百病不生，常服延年不老」等主導養生延壽的藥方。

## 2.5、「房中補益」的養生思想

《千金要方：卷二十七養性》的一節《房中補益第八》論述了男女兩性的房室生活，提倡通過陰陽交合達到健康生育與養生的效果。孫思邈之所以提出此重要性並不是為了淫佚，而是為了讓人們生育、繁衍後代。孫思邈曰：「男不可無女，女不可無男。無女則意動，意動則神勞，神勞則損壽」，「恣其情欲，則命同朝露也。」性生活是人們不可缺少的，孫思邈認為適度的房室生活有益於人體健康，但過則為災。孫思邈對房中術的論述體現出養生思想不僅提供人們應該做的事情，也包含了養生時應該注意、避免的禁忌。以房事為例，孫思邈提出了結合氣功、按摩、藥理的「御女之術」等性技巧，也點出了縱慾的大忌。因為「凡精少則病，精盡則死」，所以孫思邈提醒男性應該固精守關，以免人體虛弱、身體精氣流失。孫思邈認為房事是一門科學，是養生之道，是方法，是技術。「少年極需慎之」，「年至四十，須識房中之術」，要根據不同年齡特徵和體質來安排房事，如若能掌握「房中術」方能延年益壽，倘若忽略它只會讓身體受到損傷。

### 三、孫思邈與中國醫學、養生學

養生，是指通過各種方法頤養生命、增強體質、預防孫思邈養生思想與預防醫學、衛生學相結合，以「治未病」理論向大眾普及養生養性的醫藥知識。孫思邈引用了扁鵲的話：「濟命扶危者，醫也。」孫思邈把醫藥知識看作是為民眾謀福利的手段，而不是為

私人謀利的工具，亦是做到了養性中所謂的「淡泊名利」。孫思邈認為醫生有責任、義務讓醫學衛生知識「家家悉解，人人自知」，為此他編寫了《千金要方》，隨著隋唐時期朝廷對醫學的大肆宣傳，向世人傳播養生延壽之學。

孫思邈年齡仍舊成謎，但據史料記載，他至少活到了一百歲的高齡，身體力行地詮釋養生之道。在千金二方中，孫思邈以通俗易懂的語言提高民眾的健康意識，孫思邈專注於食治、居處、房中補益、調氣、按摩等生理調理法，以通俗易懂的言語提醒人們以「十二少」、「十要」等保持心裡平靜，養成高尚道德品質的養性、心理調理法，達到養生身心健康，延年益壽的作用，增強整個社會的健康道德意識和自我保健能力。

### 結語

藥王孫思邈通過《備急千金要方：卷二十七養性》以「養性」為覈心詳細講解了養性、道林養性、居處法、按摩法、調氣法、服食法、黃帝雜忌法、房中補益方八種系統性的「養生」、延年益壽的方法，大肆宣傳普及衛生醫藥知識。孫思邈養生養性觀當中蘊含了儒家和哲學的思想，從人體自身健康上升到社會、宇宙的層面，是自我到無我境界的一種昇華。孫思邈養生觀當中的醫學哲學思想涉及面相當廣泛，是古代人們長期經驗的積累和總結，時至今日，仍有學習繼承和借鑒的價值。

## 資料來源

Fan, Ka Wai. "Metaphysics and the Basis of Morality in the Philosophy of Wang Yangming." *The Period of Division and Tang Period*, edited by T.J.Hinrichs and Linda L.,Barnes, 2013, pp. 92-95.

Wilms, Sabine. "Nurturing Life in Classical Chinese Medicine: Sun Simiao on Healing without Drugs, Transforming Bodies and Cultivating Life." *Journal of Chinese Medicine*, no. 93, 2010, pp. 5-13.

陳明華, "論孫思邈健康倫理思想", 《中國醫學倫理學》, 2005年6月:3-101。

孫思邈, 《備急千金要方》(浙江大學圖書館), 唐652年。

巫懷微, 蘇華仁, 劉繼洪, 任芝華, 《藥王孫思邈道醫養生》(大展出版社, 2011)。

朱丹丹, 王衛, 王益民, 朱媿, 徐一蘭, 鮑嘉娣, "《千金方》養生之道淺析", 《天津中醫藥大學學報》, 2018年4月:37-2。



**Artist:** Ava Osann

**Title:** *Reconstructive memory*, 2023

**Medium:** Oil on canvas, 80 x 100 cm

**Description:** The painting explores how a central memory becomes extrapolated, abstracted, and remade but still remains similar to the original memory. The Reconstructive Memory Theory suggests that memory is altered and reconstructed when retrieved. This is reflected in how all the faces come from my memories and thus have features of familiar people but have been altered over time. The faces fading into the background show how parts of our past will inevitably fade away to make space for new.

The Independent Schools Foundation Academy  
1 Kong Sin Wan Road, Pokfulam, Hong Kong  
Tel +852 2202 2000  
Fax +852 2202 2099  
Email [enquiry@isf.edu.hk](mailto:enquiry@isf.edu.hk)

